Characterisation of flowmotion in healthy controls and type 2 diabetes

By

Sarah Blackwood

BMedRes (Hons.)

Submitted in fulfilment of the requirements for the degree of

Doctor of Philosophy (Medical Research)

Menzies Institute for Medical Research

University of Tasmania

October 2016

UNIVERSITY *of* TASMANIA

MENZIES

Institute for Medical Research

Table of contents

Acknowledgments

First and foremost, I must thank my awesome supervisors for all the time and effort they have put into me over the last 4.5 years, through honours and a PhD. Their guidance and help has inspired and pushed me to be the best researcher I can be. A particular thanks to my two main supervisors.
Prof. Steve Rattigan, thank you for trusting me with a project you are so passionate about. You have always pushed me to be better, to think more, and I know it has made me an infinitely better scientist as a result. Dr Renee Dwyer I am pretty sure you are the reason I've been able to get this PhD done no matter what life has thrown my way. I am profoundly grateful to you for always giving me time to discuss the data, checking I'm okay and making sure I kept my sanity. Your ability to edit my first drafts in a way that doesn't have me on the floor in the foetal position is also greatly to be admired.
Thanks also goes to Dr Michelle Keske, whom I think of as the voice of reason in my life. Never underestimate just how grateful I am when you say it like it and give me a straight forward way to progress. I have immense respect for you because of it. Dr Steve Richards, who swoops in to provides valuable advice whenever needed. Who is also there with a bottle of red whenever wine is needed.
I am profoundly grateful to you all for your support and friendship.

The collection of some of the data in this thesis was performed by a number of fantastic people in my group. Michelle Keske and Ryan Russell were the brains and the work behind the clinical study described in this thesis. Michelle acquired the funding and put hours into the running of the study. Ryan must be acknowledged for running the day to day operations and collecting the ultrasound blood flow data (total flow and CEU) in the clinical chapters of this thesis. Michelle, Ryan and Renee also ran and supervised the RT intervention described in chapter 5. Donghua Hu was responsible for the analysis of clinical blood chemistry data. Eloise Bradley performed the upper thigh phentolamine experiments described in chapter 6. I thank them all for providing this data so that my thesis can tell a more complete story.

There are a number of clinical studies that didn't make it into this thesis in the end. I would just like to thank Rach, Dean, James and the two Kates for being incredibly accommodating and helpful towards me. I thank them for letting me take some LDF measures on the participants of their studies. I also thank everyone that participated in all the studies I have been involved in.

A thank you to Diabetes Tasmania, as well as Staples and Konica Minolta who have both provided me with an elite top out scholarship at different times throughout my PhD.

I thank other past and present members of the MRG group for their support and friendship. Particularly Aascha, Dino, Eloise and Helena who have all helped me whenever I have asked, and put up with me singing to myself in the lab.

A profound thank you goes out to my fellow PhD students, your support and friendship has kept me afloat when I was drowning over the last 3.5 years. I thank the OHA hockey club, particularly the A-pool women, for being a second family to me and for saving me from myself. I thank all my friends and anyone I have bailed up into a corner and passionately talked science to non-stop. You have all made doing a PhD much less stressful and much more enjoyable than it otherwise would have been.

To my amazingly supportive family, no words will ever thank you enough for the unconditional love and support you give me. I know that no matter what happens, no matter what I need, you will unquestioningly come to my rescue. Because of your love and generosity, I can peruse anything my heart desires, and that is an incredible gift.

Finally, this thesis is dedicated to two wonderful people in my family who have profoundly enriched and bettered my life:
To my Grandfather Colin Milford Blackwood (1919 to 2010), a man of exceptional integrity and courage. His sacrifice and choices have meant that my life is free of limitations. Because of him I am able follow my passions without question or hesitation, something I will always be immensely grateful for.
And to my darling Nan, Joan Smythe. A person who has always inspired me with her kindness for others and passion for life, no matter what comes her way. I not only have your name, but your strength and determination that makes sure I achieve all that I am capable of and live life to the fullest. Thank you for being such a wonderful role model.

Statement

The work in this thesis has been undertaken exclusively for the use of a PhD in the area of Biochemistry and has not been used for any other higher degree or graduate diploma in any university. All written and experimental work is my own except that which has been referenced accordingly.

Sarah J. Blackwood

Authority of Access

This thesis may be available for loan and limited copying in accordance with the *Copyright Act* 1968.

Sarah J. Blackwood

Abstract

Flowmotion, the rhythmic oscillation of blood flow across a tissue, optimises nutrient delivery at rest and during states of increased metabolic demand. Five known factors influence flowmotion patterns across a tissue, each distinguishable by their rate of input; cardiac, respiratory, myogenic, neurogenic and endothelial components. In disease states such as type 2 diabetes (T2D), flowmotion is thought to be altered and may contribute to dysregulated metabolism. The aim of this thesis was to characterise flowmotion in healthy controls and T2D participants.

Flowmotion was investigated in healthy controls and T2D participants at rest, and following endogenous insulin release in response to a 50g oral glucose challenge (OGC). The effect of a resistance training (RT) intervention in T2D participants was also assessed. Total blood flow to the forearm was measured using 2D-ultrasound and skeletal muscle perfusion was measured with contrast enhanced ultrasound (CEU). Microvascular blood flow in the skin and subcutaneous tissue (skin+SC) of the forearm was examined using a combined Laser Doppler Flowmetry (LDF) and tissue oxygenation probe. Spectral analysis (wavelet transformation) was performed on the data to characterise the individual contributions of the five factors known to influence flowmotion.

Type 2 diabetics exhibited differences in total blood flow, skin+SC LDF flux and skin+SC flowmotion compared to healthy controls at rest. Flowmotion was altered in response to the OGC in healthy controls, without changes in total flow and skin+SC LDF flux. In contrast, flowmotion and skin+SC LDF flux were unaltered in response to OGC in T2D, while total blood flow to the forearm increased. In the T2D group, a 6-week RT intervention partially restored skin+SC flowmotion.

In response to OGC skeletal muscle microvascular perfusion was reduced in healthy controls, but not in T2D participants. In contrast, skin+SC microvascular perfusion did not change in response to OGC in either group, indicating skin+SC flowmotion may not represent flowmotion in skeletal muscle.

The CEU technique, used to determine skeletal muscle microvascular perfusion, was adapted to investigate flowmotion within skeletal muscle. In anaesthetised rats, skeletal muscle flowmotion patterns were measured with both the LDF and the newly adapted CEU techniques. An α-adrenoceptor antagonist, which inhibits the neurogenic component of flowmotion, was used to compare the two techniques. Both the LDF and CEU methods detected the inhibition. In addition, the CEU method enable identification of different flowmotion patterns within specific fibre types.

In conclusion, these studies demonstrate dysfunction in blood flow and flowmotion in T2D. They also highlight a difference in skin+SC and skeletal muscle microvascular blood flow in response to OGC. The newly adapted CEU technique will allow more informative assessment of flowmotion in skeletal muscle, facilitating future research into its role in regulation of muscle metabolism.

Abbreviations

1RM	1 repetition maximum
AUC	Area under the curve
BMI	Body mass index
Δ	Delta, change from basal
Ca^{2+}	Calcium
CEU	Contrast enhanced ultrasound
CNS	Central nervous system
ET-1	Endothelin 1
FBF	Femoral blood flow
GMP	Guanosine monophosphate
HR	Heart rate
LDF	Laser Doppler Flowmetry
LDF + OXY	Combined Laser Doppler Flowmetry and tissue oxygenation probe
MAP	Mean arterial pressure
MAPK	Mitogen-activated protein kinases
NA	Noradrenaline
NO	Nitric oxide
O_2 Sat	Oxygen saturation
PI3K	Phosphoinositide 3-kinase
RBC	Red blood cell
ROI	Region of interest
Skin+SC	Skin and subcutaneous tissue
SNS	Sympathetic nervous system
SNP	Sodium nitroprusside
T2D	Type 2 diabetes
tHb	Total haemoglobin
WHO	World Health Organization

Preface

Listed below are the data obtained for the present thesis that has been submitted for publication or presented at scientific meetings.

Papers accepted for publication

Michelle A. Keske, Renee M. Dwyer, Ryan D. Russell, **Sarah J. Blackwood**, Aascha A. Brown, Donghua Hu, Dino Premilovac, Stephen M. Richards, Stephen Rattigan. Regulation of Microvascular Flow and Metabolism: An Overview. *Clinical and Experimental Pharmacology and Physiology.*

Review article.

Manuscripts in progress

Sarah J. Blackwood, Renee M. Dwyer, Eloise A. Bradley, Michelle A. Keske, Stephen M. Richards, Stephen Rattigan. Determination of skeletal muscle microvascular flowmotion with novel contrast enhanced ultrasound technique. Under review at *Cardiovascular Research*.

Performed all experiments and wrote the manuscript, data from chapter 6.

Ryan D. Russell, Donghua Hu, Timothy Greenaway, **Sarah J. Blackwood**, Renee M. Dwyer, James E. Sharman, Graeme Jones, Kathryn A. Squibb, Aascha A. Brown, Meg Boman, Hayder Al-Aubaidy, Dino Premilovac, Christian K. Roberts, Samuel Hitchins, Stephen M. Richards, Stephen Rattigan, Michelle A. Keske. Skeletal Muscle Microvascular-Linked Improvements in Glucoregulatory Function from Resistance Exercise in People with Type 2 Diabetes. Intend to submit to *Diabetes Care*.

Collected and analysed LDF data and wrote methods and results section pertaining to this data (chapter 5).

Oral Presentations at conferences

Invited talk at *The Physiological Society (UK) Annual Meeting*. Cardiff, Wales, UK. July 2015. **Sarah J. Blackwood**, Renee M. Dwyer, Michelle A. Keske, Stephen M. Richards, Stephen Rattigan. Determination of skeletal muscle microvascular flowmotion with contrast enhanced ultrasound

Invited talk at *The Physiological Society (UK) Annual Meeting*. Cardiff, Wales, UK. July 2015. S. Rattigan, **S. J. Blackwood**, E. Bradley, S. Richards, R. M. Dwyer, M. A. Keske. Methods for assessing microvascular flowmotion in humans.

Invited talk at the *10th World Microcirculation Meeting in Kyoto Japan*. Tokyo Japan. September 2015. Michelle A. Keske, **Sarah J. Blackwood**, and Stephen Rattigan. Methods for the investigation of flowmotion.

Australian Physiological Society Annual Meeting. Hobart, Tasmania, Australia. November 2015. **Sarah J. Blackwood**, Ryan Russell, Renee M. Dwyer, Michelle A. Keske, Stephan Rattigan. Forearm blood flow distribution in healthy controls and T2D: Effect of exercise training.

Posters at conferences

The Physiological Society (UK) Annual Meeting. London, England, UK. July 2014. **Sarah J. Blackwood**, Eloise A. Bradley, Renee M. Dwyer, Stephen M. Richards, Michelle A. Keske and Stephen Rattigan. New techniques for the detection of microvascular flowmotion within skeletal muscle.

Pulse of Asia. Seoul, South Korea. September 2016. Rachel E. Climie, Dean S. Picone, **Sarah J. Blackwood**, Ahmad Qasem, Steven Rattigan, James E. Sharman. First evidence of pulsatile pressure interaction between the macro-vasculature and micro-vasculature: proof-of-concept by association with kidney dysfunction among patients with type 2 diabetes.

ARTERY16. Copenhagen, Denmark. October 2016. Rachel E. Climie, Dean S. Picone, **Sarah J. Blackwood**, Ahmad Qasem, Steven Rattigan, James E. Sharman. First evidence of pulsatile pressure interaction between the macro-vasculature and micro-vasculature: proof-of-concept by association with kidney dysfunction among patients with type 2 diabetes.

Chapter 1 - *Introduction*

Vascular delivery of nutrients and hormones is normally tightly coupled to the metabolic demands of the supplied cells, and has been investigated in tissues including the brain, heart, skin and skeletal muscle (1). In mammals, skeletal muscle makes up a high proportion of body mass (30-40% of body (2)) and has the potential to be highly metabolically active, which has major implications for the cardiovascular system. It is therefore critical that blood flow changes with skeletal muscle metabolic demand to efficiently couple nutrient delivery and waste removal with the function of the tissue (3). Blood flow is minimised when metabolic demand is low, in order to prevent excess circulatory demand (cardiac output), but must have the capacity to support the significant rise in oxygen consumption and nutrient utilisation for fuel production in the myocytes during exercise when the work load and thereby metabolism is greatly enhanced (4). Additionally, there are other stimuli which cause skeletal muscle metabolism and blood flow requirements to change, for example, when muscle is storing nutrients derived from diet (i.e. glucose) (5, 6). Meeting increased metabolism with sufficient blood flow to the working tissue occurs through both systemic and local mechanisms.

The capillary recruitment theory indicates that at rest when nutrient demand is low, blood flow can be reduced by intermittently perfusing fewer of the available capillaries; however, to keep nutrient delivery adequate to all myocytes the sets of perfused capillaries must be continually varied. This is in part achieved through vasomotion, a function of the vasculature that involves the rhythmical oscillation of blood vessel diameter to allow or restrict blood flow through individual vessels (7, 8). The physiological consequence of vasomotion is flowmotion, which is the rhythmical oscillation and variation of flow through tissue (7, 9). Vasomotion and flowmotion have been observed in skeletal muscle during rest, and has been seen to change in response to insulin (10, 11). Vasomotion has also been seen in other tissues in the body such as the skin and subcutaneous tissue (skin+SC) (12). It is suspected that these processes are critical for the efficient matching of nutrient and oxygen delivery to demand. Demonstration of how vasomotion and flowmotion affect metabolism, and how they are in turn affected by alterations in metabolism or pathological processes has been difficult.

Flowmotion can be assessed by techniques that are commonly used to measure blood flow through regions of tissues whereby blood flow data are collected constantly over time, (e.g. Laser Doppler Flowmetry [LDF]). These techniques can be used to assess changes in skin+SC or skeletal muscle flowmotion in response to the infusion of insulin or other vasoactive molecules, and in disease states such as insulin resistance and type 2 diabetes (T2D). The purpose of the studies in this thesis was to develop methods for the assessment of flowmotion; to investigate normal patterns of blood flow in both human participants (skin+SC) and animal models (skeletal muscle), and to assess the changes that occur in T2D.

1.1 Vascular structure

The body's vasculature is composed of three types of vessels; arteries, capillaries and veins. The arterial system consists of larger conducting arteries that move oxygenated blood from the heart to the tissues; these are comprised of an endothelial layer, layers of smooth muscle, and many elastic connective tissue fibres. The larger arteries branch into smaller arterioles which carry blood throughout organs into capillaries. Arterioles are known as resistance vessels and consist of an endothelial layer, connective tissue, and a thick layer of smooth muscle. Capillaries are comprised only of an endothelial layer, which aids their role in nutrient exchange at the cellular level as it allows for the diffusion of select nutrients out of the blood into the tissue and vice versa (13). The arrangement of arterioles in rodent cremaster, soleus, and extensor digitorum longus muscles has been described by Sweeney and Sarelius (14) and Williams and Segal (15). These studies show that blood enters the muscle through a feed artery classified as a 1st order arteriole, which then branches into smaller vessels (numbered in increasing order). 3rd order arterioles transverse the muscle tissue and 5th order arterioles lead into the capillaries. The capillaries are arranged in groups known as modules, which consist of approximately 15 capillaries that arise from each 5th order arteriole. A group of modules which arise from a 4th order arteriole is known as a capillary network (Figure 1) (16).

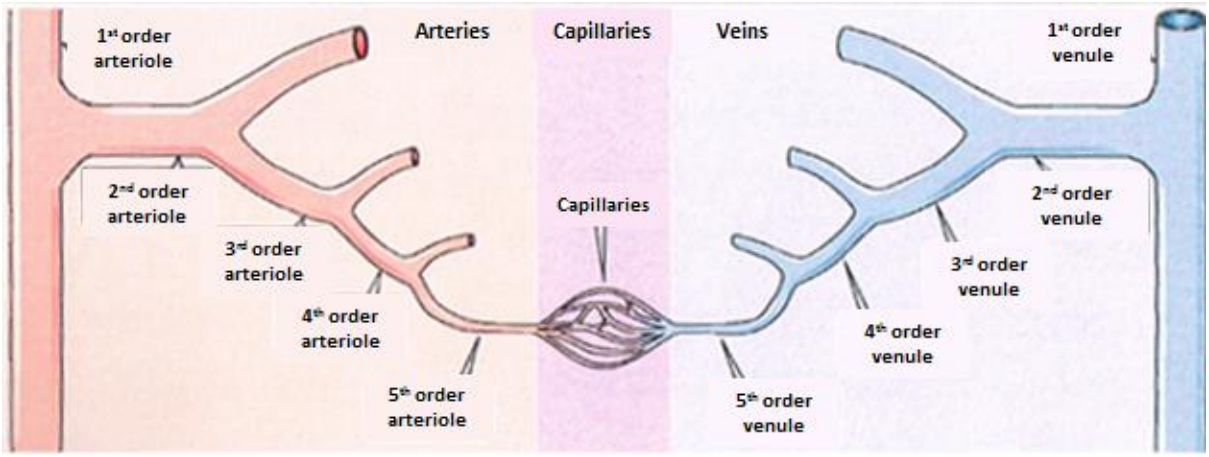

Figure 1.1: *Skeletal muscle microvasculature*. Adapted from Boron and Boulpaep 2003 (13).

The prevailing theory indicates that blood flow to the whole muscle (often referred to as bulk or total flow) is controlled by constriction and dilation of the 1st-3rd order arterioles, whereas flow to the individual capillary networks is controlled by the 3rd-5th order arterioles (16). A number of animal and human studies indicate there is intermittent and heterogeneous movement of blood through the skeletal muscle tissue, differing in both spatial and temporal structure of flow (17-19). It appears that a rhythmic oscillation of arteriole diameter (vasomotion) occurs at regular intervals so that different capillary modules are perfused at different times (20, 21). It has been proposed that at any one time not all capillaries in the muscle tissue are perfused (14, 22) and that control of this blood flow is tightly linked to changes in metabolic demand and other stimuli such as increased work during exercise or after a meal (23). Further to this, it is proposed that within skeletal muscle two different capillary routes exist and changes in distribution between these two pathways may be a means to minimise blood nutrient utilisation during rest, while also maintaining the ability to meet increased demands when they arise (24).

First alluded to by Pappenheimer in 1941 (25) using constant-pressure perfused canine gastrocnemius muscle and then later extensively investigated by Clark *et. al.* (3, 5, 23, 24) with the constant-flow perfused rat hindlimb is the idea that the skeletal muscle contains two different capillary networks, each with a different role within the tissue. It is proposed 'nutritive' and 'non-nutritive' capillary

networks run parallel to each other in skeletal muscle vasculature, with flow distribution within each changing based on metabolic demand. Structural studies of skeletal muscle vasculature support this concept of two separate blood flow routes running parallel to each other (26, 27). Clark *et. al.* (24) propose that the nutritive flow route consists of longer tortuous capillaries which wrap around muscle fibres, thereby providing a large surface area for nutrient exchange between myocytes and blood. The non-nutritive pathway, believed to consist of lower resistance, shorter and wider capillaries (28), is thought to act as a shunt through the skeletal muscle tissue. A proportion of the non-nutritive capillaries are thought to supply connective tissue such as septa and tendons (29), as well as adipocytes within the tissue (30). Clark and colleagues surmised that *in vivo* the non-nutritive flow route in skeletal muscle may act as a flow reserve which can be rapidly redistributed to the nutritive flow route in response to increased metabolic demand (24). The redistribution of blood into the two different flow routes *in vivo* is proposed to be an important component in the regulation of muscle nutrient utilisation. This allows conservation of nutrient and oxygen supply during rest, while maintaining the ability of muscle to meet increased demands in response to stimuli such as contraction (5, 24). It should be noted that the nutritive and non-nutritive capillary theory is not universally accepted, other theories indicating homogenous capillary structure and continuous perfusion of all capillaries do exist (31) and these theories have been subject to debate in the literature (32, 33).

1.1.2 Capillary perfusion

According to the capillary perfusion theory (which is postulated to accurately reflect true microvascular flow (32)), in skeletal muscle at rest, only a proportion of capillaries are believed to be perfused at any one time (14, 22), with a constant change in the regions perfused occurring via vasomotion (20, 21). During times of increased metabolic demand such as during exercise or after a meal, the number of capillaries perfused and the surface area available for nutrient exchange is

increased. However, the major alternative theory states that there is continuous perfusion of all capillaries at all time and that only the haematocrit becomes altered when demand is changed (31). The mechanisms through which this increase in perfusion occurs may vary depending upon the stimuli. Increased capillary perfusion occurs via dilation of terminal arterioles (4^{th}-5^{th} order), allowing blood flow through previously quiescent capillaries, a process known as microvascular recruitment (or capillary recruitment) (6, 34, 35). Greater distribution of flow into the capillaries can occur with or without the increase in total flow to the muscle, controlled by feeder (1^{st}-3^{rd} order) arterioles (16). Total blood flow is the bulk volume of blood moving through main arteries into the muscle tissue as a whole, as distinct from capillary perfusion, which refers to the distribution of the blood within the muscle capillaries. It is thought that because of the two different flow routes in muscle, capillary perfusion can change and increase without necessarily requiring a change in total blood flow (36). Coggins *et. al.* (37) looked at changes in total blood flow and microvascular perfusion in the forearm during a 4-hour infusion of physiological levels of insulin (0.05mU/kg/min). This showed an increase in microvascular perfusion which occurred without a significant increase in total flow to the forearm, thereby demonstrating that distribution of blood within skeletal muscle tissue can be altered without changing the total amount of blood delivered into the muscle.

Experiments looking at the vascular control by insulin may have great importance in elucidating the true behaviour of blood flow through muscle. Commonly, the euglycemic hyperinsulinemic clamp, where constant insulin infusion is coupled with variable glucose infusion to stabilise blood glucose levels, is used to assess insulin action within the body. Studies involving infusion of insulin affect the whole body and allow assessment of partial changes in blood flow within muscle, unlike studies utilising contraction to assess blood flow behaviour which is a more isolated effect and generally results in large changes in blood flow. Utilising techniques which assess capillary perfusion, rather than bulk flow, in insulin studies may be an effective way of gaining greater understanding of how insulin

is able to alter blood flow distribution within the tissue, an action that has been linked to increased glucoses uptake in human (38, 39) and rat (36, 40, 41) studies.

1.1.2.1 Techniques to measure capillary perfusion

A number of techniques exist to measure the change in total flow as well as capillary perfusion. Changes in bulk blood flow have been investigated using thermodilution (42, 43), dye dilution (44), plethysmography (45, 46), positron emission tomography combined with [^{15}O]H_2O (47), and 2D-ultrasound (48). However, these techniques only give an insight into the total amount of blood moving through the skeletal muscle tissue (total/bulk flow), via conducting and feed arteries, and not how that blood is distributed between capillaries. Importantly, there are a number of techniques which can be used to look at changes in microvascular perfusion alone (assessing the number of capillaries which are perfusion at any one time), independent of changes in bulk blood flow (48).

A commonly used technique to measure microvascular flow is laser Doppler Flowmetry (LDF). LDF is a measure sensitive to both the velocity and number of red blood cells (RBC) within the vasculature, with the resulting LDF signal (measured as flux) being proportional to the tissue perfusion (49). LDF probes can be placed onto the skin or into tissue and consist of fibre optic cables that direct a laser light (700-800nm) into the tissue. As the RBC move through vessels in the illuminated section of tissue they interact with the laser to create a scatter pattern with a frequency change according to the Doppler effect. Sensitive photo detectors in the collecting optic fibre of the LDF probe then measure the scattered light and frequency shift (50-52). The resulting signal gives an indication of the number and speed of RBCs in the tissue that is being illuminated by the laser. However, the use of LDF to assess capillary perfusion is limited by a number of factors. LDF is only able measure blood flow in the specific region of tissue illuminated by the laser, and as such cannot be used to determine whole tissue blood flow (49). The flow measured in the area illuminated may differ to that of other regions of the tissue. For example, through experimental observation Clark *et. al.* (24) propose that if the LDF probe is

placed in a section of the non-nutritive flow route, the flow rates indicated by LDF measurements will differ from the flow-rates in another region of muscle where the nutritive pathway predominates. Additionally, in the assessment of skeletal muscle flow, the inability of the LDF laser to penetrate beyond the skin and subcutaneous tissue (skin+SC) has limited its use in assessing blood flow within deeper tissues such as skeletal muscle. The problems with the power of the laser can be overcome by removing skin and other superficial tissues and placing the probe directly on the muscle, or more recently, using high power LDF probes that can potentially penetrate into the muscle when placed on the skin. Previous studies have generally focused upon the change in the averaged LDF signal value during interventions (53, 54). The average measure gives an overall indication of microvascular blood flow status of the tissue sampled and if blood flow may have become altered during disease, but not an in-depth assessment of underlying changes in blood flow function that may be occurring. To give a greater insight into the control of microvascular blood flow patterns and to identify what specific changes in microvascular blood flow behaviour may be occurring during diseases such as T2D, mathematical modelling can be applied to the LDF data to analyse different aspects of the signal. These include spectral analysis such as Fourier analysis or wavelet transformation which determine different frequencies in the signal (55-57) and complexity measures which assess the randomness of the LDF flux (58, 59).

Interestingly, recent advances in technology have produced combined LDF flux and tissue oxygenation probes (LDF + OXY probe), which can measure LDF flux, oxygen saturation (O_2 Sat) and total haemoglobin (tHb) concurrently at the same site. However, the different light sources for each measurement type may have different penetration into the tissue, as such these different measures are detecting blood flow in different volumes of tissue (60, 61). The oxygenation of tissue (O_2 Sat) and total number of RCB (tHb) can be measured and analysed in the same manner as LDF flux to give a more holistic assessment of microvascular perfusion. O_2 Sat and tHb measures are taken with white light spectroscopy, where oxygenated and deoxygenated haemoglobin absorb light at different

wavelengths, which is then detected by photosensors in the probe and recorded (62). Kuliga *et. al.* (63) validated the novel combined LDF flux and white light reflectance spectroscopy sensor probe. LDF + OXY measurement of forearm microvascular blood flow in healthy participants were assessed. The result showed that resting skin+SC O_2 Sat is independently associated with blood flow and skin temperature, with the relationship between blood flow and O_2 Sat best described by a one-phase association curve fit with a plateau in O_2 Sat of 84%. The study concluded that the tissue oxygenation measures are able to detect similar skin+SC microvascular blood flow as LDF flux, but through measurement of different parameters. The use of the combined LDF + OXY probe gives a platform for a more in-depth investigation of microvascular blood flow under different metabolic and disease conditions.

1-MX metabolism is a biochemical technique used to determine the microvascular perfusion in rat skeletal muscle (48). It has an advantage over LDF as it can assess whole tissue microvascular perfusion. This technique relies upon the presence of the enzyme xanthine oxidase (XO) on the surface of all capillaries in skeletal muscle tissue. XO can metabolise 1-MX into one product, 1-methylurate (1-MU). The difference between the amount of 1-MX infused into the rat skeletal muscle and the amount of 1-MU in the venous blood, measured by high performance liquid chromatography, gives an indication of microvascular perfusion. The 1-MX metabolism technique essentially looks at the total surface area of microvasculature within the muscle through which the blood passes. With greater microvascular perfusion, the blood is exposed to a greater surface area of the microvascular endothelium, and thereby greater metabolism of 1-MX occurs (48). Studies of 1-MX metabolism in the constant-flow perfusion hindlimb, where the perfusion rate was altered to give more or less total flow into the muscle, have shown that 1-MX metabolism is not significantly changed with changes in muscle flow rate, verifying that this technique is a measure of flow redistribution alone (5). There are, however, limitations to this technique, as it is an indirect measure of microvascular perfusion, and it also cannot be used in humans as the clearance of 1-MX across human skeletal muscle beds is

insufficient for the assay, due to inadequate levels of XO (64). Additionally, 1-MX metabolism cannot look at changes in microvascular perfusion in real time, only giving an average value for a time period (usually 60mins) (48). The 1-MX technique is therefore unsuitable for the assessment of flowmotion, which requires continuously collected data for spectral analysis.

Contrast enhanced ultrasound (CEU) is another means of measuring microvasculature blood flow. It has an advantage over 1-MX metabolism as it can monitor real time changes in microvascular responses in the tissue of both rats (40) and humans (65), however it is a more invasive measure as compared to surface LDF. CEU allows visualisation and quantification of blood flow through a specific tissue region of interest (ROI). Ultrasound uses sound waves to visualise regions of the body. Within a specific ROI, contrast agents (which are infused into circulation) can be visualised as each sound wave emitted from the transducer results in an acoustic signal produced by the contrast agent (66). Gas filled phospholipid bubbles, known as microbubbles, are commonly used as contrast agents in animal and human experiments. The phospholipid microbubbles are introduced into the vasculature via constant venous infusion and travel in the blood. They are on average 4μm in diameter, constraining them to the vasculature and allowing them to travel in a similar manner to RBC (67). The acoustic intensity (AI) of microbubbles that are within the microvasculature can be detected. The AI signal is proportional to the concentration of microbubbles within the ROI, therefore when the arterial concentration of microbubbles is constant the AI is related to the blood volume. By imaging a muscle and measuring its AI signal, an indication of blood volume can be determined. CEU is able to track changes in blood volume in real time, and can be used to detect differences in microvascular perfusion with different treatments. Vincent *et. al.* (41) showed total blood flow (measured with an ultrasonic flow probe placed around the femoral artery) and microvascular blood volume (measured by CEU), were monitored during a euglycemic hyperinsulinemic clamp with physiological levels of insulin (3mU/kg/min) in an anaesthetised rat hindlimb. There was a rapid increase (55% 5-10min into insulin infusion) in microvascular volume observed via CEU, which occurred without any significant change to

the total blood flow to the hindlimb. The observed increase in microvascular blood volume indicates that microvascular perfusion has been increased by insulin, independently of change in total blood flow to the hindlimb.

The minimally invasive nature of the LDF + OXY and CEU techniques is believed to more likely produce observations of true, non-artificial blood flow changes in muscle, thus eliminating any potential changes in blood flow that can be caused by experimental intervention. These techniques also allow the assessment of blood flow through the large load-bearing muscle which makes up the majority of skeletal muscle tissue in the body. An additional advantage is that blood flow analysis utilising these minimally invasive techniques can be performed in both animals (36, 48, 68) and humans (65), combined with measurements of total blood flow, allowing a more holistic assessment blood flow physiology.

Table 1.1: *Summary of microvascular blood flow techniques advantages and disadvantages*.

Technique	**Advantages**	**Disadvantages**
LDF + OXY	Real-time measurements Skin measures non-invasive and easy to perform RBC number and tissue oxygenation combined Animal and human applications LDF flux measures RBC number and velocity	Small tissue section Invasive to measure deeper tissues
1-MX	Whole tissue measurement Assessment of microvascular surface exposure Measure of flow redistribution alone	Cannot be used in humans Not real-time Indirect measure
CEU	Real-time measurements Animal and human applications Non-invasive to muscle Able to measure large load bearing muscles Large tissue sections Measure of microvascular blood volume alone	Contrast agent required

Techniques to assess muscle blood flow directly do also exist, but are inherently more invasive. Intravital microscopy is a common method used to directly observe many different biological functions *in vivo*, including blood flow in skeletal muscle tissue (69-71). Using this technique, muscle in a live sedated animal is surgically exposed, and a high resolution microscope is used to directly observe blood flow patterns in the muscle. Intravital microscopy is generally used to assess blood flow in thin, more specialised muscle, as they are more easily accessed (31). This is as opposed to the less invasive techniques, which can also assess bulk load-bearing muscle (32). The technique is advantageous as it allows for direct assessment of blood flow in the muscle tissues, however, the highly intrusive nature of this method could potentially result in unnatural alteration of blood flow in the muscle, and thereby not give a true representation of normal blood flow and distribution through the tissue. Additionally, due to the surgery required, intravital microscopy cannot be used to assess human muscle blood flow. The only assessable vascular beds for intravital microscopy in humans are the nail fold microvasculature (12), retinal (72) and oral mucosa (73); studies of blood flow in these tissues are unlikely to reflect muscle flow, which is the primary tissue of interest when assessing metabolism and vascular dysfunction during disease. Each method used to assess *in vivo* muscle blood flow has inherent flaws, and as such the use of multiple and different techniques may be the best approach to the assessment of skeletal muscle blood flow.

1.1.2.2 Alternative skeletal muscle blood flow hypotheses

In 1917 Krogh (74) first proposed the idea of capillary perfusion from observations made in experiments where dye was passed through muscle microvasculature. Krogh noted that not all capillaries in the tissue gave passage to the dye and hypothesised that in the vasculature there is a reserve of unperfused capillaries, a concept that is still believed to hold true by many microvascular researchers (5, 6, 75). However, there are other theories as to how blood flow acts and changes in skeletal muscle. Primarily it is the work and opinions of Poole *et. al.* (31) who disagree with the concept

of capillary recruitment and through their study of blood flow at rest and during contraction suggest an alternative hypothesis. Poole *et. al.* propose that instead of only a proportion of capillaries being perfused any one time during rest, all capillaries within a tissue support plasma flow and almost all RBC flux, at all times. It is proposed that the haematocrit in capillaries is altered upon changes in metabolic demand within the muscle tissue (from 15% to 45%) (31). The manner in which the different components of blood interact with the vessel wall is theorised to allow for this change in haematocrit. During rest molecules on the vessel wall interact and hold up RBC but not the plasma and upon stimulation by increased metabolic demand (i.e. exercise) the RBC are released and haematocrit subsequently increases. Additionally they propose that 'longitudinal recruitment' occurs where the capillaries extend in length upon increased metabolic demand, to increase surface area on which exchange can take place (31). Poole *et. al.* based their hypothesis upon studies mostly done using intravital microscopy of thin more specialised muscle which is observed at 'basal' and then under electrical stimulation to induce contraction (76). The manner of these studies highlights potential issues with the resulting hypothesis that RBC concentration increases in capillaries during contraction, not whole blood flow. It is likely that the invasive nature of the techniques itself used by Poole *et. al.* may result in capillary recruitment and that 'basal' measurements of capillary RBC content may not be accurate. Questions are also raised about how haematocrit is able to dynamically change in a closed system. Additionally, Poole *et. al.* focus upon changes which result from contraction and mention little about the changes induced by insulin – such as increased glucose uptake (which travels in the plasma) resulting from an increased capillary flow (6) – or vasomotion within muscle vasculature (77), two key processes in the overall behaviour of blood flow in skeletal muscle.

1.2 Vasomotion and flowmotion

Vasomotion is the rhythmic oscillation of vasculature diameter (7, 8, 78) which occurs in many, if not all, tissues throughout the body (10). The consequence of vasomotion is oscillations of flow into or

within tissues; flowmotion (9). Vasomotion and the subsequent flowmotion which occurs are thought to be an important component in the distribution of blood flow within tissues such as muscle and skin+SC. Vasomotion was first described over 150 years ago by Jones (1852) (79), who observed rhythmical changes in vessel diameter in bat wings. Many *in vivo* and *in vitro* studies have since reported the presence of vasomotion (80). Studies of vasomotion and flowmotion have been conducted upon a number of different tissues including the testes (81), mesenteric vasculature (11), skin (82) and skeletal muscle (57), indicating a widespread occurrence throughout the body. Vasomotion is thought to be generated locally from within the vascular wall, not from systemic mediators such as heart beat, respiration or nervous system input; though synchronisation of vasomotion has been reported to occur through neurogenic input (83, 84). Studies by Colantuoni *et. al.* (85-88) using the hamster skin-fold window preparations show that the frequency of vasomotion is greater in smaller arteries, thus terminal arterioles have higher occurrence of vasomotion when compared to higher order arterioles. Additionally, experimental conditions may affect the study of vasomotion with varied reports of the presence of vasomotion in animals observed during rest, both with or without anaesthetic (10). Importantly, in human studies the presence of vasomotion and flowmotion has consistently been observed during and without anaesthesia (82, 89, 90). The study of vasomotion since its discovery in 1852, has been difficult due to the limited techniques with the appropriate sensitivity available to observe and measure vasomotion. There are two fundamental questions regarding vasomotion which are yet to be fully answered. 1) What are the cellular mechanisms that produce vasomotion and 2) what is the physiological role of vasomotion?

The physiological consequence of vasomotion, flowmotion, is in contrast relatively easy to detect and has been assessed using techniques such as oxygen tension measures, local blood pressure measures, and LDF (81, 90-93). Importantly, flowmotion is not only controlled by vasomotion but is also influenced by the central factors; cardiac, respiratory and neurological activity. Five different oscillation frequencies (between 0.0095 and 1.6Hz) are present in human flowmotion measures (55).

These distinct frequencies correspond to the above factors (10, 11, 94) and have been identified *in vivo* using LDF (90, 91, 95-98), oxygen tension measures (99) and through direct observation (92, 100). Two of the oscillating bands occur at higher frequency and originate from cardiac (0.4-1.6Hz) and respiratory (0.15-0.4Hz) input (the range of these frequencies are increased in rats due to higher respiratory and heart rates). The other three factors are present at lower frequencies and through pharmaceutical intervention it has been established that the mechanistic backgrounds for each is intrinsic smooth muscle activity (myogenic, 0.06-0.15Hz), nervous system input (neurogenic, 0.02-0.06Hz) and vascular endothelium (endothelial, 0.0095-0.02Hz) (55, 94). Studies *in vitro* looking at vasomotion in isolated small arteries suggests that the myogenic frequency of flowmotion at 0.06-0.15Hz seen *in vivo* is due to vasomotion (11). It is also thought that the endothelium has a role in the control of vasomotion as vessels stripped of their endothelial layer show an inhibition of vasomotion that can be rescued by application of endothelial derived agents such as nitric oxide (NO) (10).

1.2.1 *In vivo* measurement of flowmotion

In the 1990's Stefanovska *et. al*. (55, 56, 96) showed that the contribution of different frequency components of flowmotion could be revealed by mathematically transforming skin+SC LDF flux data with spectral analysis. The presence and relative input of each of the five factors influencing flowmotion can be determined by performing the mathematical transformation on raw LDF data. Spectral analysis applies a mathematical equation to the LDF data, which is expressed as perfusion units (PU) verses time, and transforms the data into average wavelet transformation (PU) verses frequency (Hz) (101, 102). LDF is unable to measure blood flow in absolute perfusion values, the PU measurements are therefore an arbitrary, relative measure of flux. It is therefore essential that LDF probes are correctly calibrated before measures are taken to enable comparison of results. A peak representing each of the five influencing factors is then able to be identified. Fast Fourier analysis and wavelet transformation are two forms of spectral analysis that can be used to analyse the LDF flux

data. Wavelet transformation is considered advantageous over fast Fourier analysis as it allows a more precise determination of the lower frequency components of a signal (103). As described by Stefanovska *et al*. (55), wavelet transformation also takes time into consideration, producing a 3D output with wavelet transformation, frequency and time considered (Figure 1.2A). The temporal information provided by performing a wavelet transformation indicates the variance of the signal and how often a modulating factor exerts its influence over blood flow. For example, the endothelial component which influences blood flow at a lower frequency has a great variation over time as the oscillating signal only occurs at 50-105 second intervals. The cardiac component however, exerts its influence at a much higher frequency, therefore there is less variation as the oscillations occur at 0.6-2.5 seconds. In most biological circumstances, the wavelet transformation is averaged over time to give a 2D measure of wavelet transformation against frequency (Figure 1.2B), allowing easier handling and interpretation of the complex data. The averaging of wavelet transformation data over time for the interpretation of flowmotion patterns results in the loss of temporal information. In the context of the data described in this thesis, the temporal data is only of importance in the consideration of the time period on which the wavelet transformation is performed. To adequately measure the influence of the lower frequency components on flowmotion longer periods of time (20min or more) need to be used to overcome the variance in the signal and obtain an accurate reading of the endothelial influence on flowmotion.

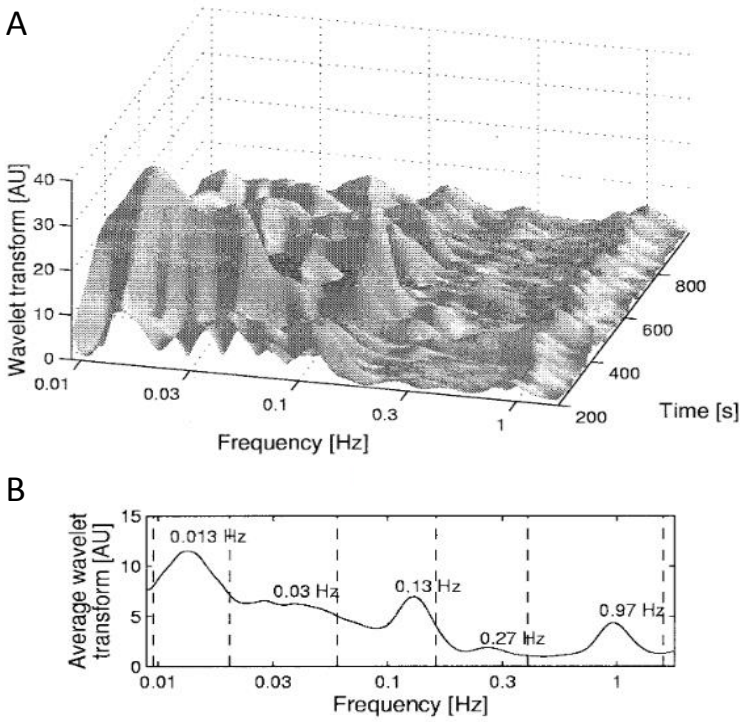

Figure 1.2: *Wavelet transformation of human skin LDF signal*. Figure taken from Stefanovska *et al*. (55) (Figure 2) demonstrates the A) 3D output of wavelet transformation where average transformation (Z axis), frequency (X axis) and time (Y axis) are all taken into consideration. Data is averaged over time to give B) 2D average wavelet transformation against frequency for easier interpretation of data.

By applying a normalisation calculation to the average wavelet transform values – achieved from wavelet transformation of LDF flux data – the relative contribution of each frequency to flowmotion can be established. A calculation to establish the relative contribution of each frequency allows the changes in flowmotion that are induced by interventions such as insulin infusion to be established.

Wavelet transformation of LDF flux data provides an effective means of determining overall flowmotion patterns and the contribution of each frequency component within this. However, the use of LDF flux to assess flowmotion is limited in that it can only assess blood flow in one small section of a tissue. Flowmotion is the oscillation of flow across a whole tissue and it may be blood flow in different sections of the same tissue differ. LDF does not allow adequate investigation into the idea of varied flow distribution across a tissue. To overcome this limitation, the same analysis technique (wavelet transformation) could be applied to blood flow measurement techniques that assess flow

over larger regions of tissue (i.e. CEU), which can be performed on both animal models and human subjects.

In order to understand and interpret changes in flowmotion observed by wavelet transformation; it is first important to understand the cellular mechanisms through which flowmotion is controlled.

1.2.2 Cellular mechanism of vasomotion

1.2.2.1 Myogenic input

The myogenic input is often itself called vasomotion as it is the intrinsic contraction within the vessel smooth muscle per se. The cellular mechanisms in the smooth muscle which bring about vasomotion and the mediators which induce these mechanisms have been previously investigated, but are still not fully understood. The majority of investigations into the mechanism of vasomotion have been done with intravital microscopy and isolated larger arteries using various agonists and inhibitors of vasomotion (reviewed by Aalkjaer and Nilsson in (10, 11)). It is thought that two important processes induce vasomotion in arteries; firstly, generation of Ca^{2+}-dependent oscillators within smooth muscle cells, which induces cellular depolarisation and secondly, synchronisation of that depolarisation between the smooth muscle cells (10). Oscillators within the smooth muscles cells are thought to be generated from cytosolic and membrane actions (80, 104). Vasomotion is thought to be initiated by release of cellular stores of Ca^{2+} (from sarcoplasmic reticulum) into the cytosol by cytosolic oscillators (105, 106). Vasomotion is only established when intercellular Ca^{2+} release is formed into synchronised waves (106-108). Prominent vasomotion researchers Aalkjaer and Nilsson hypothesise that the membrane oscillators induce the intracellular synchronisation (109-111). The waves of Ca^{2+} within the smooth muscle cells are believed to induce activation of many Ca^{2+}-dependent membrane bound ion channels such as Cl^- and K^+ channels (112-115). Activation of these membrane channels is believed to induce the depolarisation of smooth muscle cells responsible for vasomotion activation (106). A study

by Bartlett *et. al.* (116) showed an abolishment of vasomotion in hamster cheek vasculature upon blockade of K^+ channels, indicating the importance of membrane K^+ channels in the activation of vasomotion through cellular depolarisation. It is proposed that in order for vasomotion to occur in a whole vessels, a synchronisation of the oscillating depolarisation between smooth muscle cells is required (10). The depolarisation initiated through generation of Ca^{2+} waves within cells can be propagated to the surrounding smooth muscle myocytes via gap junctions, forming an electrical signal (reviewed in (10)). Through the gap junction mediated synchronisation of cellular depolarisation, vasomotion in a vessel is believed to occur. Matchkov *et. al.* (117) used gap junction inhibitors on isolated rat mesenteric arteries to show a desynchronisation of membrane potential oscillations between vessel smooth muscle cells, which resulted in an inhibition of vasomotion. The desynchronisation of membrane potential oscillations was shown to occur without effecting Ca^{2+} waves within individual smooth muscle cells of the isolated arteries, indicating an inhibition in the synchronisation required to produce vasomotion, not the cellular mechanism involved. The observations by Matchkov *et. al.* (117) has been repeated in other studies which utilise gap junction inhibitors (117-120). These studies have formed the idea that gap junction mediated synchronisation of the Ca^{2+}-dependant depolarisation is essential for induction of vasomotion in a vessel. While there are many studies outlining the possible mechanisms through which vasomotion occurs, the question of what induces these actions within the smooth muscle cells to bring about vessel vasomotion still remains and requires a great deal of further investigation.

1.2.2.2 Neurogenic input

Neurogenic input to flowmotion is primarily generated centrally in the brain, constantly outputting signal to cause vasoconstriction in the smooth muscle of vessel in order to maintain a balanced vascular tone (121). However, the effector of this process, noradrenaline (NA), acts locally at the tissue site to induce vasoconstriction. Using skin LDF measures, Kastrup *et. al.* (122) demonstrated with denervation studies that the neurogenic component of flowmotion exerts its control at a frequency

of about 0.04Hz. Neurogenic input to the skin was removed after both local and ganglionic nerve block and after a sympathectomy. The control of vasoconstriction by the neurogenic input periodically modulates the vascular tone of vessels and thereby influences vasomotion patterns. NA is released by the axons of nerves, which then binds to and activates alpha1-adrenoceptors on the vessel smooth muscle to result in increased intracellular Ca^{2+}. Increases in intracellular Ca^{2+} causes contraction of the myocytes and thereby vasoconstriction (123, 124). Under basal situations, neurogenic input to vascular smooth muscle is constant to produce a basal level of vasoconstriction in order to maintain normal blood pressure (121). However, neurogenic control can be more complicated and response to neurogenic input can vary at different vascular sites (26), likely due to the varied presence of alpha2-adrenoceptors on vascular pre-synaptic neurons. Alpha2-adrenoceptors modulate alpha1-adrenoceptors mediated vasodilation through the inhibition of NA release into the synapses, thereby inhibiting neurogenic mediated vasodilation (125). It is worth noting that NA can also be released from the adrenal gland into circulation as a stress response (126), which may then influence the neurogenic component of flowmotion.

1.2.2.3 Endothelial input

In addition to smooth muscle cell mechanisms, the endothelium is thought to be of great importance in the generation of vasomotion (11). Jackson *et. al.* (127) used α1-adrenergic agonists to stimulate vasomotion in isolated hamster aortas. This rhythmic activity was not simulated in vessels where the endothelium had been removed. Jackson *et. al.* (127) concluded that localised mechanisms within the endothelium were influencing and controlling the generation of vasomotion in the vessel smooth muscle. To establish the frequency at which the endothelial component of flowmotion exerts its effect, Kvernmo *et. al.* (128) performed wavelet transformation analysis of skin LDF measures during basal, endothelial-dependent (acetylcholine) and endothelial-independent (sodium nitroprusside) stimulation of vasodilation. During endothelial-dependent vasodilation there was a significant increase in the contribution of the frequency component at 0.01Hz, indicating that it is at this low

frequency that the endothelial input exerts control over flowmotion. Several different endothelium-derived molecules have been suggested to be important for the activation of vasomotion. Restoration of vasomotion in hamster aorta stripped of the endothelial layer by sodium nitroprusside (SNP) and cyclic GMP (cGMP) has also been observed by Jackson *et. al.* (129). The ability of SNP and cGMP analogues to recovery oscillatory behaviour when vessel endothelium is removed suggests that the nitric oxide (NO) system (which is initiated in the endothelium) may play an important role in vasomotion generation. In another study by Gustafsson *et. al.* (130) isolated rat mesenteric arterioles and stripped the endothelial cells, resulting in an inhibition of vasomotion, which was then restored with the addition of the NO donor SNP and a cyclic GMP (cGMP) analogue. Additionally, high concentrations of cGMP introduced to smooth muscle in the absence of vessel endothelial cells has been shown to induce synchronisation of Ca^{2+} waves (106, 131). It appears that NO-mediated process are important in vasomotion, but other factors such as endothelium-derived hyperpolarising factor (EDHF) are thought to also play a role (132). Both NO and EDHF have been shown to modulate Ca^{2+} release in vascular smooth muscle cells (104). The release and synchronisation of Ca^{2+} is proposed to be the mechanism by which vasomotion is generated (10), thereby providing a mechanistic link for the endothelial modulation of flowmotion. The perceived importance of NO-mediated pathways in vasomotion is perhaps an important point in understanding the physiological role of vasomotion. Insulin induces NO production in vessel endothelium (133), and it has been shown that insulin induces vasomotion (57). It is thought that there is a link between insulin-mediated vasomotion and redistribution of blood flow within skeletal muscle tissue. In the current thesis, the relationship between insulin and flowmotion will be studied more extensively in an attempt to better understand the physiological role of vasomotion and flowmotion.

1.3 Insulin-mediated changes to skeletal muscle haemodynamics and their effect on metabolism

1.3.1 Insulin-mediated changes in blood flow

The vasoactivity of insulin was first described in 1939 when schizophrenic patients were treated with large doses of insulin (134). A bolus dose of 40-280U of insulin resulted in bulk increases in blood flow to the leg, forearm and hand. The ability of insulin to increase bulk blood flow to skeletal muscle has been reported in some subsequent studies (43, 45, 48, 135), but others studies have shown no change (136-139). Differences in the outcomes of total flow studies are not only attributed to the techniques used, but to the varied concentration of insulin employed in each case. At a relatively low dose (75mU/mL) Kelley *et. al.* (137) failed to see any increase in total blood flow to the leg. However, Laakso et. al. (43) using a euglycemic hyperinsulinemic clamp, found changes in total leg blood flow were related to insulin dose. The study used a ramped protocol in which insulin was infused at 10mU/m^2/min increasing to 600mU/m^2/min and found total leg blood flow increased in a graded fashion relating to the insulin infusion. In addition to the changes in total flow, studies in humans (65) and rats (41, 48, 140) exploring insulin mediated distribution of blood within the skeletal muscle capillary beds have shown that insulin causes an increase in capillary perfusion. Insulin promotes capillary recruitment through the redistribution of blood flow amongst a greater number of capillaries, even at lower physiological doses, prior to any changes in whole-limb flow (36). Changes in microvascular perfusion, leading to enhanced glucose uptake occur primarily via insulin binding to the endothelial cells of the arterioles, as opposed to acting upon the smooth muscle cells that surround the vessel. Insulin signalling results in activation of several different pathways in the microvasculature to alter the tone of vessels, mediating both vasodilation and vasoconstriction, with the overall vascular tone achieved resulting from a balance of these two actions (Figure 1.3).

Insulin mediates vasodilation of arterioles by inhibiting vasoconstriction in vessel smooth muscle cells. Insulin-mediated vasodilation of the terminal arterioles is believed to induce microvascular recruitment (6). Binding of the insulin receptor on the endothelial cells leads to phosphorylation – therefore activation of – the endothelial form of the NO synthase (eNOS) via the phosphoinositide 3-kinase (PI3K) pathway (140-142); resulting in NO production in the endothelial cells (Figure 1.3) (143). NO then diffuses into the surrounding smooth muscle, where it binds to and activates the enzyme guanylate cyclase (GC). Activation of GC leads to increased production of cGMP within the smooth muscle cells (144, 145) and allosteric activation of protein kinase G (PKG), which in turn causes vasodilation of the vascular smooth muscle cells. PKG inhibits the actions of vasoconstrictors by removing calcium from the cytosol and de-phosphorylating myosin light kinase (146-149), thus preventing contraction and producing relaxation.

As can be seen in Figure 1.3, insulin binding to the receptor on endothelial cells also induces an endothelin-1 (ET-1) dependent vasoconstriction (150, 151). Activation of insulin receptors on an endothelial cell results in activation of the MAP-Kinase (MAPK) signalling pathway in addition the activation of the PI3K pathway (152). Activation of the MAPK pathway stimulates the release of the powerful vasoconstrictor ET-1 (153). The activation of ET-1 in addition to NO by insulin is important in the regulation of skeletal muscle vascular tone, ensuring a correct balance is maintained. In healthy individuals insulin stimulation results in controlled vasodilation (133).

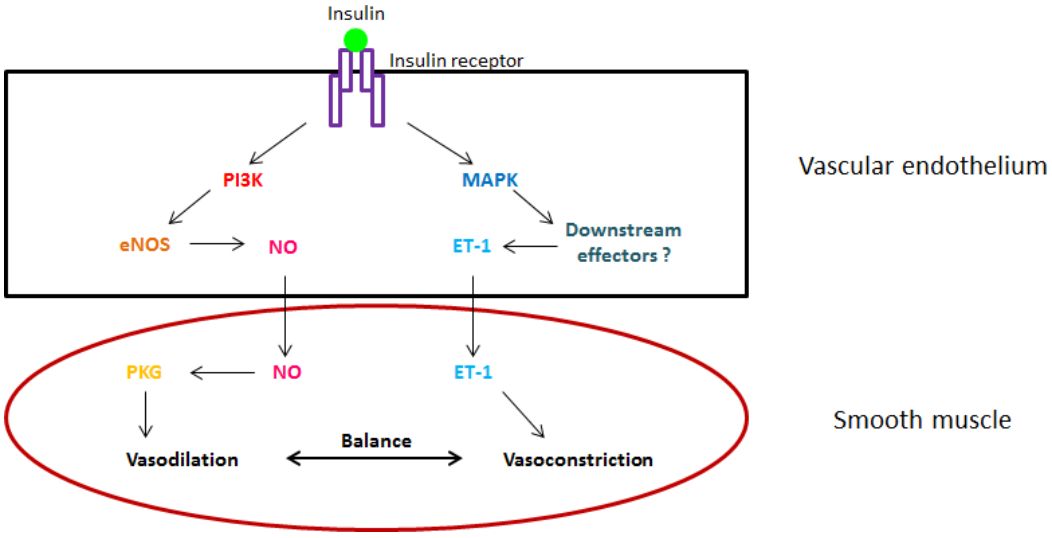

Figure 1.3: *Comparison of endothelial insulin-mediated vascular responses.* Insulin induces two different pathways which effect vascular tone. The **PI3K** pathway leads to **NO**-mediated vasodilation. Activation of the **MAPK** pathway leads to **ET-1** –mediated vasoconstriction. Overall vasculature tone results from the balances between the two pathways. Adapted from Kim *et. al.* (152).

Additionally, insulin is known to activate the sympathetic nervous system (SNS) (reviewed in (154)). In healthy participants physiological concentrations of insulin have been shown to increase venous catecholamine levels and sympathetic nerve activity (155-157). Activation of the SNS generally leads to vasoconstriction, which is thought to oppose insulin-mediated NO vasodilation (158). There is however, evidence of varied responses to insulin by different vessels based on their position on the vascular tree (6, 159). With elevated SNS activity, distal arterioles have been shown to vasodilate in response to insulin, whereas proximal arterioles have been shown to vasoconstrict (160). However, other studies have shown that SNS activity is not involved in insulin-mediated vasodilation (161). It is clear that the vasoactive interaction between insulin and the SNS is complex and it maybe that different levels and regions of the vasculature controlled by the SNS respond separately to insulin, thereby potentially altering the overall outcome of insulin stimulation at different sights in the vasculature.

1.3.2 Insulin-mediated skeletal muscle glucose uptake

Insulin promotes removal of glucose from the blood in order for it to be stored as glycogen within skeletal muscle (162). The importance of skeletal muscle as a target tissue can be seen after a meal, where 65-90% of the glucose ingested is stored as glycogen in the skeletal muscle myocytes (162-164). Bergman *et. al.* (165, 166) hypothesize that insulin delivery to the skeletal muscle interstitium is the rate-limiting step in insulin-stimulated glucose uptake by skeletal muscle. Actions of insulin on both the myocyte cells themselves and the surrounding vasculature are important in efficient uptake of glucose by the muscle.

Binding of the insulin receptor on myocytes induces the PI3K signalling pathway to translocate vesicle bound glucose transporters (GLUT4) to the cell membrane where they become active (140, 141, 167), thereby allowing increased glucose uptake from the blood into cells. As discussed, in addition to the changes insulin induces within the myocyte cells, insulin is able to elicit vasodilation in the skeletal muscle microvasculature; a process that plays an important role in the overall ability of the tissue to take up glucose. Insulin stimulation induces balanced vasodilation the terminal arterioles, which leads to microvascular recruitment and therefore an enhanced flow of blood to the myocytes (36, 168, 169). It is thought that insulin stimulation increases blood flow into the nutritive pathway (5). With greater blood flow to the myocyte cells there is a greater surface area by which insulin and glucose are exposed in the skeletal muscle tissue. Greater exposure of insulin and glucose to myocytes enhances GLUT4 translocation by insulin and thereby allows greater uptake of the increased amounts of glucose exposed to the cells (reviewed in (6)). An *in vivo* rat hindlimb study by Vincent *et. al.* (40) where NO production was inhibited by L-arginine methyl ester (L-NAME) during a euglycemic hyperinsulinemic clamp (10mU/kg/min) showed a 40% reduction in glucose uptake induced by insulin in the skeletal muscle tissue. The 40% reduction in glucose uptake was attributed to the reduction in capillary perfusion and total blood flow that was observed. The decrease in glucose uptake with L-NAME

infusion was thought to be because the inhibition of NO-mediated vasodilation decreased blood flow to the myocytes and therefore less glucose and insulin exposure to the muscle cells, resulting in the reduced glucose uptake seen. Other studies inhibiting NO production during insulin infusion in animals (170) and humans (171) have also shown similar results, indicating the importance of insulin-mediated vasodilation upon normal glucose uptake into skeletal muscle. It is currently unknown whether flowmotion in skeletal muscle plays an important role in regulating the glucose uptake in this tissue.

1.3.4 Insulin resistance and microvascular dysfunction

Insulin resistance is a state where cells in the body become less sensitive to insulin. Insulin resistance over a prolonged time period is causative of T2D. There are a number of factors that lead to the development of insulin resistance, most relate to the weight status of the individual (172). Currently the most accepted theories indicate that inhibition of the PI3K insulin signalling pathways by aberrant lipid storage in muscle (133, 173, 174), and in later stages markers of low-grade inflammation (175-177), result in cellular insulin resistance and therefore in a failure of glucose uptake by skeletal muscle cells (178). The resulting insulin resistance from inhibition of the insulin signalling pathway causes an attenuation in normal glucose metabolism in skeletal muscle (affecting both myocytes and the vasculature), and other insulin-dependent tissues such as liver and adipose cells. The result is a decrease in glucose disposal resulting in hyperglycaemia as less glucose is taken up into the skeletal muscle cells. Greater insulin concentrations are therefore required to achieve normal glucose uptake (179). In humans with T2D (180) and models of insulin resistance such as the obese Zucker rats (181), insulin resistance in skeletal muscle is associated with a failure of myocytes to take up glucose and an inability to adequately deliver glucose to the cells (182-184).

As insulin resistance is thought to result from an inhibition in the PI3K signalling pathway, it impacts not only on GLUT4 translocation in myocytes, but also upon insulin-mediated vasodilation in the arterioles, which is believed to result in microvascular dysfunction. A study by Cusi et. al. (185) performed euglycemic hyperinsulinemic clamps in healthy and type two diabetic patients. Muscle biopsies before, during and after the clamp where taken to determine activation levels of the PI3K and MAPK pathways. They found a significant decrease in the phosphorylation (therefore activation) of the PI3K pathway in T2D in response to insulin, without any change in activation of the MAPK pathway. In insulin resistance it is thought that the PI3K pathway is no longer able to induce adequate release of NO in the vasculature, but the MAPK pathway is unaffected and ET-1 production still occurs (reviewed in (152)). Indeed, some studies have found an increase in ET-1 in the vasculature and have proposed that markers of low grade inflammation, which occurs in later stages of insulin resistance, may be responsible for increased production (186, 187). The net result is an aberrant vasoconstriction of the microvasculature, which impedes blood flow to the myocytes and glucose uptake is consequently attenuated (75, 151, 152, 188). In anaesthetised rat studies where acute insulin resistance was induced by infusion of TNF-α (184) or free fatty acids (189), glucose uptake was reduced by 50% and 69% respectively, while NO-mediated vasodilation was impaired and capillary recruitment was shown to be attenuated. As previously described, the Vincent *et. al.* (40) study where NO production was blocked with L-NAME during an euglycemic hyperinsulinemic clamp (10mU/kg/min) reported a reduction in microvascular recruitment and a 40% reduction in glucose uptake. Even though the decrease in glucose uptake is varied in these studies, it is clear that normal vasculature function is important in the overall glucose uptake of skeletal muscle and this is attenuated in insulin resistance. Additionally, a reduced production and response to NO has been reported in insulin resistance (190) and T2D (191). In obese Zucker (192, 193) and high fat fed (194) rats, insulin-mediated microvascular recruitment has been shown to be impaired. Premilovac *et. al.* (194) studied high fat fed rats and compared their microvascular recruitment during a euglycemic hyperinsulinemic clamp with lean animals. Using the 1-MX technique Premilovac *et. al.* (194) showed 32% decrease in 1-MX

metabolism in the high fat animals as compared to the lean animals. The observed decrease in the insulin-mediated microvascular perfusion in the high fat feed animals was accompanied by a reduction in insulin-mediated skeletal muscle glucose uptake. There is significant evidence to suggest that microvascular dysfunction occurs in insulin resistance and T2D (reviewed in (133, 195)) and that it is involved in the attenuation of skeletal muscle glucose uptake seen in these conditions. In addition to insulin resistance causing vascular dysfunction in T2D other pathological changes in the disease also impact of vascular function. Capillary density and morphology become pathologically altered throughout the progression of T2D, leading to reduced capillary perfusion in key tissues such as skeletal muscle (196). A study by Barchetta *et. al.* (197) directly examining nailfold capillaries using videocapillaroscopy in healthy controls and participants with either type 1 or 2 diabetes mellitus, observed decreased capillary length, reduced and irregular capillary density and abnormal capillary morphology in the diabetic participants. Autonomic dysfunction is known to occur in T2D (198, 199), which results in increased neurogenic input to the vasculature and thereby an aberrant vasoconstrictive state, in addition to attenuation of insulin-mediated vasodilation. The result is a reduction in blood flow in key tissues such as skeletal muscle and thus an attenuation in skeletal muscle glucose uptake. Obesity and T2D are also commonly associated with increased cardiac output and respiratory rate due to pathological changes to the vasculature (200). Of particular interest in this thesis, is the observation of flowmotion dysfunction, altered contributions of the frequency components, in insulin resistance and T2D (reviewed in (10)). It is likely that in addition to the overall changes in vascular function seen in insulin resistance and T2D, changes to flowmotion may also be contributing to the metabolic dysfunction seen in these disease sates.

The pathological changes that occur to the vasculature in T2D are extremely important in the progression of the disease over time and development of the adverse health outcomes associated with the disease such as retinopathy, neuropathy, nephropathy and increased risk of acute myocardial infarction and stroke (201). It is therefore important to minimise the progression of these

cardiovascular complications. While most of the anti-diabetic medications focus on increasing insulin production in the beta cells and insulin sensitivity in peripheral cells (202), improvements in cardiovascular function can be achieved through exercise intervention (203). Resistance training (RT) is one form of exercise that has been shown to improve several cardiovascular functions and risk factors including arterial stiffness (204), lipid profile (205), visceral adiposity (206), HbA1c control and insulin sensitivity (207). Importantly for the current studies, RT also improves endothelial function in both healthy (208, 209) and disease states (210, 211), in particular endothelial function has been shown to be improved with RT in T2D (212). The prevailing theory on how endothelial function is improved with RT is that with the continual enhanced shear stress placed on the endothelial cells during RT, NO-mediated vasodilation mechanisms are enhanced and the bioavailability of NO (213), through such mechanisms as upregulated eNOS expression (214) , is subsequently increased. The improvement of endothelial function with RT is of particular interest in the current thesis as little is known about the effect RT has upon microvascular flowmotion, and more particularly if it can be improved with training in type 2 diabetes. The improvement in endothelial function with RT in T2D may potentially also improve microvascular flowmotion.

1.3.5 Flowmotion: Insulin-mediated changes and dysfunction in insulin resistance and T2D

Alterations to flowmotion have been observed with the development of insulin resistance and T2D; shown in studies of acute vasoconstriction in *in vivo* rat skeletal muscle (57), as well as in skin+SC of obese (215, 216) and T2D (217, 218) populations. Investigation into flowmotion dysfunction in insulin resistance has primarily been determined with spectral analysis of skin+SC LDF measures and aberrant changes in a number of the different component frequencies have been observed. In a study by de Jongh *et. al.* (219) blood flow in the skin+SC was measured by LDF on healthy and obese female subjects, with and without the introduction of insulin through iontophoresis. Total LDF flux was assessed to determine blood flow and spectral analysis was performed on the LDF data to give a measure of flowmotion. Local administration of insulin to the skin+SC (iontophoresis) produced a

vasodilatory response in the healthy women, but not in the obese. In the basal state, flowmotion as a whole (the contribution of the total frequency spectrum) as well as the endothelial and neurogenic activity of flowmotion was lower in the obese subjects. The authors surmised that obesity involves an impaired microvascular vasodilatory effects and decrease in skin+SC microvasculature flowmotion. A study by Montero *et. al.* (216) comparing lean and severely obese adolescent participants, also using insulin iontophoresis and LDF flux measures, showed a reduction in insulin-induced myogenic activity in the obese individuals. The authors suggested dysfunction in the myogenic response to insulin may be an early step in the development of insulin resistance and T2D. Studies describing disruption of vascular smooth muscle Ca^{2+} release and signalling resulting from hyperglycaemia (220) and in an obese rat model (104) support the idea that the myogenic component of flowmotion (vasomotion) is disrupted in the development of T2D. Another study by Clough *et. al.* (215) measuring skin+SC flowmotion with LDF flux in participants with central obesity, showed an increased neurogenic input during a euglycemic hyperinsulinemic clamp as compared to previously reported healthy participants. Furthermore, an association study by de Boer *et. al.* (221) showed an inverse relationship between BMI and normalised neurogenic component of flowmotion. Additionally, the cardiac component of flowmotion was positively associated with BMI. These studies show a link between an obese state, which is known to be causative of insulin resistance, and changes in flowmotion patterns and contribution. The results are quite varied based on the technique and participant populations, highlighting the need for further study into the area to elucidate what changes in flowmotion may be occurring in different stages of disease progression.

Flowmotion studies in patients with clinically diagnosed type 2 diabetics show similar dysfunction in flowmotion frequency components. Most studies in this area focus on patients with clinically diagnosed T2D at the later stages of disease progression when complications such as neuropathy and retinopathy have manifested. Studies by Sun *et. al.* (217, 218) investigating flowmotion dysfunction in T2D patients with various severity of neuropathy, show changes (decreased input) in the endothelial

and neurogenic components of flowmotion in the early stages of neuropathy development. The two studies indicate dysfunction in these frequency components may be causative of disease development. These studies measured skin+SC flowmotion with LDF flux on the foot of participants, but skin+SC LDF measures are not the only means to investigate changes in flowmotion that occur in T2D. A study by Bek et. al. (72) examined changes in retinal arteriole flowmotion over 180seconds by applying spectral analysis to video recordings of vasomotion activity in healthy controls and T2D with increasing severity of retinopathy. The study found a significant reduction in spontaneous high frequency oscillations (attributed to changes to cardiac function) and noted a reduction in overall frequencies with increasing severity of disease. Studying the changes in flowmotion at different stages of disease development, from insulin resistance through to severe microvascular disease state such as retinopathy, nephropathy and neuropathy, in a number of different tissue types may greatly enhance knowledge about how T2D develops and progresses over time.

A key tissue in the development of T2D is skeletal muscle, but due to technique difficulties there are a limited number of studies on skeletal muscle flowmotion in insulin resistances states. A previous study by Newman *et. al.* (57) on flowmotion in anesthetised rat skeletal muscle during a 10mU/min/kg euglycemic hyperinsulinemic clamp found (using LDF wavelet transformation from an implanted probe) an increase in the myogenic component (vasomotion) of flowmotion. Newman *et. al*. (57) then induced an acute state of insulin resistance with the peripheral vasoconstrictor α-methylserotonin and found a reduction in insulin-mediated glucose uptake and blockade of the myogenic component of flowmotion. The authors suggested that insulin-mediated microvascular recruitment may in part involve action on the vasculature smooth muscle to increase vasomotion, thereby enhancing capillary perfusion and glucose uptake. A concept supported by the evidence for NO-dependent endothelial mediated control of vasomotion.

The numerous changes in overall flowmotion as well as input from the individual frequency components is widely reported in abhorrent disease states such as insulin resistance and T2D. These changes may contribute to the development of disease and advancement of adverse outcomes. However, the results are varied based upon the tissue type and technique used, highlighting a need to better define changes that occur over the progression of disease. Importantly, the actions of flowmotion in tissues such as skeletal muscle may play an important role in normal glucose metabolism and thus dysfunction could play a role in early disease progression. A study by de Boer *et. al.* (12) on healthy individuals concurrently measuring skin+SC microvascular flowmotion and capillary perfusion in the nailfold during a euglycemic hyperinsulinemia clamp, showed an increase in normalised neurogenic input was associated with increased capillary perfusion, with both increases also associated with enhanced glucose uptake. The study concluded that lower insulin-mediated capillary recruitment and glucose uptake was associated with a decreased in neurogenic input during infusion of physiological levels of insulin (1mU/kg/min clamp). This study thereby indicates the potential importance in insulin-mediated changes in flowmotion. However, as the study was performed in skin+SC and nailfold, thus the translation of these results to the more metabolically important tissue of skeletal muscle is yet to be investigated.

1.4 Summary of study aims: characterisation of flowmotion

As previously discussed, vasomotion and the other factors that influence flowmotion are thought to regulate blood flow distribution in skin+SC and skeletal muscle. Dysregulation of blood flow patterns is believed to contribute to the development T2D and the adverse health outcomes associated with this disease such as neuropathy, retinopathy and nephropathy. Further studies into the basic control of flowmotion, particularly by the lower frequency mediators (endothelial, neurogenic and myogenic), is still required to better understand its function. Developing understanding of insulin-mediated changes to flowmotion is of particular interest in this thesis. It is thought that insulin alters vasomotion in terminal arterioles to induce flow redistribution, between non-nutritive and nutritive flow routes.

A more in-depth understanding of how insulin mediates changes into microvascular distribution and how this may be altered in pathological states, such as insulin resistance and T2D, would give further insight into how changes in blood flow are able to regulate glucose metabolism in skeletal muscle.

In the current study the techniques of LDF flux, tissue oxygenation and CEU were used to investigate flowmotion function both clinically, comparing healthy and type 2 diabetic participants, as well as in an *in vivo* anaesthetised rat model. The overarching hypothesis of this thesis is that flowmotion is important for normal metabolic activity in a tissue, and therefore as a corollary, that vascular dysfunction will lead to impaired flowmotion. In this thesis there are a number of sub-hypothesis and aims to address this overall idea of flowmotion.

1.4.1 Clinical hypothesis and aims

Cardiac, respiratory, autonomic and endothelial dysfunction often occur in people with T2D. Therefore, it is hypothesised that people with T2D will have identifiable changes in these components of flowmotion compared to healthy controls.

> **Aim 1:** To determine whether differences occur in skin+SC flowmotion at rest between healthy controls and type 2 diabetics.

Insulin is a vasomodulator that acts on the endothelium and the sympathetic nervous system. Therefore, it is hypothesised that insulin modifies blood flow patterns by altering flowmotion, and this process is dysregulated during states of insulin resistance such as T2D.

> **Aim 2:** To determine whether skin+SC flowmotion increases in response to oral glucose challenge (OGC) in healthy controls and type 2 diabetics.

Resistance training (RT) can improve insulin sensitivity and glucoregulatory control in healthy and type 2 diabetic individuals (222-224). Whether RT can alter flowmotion is unknown. It is hypothesised that a 6-week RT intervention will improve skin+SC flowmotion in people with T2D.

Aim 3: To determine if a 6-week RT intervention in T2D group improves skin+SC flowmotion at rest or in response to an OGC.

The majority of clinical studies investigating flowmotion changes in insulin resistance and T2D are performed using skin+SC flowmotion measures (for practical reasons). However, measuring skin blood flow may not be reflective of blood flow patterns in skeletal muscle. It is hypothesised that skin+SC microvascular blood flow measures will reflect those of skeletal muscle blood flow.

Aim 4: To determine whether skin+SC and skeletal muscle blood flow show the same response to an OGC.

1.4.2 Animal studies hypothesis and aims

Flowmotion in the skeletal muscle microvasculature plays a role in the regulation of glucose and insulin delivery to muscle myocytes and thus impacts upon muscle metabolism. However, techniques for measuring skeletal muscle flowmotion are limited. It is hypothesised that CEU can be used to detect changes in flowmotion in skeletal muscle.

Aim 5: Adapt the CEU technique for the measurement of skeletal muscle flowmotion in an animal model.

Chapter 2 - *General Methods*

2.1 Clinical studies

All studies were approved by the University of Tasmania ethics committee and comply with the Australian Code for the Responsible Conduct of Research 2013. Details of studies were outlined to each participant and informed consent was obtained before commencement of testing.

2.1.1 Testing conditions

All clinical studies were undertaken in the clinical rooms at the Menzies Institute for Medical Research. Rooms were maintained at an ambient temperature between 20 and 25°C. During testing participants lay semi-recumbent (at about 45°) on a bed, right arm was extended out from the body with ventral side of forearm facing upward. The arm was held in place with a table and pillow at approximately the same height as participant's heart. Participants were asked to limit arm movement as much as possible throughout testing.

2.1.2 Skin and subcutaneous tissue microvascular measures

Skin+SC microvascular blood flow was measured with Moor Instruments (Devon, UK) CP1-1000 combined high power LDF (fibre separation 0.5mm) and tissue oxygenation (fibre separation 1mm, which indicates the depth of penetration into tissue) probe, which measures skin+SC LDF flux, oxygen saturation (O_2 Sat), total haemoglobin (tHb) and skin temperature (LDF + OXY probe). The LDF component of the probe emits a laser light at a 785 ± 10nm wavelength which penetrates into the tissue and interacts with red blood cells in the section of tissue illuminated by the laser. The scattered and reflected light is then collected by optic fibres on the probe which then provides a perfusion flux value, indicating the number and velocity of red blood cells (Doppler shift) in the section illuminated by the laser light. Modern high power LDF probes have enhanced penetration of light into the tissue and are therefore able to measure both skin and subcutaneous blood flow. A variation in volume of skin and subcutaneous tissue between different individuals could potentially influence the LDF + OXY measurements of microvascular blood flow as the different tissue type may have different capillary

densities and blood flow controls. Potentially, to account for this variation, measurements of subcutaneous tissue volume at the site of LDF + OXY blood flow measurements could be performed and data corrected for any variation between participants. LDF is unable to measure blood flow in absolute perfusion values. As such, the output is LDF flux over time given as perfusion units (PU), an arbitrary measure, as demonstrated in Figure 2.1. The tissue oxygenation component of the probe uses white light spectroscopy to determine tissues O_2 Sat and tHb concentrations in real time at the same site as the LDF (tissues separation 1mm). O_2 Sat output is in percentage (%) and tHb as arbitrary units (AU) over time (Figure 2.1). The compound signals of O_2 Sat and tHb were chosen as blood flow measures over oxy and deoxy signals as they each provide additional information useful to the aims of this thesis. O_2 Sat also provides a measure of the metabolism occurring within the tissue, while tHb is a measure of blood volume which can then be linked to the CEU measure also taken throughout this thesis. Data were continuously recorded at a sampling rate of 40Hz and interfaced with Moor Instruments software (moorVMS-PC V3.1, Moor Instruments, Devon, United Kingdom). A frequency of 40Hz which, samples data at every 0.025second, was chosen as it was the default setting of the Moor Instruments equipment and was adequate to sufficiently sample the higher frequency flowmotion components which occur at a rate of 0.6-2.5 seconds.

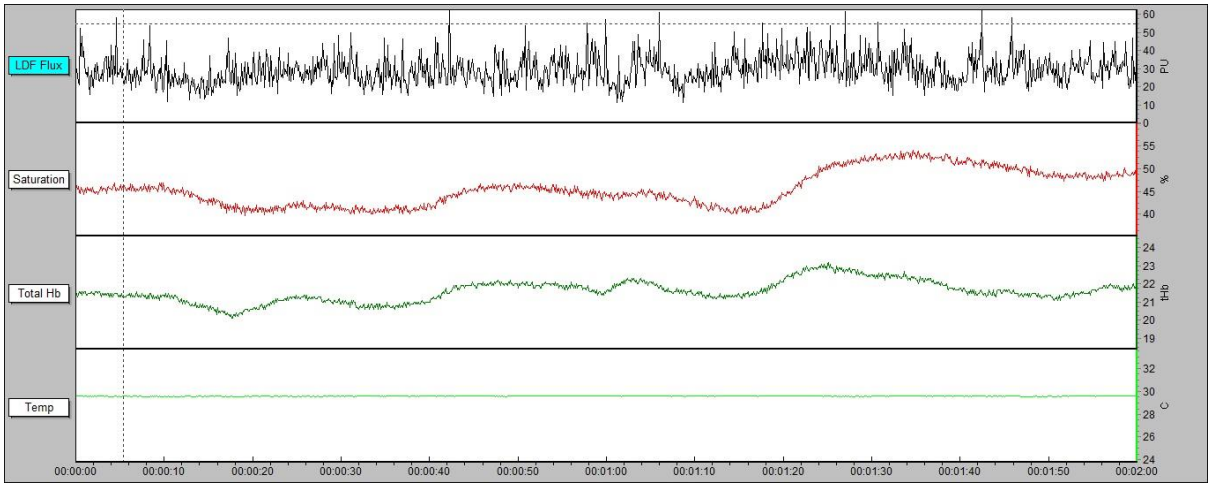

Figure 2.1: *Typical LDF output*. High power LDF probes (as recorded by Moor instruments software) typical output of LDF + OXY probe LDF flux (perfusion units, upper panel), O_2 Sat (percentage, upper middle panel), tHb (arbitrary units, lower middle panel) and temperature (degrees Celsius, lower panel).

On the forearm of each participant, the distance between cubital fossa and wrist joint was measured and midpoint marked. The LDF + OXY probe was placed on the forearm (volar surface) at the midway point avoiding any obvious veins on the skin, as demonstrated in Figure 2.2. Care must be taken while performing LDF measurements as the probes are sensitive to movement artifacts and should not be moved throughout testing. An additional limitation of LDF and tissue oxygenation measures in the skin+SC is the reproducibility of results over different days of testing as microvascular structure in the skin+SC varies significantly at different sites of the tissue. To minimize the impact of this on the data care was taken in the positioning of probes during testing, with probes placed at specific sites in the forearm and the avoidance of probe placement over large vessels.

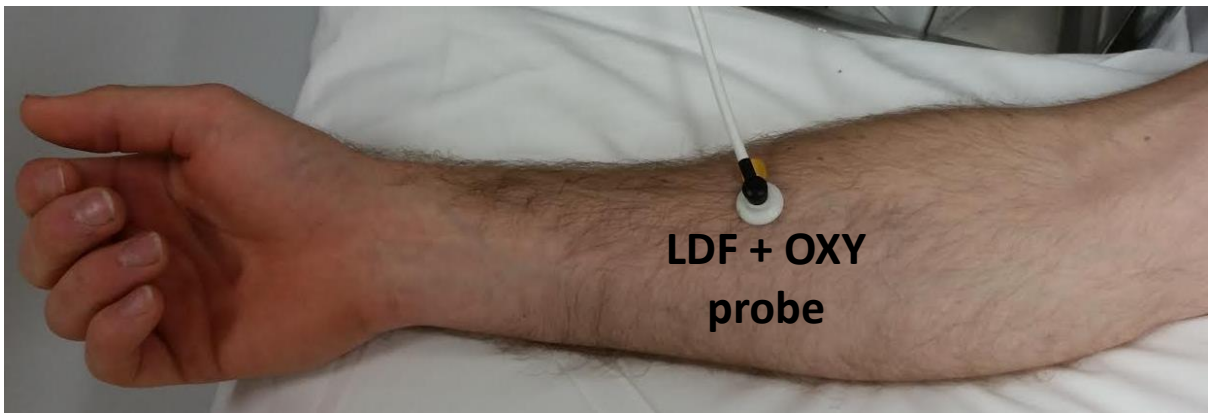

Figure 2.2: *LDF probe placement of participant forearm*. Distance between cubital fossa and wrist joint measured and midpoint marked. LDF + OXY probe placed at midpoint of forearm, avoiding any obvious veins in skin.

2.1.3 Skeletal muscle microvascular perfusion

CEU was used to determine the microvascular perfusion in forearm skeletal muscle. A linear-array L9-3 ultrasound transducer was placed over the right deep flexor muscle of the forearm. The acoustic power of ultrasound, the mechanical index ([peak acoustic pressure] x [frequency]$^{-1/2}$), was set to 0.10 and gain settings optimised and held constant. The transducer was interfaced with an ultrasound system (iU22, Phillips Medical Systems, Andover, MA) on which CEU measures were taken. Contrast agent, gas filled phospholipid microbubbles (DEFINITY® Perflutren Lipid Microsphere, Lantheus

Medical Imaging, MA, USA) were diluted (1.5mL added to 30mL saline) and continuously infused intravenously at 0.03mL/min/kg body weight throughout skeletal muscle blood volume measurements. Microbubbles are continually infused at the same rate to produce a constant concentration of the contrast agent in the blood, which is very important to accurately measure blood volume. Therefore, before each skeletal muscle CEU measure the consistency of blood microbubble concentration was established by measuring in triplicate, the AI in the brachial artery of participants. Microbubbles are echogenic and thus create acoustic signal by expanding and compressing in response to the ultrasound pressure waves. When microbubbles move into the imaged region they interact with the ultrasound output to create an acoustic intensity (AI) which can be recorded by the ultrasound system. As microbubbles concentration is constant in the blood, the AI signal created can be related to blood volume in the imaged region. The use of CEU to measure skeletal muscle microvascular perfusion is quite sensitive, but can be limited its reproducibility over different time points. The ultrasound probe needs to be placed in the same position when comparison of skeletal muscle microvascular perfusion is being made over different times points. To minimise the impact of this limitation on the current study highly trained individuals performed the CEU measures and used land marks such as veins to correctly position the ultrasound probe over the same section of muscle tissue for each measurement.

Microvascular perfusion was determined by destroying microbubbles in the imaged region with a high energy ultrasound pulse (mechanical index set at 1.15) and then recording the replenishment of microbubbles into the skeletal muscle tissue over 45 seconds. CEU data were analysed using Qlab advanced quantification software (Philips Medical Systems, Eindhoven, The Netherlands). Refilling measures were taken in triplicate and then averaged, with the signal from the larger vessels and background subtracted (1 second). Microvascular refilling curve was created by plotting time (seconds) verses AI, giving an exponential rise to maximum plot (Figure 2.3). Microvascular volume (A)

and microvascular filling rate (β) where determined from the graph via SigmaPlot graphing software (Systat Software Inc., CA, USA) with the equation:

$$Y = A(1-e^{-\beta(x(t)-bkg(t))})$$

Where:

Y = Acoustic intensity
X = time (seconds)
A = Acoustic intensity at the plateau position (an indicator of microvascular volume)
β = Rate constant which provides a measure of the microvascular filling rate
bkg = time of background image

Microvascular blood flow is indicated by multiplying A and β values.

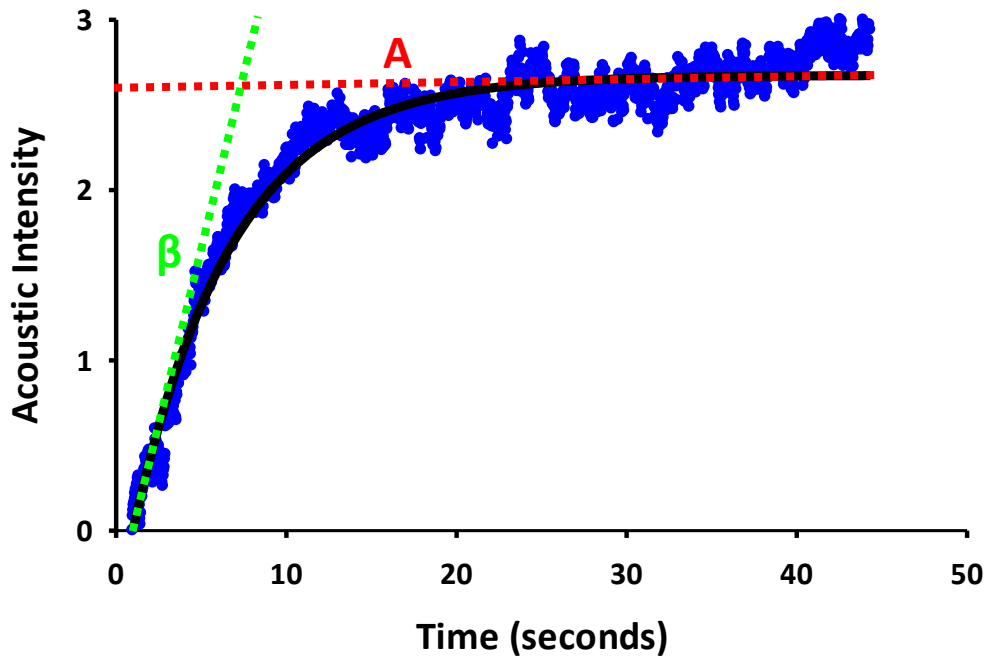

Figure 2.3: *Microvascular volume and filling rate calculation*. Plot was constructed after high energy ultrasound pules destroyed microbubbles in imaged region at t=0. Microvascular volume is indicated by the plateau position (A), and the rate of microvascular refilling is indicated but the rate of increase (β). Microvascular perfusion is calculation by Axβ.

2.1.4 Brachial artery blood flow

Brachial artery blood flow measures were made using a high frequency L12-5 linear array ultrasound transducer (iU22 ultrasound, Philips Medical Systems, Andover, MA) placed ~ 10cm proximal to the

antecubital fold. The diameter of the brachial artery was measured to determine the distance between the upper and lower inner edge of arterial intima. Measurements of the brachial artery diameter were performed manually by trained technician in triplicate using 2-D imaging of the artery at one-time point during both rest and treatment. The manual nature of this measurement does introduce a margin for error, to minimise the impact of this all measurements were performed by the same individual. Pulse-wave Doppler was used to determine the velocity of blood flow in the brachial artery. Brachial artery blood flow (BBF) was then calculated from the diameter and velocity measures:

BBF (mL/min) = π x (½ x diameter)^2 x velocity x 60

Where diameter is in cm and velocity is in cm/sec.

2.1.5 Blood pressure

Resting systolic and diastolic brachial blood pressure (BP) measures were taken in triplicate with a Mobil-O-Graph monitor (I.E.M. Stolberg, Germany) while participants lay semi-recumbent on a bed. The Mobil-O-Graph monitor is a highly sensitive and reproducible method for measuring brachial blood pressure.

2.1.6 Blood analysis

Fasting blood was collected by a trained phlebotomist and blood chemistries (HbA1c, cholesterol, high density lipoprotein cholesterol (HDL), low density lipoprotein cholesterol (LDL), and triglycerides) determined at a nationally accredited pathology laboratory (Royal Hobart Hospital, TAS). Blood glucose measures taken throughout the protocol were determined using a bench top glucose analyser (YSI Model 2300 Stat plus, Yellow Springs Instruments, OH). Plasma insulin concentrations were determined by ELISA (Mercodia AB, Uppsala, Sweden). These blood analysis techniques are considered highly sensitive and reproducible when performed by trained individuals, as is the case in these studies.

2.1.7 Body composition

To determine percentage body fat and percentage lean muscle mass participants underwent a whole-body scan by dual-energy X-ray absorptiometry (DEXA; Hologic Delphi densitometer, Hologic, Waltham, USA). Each parameter was calculated as previously reported (225). DEXA is considered the gold standard measure of body composition.

2.1.8 Analysis

2.1.8.1 Microvascular blood flow averages

All data are expressed in a scatter graph or as mean ± SE. For high power LDF + OXY probe 10 minute averages of skin+SC microvascular blood flow measures (LDF flux, O_2 Sat and tHb) and skin temperature were determined using Moor Instruments software (moorVMS-PC V3.1, Devon, UK).

2.1.8.2 Complexity

Complexity analysis is a means of assessing the randomness of a recorded signal, the more random the collected data is (less regular reoccurring patterns within a signal) the higher the complexity value will be. It is hypothesised that in healthy individuals there is a high level of randomness in microvascular blood flow patterns and that with increasing severity of diseases such as T2D the randomness of blood flow patterns is reduced (226). Complexity analysis could therefore possibly be used to identify dysregulation of microvascular blood flow in T2D, when compared to healthy control data. MATLAB program (MathWorks, Natick, MA, USA) was used to perform Lempel-Ziv (LZ) complexity measurements (226, 227) on skin+SC microvascular blood flow measures. Briefly, the LZ complexity analysis technique determines the average value of a data set and then for each individual data point assigns a 0 if the data point is below or equal to the mean value, or a 1 if data point is above

mean value. The resulting output of numbers (e.g. 11000110101010…. etc.) is then analysed and reoccurring patterns in the signal determined. If there are large numbers of reoccurring patterns the resulting complexity value will be low, if there are only small numbers of reoccurring patterns within the signal the complexity value will be higher. Complexity determination is limited by the amount of random noise in the signal, depending upon the period of time analysed, the complexity value maxes out at a particular point. LZ complexity analysis was performed in MATLAB on 10 x 1min of high power LDF, O_2 Sat and tHb (exported from Moor Instruments software). The complexity value of each of the 10 x 1min data sections was averaged to give an overall complexity value for each blood flow measure. For 1min complexity analysis, the complexity value maxes out due to random noise in the signal at a value of 224.

MATLAB script for complexity analysis:

```
%%Enter data frequency and EPOH time
a = 40;
b = 60;
c=a*b;

%generate LZcomplex number for probe1 basal data1 and for EPOHs
LZBP1a=lzcomplex(data1(1:c,2));
LZBP1b=lzcomplex(data1(c+1:2*c,2));
LZBP1c=lzcomplex(data1(2*c+1:3*c,2));
LZBP1d=lzcomplex(data1(3*c+1:4*c,2));
LZBP1e=lzcomplex(data1(4*c+1:5*c,2));
LZBP1f=lzcomplex(data1(5*c+1:6*c,2));
LZBP1g=lzcomplex(data1(6*c+1:7*c,2));
LZBP1h=lzcomplex(data1(7*c+1:8*c,2));
LZBP1i=lzcomplex(data1(8*c+1:9*c,2));
LZBP1j=lzcomplex(data1(9*c+1:10*c,2));

EPOH=[ 1; 2; 3; 4; 5; 6; 7; 8; 9; 10];
complexity=[LZBP1a;LZBP1b;LZBP1c;LZBP1d;LZBP1e;LZBP1f;LZBP1g;LZBP1h;LZBP1i; LZBP1j];
xls1=[EPOH,complexity];
[filename,pathname]=uiputfile('*.xls','give name to save file');
filenameinclpath=[pathname,filename];
s=xlswrite(filenameinclpath,xls1,'a1:b11');
```

2.1.8.3 Flowmotion

Wavelet transformation analysis was performed on all microvascular blood flow measures to assess skin+SC flowmotion patterns. LDF flux, O_2 Sat and tHb measures were exported from Moor instruments software. MATLAB program (MathWorks, Natick, MA, USA) was used to perform wavelet transformation. Prior to wavelet transformation, average value of data set was determined and then subtracted from each data point as a means of controlling for data variation and optimising the wavelet transformation analysis by removing edge effects. 8:1 cmor morlet wavelet was used in wavelet transformation analysis of clinical data.

Plotting wavelet transformation of blood flow data against frequency provides a picture of overall flowmotion pattern occurring in tissue. However, to determine any differences in frequency component contribution between treatments and disease states the data must be quantified. Previously in the literature the contribution of each frequency component has been quantified by determining the mean wavelet transformation value over each frequency range, which is then normalised by dividing the mean of the entire frequency range assessed (55). Initially this technique was employed to the current data set, but proved to be problematic the as some of the sensitivity of the wavelet transformation analysis was lost through the averaging across the whole frequency region. The difference is baseline values between participants was an additional concern. It is the peaks in the wavelet transformation analysis that are of particular interest in this thesis as it is believed that the sum of these provided information about the contribution of each different frequency component to flowmotion. To better measure the contribution of each component to flowmotion and overcome the impact of varied baseline values, the area under the curve (AUC) of all the peaks in a frequency range was determined and summed together. Separate to the contribution of each component to flowmotion, the most prominent frequency at which each component exerted influence over flowmotion was also of interest. This was measured by determining the frequency at

which the highest peak in each region (i.e. the most prominent signal) occurred at. AUC of peaks and peak frequency was calculated using PeakFit software (Systat Software Inc. CA, USA).

Each wavelet transformation from LDF flux, O_2 Sat and tHb measures was individually uploaded into PeakFit software on a linear scale and the best baseline for graph selected (Figure 2.4A). The linear data points were used to distinguish peaks in different frequency components. The highest peak in each region was determine and then referenced back to the corresponding frequency at which it occurred (Figure 2.4B). The AUC of peaks in each region were then determined by the software, if multiple peaks were present in frequency range the AUC of all peaks was summed (Figure 2.4C).

LDF flux wavelet transformation measures adequately detected all five frequency components (endothelial, neurogenic, myogenic, respiratory and cardiac), but tissue oxygenation measures were only able to adequately detect the three lower frequency components (endothelial, neurogenic and myogenic). AUC and peak frequencies for O_2 Sat and tHb were therefore only determined for lower frequency components.

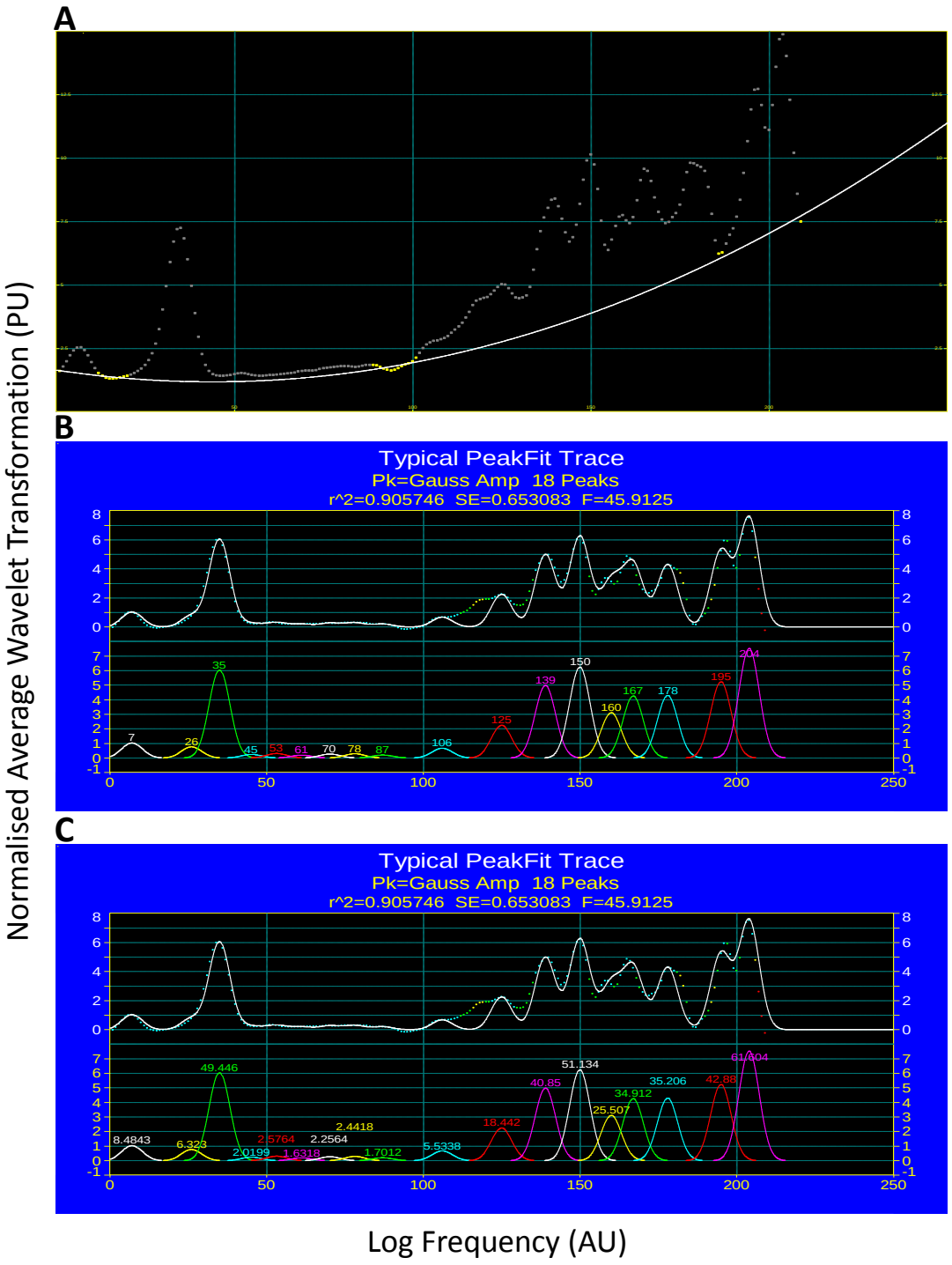

Figure 2.4: *Typical PeakFit analysis output.* Wavelet transformation data is uploaded into PeakFit software on linear scale and the A) best baseline is selected B) peaks in each frequency region are identified by position and then C) AUC for each peak is determined by software and recorded.

2.2 Laboratory experiments

2.2.1 Animal care

Male Sprague Dawley rats (288g ± 8) reared and housed in the University of Tasmania animal facilities were used for all experiments. Animals were maintained at 21-22˚C and kept in a 12hr dark/light schedule. Animals were given access to water and commercial diet (4.8% lipid, 19.4 % protein, 70.7% carbohydrate, 5.1% crude fibre with added vitamins and minerals, Specialty Feeds, Glen Forest, WA, Australia) *ad libitum* up to the morning of experiments. All procedures and experiments were approved by the University of Tasmania Animal Ethics Committee in accordance with the 2013 Australian Code of Practice for the Care and Use of Animals for Scientific Purposes (#A13384).

2.2.2 *In vivo* protocol

2.2.2.1 Surgery

On the morning of the experiment rats were anaesthetised with an intraperitoneal injection of sodium pentobarbital (50mg/100g body weight) prior to surgery. Once animals were non-responsive, a tracheotomy was performed to allow for spontaneous breathing throughout experiment. Both jugular veins and a carotid artery were cannulated with polyethylene tubing (Figure 2.5). The left jugular vein was cannulated (PE60 Intramedic®) to allow for continuous anaesthetic infusion (~0.6mg/min/kg sodium pentobarbital, maintaining anaesthesia) and delivery of intravenous solutions. The right jugular was cannulated (PE40 Intramedic®) to allow intravenous infusion of microbubbles (ultrasound contrast agent). Cannula inserted into the carotid artery (PE60 Intramedic®) was used to continuously determine animals mean arterial pressure (MAP) and heart rate (HR) via a pressure transducer (Transpac IV, Abbott Critical Systems, Morgan Hill, CA USA) and for arterial blood sampling. All cannulas were secured with size 3/0 waxed braided silk ligatures. Continuous monitoring of total blood flow to the rat hindlimb was achieved by an ultrasonic flow probe (Transonic Systems™, VB series

0.5mm, Ithaca, NY, USA) placed around the femoral artery in a position distal to the rectus abdominal muscle. To allow flow probe placement, ~1cm section of skin was removed from the region above the femoral artery and vein, the epididymal fat pad separated, epigastric artery ligated and artery separated from femoral vein and saphenous nerve. The flow probe and pressure transducer were interfaced with an IBM compatible PC computer. The computer acquired data at a sampling frequency of 100 Hz for femoral blood flow (FBF), HR and MAP using WINDAQ data acquisition software (DATAQ instruments, Akron, OH USA).

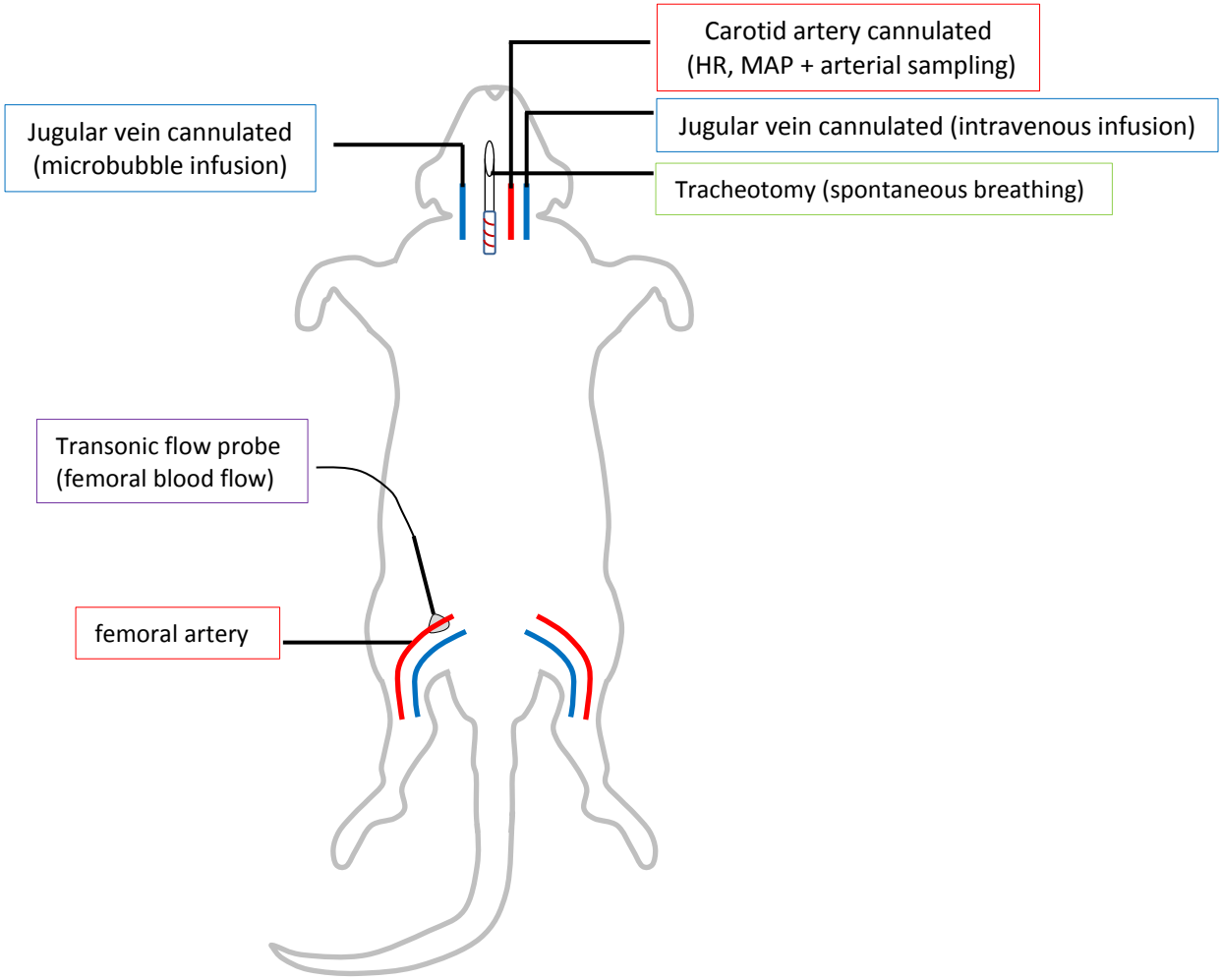

Figure 2.5: *Schematic diagram of the* in vivo *surgery*. Surgery details are given in section 2.1.2.1. The above picture illustrates the ventral view of the rat after surgery. A tracheotomy tube was inserted to allow spontaneous breathing of room air. The cannulation of both jugular veins (used for intravenous infusion) and right carotid artery (used for continued measurement of MAP and HR as well as arterial blood sampling) is shown. Transonic™ flow probes which allow continual FBF measurements were placed around right femoral artery. Diagram adapted from Mahajan *et al* (228).

2.2.2.2 Laser Doppler Flowmetry

Microvascular blood flow of the rat tibialis anterior muscle was determined using LDF flux and tissue oxygenation measures. A small section of skin (~0.5cm) was removed from above the upper section of the left tibialis anterior muscle, exposing the muscle and a small layer of connective tissue. The CP3-500 is a combined laser Doppler and tissue oxygenation probe (LDF + OXY, Moor Instruments, Devon, UK, tissues separation 0.5mm) was placed directly onto the surface of the exposed muscle (Figure 2.7) and data collected at a frequency of 40Hz using Moor Instruments recording software (moorVMS-PC V3.1, Devon, UK) as demonstrated in Figure 2.6.

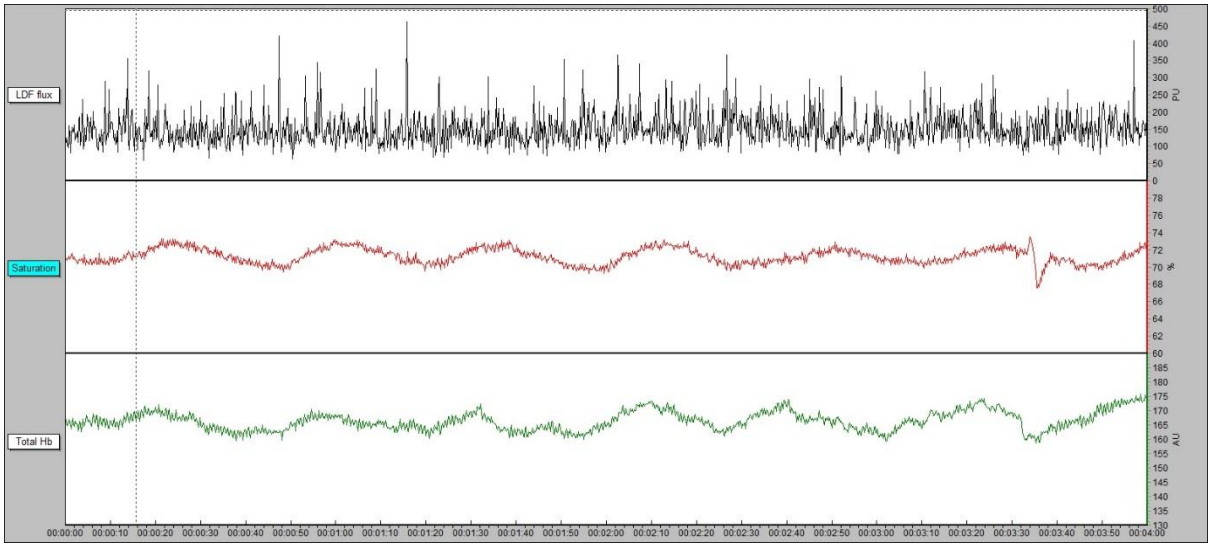

Figure 2.6: *Typical CP3-500 probe output*. LDF flux (perfusion units, upper panel), O_2 Sat (percentage, middle panel), tHb (arbitrary units, lower panel) over time is demonstrated.

2.2.2.3 Contrast enhanced ultrasound

Microvascular blood flow in the rat calf (soleus, plantaris, and red, white and mixed gastrocnemius muscles) and upper thigh (biceps femoris anterior and posterior, adductor magnus and brevis, semimembranosus red and white, and semitendinosus) was assessed using the CEU technique. A

linear-array L9-3 ultrasound transducer was placed over the rat left calf or upper thigh, with ultrasound conductive gel (Conductive Gel, Medical Equipment Services Pty Ltd, Melbourne, AUS) between probe and hindlimb to allow for imaging (Figure 2.7). The transducer was interfaced with the iU22 ultrasound system on which CEU measures were taken (Figure 2.7).

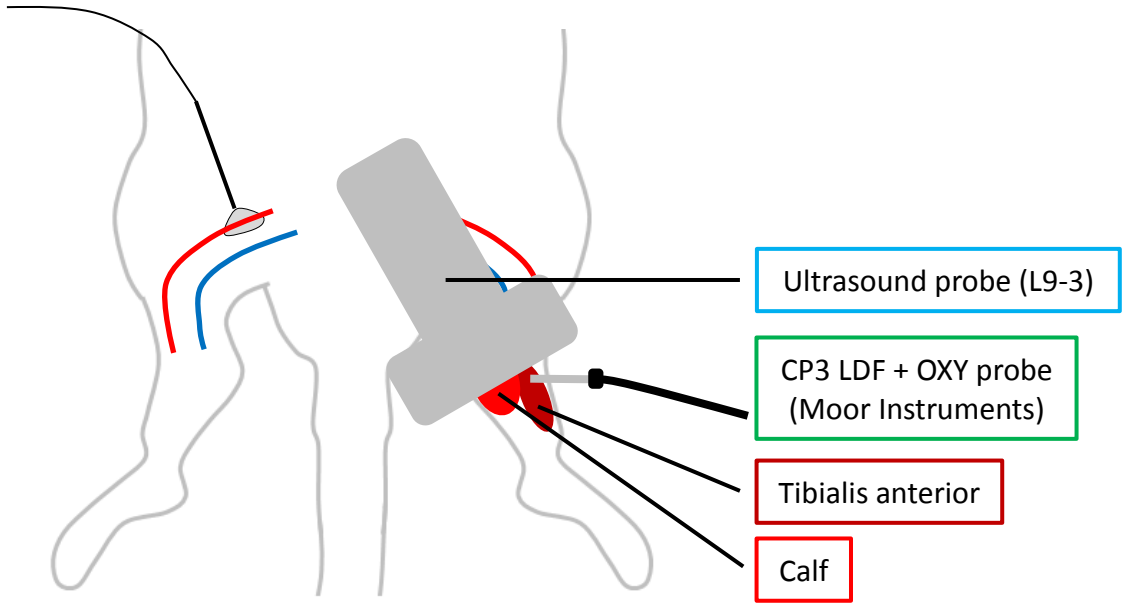

Figure 2.7: *Schematic diagram of probe placements.* As describe in sections 2.1.2.2 and 2.1.2.3, skin above left tibialis anterior muscle was removed and CP3-500 probe place directly onto muscle tissue. L9-3 ultrasound probe was placed over the rat left calf muscle to image soleus, plantaris and white, red and mixed gastrocnemius.

The contrast agent, gas filled phospholipid microbubbles, were continuously infused intravenously via the right jugular vein (approximately 2.14×10^6 microbubbles/min), allowing steady state concentration to be reach in the blood. The mechanical index was set to 0.08 and the gain settings optimised for each individual experiment (2D 87-89%, C 30, P off). An example of ultrasound images on the rat calf with and without microbubbles, as well as an overlay of muscle positioning is demonstrated in Figure 2.8.

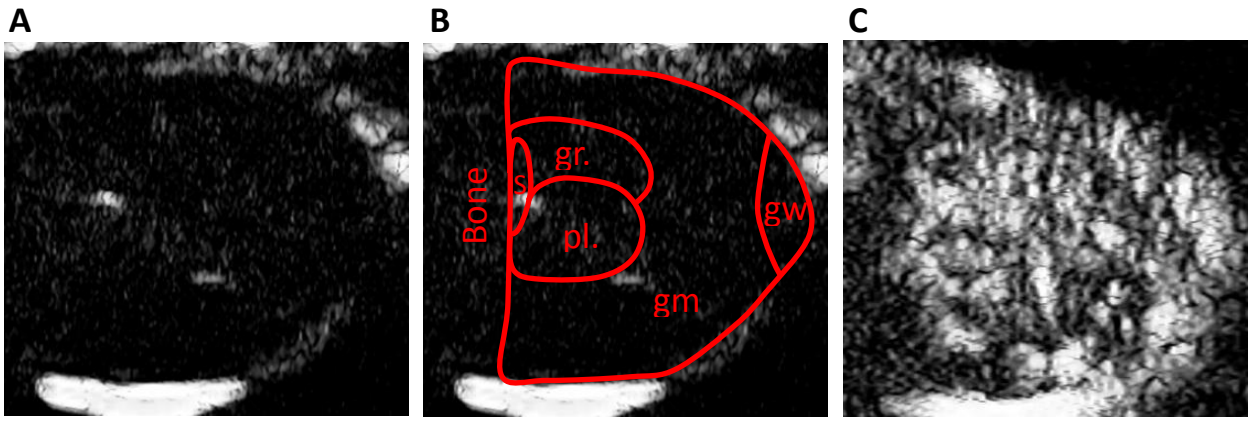

Figure 2.8: *CEU images of rat calf*. A) Ultrasound image of the rat calf with B) an overlay of muscle positioning based upon R. Armstrong and M. Laughlin 1984 description (229). Abbreviations: s., soleus; pl., plantaris; gr., gastrocnemius red; gm., gastrocnemius mixed; gastrocnemius white. C) CEU image with contrast agent in rat calf muscle.

CEU data were analysed using Qlab advanced quantification software, which allows for selection of many different regions of interest (ROI). CEU was used to asses both flowmotion changes and microvascular perfusion during different treatments. To assess changes in skeletal muscle flowmotion, recording of CEU images was triggered for ever 50ms (frequency of 20Hz) and continuously collected for 30min under the different treatment conditions. The sampling frequency of 20Hz is utilised in these experiments due to the limitations of the iU22 ultrasound system. A frequency of 20Hz allows sampling of data every 0.05 seconds. Sampling at 20Hz is therefore is considered appropriate for the collection of blood flow for the analysis of flowmotion via wavelet transformation as the highest frequency component (cardiac) occurs and a rate of 0.6-2.5 seconds. Microvascular perfusion was determined at the end of each treatment period using the same technique described in section 2.1.3. Microbubbles in the imaged region are destroyed and the replenishment over 45sec, which was recorded and fitted to an exponential rise to maximum plot, from which microvascular volume, filling rate and perfusion were determined.

2.2.3 Haemodynamic and LDF data analysis

All data are expressed as mean ± SEM. Five second sub-sample of WINDAQ data were used to calculate MAP (mmHg), HR (bpm) and FBF (mL/min) at various time points. Over the course of the entire experiment, 5min averages of LDF flux, O_2 Sat and tHb were determined using Moor Instruments software (moorVMS-PC V3.1, Devon, UK).

2.2.4 CEU and LDF flowmotion analysis

CEU (20Hz) and LDF + OXY (40Hz) data (30min, collected at the same time points) were exported from Qlab and Moor instruments software respectively. MATLAB program (MathWorks, Natick, MA, USA) was used to perform wavelet transformation. Prior to wavelet transformation, average value of data set was determined and then subtracted from each data point as a means of optimising the wavelet transformation analysis and removing edge effects. Different to the clinical data, a 2:1 cmor morlet wavelet was used in wavelet transformation analysis of animal data. The change from 8:1 to 2:1 cmor morlet in the analysis of animal blood flow data is due to the difference in quality of the data in each study. 8:1 cmor morlet was used to analyse the clinical data as a higher ratio produces more distinctive peaks, this was necessary for the clinical data as it was less controlled than in the laboratory setting and therefore contained greater random signal. In the laboratory experiments the animals were anesthetised and measures taken to minimise external influences on data collection, thereby there was no need to alter the morlet parameters as peaks in each region were already well defined at a lower ratio.

As with clinical data (described in section 2.1.2.3) comparison of each frequency range contribution to flowmotion between treatment or control groups was determined by comparing the AUC of peaks in each frequency range. AUC of peaks and the frequency at which the highest peak in each frequency range was calculated using PeakFit software (Systat Software Inc. CA, USA). Analysis using PeakFit for animal data varied slightly from clinical (section 2.1.2.3) as respiratory and cardiac input occur at

higher frequency to humans and therefore data input to PeakFit program was on a different linear scale. Each wavelet transformation was individually loaded into PeakFit software and the best baseline for graph selected, AUC of peaks in each region were then determined by the software, if multiple peaks were present in frequency rage the AUC was summed.

2.3 Summary of blood flow measures

Table 2.1: *Summary of blood flow measures and implications of this on flowmotion analysis*.

Technique	Component of Blood flow measured	Flowmotion Implications
Blood pressure	Pressure in circulatory system	Not measured
Limb blood flow	Total/bulk flow into limb	Not measured
CEU	Blood volume	Blood volume influenced by local factors
LDF	RBC number and velocity	Influenced by mediators of velocity as well as blood volume
O_2 Sat	Oxygenated RBC and metabolism in the tissue	Metabolism measure potentially has additional influence from components such as neurogenic input
tHb	RCB number (blood volume)	Blood volume influenced by local factors

2.4 Statistical analysis

All tests were performed using SigmaStat software (Systat Software Inc. CA, USA). The tests performed are outlined in each individual chapter. For each data set normality (Shapiro-Wilk) was assessed in SigmaPlot, and a suitable test selected if data was parametric or non- parametric. Significance was assumed at $p < 0.05$ and was assessed using Student's t-test when there were two groups and Student-Newman-Keuls post hoc test for multiple groups.

Chapter 3 - *Microvascular flowmotion in the skin and subcutaneous tissue: healthy control versus T2D*

3.1 Introduction

The vascular system is an integral component of normal cellular function, providing a means of nutrient delivery and waste removal from the cells. It thereby allows the maintenance of homeostasis during rest and periods of increased metabolic demand (1). Disruption of normal vascular function can contribute to pathological disease states such as T2D (191). Insulin resistance alters vessel function and blood flow early on in T2D development, via the attenuation of endothelial derived insulin-mediated vasodilation (endothelial insulin resistance). This aberrant change in insulin-mediated vasodilation is of particular importance in skeletal muscle (230) as it results in reduction in insulin-mediated blood flow directly to the myocytes and thus an attenuation of skeletal muscle glucose uptake (168). Endothelial insulin resistance is therefore, in part, causative of the characteristic high blood glucose levels seen in T2D. As the disease progresses, T2D results in direct damage to the vasculature as glucose is a highly reactive molecule. Glucose binds to proteins on vessels to form advanced glycation end-product, which disrupts normal structure and therefore function (231, 232). The chronic pathological levels of blood glucose in T2D thus result in damage to both the macrovasculature and the microvasculature, and are causative of the long term adverse health outcomes of T2D such as cardiovascular disease, nephropathy, neuropathy and retinopathy (233). Disruption of normal microvascular function in T2D, through endothelial insulin resistance and glucose induced vessel damage, is therefore involved in both the early development of the disease and the development of the serious adverse health outcomes. To investigate the changes in blood flow that occur in T2D in both skin+SC and the more metabolically important tissue skeletal muscle, skin+SC LDF + OXY and skeletal muscle CEU measures were taken.

Pathological changes in vascular function could be mediated by changes in blood flow patterns and distribution. Investigating flowmotion and determining whether any or all of the controlling influences (endothelial, neurogenic, myogenic, respiratory and cardiac) are altered in T2D is important in understanding the pathogenesis of the disease (72, 217, 218). Developing our understanding of the

affected components may also provide potential treatment targets to improve the function of the microvascular blood flow, thereby improving the long-term health outcomes of patients.

LDF is the most commonly used technique to measure flowmotion in humans. High power LDF probes are used to measure blood flow from the skin and underlying subcutaneous tissue (skin+SC). Tissue oxygenation measures are also becoming more frequently used to determine human skin+SC blood flow. Spectral analysis such as wavelet transformation can be applied to skin+SC LDF flux, O_2 Sat and tHb data for the assessment of flowmotion. Determination of the contribution of each individual frequency component to flowmotion and the peak frequency at which the component is exerting influence, can give an extensive insight to blood flow patterns and help to identify areas of dysregulation.

Wavelet transformation does however require larger data sampling times (a minimum of 20min) as the lower frequency components, such as the endothelial, occur at slower rates of one cycle every 50-105sec (55, 56). Thus to ensure there are sufficient cycles measured, longer sample times are required. This imparts some practical limitations on data collection, which may be overcome by using complexity analysis, an assessment of the randomness of a signal, which only requires shorter sampling periods. While complexity analysis does not give a measure of the differing contribution of each frequency component within flowmotion, it will give an indication of how random the LDF signal is, with a more random signal indicating less regular control of blood flow, which is believed to be a healthy state. The more random the signal, the higher the complexity output. The use of complexity analysis on skin+SC LDF flux and tissue oxygenation measures could indicate if flowmotion dysfunction (i.e. decreased complexity) is occurring within an individual, giving an overall indication of vascular function. It has previously been shown in monkeys that the randomness of skin+SC LDF flux measures decreases with advancing insulin resistance and T2D (226). The use of this analysis technique may therefore offer a more practical means of assessing microvascular function in human participants.

The aim of this study was to determine if forearm blood flow distribution and microvascular flowmotion in skin+SC is altered in T2D participants. Forearm total blood flow, average skin+SC flux and skeletal muscle microvascular perfusion were measured to determine the distribution of blood flow within the forearm. Wavelet transformation of skin+SC LDF flux, O_2 Sat and tHb measures were used to identify changes in any of the five controlling components of flowmotion, while complexity analysis was performed to determine if this more simplistic mathematical analysis could be used to detect microvascular dysfunction.

3.2 Methods

This study was approved by the University of Tasmania Human Research Ethics Committee (#H14086) and conducted at the Menzies Institute for Medical Research. Through community advertisement, 23 healthy controls and 18 sedentary (self-reported <30min of moderate exercise per week) clinically diagnosed type 2 diabetics were recruited for the study. Inclusion criteria for the study were participants aged between 18-60 years who were normal to overweight (BMI = 19 – 35 kg/m^2). Exclusion criteria for study was a BMI>35 kg/m^2, a history of smoking, cardiovascular disease, stroke, myocardial infarction, uncontrolled hypertension (resting brachial blood pressure >160/100mmHg), peripheral arterial disease, pulmonary disease, arthritis/muscular skeletal disease, malignancy within past 5 years or severe liver disease.

3.2.1 Screening visit

Eligibility for the study was determined at an onsite screening visit after first giving informed consent. Participants provided a detailed medical background. Anthropometric measures (height and weight) as well as resting blood pressure were taken on the day in the clinical setting. Body composition was determined using DEXA whole body scan as described in section 2.1.7.

3.2.2 Clinic visit

Participants presented to the clinic on the morning of testing overnight fasted and having refrained from alcohol and vigorous exercise for 48 hours prior. Type 2 diabetics ceased diabetes medications for 48 hrs prior to testing, which is standard practice and allows for accurate assessment of severity of insulin resistance. All other medication i.e. hypertension was taken as usual. Testing conditions were as described in section 2.1.1, with measures taken at ambient temperature (20-25°C) and participants laying semi-recumbent on a bed. The right arm was extended out from the body with the ventral side of forearm facing upward. All measures were taken under resting and fasted conditions,

after an initial period of equilibration (~20min). Due to experimental issues and loss of data some data points are missing for various measure for some participants.

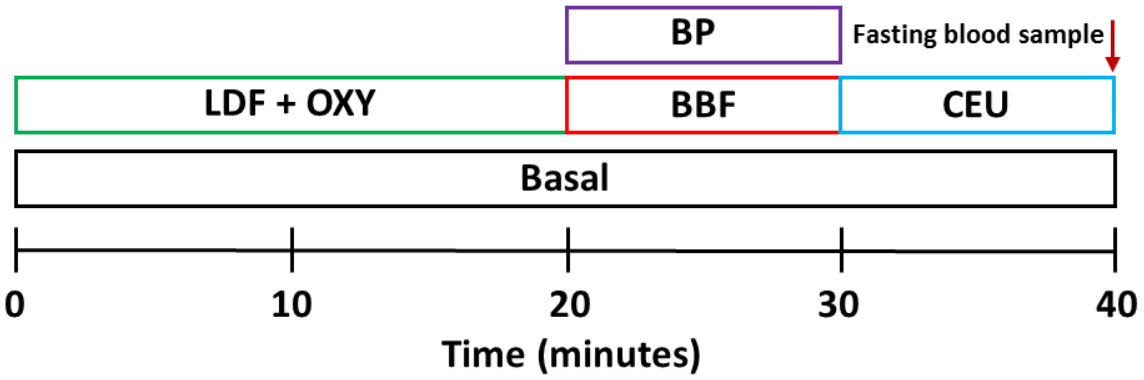

Figure 3.1: *Study protocol.* All measures were taken under basal (resting) conditions. Skin+SC LDF flux and tissue oxygenation (**LDF + OXY**) was measured from 0 to 20mins. Resting **BP** was then repeatedly measured over 10min time period while brachial blood flow (**BBF**) was concurrently measured using ultrasound. The antecubital vein of the non-dominant arm was cannulated and a fasting blood sample was acquired at 40mins. Forearm skeletal muscle microvascular perfusion was then assessed from 30-40mins using contrast enhanced ultrasound (**CEU**).

3.2.2.1 Skin and subcutaneous tissue microvascular blood flow

The LDF + OXY probe (described in section 2.1.2) was attached to the midsection of the ventral side of the right forearm. Skin+SC microvascular blood flow was assessed with LDF flux and tissue oxygenation measures over a 20min period (Figure 3.1).

3.2.2.2 Total forearm blood flow

Brachial artery blood flow at rest was determined as a measure of forearm total flow (figure 3.1). As describe in section 2.1.4, a L12-5 linear array ultrasound transducer was used to measure brachial artery diameter and then blood velocity. Brachial blood flow (BBF) is then calculated from velocity and diameter measures (BBF mL/min = π x (½ x diameter)^2 x velocity x 60). Where diameter is in cm, and velocity is in cm/sec.

3.2.2.3 Forearm skeletal muscle microvascular perfusion

Microvascular blood volume, filling rate and perfusion of forearm deep flexor muscle was determined as described in section 2.1.3. CEU measures of skeletal muscle microvascular blood flow were taken using a linear-array L9-3 ultrasound transducer while contrast agent (phospholipid microbubbles) were constantly infused. Microbubbles within the region under the ultrasound beam were destroyed and the replenishment of microbubbles back into the tissue was recorded over 45 seconds to determine microvascular perfusion measures (Figure 3.1). For a number of participants, CEU skeletal muscle microvascular perfusion measures were lost or not recorded correctly. As such participant numbers for forearm muscle blood flow are lower than other measures.

3.2.2.4 Blood pressure and heart rate

Resting systolic and diastolic blood pressure and heart rate measures were repeatedly taken over a 10min time period with a Mobil-O-Graph monitor as described in section 2.1.5 (Figure 3.1). Vascular resistance was calculated from MAP and BBF to give an indication of vasodilatory state.

Vascular resistance = MAP (mmHg)/BBF (min/mL)

3.2.2.5 Blood analysis

Fasting blood samples were taken from an antecubital vein of the non-dominant arm and analysed for fasting blood glucose, fasting plasma insulin, HbA1c and lipid profile as described in section 2.1.6.

3.2.3 Data analysis

3.2.3.1 Microvascular blood flow averages

The mean LDF flux and tissue oxygenation measures were determined over a 10min period as described in section 2.1.8.1.

3.2.3.2 Complexity measures

Mean complexity measures over the same 10min time period as average LDF flux and tissue oxygenation measures was calculated as described in section 2.1.8.2.

3.2.3.3 Flowmotion measures

Flowmotion analysis using wavelet transformation was performed on 20min of resting LDF flux and tissue oxygenation measures. Wavelet transformation data were then quantified by determining AUC of peaks within each flowmotion component and peak frequency, as described in section 2.1.8.3.

3.2.4 Statistical analysis

For all anthropometric, blood chemistry, blood flow and flowmotion measures, unpaired Student's t-tests were performed to determine differences between healthy controls and T2D, as described in section 2.1.9.

3.3 Results

3.3.1 Participant characteristics

Populations similar in age and gender were recruited to allow comparison between healthy controls and clinically diagnosed type 2 diabetics (Table 3.1). While on average the type 2 diabetics were five years older than healthy controls, this was not statistically different ($p = 0.379$). Likewise, the male to female ratio was similar between the two populations with 35% females in healthy controls and 33% in T2D group.

Several anthropometric and blood chemistry analyses were performed (Table 3.1). Body weight ($p = 0.001$), percentage body fat ($p = 0.025$) and BMI ($p < 0.001$) were all significantly higher in T2D group as compared to the healthy controls. Systolic blood pressure was significantly elevated (10.9mmHg difference) in type 2 diabetics ($p = 0.018$). There was no difference in the vascular resistance between healthy controls and T2D at rest. T2D participants also displayed significantly higher fasting ($p < 0.001$) blood glucose, HbA1c ($p < 0.001$) and fasting plasma insulin ($p < 0.001$), as well as significantly lower HDL ($p = 0.041$) compared to healthy controls. The average duration of T2D was 7.08 ± 1.4 years within the T2D group (Table 3.2). The number of participants on different medications is indicated in Table 3.2, all but two participants were taking metformin to control their diabetes, while two participants were taking insulin.

T**able 3.1:** *Anthropometric and blood chemistry results of healthy controls and T2D participants*. Data expressed as mean ± SE.

	Healthy Control	T2D	P value
Age (yr)	47 ± 2	52 ± 2	0.379
Sex (M/F)	15/8	12/6	-
Weight (kg)	75.2 ± 2.3	94.4 ± 6.5	**0.001**
Body Fat (%)	26.1 ± 1.9	31.6 ± 1.5	**0.025**
BMI (kg/m^2)	25.3 ± 0.6	30.9 ± 1.1	**<0.001**
Blood Pressure (mmHg)			
Systolic	121.0 ± 3.1	131.9 ± 3.9	**0.018**
Diastolic	77.0 ± 1.9	80. ± 3.0	0.209
Fasting Blood glucose (mM)	4.9 ± 0.1	10.2 ± 1.0	**<0.001**
HbA1c (%)	5.4 ± 0.1	7.9 ± 0.4	**<0.001**
Plasma Insulin (pM)	40.5 ± 1.7	97.3 ± 17.8	**<0.001**
Fasting Blood Lipids (mmol/L)			
HDL	1.5 ± 0.1	1.4 ± 0.2	**0.041**
LDL	3.1 ± 0.2	2.6 ± 0.3	0.056
Total Cholesterol	3.6 ± 0.2	3.9 ± 0.3	0.303

Table 3.2: *Diabetes duration and medication taken by type 2 diabetics.* Data expressed as mean ± SE.

Type 2 Diabetics	
Number	13
Diabetes duration (years)	7.08 ± 1.4
Medication	**Number of participants on medication**
Hypertension	8
Hypercholesterol	10
Metformin	12
GLP	0
SGLT2 inhibitor	1
DDP	0
Insulin	2
Diuretic	6
Calcium channel blocker	3
Beta blocker	0
Statin	5
Other	8

3.3.2 Forearm total flow

Brachial artery blood flow was measured with 2D-ultrasound to determine the total amount of blood flow to the forearm. As shown in Figure 3.2, total forearm blood flow was significantly higher in the T2D group compared to the healthy controls at rest ($p = 0.003$).

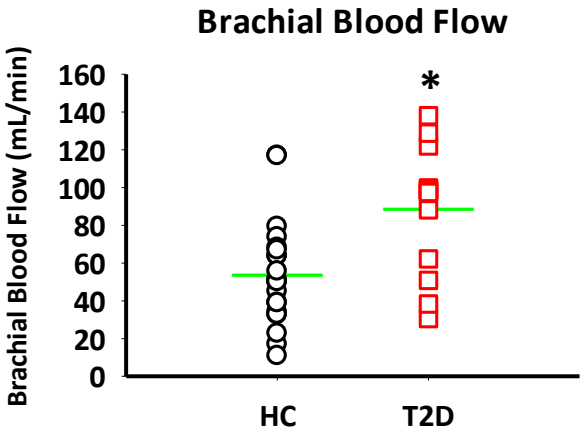

Figure 3.2: *Brachial artery blood flow.* Brachial artery blood flow (mL/min) measured with 2D-ultrasound for **healthy control** (**HC**; n=22) and **T2D** (n=12) groups. — indicates mean. ***** significant difference between healthy **controls** and **T2D** ($p = 0.003$).

3.3.3 Skin and subcutaneous tissue microvascular blood flow and tissue oxygenation

LDF flux measures red blood cell number and velocity in forearm skin+SC. A higher resting forearm skin+SC LDF flux (Figure 3.3A), and thus skin+SC microvascular blood flow, was seen in the T2D participants ($p = 0.009$). There were no significant differences in the tissue oxygenation measures (Figure 3.3B-C), which were measured at the same site as LDF flux. Skin temperature measured by the LDF + OXY probe showed no difference between healthy control (28.9 ± 0.2°C) and T2D (29.0 ± 0.2°C) groups.

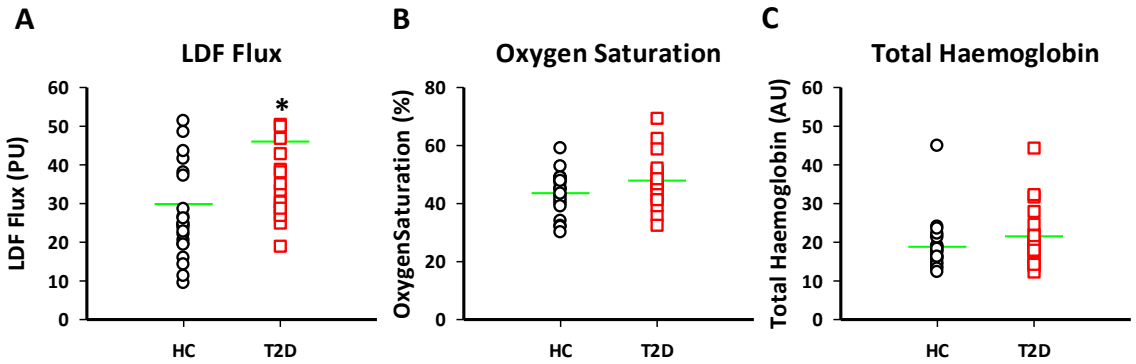

Figure 3.3: *LDF flux and tissue oxygenation measures*. Average over 10mins for **healthy control** (○ **HC**; n=23) and **T2D** (□ n=18) groups of skin+SC A) LDF flux B) O_2 Sat and C) tHb measures. — indicates mean. ***** indicates significant difference between healthy **controls** and **T2D** ($p = 0.006$).

3.3.4 Skin and subcutaneous tissue complexity measures

Complexity analysis was performed on the same 10min LDF flux and tissue oxygenation data used to determine average flux (Figure 3.3). The complexity measures of LDF flux, which determines RBC number and velocity, are much higher than those of O_2 Sat and tHb, indicating there is greater randomness in the LDF flux than the tissue oxygenation measures. No significant differences in complexity between healthy controls and type 2 diabetics were seen in any of the microvascular blood flow measures (Figure 3.4).

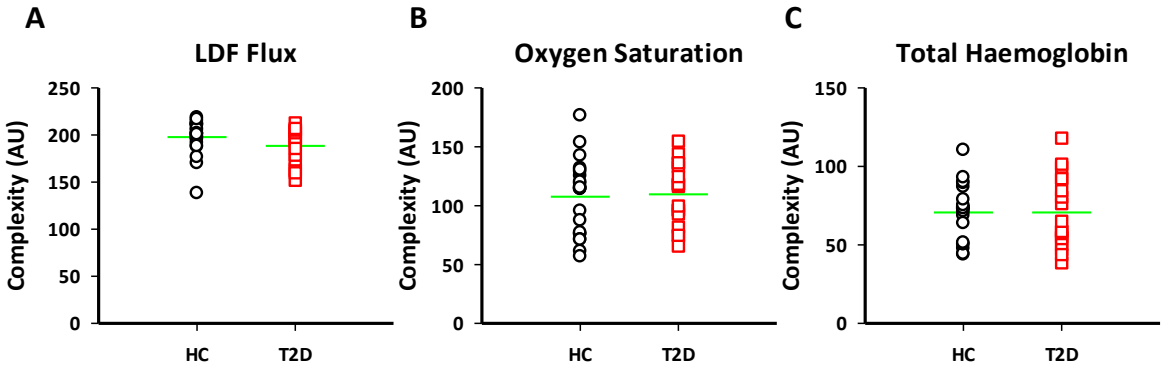

Figure 3.4: *Complexity analysis.* Complexity was calculated from 10min of skin+SC LDF flux and tissue oxygenation measures. A) LDF flux, B) O_2 Sat and C) tHb, **healthy control** (○ **HC**; n=23) and **T2D** (□ n=18) groups. — indicates mean.

3.3.5 Forearm skeletal muscle microvascular perfusion.

CEU was used to determine forearm microvascular perfusion of skeletal muscle (deep flexor) to give an indication of the distribution of the blood flow within the forearm. No difference in the skeletal muscle microvascular blood volume, filling rate or overall perfusion measure were seen between healthy control and T2D groups at rest (Figure 3.5).

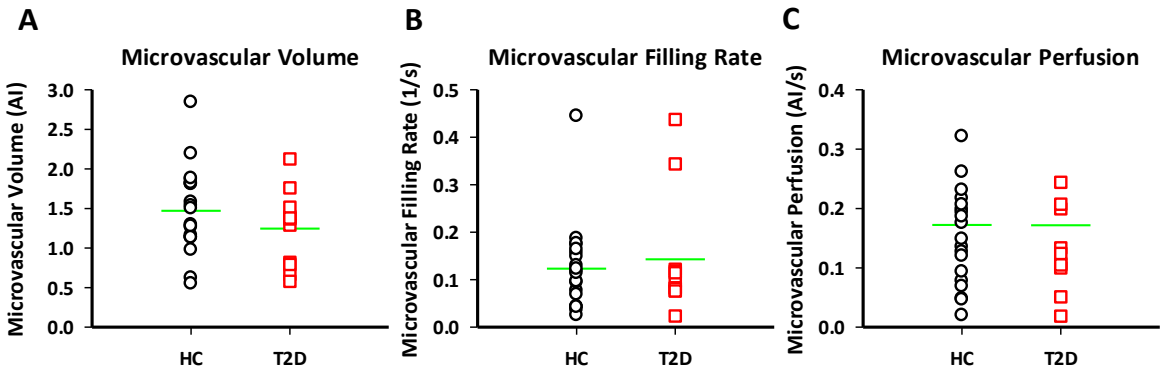

Figure 3.5: *Microvascular blood perfusion as assessed by CEU in forearm skeletal muscle.* Data were collected over 3 x 45sec loops using CEU to assess A) microvascular blood volume, B) microvascular filling rate and C) microvascular perfusion, **healthy control** (○ **HC**; n=20) and **T2D** (□ n=11) groups. — indicates mean.

3.3.6 Skin and subcutaneous tissue flowmotion measures

Figure 3.6 shows representative wavelet transformations traces of LDF flux, O_2 Sat and tHb measures plotted on a log frequency scale. The average wavelet transformation plots demonstrate overall flowmotion patterns and the contribution of each frequency component for a healthy control and type 2 diabetic.

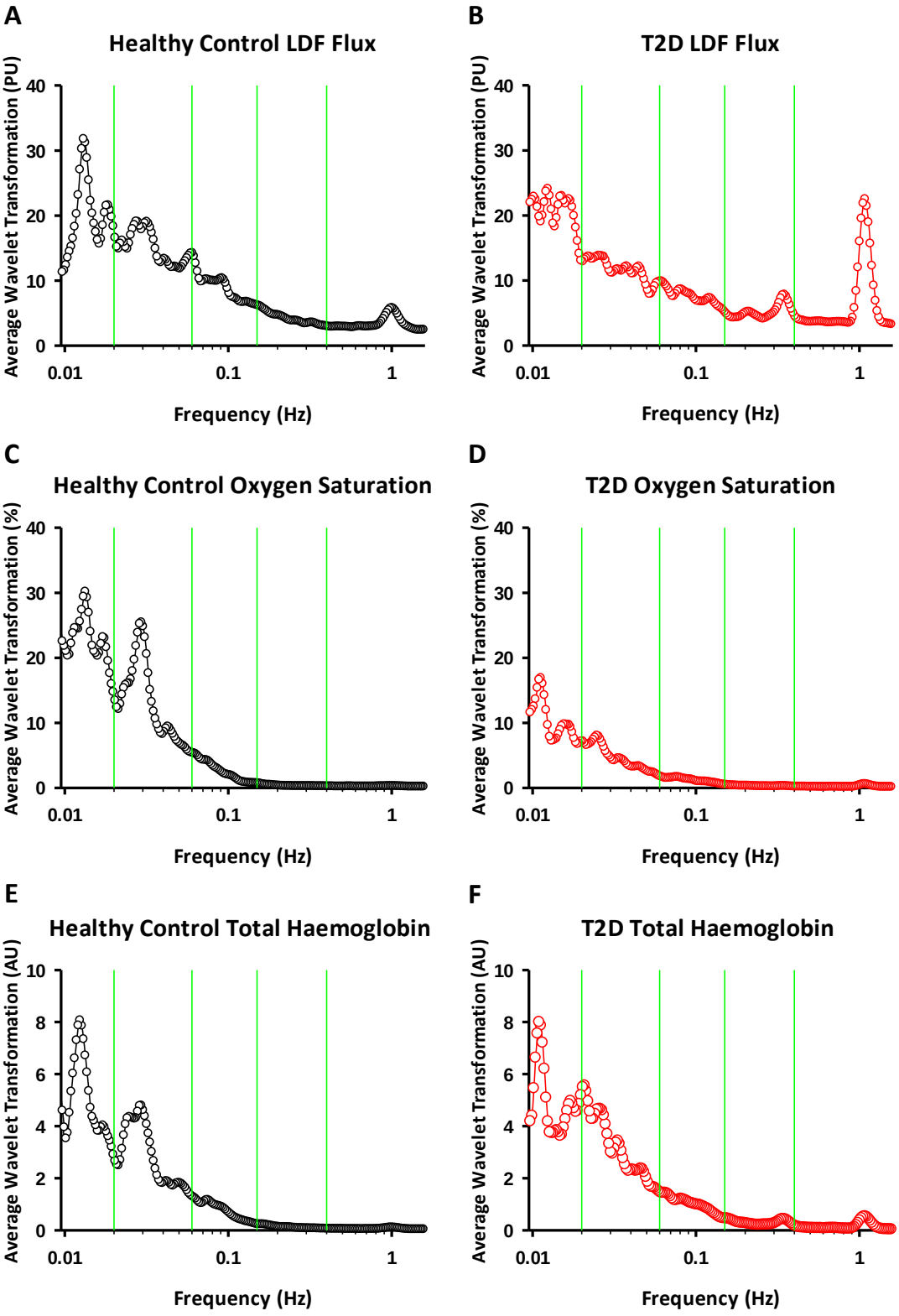

Figure 3.6: *Wavelet transformation of skin and subcutaneous tissue blood flow measures.* This figure shows wavelet transformations of skin+SC LDF flux (Panel A and B), O_2 Sat (Panel C and D) and tHb (Panel E and F) in **healthy control** and **T2D** participants. These traces are representative of the data collected in each group.

In order to quantify each frequency component within the wavelet transformation, peak AUC for each frequency range and the frequency at which the highest peak occurs was quantified with PeakFit software. Flowmotion assessed by LDF flux showed significant differences between healthy control and T2D groups in peak AUC (Figure 3.7). In both the respiratory and cardiac frequency components peak AUC in T2D group was significantly increased as compared to healthy controls, p = 0.010 and 0.028 respectively (Figure 3.7D and E). In addition, T2D participants tended to have a decreased input (assess by peak AUC) from the myogenic component (p = 0.072).

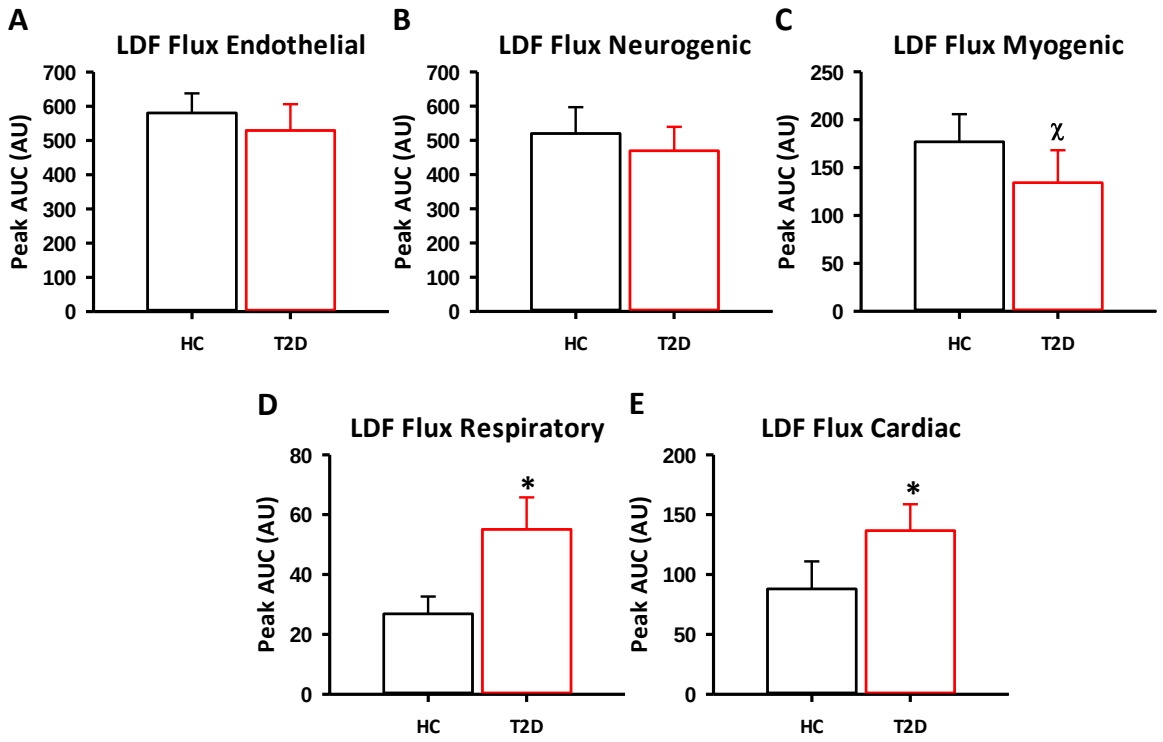

Figure 3.7: *LDF flux wavelet transformation: peak area under the curve for each flowmotion component.* The average peak AUC of wavelet transformed LDF flux measures for frequency regions A) endothelial B) neurogenic C) myogenic D) respiratory and E) cardiac. **Healthy control** (**HC**; n=23) and **T2D** (n=18). Data expressed as mean ± SE. * indicates significant difference between **healthy control** and **T2D** groups ($p < 0.05$). χ $p = 0.072$ between **T2D** compared to **healthy control**.

In each wavelet transformation, the frequency at which the highest peak occurred within each flowmotion component measured by LDF flux was identified (Table 3.3). For the cardiac component frequency was significantly higher ($p < 0.001$) in T2D group, indicating a higher heart rate. Using the

wavelet transformation, average heart rate was calculated for each group. The resting heart rate was 53.5 ± 1.7bpm for healthy controls compared to 67.6 ± 1.9bpm in T2D group. Peak frequency of the respiratory component was also significantly elevated in the T2D group (p = 0.007), indicating a higher average breathing rate, with rate 12.8 ± 1.0 breaths/min for healthy control and 15.4 ± 0.8 breaths/min in T2D group. In the lower frequency components there was a tendency for T2D participants to have slightly elevated rate of input from the endothelial, neurogenic and myogenic components, but this did not reach significance.

Table 3.3: *LDF flux wavelet transformation: peak frequency for flowmotion components.*

LDF Flux				
		Healthy Control	**T2D**	**P value**
Endothelial	*Frequency (Hz)*	0.012 ± 0.000	0.013 ±0.001	0.073
	Cycle period (secs)	85.6 ± 2.7	78.0 ± 3.6	
Neurogenic	*Frequency (Hz)*	0.028 ± 0.002	0.032 ± 0.002	0.068
	Cycle period (secs)	37.2 ± 1.7	32.8 ± 1.7	
Myogenic	*Frequency (Hz)*	0.070 ± 0.003	0.076 ± 0.003	0.108
	Cycle period (secs)	14.7 ± 0.52	13.4 ± 0.48	
Respiratory	*Frequency (Hz)*	0.214 ± 0.017	0.257 ± 0.013	**0.008**
	Cycle period (secs)	5.2 ± 0.34	4.1 ± 0.19	
Cardiac	*Frequency (Hz)*	0.892 ± 0.028	1.128 ± 0.036	**< 0.001**
	Cycle period (secs)	1.15 ± 0.04	0.899 ± 0.03	

Average peak frequency of each frequency region, expressed as frequency (Hz) and cycle period (seconds). Healthy control (n=23) and T2D (n=18) groups. Data expressed as Mean ± SE.

Wavelet transformation of tissue oxygenation measures are only able to adequately detect peaks in the three lower frequency, locally acting, flowmotion components (endothelial, neurogenic and myogenic). Quantification of O_2 Sat flowmotion measures showed a significantly lower (p = 0.017) endothelial peak AUC in T2D group (Figure 3.8A). However, while there was a similar trend of lower

contribution in T2D group, there was no difference in peak AUC in the neurogenic and myogenic components (Figure 3.8B-C).

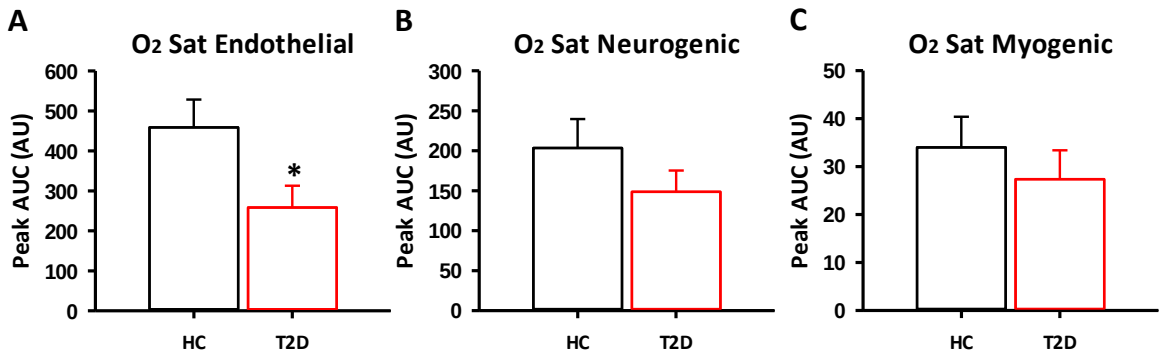

Figure 3.8: *O_2 Sat wavelet transformation: peak area under the curve for flowmotion components.* Average peak AUC of wavelet transformed O_2 Sat measures for frequency regions A) endothelial, B) neurogenic and C) myogenic. **Healthy control** (**HC**; n=23) and **T2D** (n=18) groups. Data expressed as mean ± SE. * indicates significant difference between **healthy control** and **T2D** groups (p = 0.017).

Table 3.4 shows the peak frequency for each component, or rate of input, which were similar between the two groups.

Table 3.4: *O_2 Sat wavelet transformation: peak frequency for flowmotion components.*

Oxygen Saturation				
		Healthy Control	**T2D**	**P value**
Endothelial	*Frequency (Hz)*	0.014 ± 0.001	0.013 ±0.001	0.469
	Cycle period (secs)	77.0 ± 3.5	80.2 ± 4.1	
Neurogenic	*Frequency (Hz)*	0.027 ± 0.001	0.030 ±0.002	0.221
	Cycle period (secs)	37.4 ± 1.2	34.6 ± 1.8	
Myogenic	*Frequency (Hz)*	0.075 ± 0.004	0.084 ±0.005	0.317
	Cycle period (secs)	14.1 ± 0.77	12.3 ± 0.54	

Average peak frequency of each frequency region, expressed as frequency (Hz) and cycle period (seconds). Healthy control (n=23) and T2D (n=18) groups. Data expressed as mean ± SE.

For tHb measure, wavelet transformation peak AUC in endothelial and myogenic frequency components (Figure 3.9) was significantly lower in the T2D as compared to healthy control (p = 0.017 and p = 0.047 respectively). In the neurogenic frequency component there was a trend of decreased T2D peak AUC compared to healthy controls (p= 0.101).

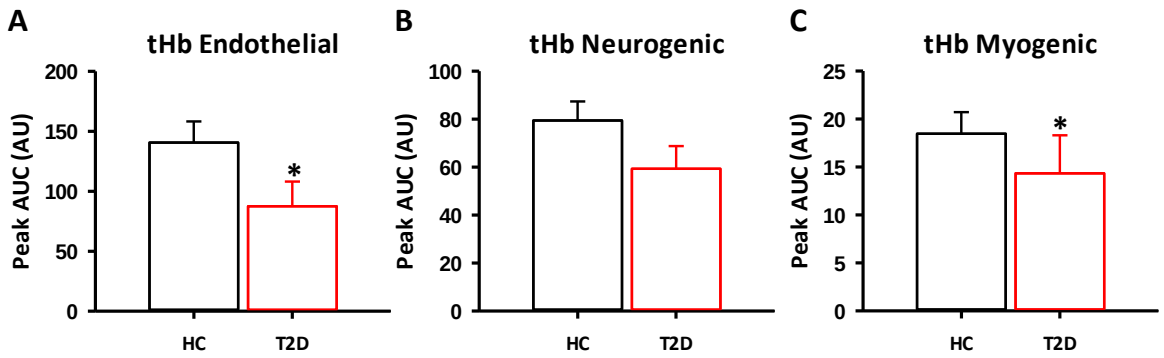

Figure 3.9: *tHb wavelet transformation: peak area under the curve for flowmotion components.* Average peak AUC of wavelet transformed tHb measures for frequency regions A) endothelial, B) neurogenic and C) myogenic. **Healthy control** (**HC**; n=23) and **T2D** (n=18) groups. Data expressed as mean ± SE. * indicates significant difference between **healthy controls** and **T2D** groups ($p < 0.05$).

In the tHb measures, no significant difference in peak frequency between the two groups were seen (Table 3.5).

Table 3.5: *tHb wavelet transformation: peak frequency for flowmotion components.*

Total Haemoglobin				
		Healthy Control	**T2D**	**P value**
Endothelial	*Frequency (Hz)*	0.0 14 ± 0.001	0.013 ±0.001	0.286
	Cycle period (secs)	77.2 ± 3.8	84.3 ± 4.5	
Neurogenic	*Frequency (Hz)*	0.029 ± 0.002	0.031 ± 0.002	0.247
	Cycle period (secs)	36.5 ± 1.4	34.1 ± 1.7	
Myogenic	*Frequency (Hz)*	0.070 ± 0.002	0.074 ± 0.003	0.082
	Cycle period (secs)	14.5 ± 0.42	13.7 ± 0.42	

Average peak frequency of each frequency region, expressed as frequency (Hz) and cycle period (seconds). Healthy control (n=23) and T2D (n=18) groups. Data expressed as Mean ± SE.

3.4 Discussion

This study determined several differences in skin+SC microvascular flowmotion between healthy control and T2D groups at rest. An elevated rate and contribution to flowmotion was seen in the higher frequency components (cardiac and respiratory) in the T2D group (Figure 3.7 and Table 3.2). Whilst the lower frequency components (endothelial, neurogenic and myogenic) showed a lower contribution to flowmotion compared to healthy controls (Figure 3.8 and 3.9). There were also differences in total blood flow to the forearm and the distribution of that flow throughout, with elevated brachial blood flow and skin+SC perfusion in the T2D group (Figure 3.2 and 3.3). Complexity analysis of LDF + OXY data failed to show any differences in randomness of signal between the healthy control and T2D groups at rest (Figure 3.4).

The anthropometric measures and clinical blood chemistries show a clear, expected difference in health parameters of healthy controls and the diagnosed type 2 diabetics (Table 3.1). Anthropometric measures in the T2D group show an overt disease state with increased body mass and BMI (30.9 ± 1.5kg/m^2, indicating obesity) compared to the healthy controls (25.3 ± 0.6kg/m^2, on the upper end of normal) (234)), and significantly elevated fasting blood glucose, HbA1c and plasma insulin. T2D participants were hypertensive (systolic BP = 131.9 ± 3.9mmHg), indicating dysfunction in the cardiovascular system. All type 2 diabetes were on a form of antidiabetic medication, with the majority (92%) taking metformin, while only 15% were taking insulin. Additionally, 62% were taking antihypertensive medication and 77% on cholesterol lower medication. The need of the medications, again highlights an overt disease state in these individuals.

The activity threshold of <30min of moderate exercise per week was only applied to the T2D group, activity level. As such, there is potentially varied level of activity within the healthy control group which is likely to result in difference in the cardiovascular health of the control group. This gives a more

accurate sample of the general healthy population and the variation within the healthy control group adds power to the study.

Several different measures were used to assess blood flow distribution in the forearm. Brachial artery blood flow (total flow measured by 2D-ultrasound) was significantly elevated in the T2D group at rest (Figure 3.2). Likewise, skin+SC microvascular blood flow (assessed by LDF flux) was also elevated in the T2D group (Figure 3.3), indicating a greater amount of blood flow within the skin+SC microvasculature at rest. Importantly, there was no influence of skin temperature on perfusion. LDF flux is affected by temperature, with flux increasing as temperatures rise (235). It therefore appears that in response to the higher total blood flow to the forearm, there was a greater amount of blood flow to the skin+SC in these T2D participants. Tissue oxygenation measures in the skin+SC were no different between the two groups. Interestingly, there were no differences in skeletal muscle perfusion between the two groups (measured by CEU) at rest. The average duration of diabetes was 7.08 ± 1.4 years and as such the lack of difference in skeletal muscle perfusion is not all that surprising as capillary rarefaction in the skeletal muscle develops in T2D over prolonged periods of time (236, 237). Blood flow in the underlying skeletal muscle of the forearm at rest therefore appears to not be affected by T2D, whereas the skin+SC flux and total flow of the forearm does.

The assessment of skin+SC flowmotion in healthy control and T2D participants showed a number of interesting results. Upon wavelet transformation of skin+SC LDF flux microvascular blood flow measures, it was found that the higher frequency components (respiratory and cardiac) are only adequately detected with the LDF flux measure, not the tissue oxygenation (section 3.3.6). This result is most like due to the ability of LDF to detect both RBC cell number (volume) as well as the velocity at which they travel, while it is thought that the tissue oxygenation measures mostly just RBC number (volume) (63). Therefore, based on the observations made with wavelet transformation of blood flow

data it is thought that the higher frequency components may exert their effect on flowmotion primarily by controlling velocity of blood flow.

Both the rate and contribution to flowmotion of cardiac and respiratory components was elevated in the T2D group (Figure 3.7 and Table 3.2). Patients with T2D are known to have cardiovascular dysfunction that leads to increased heart rate and respiration (238-240). The elevated rate of cardiac and respiratory components to flowmotion is therefore consistent with the literature and the problems associated with the disease (72). The pathological changes to the cardiovascular system seen in T2D, such as arterial stiffening (200), may also account for the increased contribution of the cardiac and respiratory component of flowmotion. In these participants the greater stress placed upon the heart and larger blood vessels may have led to a pathological change in the contribution of the higher frequency components to flowmotion through such changes as the development of atherosclerosis and medial calcification (241).

The contribution to flowmotion of the endothelial (detected by O_2 Sat and tHb, Figure 3.8 and 3.9) and myogenic (detected by tHb, Figure 3.9) components was decreased in the T2D group. A reduced input in these lower frequency components have been seen previously. Stansberry et. al. (242) examined flowmotion patterns in the fingers of healthy and T2D participants, and found reduced input of the lower frequency components to flowmotion in T2D, as is also seen in the current study. Differences in the contribution to flowmotion in the lower frequency components were seen in the tissue oxygenation measures, but not the LDF flux. These differences in the flowmotion measures may relate to the differing penetration of each type of measure. It is thought that the white light spectroscopy (400-700nm) used to determine tissue oxygenation measures has less penetration into the skin+SC than the LDF flux (785 ± 10nm) (60, 61). As such, the two different microvascular blood flow measures may determine RBC movement in slightly different tissue volumes at the same skin site. Tissue oxygenation measures determine flow in more superficial layers of the skin+SC, whereas

LDF flux can measure flow in both the superficial skin layers and deeper into the subcutaneous tissue. Therefore, the difference in skin+SC flowmotion measures by LDF flux and tissue oxygenation at the same skin sight may be explained by the different volumes and combination of tissues each light source is able to illuminate.

The reduction in lower frequency contribution to flowmotion in the T2D group is not surprising due to the pathological changes in microvascular function commonly seen in this disease. Endothelial dysfunction in insulin resistance leads to an attenuated response to insulin-mediated, NO-dependant vasodilation, while the concurrent ET-1 induced vasoconstriction activated by insulin (to maintain a balanced vascular tone) is not affected. The result is a pathological vasoconstriction in the microvasculature (191). Additionally, chronic elevation of blood glucose levels leads to pathological changes to endothelial proteins (due to glucose induced damage) and a dysregulation of endothelial cell function (233). The changes in endothelial signalling pathways and protein destruction result in dysfunction of normal endothelial activity, and thus may explain the reduction in endothelial contribution to flowmotion in T2D group.

A reduction in the contribution of the myogenic component in T2D participants indicates an altered vasomotion or intrinsic contraction of vessel smooth muscle cells. The specific mechanism altering vasomotion in T2D is not clear, but it may be causing disruption to the intracellular synchronisation of Ca^{2+} release within the vessel smooth muscle cells, which is hypothesised to drive vasomotion activity (106, 109). Changes to the regulation of Ca^{2+} release within the smooth muscle cells results in changes to cellular contraction and thus could be altered in T2D, therefore changing the contribution of myogenic input to overall flowmotion patterns (10).

It was surprising that no difference in the neurogenic component, either contribution to flowmotion or frequency of input, was seen in this study as T2D is known to involve autonomic dysfunction (198,

199). A number of previous studies looking at skin+SC flowmotion in obesity and T2D have reported changes in the neurogenic component at rest (95, 98, 215, 217). However, the participants in these studies were measured at different time points in disease progression to the current study. A number of the studies that describe changes in the neurogenic component measured skin+SC flowmotion in obese individuals who were not yet clinically diagnosed with T2D (95, 215, 243). These studies showed dysfunction in the neurogenic component, perhaps indicating that changes to this component of flowmotion may be involved in the early progression of the disease. Other studies reporting changes to the neurogenic component were performed on T2D participants with advanced disease who had developed neuropathy as a consequence of T2D (98, 217, 218). Again, neurogenic dysregulation may have been involved in the advancement of disease state either contributing to the development of neuropathy or resulting from the damage to the nervous system which occurs in this disease. In the current study where T2D participants are clinically diagnosed, but have no additional disease (including cardiovascular disease, neuropathy, retinopathy and nephropathy), the lack of difference to the healthy controls in the neurogenic component at rest may be attributed to the stage of disease progression of these participants. Changes in the neurogenic component of flowmotion in T2D may vary based on the duration of disease in an individual and the development of further complications such as neuropathy.

Complexity measures have previously been used to show dysfunction in skin microvascular blood flow in type 2 diabetic monkeys (226), with disease progression associated with a reduction in skin+SC blood flow complexity. Analysis of flowmotion with wavelet transformation in this study showed differences between healthy control and T2D groups. It was therefore thought that transformation of human skin+SC LDF flux and tissue oxygenation measures with complexity analysis would show a difference in the randomness in T2D skin+SC blood flow and provide a means of quickly and easily determining the presence of skin+SC blood flow dysfunction in an individual. However, at rest no difference in complexity of LDF flux or tissue oxygenation measures were seen between healthy

control and T2D groups (Figure 3.6), indicating skin+SC complexity measures in humans may not be suitable for identifying blood flow dysfunction.

An important factor when comparing the difference in flowmotion patterns between healthy controls and type 2 diabetics not taken into consideration here is the influence of insulin upon flowmotion measures. In order to fully understand the flowmotion dysregulation which occurs in T2D, an understanding of how insulin changes flowmotion in healthy controls and how this may be attenuated in T2D needs to be investigated. Due to the endothelial-dependent pathway through which insulin stimulates blood flow changes, and insulin stimulation of the SNS (157, 244), respiration and cardiac output (245, 246), it is thought that insulin alters flowmotion patterns. A number of studies examining skin+SC flowmotion in response to insulin stimulation (either a euglycemic hyperinsulinemic clamp (216) , consumption of a mixed meal (247) or direct delivery of insulin to the skin+SC via iontophoresis (215)) show changes to overall flowmotion and the contribution of lower frequency components. It was therefore expected that in the healthy control group of this study, insulin release would cause changes to skin+SC flowmotion patterns. While in the T2D group assessed in this study, where insulin resistance and pancreatic failure have led to glucoregulatory and cardiovascular dysfunction (elevated heart rate, respiration, systolic blood pressure, total flow and skin+SC microvascular perfusion), it is thought that insulin release will not result in a stimulation of flowmotion.

Chapter 4 - *Microvascular flowmotion in the skin and subcutaneous tissue in healthy controls and type 2 diabetics: oral glucose challenge*

4.1 Introduction

Insulin modifies skeletal muscle blood flow by stimulating NO-dependent smooth muscle vasodilation, resulting in enhanced blood flow through the tissue and promoting glucose uptake (248). There is evidence to suggest that insulin induces a change in flowmotion (157, 244, 245), complementing the enhanced level of capillary perfusion and facilitating further delivery of insulin and glucose to the myocyte. However, there is significant variation in the literature in regards to which components of flowmotion insulin affects. Most of these discrepancies can be attributed to differences in study design and the characteristics of participants, which lead to inconsistent findings regarding the mechanism by which insulin may influence flowmotion. For example, de Jongh *et. al.* (249), using an LDF probe implanted directly into skeletal muscle tissue, showed increased activity in endothelial and neurogenic components of flowmotion in response to a euglycemic hyperinsulinemic clamp. In contrast, using a LDF probe on the skin, Rossi *et. al.* (250) used spectral analysis of skin+SC LDF flux to demonstrate an increased myogenic component of flowmotion upon local insulin stimulation, delivered by iontophoresis. Additionally, Jonk *et. al.* (247), also measuring skin+SC flowmotion with LDF, observed an increase in the contribution of all components of flowmotion in response to consumption of a mixed meal. These studies highlight the varied observations in insulin-mediated flowmotion changes, and thereby the need to further investigate the changes in flowmotion that occur in response to insulin.

Aberrant changes in flowmotion have been observed during both acute and chronic insulin resistance. A study by Newman *et. al.* (57) performed in an anaesthetised rat model, showed an increase in the myogenic component of flowmotion with insulin infusion, which was then attenuated during an acute insulin-resistant state induced by the vasoconstrictor α-methylserotonin. Clough *et. al.* (215) observed an increased contribution to skin+SC flowmotion (LDF flux) in the endothelial component in response to insulin stimulation (iontophoresis) in healthy controls, which was significantly attenuated in participants with central obesity. Similarly, using skin+SC LDF flux measures, de Jongh *et. al.* (219)

showed an attenuated response to insulin stimulation (iontophoresis) in the skin+SC of obese women, with reduced endothelial and neurogenic contribution. These studies demonstrate an attenuation of insulin-mediated flowmotion in insulin resistance. Changes to skin+SC vasomotion have been observed in T2D (242, 251). Using skin+SC LDF flux measures and Fast Fourier analyses, Stansberry *et. al.* (242) showed an impairment in lower-frequency vasomotion in 75% of type 2 diabetics compared to age matched healthy controls. Changes to flowmotion in key metabolic tissues such as skeletal muscle may reduce blood flow directly to myocytes, and thereby contribute to the reduced glucose disposal in insulin resistance and T2D. It is therefore important to understand the changes in flowmotion induced by insulin and how these may become dysfunctional in T2D.

The primary aim of this study was to determine the difference in skin+SC flowmotion response to an endogenous release of insulin, via an oral glucose challenge (OGC), in healthy control and T2D participants.

A limitation of most studies investigating changes in flowmotion in disease states such as obesity, insulin resistance and T2D is that blood flow measures are performed primarily on skin using LDF flux. Changes in flowmotion in more metabolically important tissues such as skeletal muscle are of greater interest in understanding the dysfunction and pathogenesis of these diseases. It is not clear if skin+SC measures of blood flow are an appropriate substitute for blood flow in deeper more metabolically relevant tissues such as skeletal muscle. Due to the different roles of skin+SC (protective and thermoregulation) and skeletal muscle (highly metabolic tissue) (252) in the body it is unlikely that blood flow patterns would be similar between the two tissues. A secondary aim of this study was therefore to determine if there is a consistent response to OGC in measures of forearm total blood flow, skin+SC microvascular flux and skeletal muscle microvascular perfusion. This comparison was to determine whether skin+SC flowmotion measures are representative of skeletal muscle flowmotion, a more metabolically active tissue and target of insulin.

4.2 Methods

The study outlined in this chapter was performed on the same day and same participants descried in chapter 3. After basal measures were taken, participants (characteristics reported in section 3.2) underwent an oral glucose challenge. While a 75g glucose load is used clinically for the diagnosis of T2D, this study used a 50g glucose load. Preliminary experiments showed that when administered in healthy participants, a 75g glucose load resulted in significantly reduced skeletal muscle blood flow response (when an increase was expected with endogenous insulin release (247)) and participants feeling ill (nauseous and/or light headed). This was thought to occur due to an excessive activation of the SNS in these insulin sensitive participants (253). Therefore, a modified 50g glucose load was used in the current study as it has previously been shown to be well tolerated in healthy participants, while still eliciting a significant change in blood glucose and plasma insulin levels in both healthy control and T2D participants (254).

4.2.1 Protocol

Before commencement of the OGC, a fasting blood glucose sample was obtained from the antecubital vein of the non-dominant arm. A 50g glucose drink (GLUCO SCAN, SteriHealth, Australia) was then consumed orally at t = 0 mins. Participants had 5mins to fully consume the drink. Blood glucose and plasma insulin levels were monitored over 120min after the consumption of glucose via venous samples from the antecubital vein at t = 15min, t = 30min and then every 30min up to the 120min time point (Figure 4.1). A time-course of blood glucose and plasma insulin was plotted and the AUC of each time course was determined to give an overall indication of glucoregulatory function in healthy control and T2D groups.

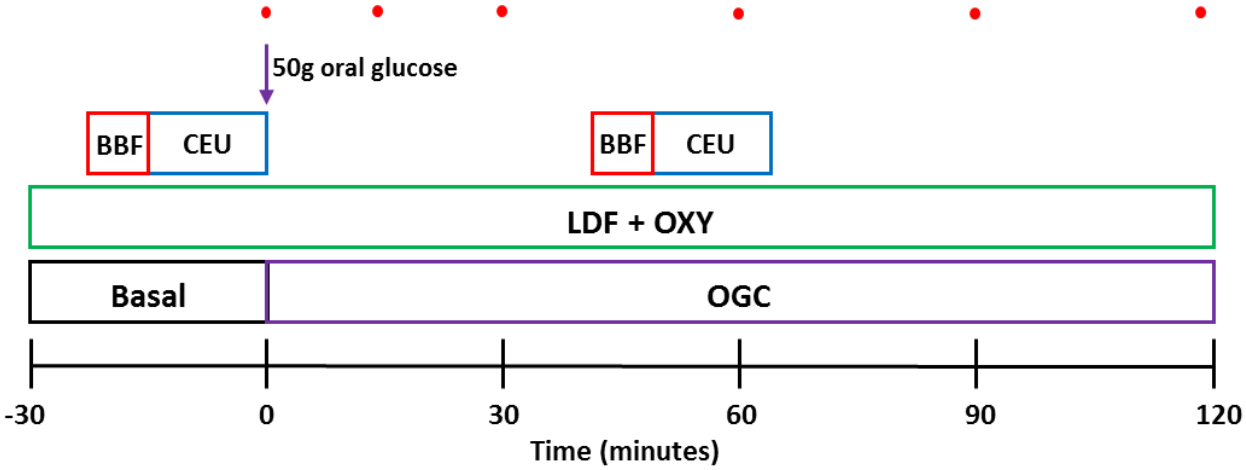

Figure 4.1: *Oral glucose chanllenge (OGC) study protocol.* Participants lay in a semi-recumbent possition thoughout testing. An initial **basal** period was observed and then 50g of liguid glucose was comsumed orally. Forearm skin+SC **LDF + OXY** measures where taken throughout **basal** and **OGC**. Total forearm blood flow was determined by measuring **BBF** during **basal** and at t = 45min into **OGC**. Skeletal muscle micorvascuar perfusion was determned using **CEU** at rest and at = 60min of **OGC**. Venous blood samples where taken before and then thoughout **OGC** (●).

The blood flow measures taken previously at rest (described in section 3.2.2) were repeated during the OGC as described below. Timing of measurements was based on the peak glucose concentration in the blood, while trying to minimise the influence of other measurements occurring around the same time. Vascular resistance was calculated from MAP and BBF to give an indication of vasodilatory state.

Vascular resistance = MAP (mmHg)/BBF (min/mL)

4.2.1.1 Skin and subcutaneous tissue microvascular blood flow

The LDF + OXY probe (described in section 2.1.2) was attached to the midsection of the ventral side of the right forearm. Skin+SC LDF flux and tissue oxygenation measures were continuously recorded throughout basal and OGC (Figure 4.1). Skin+SC microvascular flowmotion was assessed with LDF flux and tissue oxygenation measures over two 20min time periods during basal (t = -30 to -10min) and then during OGC (t = 35-45min).

4.2.1.2 Total forearm blood flow

Total flow into the forearm was determined by measuring the brachial artery blood flow with a L12-5 linear array ultrasound transducer (describe in section 2.1.4). Brachial artery diameter and blood velocity were determined, and brachial blood flow (BBF) calculated as described previously in 2.1.4. BBF measures were taken at basal (t = -20min) and then at t = 45min into OGC (Figure 4.1).

4.2.1.3 Forearm skeletal muscle microvascular perfusion

Microvascular blood volume, filling rate and perfusion of forearm deep flexor muscle was determined with CEU as described in section 2.1.3. CEU measures were taken in triplicate during basal period (t = -10min) and then at t = 60min of OGC.

4.2.1.4 Blood analysis

Blood samples taken at fasting and throughout OGC (Figure 4.1) were analysed for blood glucose and plasma insulin as described in section 2.1.6.

4.2.2 Data analysis

4.2.2.1 Microvascular blood flow averages

Mean LDF flux and tissue oxygenation measures over a 10min time period during basal (t = -30 to -20min) and at t = 50 to 60min of OGC were determined as described in section 2.1.8.1.

4.2.2.2 Complexity measures

Mean complexity measures over the same 10min time period during basal (t = -30 to -20min) and OGC (t = 50 to 60min) as average LDF flux and tissue oxygenation measures was calculated as described in

section 2.1.8.2. The timing of measure is based on the peak glucose concentrating into the blood and ensuring clean data was analysed that had not been influenced by other measures.

4.2.2.3 Flowmotion measures

Flowmotion analysis using wavelet transformation was performed on 20min of basal (t = -30 to -10min) and OGC (t = 35 to 55min) LDF flux and tissue oxygenation measures. Wavelet transformation data were then quantified by determining AUC of peaks within each flowmotion frequency component and peak frequency, as described in section 2.1.8.3. The timing of measure is based on the peak glucose concentrating into the blood and ensuring clean data was analysed that had not been influenced by other measures.

4.3 Statistical analysis

Two-way repeated measures ANOVA were performed to determine difference at basal and during OGC between healthy control and T2D groups with a Student-Newman-Keuls post hoc test, as described in section 2.4. An unpaired Student's t-test was used to determine the difference in change during OGC from basal between healthy control and T2D groups. The correlation between change during OGC from basal in LDF flux and microvascular perfusion measures in all participants (healthy control and T2D groups were combined) was performed with a linear regression on parametric data and Spearman Correlation analysis on non-parametric, as described in section 2.4.

4.3 Results

4.3.1 OGC blood glucose and plasma insulin

After overnight fasting participants were given a 50g oral glucose load (OGC) to assess insulin sensitivity. Blood glucose and plasma insulin response to OGC was monitored throughout the protocol. Fasting blood glucose levels were significantly elevated ($p < 0.001$) in the T2D group, compared to healthy controls (10.2 ± 1.0 and 4.9 ± 0.0 mM respectively). Throughout the OGC the blood glucose concentrations were significantly higher ($p < 0.001$) in the T2D group (Figure 4.2A), resulting in a significantly larger ($p < 0.001$) AUC in the T2D group (Figure 4.2B). From t = 30min onwards the change from basal of blood glucose during OGC was significantly elevated ($p < 0.002$) in T2D group (Figure 4.2C). While fasting plasma insulin was significantly elevated ($p < 0.001$) in T2D participants (97.3 ± 17.8pM) compared to healthy controls (40.5 ±1.7pM), there was no difference between the two groups during the OGC (Figure 4.2D), and no difference in the calculated absolute AUC (Figure 4.2E). Despite the difference in fasting plasma insulin levels, there was no difference in the change from basal at any time point throughout OGC (Figure 4.2F).

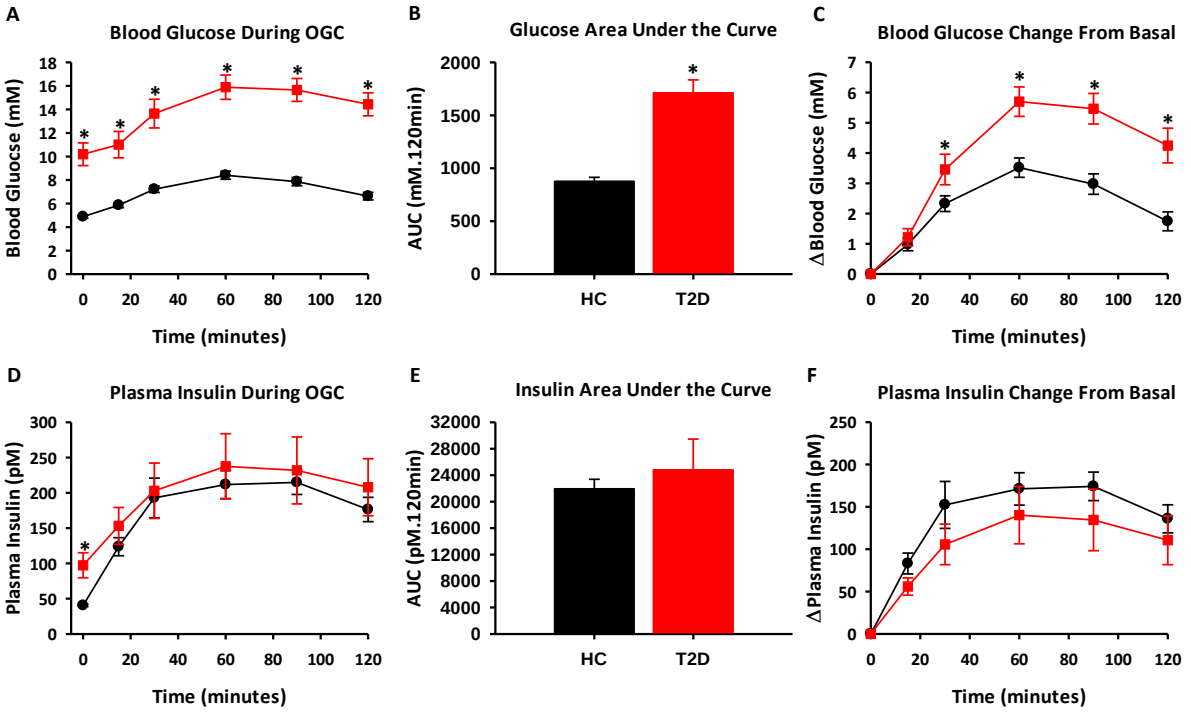

Figure 4.2: *Blood glucose and plasma insulin response to OGC.* A) Blood glucose response to OGC, the B) calculated area under the curve (AUC) of OGC time course, and C) blood glucose during OGC represented as change from basal. D) Plasma insulin response to OGC, the E) calculated AUC of OGC time course and F) plasma insulin during OGC represented as change from basal. **Healthy control** (● **HC**; n=23) and **T2D** (■ , n=18) groups. Data expressed as mean ± SE. * indicates significant difference between **healthy control** and **T2D** groups ($p < 0.02$).

4.3.2 Forearm total flow

Total blood flow to the arm was measured by determining brachial artery blood flow (BBF) using 2D-ultrasound at basal (t = -20min) and at t = 45min of OGC (Figure 4.3). In the healthy control group there was no change in total flow to the forearm with the OGC. In the T2D group, BBF was significantly elevated ($p = 0.006$) 45mins post OGC from basal. Total flow to the arm in the T2D group was significantly higher than healthy controls both during basal and t = 45min into OGC ($p = 0.039$ and $p < 0.001$ respectively).

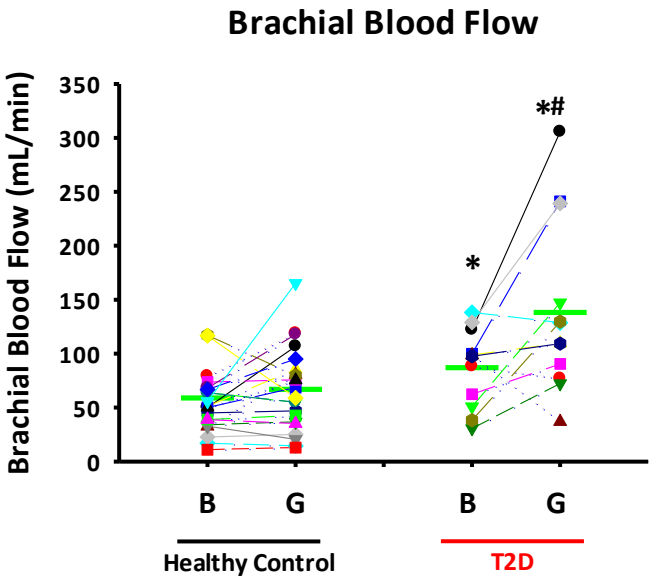

Figure 4.3: *Brachial artery blood flow in response to OGC.* Brachial artery blood flow (mL/min) measured during basal (B) and 45min after OGC (G). **Healthy control** (**HC**; n=23) and **T2D** (n=15) groups. Time points of each individual participant is represented by a different signal, — indicates mean. ***** indicates significant difference between **healthy controls** and **T2D** ($p < 0.05$). **#** indicates significant difference from basal to OGC in **T2D** group ($p = 0.006$).

4.3.3 Skin and subcutaneous tissue microvascular blood flow and tissue oxygenation

LDF flux, O_2 Sat and tHb data were determined by calculating a 10min average during basal (t = -30min) and 60min post OGC (Figure 4.4A-C). In the healthy control group, there were no changes in microvascular blood flow measures (LDF flux, O_2 Sat and tHb) during OGC compared to basal. The T2D group, had significnatly higher basal ($p = 0.027$) and OGC ($p = 0.004$) LDF flux than healthy controls. Within the T2D group O_2 Sat, but not tHb, was significantly elevated ($p < 0.001$) in OGC compared to basal. The change during OGC from basal was calculated for each blood flow measure to determine difference in response to OGC in each group (Figure 4.4D-E). The only difference in the change from basal was in the O_2 Sat measure, where the increase from basal during OGC in T2D group was a significantly different to the decrease from basal during OGC in the healthy controls ($p = 0.010$).

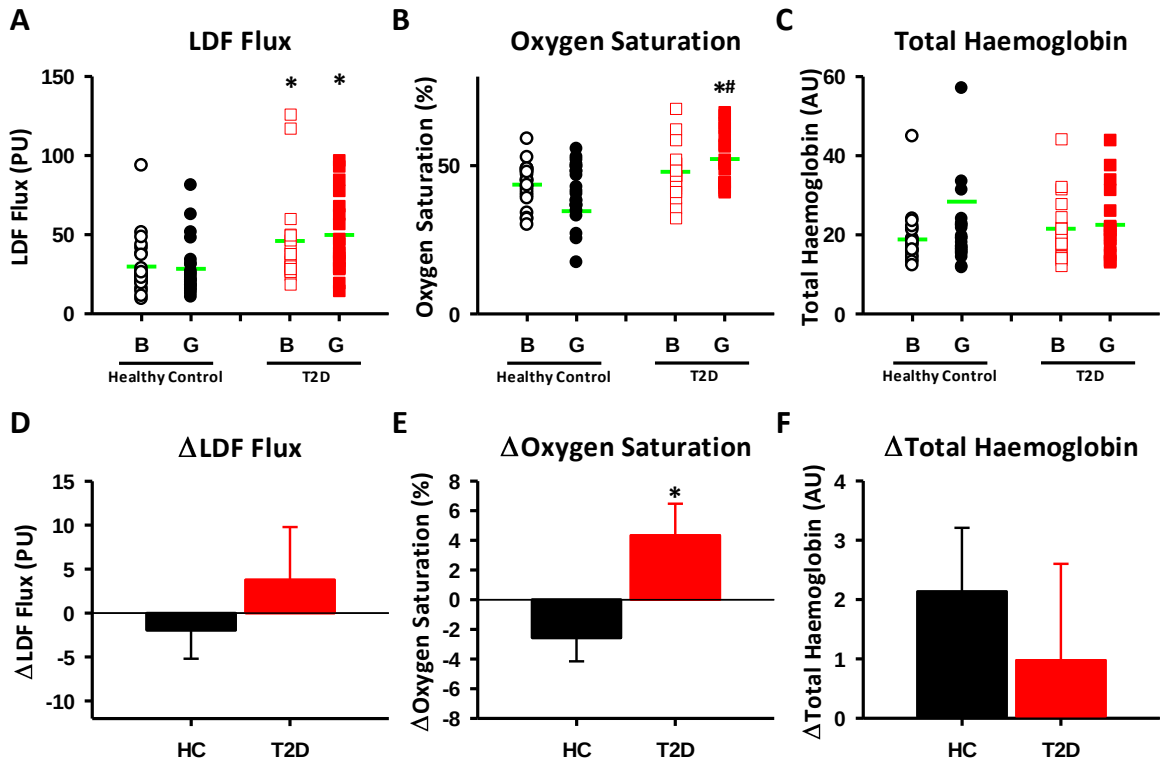

Figure 4.4: *LDF flux and tissue oxygenation response to OGC.* A) LDF flux B) O_2 Sat and C) tHb in the skin+SC were determined over a 10min time period at basal (B; open symbol) and 60min post OGC (G, filled symbol). Change during OGC from basal for each measure was determined to give D) ΔLDF flux E) ΔO_2 Sat and F) ΔtHb. **Healthy control** (● **HC**; n=23) and **T2D** (■, n=18) groups. Data expressed as mean ± SE. * indicates significant difference between healthy **controls** and **T2D** ($p < 0.05$). **#** indicates significant difference from basal to OGC in T2D group ($p = 0.027$).

4.3.4 Skin and subcutaneous complexity measures

Complexity analysis was performed on the average LDF flux and tissue oxygenation measures using the same 10min time points used to calculate average flux (during basal, t = -30min and at t = 60min of OGC), to determine randomness of skin+SC blood flow (Figure 4.5). No significant changes from basal to OGC were seen in LDF flux or tHb measures. In the T2D group complexity calculated from the O_2 Sat measures showed a significant increase from basal during OGC ($p = 0.013$).

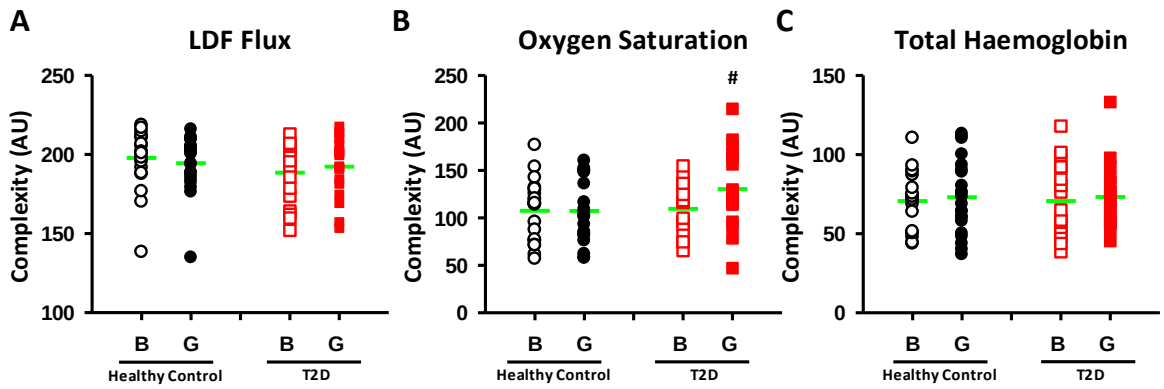

Figure 4.5: *Complexity analysis pre and post OGC.* Complexity was calculated from 10min of LDF flux and tissue oxygenation measures during basal (B, open symbol) and OGC (G, filled symbol). A) LDF flux B) O_2 Sat and C) tHb measures**.** (● **HC**; n=23) and **T2D** (■, n=18) groups. — indicates mean. **#** indicates significant difference from basal to OGC, p = 0.013.

4.3.5 Forearm skeletal muscle microvascular perfusion

Skeletal muscle microvascular perfusion in the forearm was measured to determine changes in blood flow distribution from basal to OGC (Figure 4.7). In the healthy controls microvascular blood volume and perfusion were significantly decreased during the OGC compared to basal (p = 0.024 and p = 0.001 respectively). There was no change in microvascular blood volume, filling rate or perfusion between basal and at 50-60mins into the OGC in the T2D group (Figure 4.7A-C). The change during OGC from basal was calculated for each blood flow measure to determine difference in response to OGC in each group (Figure 4.7D-E). There was a trend (p = 0.099) for a greater decrease in microvascular volume during the OGC in healthy control compared to T2D group, but no significant difference in change during the OGC from basal in any of the skeletal muscle microvascular perfusion measures.

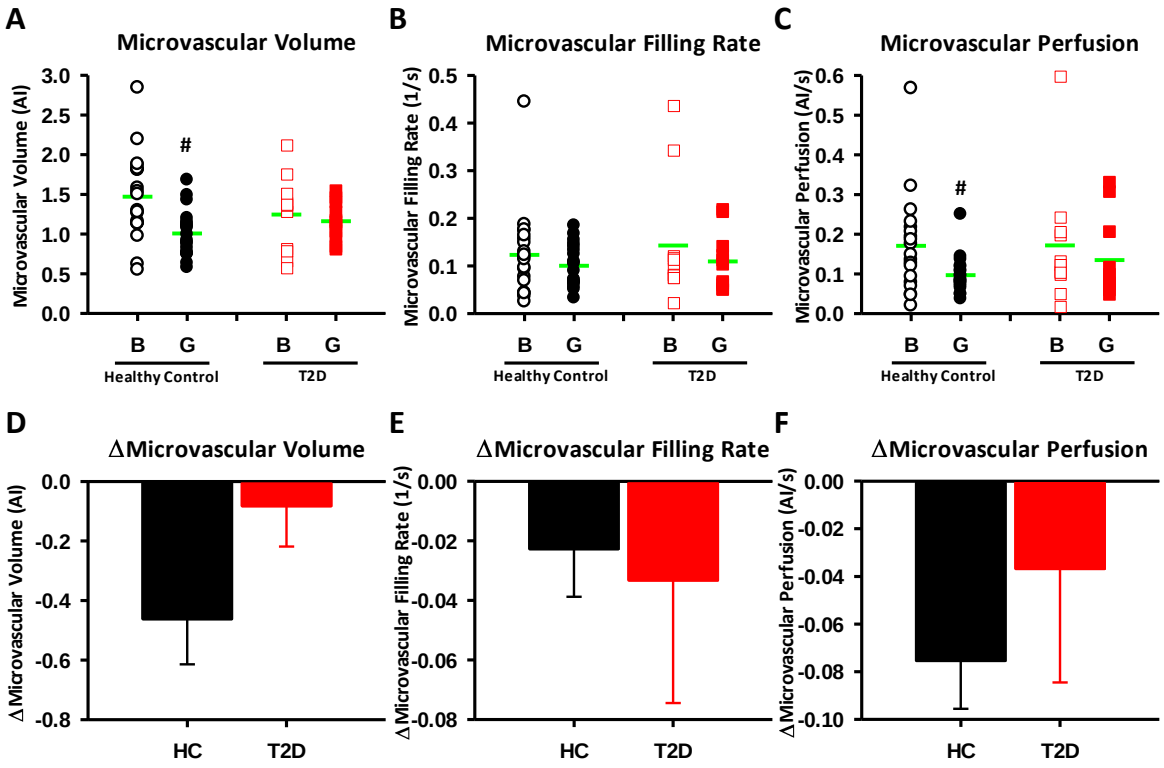

Figure 4.6: *Response to OGC of microvascular blood perfusion as assessed by CEU in forearm skeletal muscle.* Basal (B, open symbol) and OGC (G, filled symbol) data were collected over 3 x 45sec using CEU to assess A) microvascular blood volume, B) microvascular filling rate and C) microvascular perfusion. Change during OGC from basal for each measure was determined to give D) Δmicrovascular blood volume, E) Δmicrovascular filling rate and F) Δmicrovascular perfusion. **Healthy control** (● **HC**; n=23) and **T2D** (■, n=15) groups. Data expressed as mean ± SE. **#** indicates significant difference from basal to OGC ($p < 0.01$).

4.3.6 Correlation between skin and subcutaneous tissue flux and skeletal muscle perfusion

To determine if skeletal muscle and skin+SC had a similar vascular response to the OGC, a correlation analysis was performed. The change in skin+SC LDF flux was compared to the change in skeletal muscle microvascular blood volume (Figure 4.7A) and perfusion (Figure 4.7B) in response to the OGC. Healthy control and T2D groups were combined in the analysis to give an n of 30. There was no significant correlation (R = 0.175, p = 0.809) between the change in skin+SC LDF flux and the change in skeletal muscle microvascular blood volume between basal and OGC (Figure 4.7A). Similarly, there was no significant correlation (R = 0.0477, p = 0.834) between the change in skin+SC LDF flux and the change in skeletal muscle microvascular perfusion (Figure 4.7B).

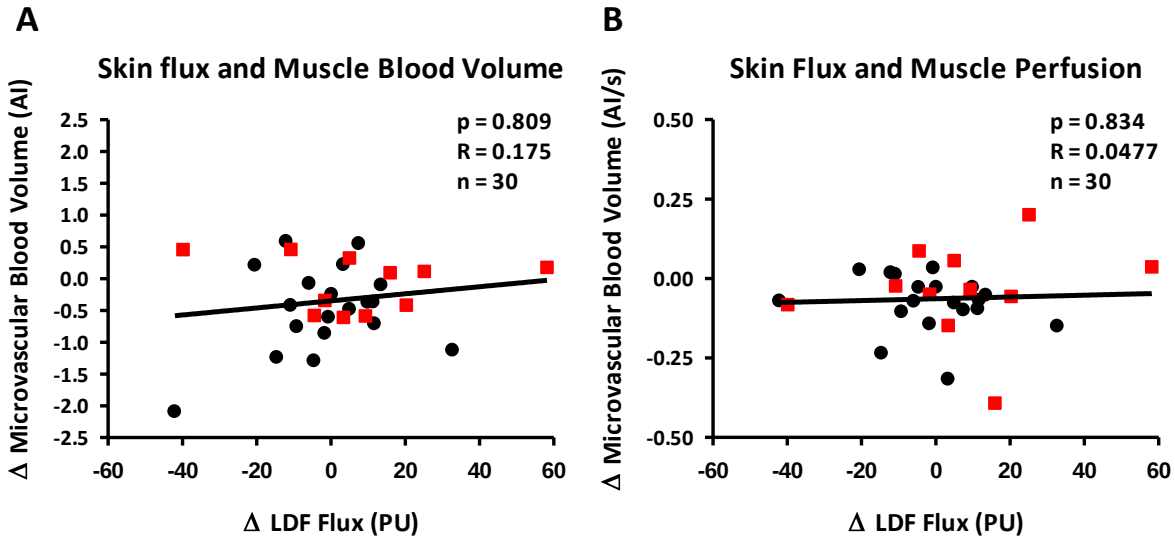

Figure 4.7: *Correlation of skin and subcutaneous tissue with skeletal muscle blood flow.* Panel A shows the correlation between the change in skin+SC LDF flux during OGC and the change in skeletal muscle microvascular blood volume during OGC. Panel B shows the correlation between the change in skin+SC LDF flux during OGC and the change in skeletal muscle microvascular perfusion during OGC. The two groups were combined for correlation analysis, healthy control (●) and T2D (■) groups (n = 30).

4.3.7 Correlation between diabetes duration and blood flow measures

To determine if diabetes duration influences a number of blood flow measures regression analysis was performed (Table 4.1). At both basal and during OGC there is a significant negative relationship between skin+SC LDF and T2D duration (p = 0.0087 R = -0.587 and p = 0.039 R = -0.577 respectively). There is a similar trend for skin+SC O_2 Sat and brachial blood flow decreasing as duration of T2D increase. During basal state only, there is a significant positive relationship between skeletal muscle microvascular volume and T2D duration (p = 0.013 R = 0.748).

Table 4.1: *Correlation analysis of diabetes duration and blood flow measures.*

Regression analysis against Diabetes Duration	**Basal**		**OGC**	
Measure	**P value**	**R value**	**P value**	**R value**
Skin+SC LDF Flux	**0.0087**	-0.587	**0.039**	-0.577
Skin+SC O_2 Sat	*0.076*	-0.509	*0.056*	-0.541
Brachial Blood Flow	*0.078*	-0.553	*0.057*	-0.588
Skeletal Muscle Microvascular Volume	**0.013**	0.748	0.304	0.362

4.3.8 Skin and subcutaneous tissue flowmotion measures

Insulin release in response to an OGC induces changes in cardiac, respiratory, neurogenic and endothelial activity. As a result, skin+SC microvascular flowmotion patterns became altered in response to the OGC. Representative traces from individual participants during basal and the OGC are shown in Figure 4.8.

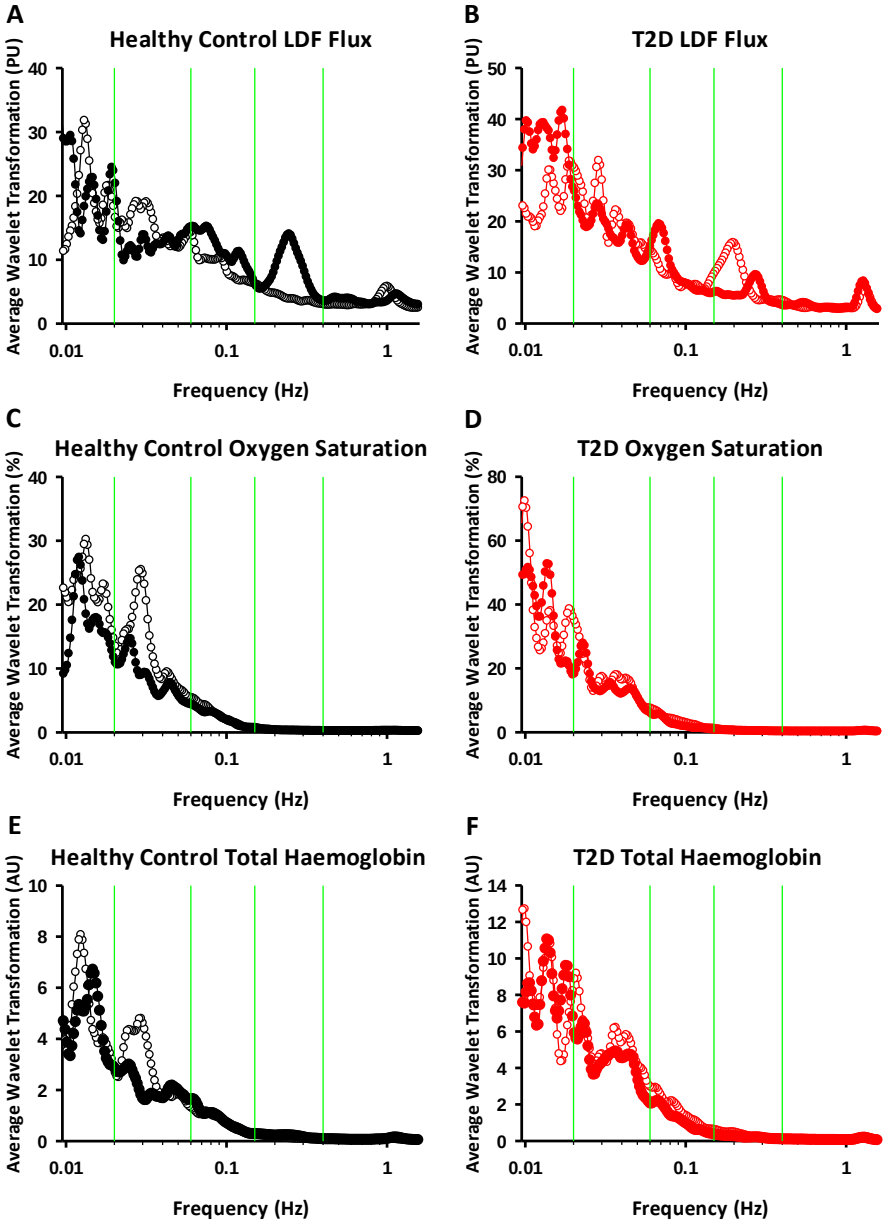

Figure 4.8: *Response to OGC in wavelet transformation of skin and subcutaneous tissue blood flow measures.* This figure shows wavelet transformation during basal (open symbol) and OGC (filled symbol) of skin+SC A) LDF flux B) O_2 Sat and C) tHb measures for a **healthy control** and **T2D** participants. These traces are representative of the data collected in each group.

Quantification of the LDF flux wavelet transformation for each participant was done by calcualting the AUC of the peaks within each frequency range. Figure 4.9 shows a similar peak AUC in both groups in each of the frequency components. In the higher frequency components, compared to healthy controls there was an higher cardiac peak AUC in T2D group during OGC.

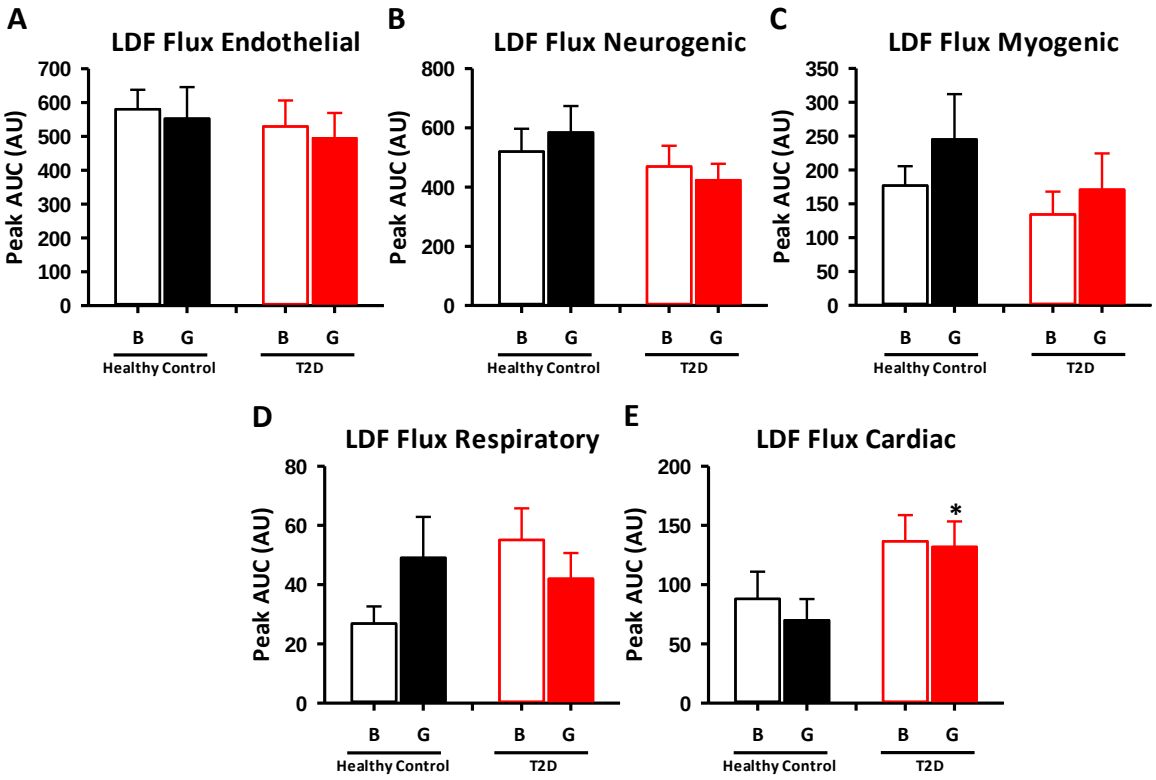

Figure 4.9: *LDF flux wavelet transformation: peak area under the curve for each flowmotion components in response to OGC.* Average peak AUC of wavelet transformed LDF flux measures during basal (B, open bar) and OGC (G, filled bar) for frequency regions A) endothelial B) neurogenic C) myogenic D) respiratory and E) cardiac. **Healthy control** (**HC**; n=23) and **T2D** (n=18). Data expressed as mean ± SE. * indicates significant difference between healthy control and T2D groups during OGC ($p = 0.030$).

In addition to AUC for each component, the peak frequency was also assessed (Table 4.2). In healthy controls, there was a significant increase in peak frequency during OGC compared to basal in the cardiac ($p < 0.01$), respiratory ($p = 0.001$) and myogenic ($p = 0.019$) components, with a near significant increase in neurogenic component ($p = 0.078$). Interestingly, in the T2D group, an increase was only observed in the peak frequency of the cardiac component of flowmotion ($p < 0.001$).

Table 4.2: *LDF flux wavelet transformation: response to OGC of peak frequency.*

LDF Flux							
		Healthy Control		P value	T2D		P value
		Basal	OGC		Basal	OGC	
Endothelial	*Hz*	0.012 ± 0.000	0.014 ± 0.001	NS	0.013 ±0.001	0.013 ± 0.001	NS
	Secs	85.6 ± 2.7	78.5 ± 4.2		78.0 ± 3.6	78.1 ± 4.4	
Neurogenic	*Hz*	0.028 ± 0.002	0.034 ± 0.002	*0.078*	0.032 ± 0.002	0.029 ± 0.002	NS
	Secs	37.2 ± 1.7	32.4 ± 2.1		32.8 ± 1.7	36.5 ± 1.9	
Myogenic	*Hz*	0.070 ± 0.003	0.079 ± 0.003	**0.019**	0.076 ± 0.003	0.071 ± 0.002	NS
	Secs	14.7 ± 0.52	13.0 ± 0.45		13.4 ± 0.48	14.3 ± 0.54	
Respiratory	*Hz*	0.214 ± 0.017	0.281 ± 0.022	**0.001**	0.257 ± 0.013	0.262 ± 0.015	NS
	Secs	5.2 ± 0.34	3.9 ± 0.24		4.05 ± 0.19	4.04 ± 0.27	
Cardiac	*Hz*	0.892 ± 0.028	0.995 ± 0.029	**< 0.001**	1.13 ± 0.036	1.19 ± 0.034	**< 0.001**
	Secs	1.15 ± 0.04	1.02 ± 0.03		0.899 ± 0.03	0.847 ± 0.02	

Average peak frequency of each frequency region during basal and OGC, expressed as frequency (Hz) and cycle period (seconds). Healthy control (n=23) and T2D (n=18) group. Data expressed as mean ± SE.

The change in peak frequency for both the healthy control and T2D groups is shown in Table 4.3. Cycle period of cardiac and respiratory components was decreased in response to the OGC in both groups, representing a faster rate of input in these components in response to the large glucose load. However, in the healthy control group the decrease in cycle period (and thus faster rate of input) in response to the OGC was significantly higher than in the T2D group in both the cardiac ($p = 0.006$) and respiratory ($p = 0.017$) components. This corresponds with the change in heart rate which was significantly elevated from basal during OGC in both healthy control (54.0 ± 0.4 bpm to 59.9 ± 0.4 bpm) and T2D (67.2 ± 0.5 bpm to 71.2 ± 0.5 bpm) groups. In the lower frequency components, the healthy

control group cycle period decreased in response to the OGC (faster rate of input), whereas in the T2D group the cycle period tended to increase. As such, a significant difference in the change in peak frequency during the OGC between healthy control and T2D groups was seen in the neurogenic ($p = 0.029$) and myogenic ($p = 0.011$) components.

Table 4.3: *LDF flux wavelet transformation: change from basal in peak frequency.*

Change from basal to OGC LDF Flux				
		Healthy Control	**T2D**	**P value**
Endothelial	*Cycle period (secs)*	-7.5 ± 1.1	0.14 ± 1.6	0.342
Neurogenic	*Cycle period (secs)*	-4.4 ± 0.64	4.1 ± 0.57	**0.029**
Myogenic	*Cycle period (secs)*	-1.8 ± 0.17	0.96 ± 0.17	**0.011**
Respiratory	*Cycle period (secs)*	-1.4 ± 0.10	-0.08 ± 0.08	**0.017**
Cardiac	*Cycle period (secs)*	-0.07 ± 0.01	-0.05 ± 0.00	**0.006**

Average change from basal in peak frequency each frequency region, expressed as cycle period (seconds). Healthy control (n=23) and T2D (n=18) group. Data expressed as mean ± SE.

At basal, the O_2 Sat wavelet tranformation measures show a significantly lower ($p = 0.005$) peak AUC in the endothelial region of the T2D group compared to healthy controls (Figure 4.10). In response to the OGC, the peak AUC in the endothelial region of healthy controls was significantly decreased from basal ($p < 0.001$).

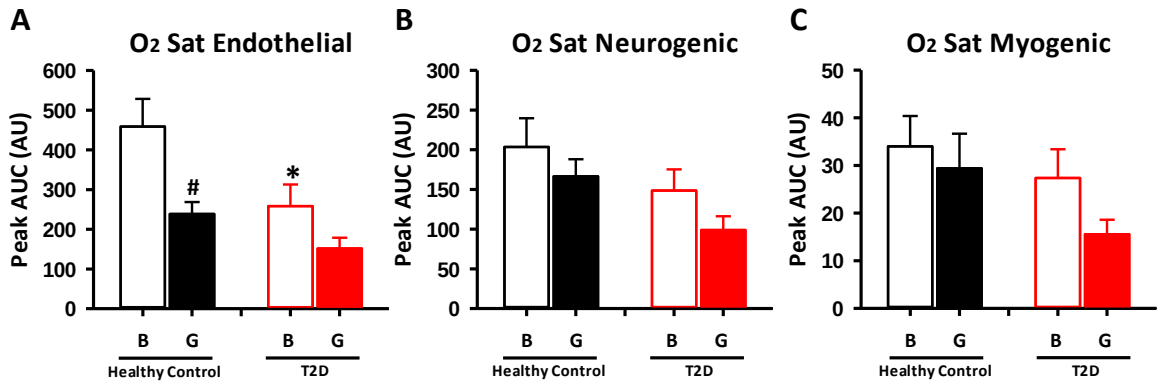

Figure 4.10: *O_2 Sat wavelet transformation: peak area under the curve for flowmotion components in response to OGC.* Average peak AUC of wavelet transformed O_2 Sat measures during basal (B, open bar) and OGC (G, filled bar) for frequency regions A) endothelial B) neurogenic and C) myogenic. **Healthy control** (**HC**; n=23) and **T2D** (n=18). Data expressed as mean ± SE. **#** indicates significant difference from basal to OGC in healthy control group ($p < 0.001$) in endothelial component. ***** indicates significant difference between **healthy controls** and **T2D** ($p = 0.005$) in endothelial component.

Unlike the LDF flux measures, there was no difference in peak frequency from basal to OGC seen in any frequency component measure by O_2 Sat in either healthy control or T2D groups (Table 4.4).

Table 4.4: *O_2 Sat wavelet transformation: response to OGC of peak frequency.*

Oxygen Saturation							
		Healthy Control		P value	T2D		P value
		Basal	OGC		Basal	OGC	
Endothelial	*Hz*	0.014 ± 0.001	0.014 ± 0.001	NS	0.013 ±0.001	0.013 ± 0.00	NS
	Secs	77.0 ± 3.5	75.5 ± 4.2		80.2 ± 4.1	77.5± 2.7	
Neurogenic	*Hz*	0.027 ± 0.001	0.028 ± 0.002	NS	0.030 ±0.002	0.029 ± 0.002	NS
	Secs	37.4 ± 1.2	37.0 ± 1.7		34.6 ± 1.8	36.4 ± 2.3	
Myogenic	*Hz*	0.075 ± 0.004	0.075 ± 0.003	NS	0.084 ±0.005	0.074 ± 0.004	NS
	Secs	14.1 ± 0.77	13.7 ± 0.47		12.3 ± 0.54	14.4 ± 0.73	

Average peak frequency of each frequency region during basal and OGC, expressed as frequency (Hz) and cycle period (seconds). Healthy control (n=23) and T2D (n=18) group. Data expressed as mean ± SE.

The change in peak frequency during OGC measured by O_2 Sat between healthy control and T2D groups is shown in Table 4.5. The change in peak frequency in response to the OGC measured by O_2 Sat was not significantly different between the two groups.

Table 4.5: *O_2 Sat wavelet transformation: change from basal in peak frequency.*

Change from basal to OGC Oxygen Saturation				
		Healthy Control	T2D	P value
Endothelial	*Cycle period (secs)*	-0.64 ± 1.2	-2.7 ± 1.3	0.780
Neurogenic	*Cycle period (secs)*	-0.57 ± 0.41	1.8 ± 0.75	0.482
Myogenic	*Cycle period (secs)*	-0.75 ± 0.26	1.2 ± 0.21	0.283

Average change from basal in peak frequency each frequency region, expressed as cycle period (seconds). Healthy control (n=23) and T2D (n=18) group. Data expressed as mean ± SE.

Figure 4.11 shows a number of changes in peak AUC in response to OGC measured by tHb. Quantification of wavelet transformation measures show a significantly lower peak AUC in T2D group at basal in endothelial ($p = 0.011$) and a near signficant decrease in neurogenic ($p = 0.057$) frequency components, compared to healthy controls. In response to OGC, the endothelial ($p < 0.001$) and neurogenic ($p = 0.001$) frequency components in healthy control group were significantly reduced from basal. In the T2D group, peak AUC of neurogenic component was also significantly reduced ($p = 0.022$).

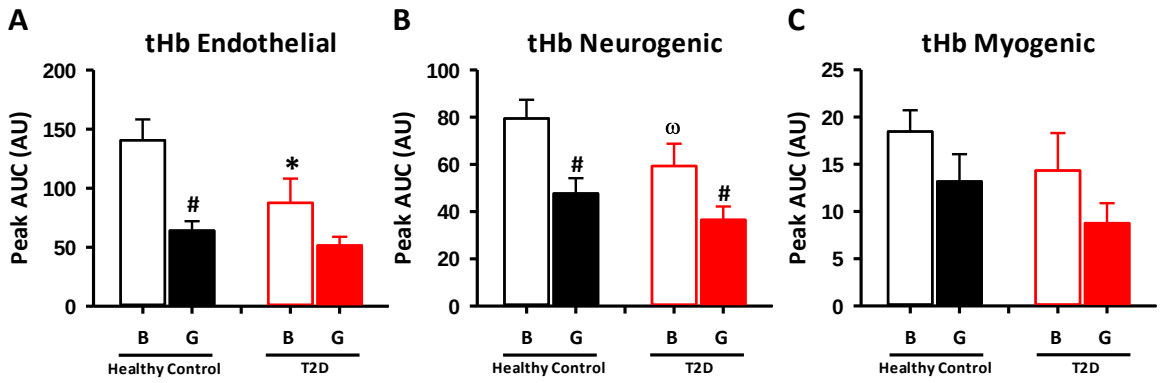

Figure 4.11: *tHb wavelet transformation: peak area under the curve for flowmotion components in response to OGC.* Average peak AUC of wavelet transformed tHb measures during basal (B, open bar) and OGC (G, filled bar) for frequency regions A) endothelial B) neurogenic and C) myogenic. **Healthy control** (**HC**; n=23) and **T2D** (n=18). Data expressed as mean ± SE. **#** indicates significant difference from basal to OGC in healthy control ($p < 0.001$) and T2D ($p = 0.022$) groups. ***** indicates significant difference between healthy **controls** and **T2D** in endothelial ($p = 0.011$) component. **ω** $p = 0.057$ between **healthy controls** and **T2D**.

The rate of input for each component as measured by tHb is shown in Table 4.6. There was no difference seen in peak frequency from basal to OGC in any frequency component in either healthy control or T2D groups.

Table 4.6: *tHb wavelet transformation: response to OGC of peak frequency.*

Total Haemoglobin							
		Healthy Control			T2D		
		Basal	OGC	P value	Basal	OGC	P value
Endothelial	*Hz*	0.0 14 ± 0.001	0.014 ± 0.001	NS	0.013 ±0.001	0.014 ± 0.001	NS
	Secs	77.2 ± 3.8	77.4 ± 3.5		84.3 ± 4.5	77.8 ± 4.2	
Neurogenic	*Hz*	0.029 ± 0.002	0.030 ± 0.001	NS	0.031 ± 0.002	0.032 ± 0.002	NS
	Secs	36.5 ± 1.4	33.8 ± 1.2		34.1 ± 1.7	32.7 ± 1.9	
Myogenic	*Hz*	0.070 ± 0.002	0.070 ± 0.002	NS	0.074 ± 0.003	0.077 ± 0.004	NS
	Secs	14.5 ± 0.42	14.5 ± 0.33		13.7 ± 0.42	13.4 ± 0.61	

Average peak frequency of each frequency region during basal and OGC, expressed as frequency (Hz) and cycle period (seconds). Healthy control (n=23) and T2D (n=18) group. Data expressed as mean ± SE.

Similarly, when the change in peak frequency in response to OGC was calculated, there was no discernible difference between the healthy control and T2D groups in the tHb measure of skin+SC flowmotion (Table 4.7).

Table 4.7: *tHb wavelet transformation: change from basal in peak frequency.*

Change from basal to OGC Total Haemoglobin				
		Healthy Control	T2D	P value
Endothelial	*Cycle period (secs)*	-0.40 ± 1.2	-6.48 ± 1.6	0.482
Neurogenic	*Cycle period (secs)*	-2.84 ± 0.41	-1.4 ± 0.74	0.677
Myogenic	*Cycle period (secs)*	0.13 ± 0.12	-0.30 ± 0.21	0.656

Average change from basal in peak frequency each frequency region, expressed as cycle period (seconds). Healthy control (n=23) and T2D (n=18) group. Data expressed as mean ± SE.

4.4 Discussion

A 50g OGC induced different blood glucose and blood flow responses in healthy controls compared to T2D participants. As expected, the T2D participants had higher blood glucose AUC in response to the OGC, indicating insulin resistance and glucoregulatory dysfunction (Figure 4.2). In response to the OGC, flowmotion measures in the healthy controls were expected to increase upon endogenous insulin secretion as insulin is known to stimulate endothelial and neurogenic components (6), but showed an unexpected decrease in contribution and increased rate of components, while in the T2D group flowmotion remained mostly unaltered in response to OGC (Figure 4.10, 4.11 and Table 4.1). There were also differences between forearm total and skin+SC blood flow response compared to skeletal muscle perfusion during the OGC in both groups (Figure 4.3, 4.4 and 4.6).

As is characteristic of the disease, the T2D group showed poor blood glucose control over the course of the OGC (Figure 4.2). While fasting plasma insulin levels were elevated in the T2D group compared to healthy controls, plasma insulin concentrations throughout the OGC were similar between the two groups. The lack of difference between healthy control and T2D insulin concentrations throughout the OGC not unexpected. The average duration from diagnosis of type 2 diabetes is 7.08 ± 1.4 years and as such it is expected that the T2D group will have decreased capacity to secrete insulin from beta cells as well as insulin resistance in cells, leading to even poorer control of blood glucose (255). Healthy controls showed normal glucoregulation, with a slower increase in blood glucose in response to the OGC and blood glucose concentrations returning to near basal levels at the 120min time point. The T2D group however, show dysfunction in glucoregulatory control with a faster increase in blood glucose levels after the 50g glucose load and blood glucose remaining significantly elevated at 120min. As T2D medication was withdrawn 48hrs prior to testing, the higher blood glucose concentration, despite similar plasma insulin levels between the two groups, suggests T2D participants had some beta cell dysfunction, which is characteristic of the disease. The difference in blood glucose response to OGC shows an overt disease state in the T2D participants, thereby providing suitable populations

to investigate blood flow and skin+SC flowmotion responses in both healthy control and T2D populations.

In the healthy control group, total blood flow to the forearm (assessed with 2D-ultrasound, Figure 4.3) and skin+SC microvascular flux (LDF, Figure 4.4) were unaltered in response to OGC. In contrast, CEU measures of skeletal muscle microvascular blood volume and perfusion were significantly decreased in response to the OGC (Figure 4.6). This is a surprising result in the healthy participants as previous studies using either a mixed meal (65, 256, 257) to induce endogenous insulin release or a euglycemic hyperinsulinemic clamp (36, 37, 184, 248) have shown an increase in skeletal muscle microvascular perfusion. A possible explanation for the decrease in skeletal muscle microvascular perfusion during the OGC in healthy controls is an enhanced neurogenic input to the skeletal muscle vasculature, caused by an excessive activation of the SNS. Welle *et. al.* (258) observed a significant increase in plasma noradrenaline (NA) levels in response to a 100g oral glucose load in insulin sensitive participants. Increased circulating NA may result in augmented SNS (thereby neurogenic) activity, potentially causing increased contraction in vessel smooth muscle cells (vasoconstriction) and therefore a reduction in skeletal muscle capillary perfusion. Activation of the SNS in response to a 75g oral glucose load was also observed by Staznicky *et. al.* (253), where SNS output to muscle was increased in insulin-sensitive obese participants, but not in insulin resistant obese participants. This would suggest that in insulin sensitive participants, consumption of large oral glucose loads may result in increased SNS output. The data in this study, decreased skeletal muscle blood flow despite an endogenous release of insulin (Figure 4.6) and an increased rate of the neurogenic component in response to OGC in healthy controls but not T2D participants (Table 4.3), supports the idea that a large oral glucose load in an insulin sensitive individual induces an elevated SNS response. However, it should be noted that there was no significant change in mean arterial pressure from basal to OGC in either the control or T2D participants, which would have been expected to increase with an increased SNS output. It may still be a more local enhancement of neurogenic input is occurring to produce the

increased SNS with OGC. In contrast, this unexpected change in the vasculature has not been observed when increased insulin levels have been induced by a mixed meal (247, 256) or euglycemic hyperinsulinemic clamp (36, 37).

In response to the OGC total flow to the forearm was unaltered in healthy controls while in contrast, the T2D group there was a significant increase from basal (Figure 4.3). While skin+SC LDF flux in the T2D group was elevated both at basal and during OGC (compared to healthy controls), the OGC did not induced a significant increase in skin+SC flux within the T2D group (Figure 4.4), which is not consistent with the increase in total flow. In contrast, skin+SC O_2 Sat, as well as the resulting complexity of this measure, was increased during the OGC in T2D participants (Figure 4.4 and 4.5). This increase in the O_2 Sat suggests an increased total flow, thereby decreased blood transit time through tissue, resulting in decreased extraction of oxygen. The increase in complexity value shows an increased randomness in O_2 Sat signal, most likely brought about by a reduced control over blood flow in the skin+SC when bulk flow to the forearm is enhanced during the OGC.

The different response to the OGC in skin+SC determined by LDF flux and O_2 Sat measures in the T2D group could be explained by the penetration of the light used for each measure. O_2 Sat, measured by white light spectroscopy, is thought to only measure flow from the most superficial layers of the subcutaneous tissue and skin (exact volume unknown), as the white light has limited penetration into the skin+SC (60). The LDF laser on the other hand is believed to have greater penetration into the skin+SC (~0.55-0.79mm^2 volume of tissue measured), and thereby measures a different volume and tissue combination compared to O_2 Sat, which could explain the difference in blood flow measurements at the same skin site (61).

A significant negative correlation between duration of T2D and skin+SC perfusion was shown; with increasing years since T2D diagnosis linked to decreased skin+SC LDF flux at both basal and during

OGC. This is not surprising, as T2D progresses there is increasing damage to the microvasculature, through such mechanisms as glucose damage (241), which appears to have resulted in a reduced perfusion of skin capillaries. Additionally, changes in capillary density and morphology may have also resulted in this reduction in skin+SC perfusion (197). While not significant, there was a similar trend in the correlation of T2D duration with skin+SC O_2 Sat and brachial blood flow, indicating damage to both large and small vessels, reducing bulk blood flow and skin+SC microvascular perfusion. Interestingly, skeletal muscle blood volume was positivity correlated with T2D duration at basal, but this was no longer present during the OGC. This is a very interesting observation which indicates that skeletal muscle blood volume at basal increases as dysfunction occurs and T2D progress, but the response to endogenous insulin is attenuated as the disease progresses. Even with increased basal perfusion in later stages of the disease, microvascular blood volume does not increase with insulin stimulation.

As in chapter 3, the complexity measures of skin+SC blood flow showed very little difference between the healthy control and T2D groups (Figure 4.5). The only difference observed, an increased complexity of O_2 Sat measures during the OGC in T2D group, was likely to be accounted for by the enhanced bulk blood flow which concurrently occurred. As changes in flowmotion were seen when the LDF flux and tissue oxygenation data were analysed using wavelet transformation measures, the complexity analysis does not appear to be sensitive enough to assess microvascular function in humans.

As LDF flux was not significantly increased in response to the OGC in the T2D group (Figure 4.4), it appears that the majority of the increased flow to the forearm during OGC has not been diverted to the skin or underlying subcutaneous tissue. Interestingly, in the T2D group skeletal muscle microvascular perfusion was also not significantly altered in response to the OGC (Figure 4.6). CEU measures the perfusion of nutritive capillaries in skeletal muscle tissue, i.e. those that provide blood flow directly to the myocyte cells (259). The insulin-mediated increase in skeletal muscle nutritive

capillary recruitment is known to be attenuated in insulin resistance and T2D (6, 40, 193), and thus the lack of change in skeletal muscle microvascular perfusion in this study is not unexpected. It appears that the greater bulk blood flow to the forearm in the T2D group (Figure 4.3) is being diverted to the non-nutritive capillary pathway (which primarily services the connective tissue (28)) and thus blood flow is potentially being shunted through the muscle, resulting in decreased exposure of glucose and insulin to myocytes. Consequently, there is a decreased disposal of the glucose load into skeletal muscle, which may contribute to the prolonged elevation of blood glucose levels observed during the OGC in the T2D group (Figure 4.2) (236, 260, 261).

Skin+SC flowmotion measures in the healthy control group showed a number of changes during the OGC. There was a decrease in the contribution of the lower frequency components of flowmotion (determined from tissue oxygenation measures, Figure 4.10 and 4.11) in response to the OGC. This is surprising as insulin release in response to an OGC would be expected to stimulate endothelial derived vasodilation (248), thereby increasing the endothelial contribution to flowmotion. Instead, a reduction in endothelial as well as neurogenic contribution was seen. As described above, an increased SNS input to the muscle has been observed in response to an OGC in insulin sensitive participants (253). In the current study, the decrease in the contribution of the neurogenic component to the skin+SC in healthy controls in response to the OGC may be a result of upregulation of SNS activity in the muscle and a subsequent down regulation in the skin+SC. Alternatively, the change to the neurogenic component may be a consequence of changes in other component inputs to the skin+SC (such as endothelial) interacting with the neurogenic input, causing a reduction in contribution. In addition to the reduced contribution in lower frequency components, the rate of input of the neurogenic, myogenic, respiratory and cardiac components of flowmotion (measured by LDF flux, Table 4.1) was increased in response to the OGC in healthy controls. These surprising responses to OGC in healthy control skin+SC flowmotion are likely, in part, due to an activation of the SNS, but may also be because flowmotion

was measured on the skin+SC of participants and not in the more metabolically relevant skeletal muscle tissue.

In the type 2 diabetics the lower frequency component input to flowmotion (determined by tissue oxygenation measures, Figure 4.10 and 4.11) tended to decrease, but, with one exception (neurogenic input measured by tHb), there was no significant change. The rate of input of all but the cardiac component, which increased, also remained unchanged in response to the OGC (Table 4.1). A lack of insulin-mediated change in flowmotion in the T2D group was not unexpected as T2D commonly has both endothelial (188) and neurogenic (198) dysfunction. In T2D, insulin-mediated vasodilation in the vessel endothelial cells is attenuated and therefore no change or a decrease in the endothelial component of flowmotion was expected. Commonly in T2D there is an increase in autonomic activity (157), as such it may be that insulin-mediated increase in neurogenic input to flowmotion is not additive to basal levels, thereby the neurogenic component does not increase upon insulin stimulation. Despite the data showing unexpected changes in blood flow in healthy controls, the impaired contribution and rate of flowmotion components in response to the OGC indicates blood flow dysfunction is present within T2D participants.

It is worth noting that high levels of glucose in circulation have been shown to independently influence blood flow, separate to insulin action. Williams *et. al.* (262) showed a reduction in endothelial-dependent vasodilation of the brachial artery during acute hyperglycaemia induced through intraarterial infusion of a 50% dextrose solution. It may be that microvascular perfusion is also altered under acute hyperglycaemia. Therefore, it is possible that some of the OGC induced changes to blood flow seen in this study may be attributed to the effect of glucose itself, independent to insulin action. This may be an alternative explanation for the unexpected observations seen in measures such as OGC induced skeletal muscle microvascular blood volume changes in healthy control group.

An important observation in the current study is the different response to the OGC in skin+SC microvascular flux (Figure 4.4) and total forearm flow (Figure 4.3), compared to skeletal muscle microvascular perfusion (Figure 4.6). While total flow and skin+SC flux remained unaltered during the OGC, skeletal muscle perfusion was significantly decreased in the healthy controls. There was also no correlation between skin+SC and muscle blood flow in both groups. The differences in skin+SC and muscle response to the OGC indicates that the skin+SC flowmotion measured at basal and in response to the OGC may not represent the flowmotion occurring in the underlying, more metabolically relevant, skeletal muscle tissue.

The data in the current study demonstrates a change in flowmotion at basal and in response to an OGC in the T2D participants, compared to healthy control. As such, the next question to be addressed in this thesis is how to improve flowmotion in T2D. A restoration of flowmotion may normalise blood delivery to important metabolic tissues such as skeletal muscle, thereby enhancing glucose uptake and thus improving long term outcomes for T2D participants. Previous studies have shown improvement in glucoregulatory and cardiovascular function of both healthy controls (263) and T2D (264, 265) participants with a resistance training intervention. It is not known if a similar exercise intervention can improve flowmotion in clinically diagnosed T2D participants.

Chapter 5 - *Microvascular flowmotion in the skin and subcutaneous tissue in type 2 diabetics: the effect of resistance training*

5.1 Introduction

Treatment for T2D can involve lifestyle changes (including diet and exercise) and the use of drugs that either improve insulin sensitivity or enhance insulin production in the remaining β cells. In late stage T2D, insulin therapy also becomes necessary due to increased β cell destruction leading to decreased insulin production. Initially, the preferred intervention for treatment of T2D, and its precursor insulin resistance, is an exercise intervention which has been shown to improve glucose regulation, blood lipid profile and cardiovascular function in T2D (203).

Both aerobic and resistance based exercise interventions have been shown to improve glucoregulatory function in T2D (264, 266). Tight control of blood glucose levels in T2D is extremely important for the long-term health outcomes of the disease. If blood glucose levels are not well controlled, but are instead constantly elevated, glycosylation damage of blood vessels results, leading to the development of adverse health outcomes such as retinopathy, nephropathy and neuropathy (165). A meta-analysis by Boule *et. al.* (267) and Snowling *et. al.* (268) looked at the effect of different types of training intervention on glucoregulatory function and found there was no difference in the improvement of glucose control between the two modes of exercise intervention.

RT interventions in T2D show benefits in short time periods (6-8weeks) and are generally well tolerated by participants (224, 265, 269). Improvements in glucose control with a RT intervention have shown ameliorated HbA1c levels (264, 270), and enhanced insulin signalling, insulin mediated glucose uptake (224), and glycogen storage (264) in skeletal muscle. RT in obese and type 2 diabetic participants has also resulted in improvement of other health parameters such as weight loss (270) and cardiovascular function (271). For example, a study by Croymans *et. al.* (272) in obese young males showed a 12-week RT intervention improved a number of cardiovascular risk factors for CVD and T2D including central, systolic and diastolic blood pressure, percentage body fat, lean mass, and blood lipid profile. RT has repeatedly been shown to improve systemic cardiovascular function in T2D with

improvements in blood pressure and blood chemistry profiles (264, 270). In addition, endothelial function has also been shown to improve with RT, with studies in obese and T2D participants showing that an 8-week RT intervention improves endothelial function in conduit and resistance blood vessels (265, 269). Watts *et. al.* (269) showed that an 8-week RT intervention did not change in basal brachial artery diameter of T2D group, but there was a normalisation to the healthy control group in brachial artery flow mediated dilation (FMD) after training. FMD dilation is known to be a NO-dependant process, thereby the 8-week RT intervention improved endothelial-mediated vasodilation in a conduit blood vessel. RT therefore potentially improves the endothelial, cardiac and respiratory components that are known to influence flowmotion, yet there is little known about the changes in microvascular flowmotion that may occur after a RT intervention. Improvements to flowmotion with long-term lifestyle intervention have been reported in obese participants. Vinet *et. al.* (273) measured skin+SC flowmotion in response to insulin delivery via iontophoresis before and after a 6-month lifestyle intervention (dietary and exercise changes) and found at baseline the contribution of all (except respiratory) components of flowmotion during insulin delivery was decreased compared to healthy controls. After the lifestyle intervention participants had significant improvements in clinical parameters (decreased weight, BMI, fat mass and systolic blood pressure) and an improvement in skin+SC flowmotion response to insulin in the endothelial, neurogenic and cardiac components. Vinet *et. al.* (273) therefore showed an improvement in skin+SC flowmotion measures with a lifestyle intervention in obese individuals, but very little is known about whether a RT exercise intervention in clinically diagnosed T2D is able to improve flowmotion.

The aim of this study was to undertake a 6-week RT intervention with the T2D group previously described in this thesis, to assess the impact on flowmotion. RT was chosen as previous studies have shown improvement in glucoregulatory function in a 6-week time period and because high intensity RT is reasonably well tolerated in sedentary type 2 diabetics (224). After completing the basal and OGC measures as described and reported in chapter 4, T2D participants undertook a 6-week RT

intervention. It was hypothesised that as long-term RT is known to improve cardiovascular function, flowmotion measures would be improved with training. Flowmotion was reassessed at basal and during OGC to determine if training resulted in any changes to this response. As data from the OGC (described in chapter 4) indicated that flowmotion measures in the skin+SC may not represent changes in the underlying skeletal muscle tissue, the changes in microvascular blood perfusion for Skin+SC and skeletal muscle were again assessed independently, with LDF + OXY and CEU respectively to determine the response to RT in each tissue bed.

5.2 Methods

The characteristic of the T2D participants have been previously described in chapter 3 and 4. The T2D cohort underwent a 6-week RT intervention. Of the original 18 T2D participants who completed baseline measurements, 14 completed the RT intervention. Due to the budget of this study healthy controls were not exercise training and therefore a weakness of this study is a lack of control group to compare the changes in T2D group to. The interpretation of the results is therefore limited and conclusions can only be drawn about RT impact in T2D participants, and not compared to healthy controls.

5.2.1 Resistance training intervention

The RT program in the current study was based on a previous study by Russell *et. al.* (263) where a 6-week RT program was shown to lower fasting blood glucose levels in healthy participants. The training intervention involved three sessions a week (Monday, Wednesday and Friday) at the same time each day (1830) at a local fitness centre in Hobart, Tasmania, Australia (All Aerobic Fitness). Sessions on Monday and Friday involved a mixture of free-weight and resistance machines. The exercises were, in order, leg press, lateral pull-down, chest press, weighted lunges, seated row, back fly, bicep curl, incline chest press, dumbbell shoulder press, leg extension, leg curl, dips, lateral shoulder raise, triceps extension, dumbbell deadlift, and push-ups. One set of each exercise was performed to complete task failure (6-15reps) and time to complete each session was limited to 60mins. Throughout the intervention, exercises were recorded and load incrementally increased (maintained between 65-85% of calculated 1 repetition maximum [1RM]) as greater strength was obtained by participants, to ensure progression. In the Wednesday session of each week core and stability exercises were performed. The type of exercise was continually modified to compensate for the increased strength and fitness of participants over the 6 weeks. Types of resistance-focused techniques performed on Wednesday included dumbbell sit-ups, medicine ball toss, leg-lifts, plank positions, burpees, and weighted

farmer's walk. *Ad libitum* water consumption before, during and after training session was encouraged.

5.2.1.1 Strength assessment

To measure improvement in fitness from Pre-RT to Post-RT, relative strength of participants was determined via the Epley formula (274) as described by Russell *et. al.* (263). The 1RM for the exercises leg press, bench press and dead lift were calculated from weight (kg) lifted and repetitions performed:

1RM = kg x (1 + [repetitions/30])

1RM of leg press, bench press and dead lift were then summed to give a total 1RM, which was then divided by participant weight to determine relative strength.

5.2.2 Protocol

Within two days of completing the 6-week RT intervention participants were reassessed using the same testing as at baseline, described in section 4.2.1. Briefly, participants were overnight fasted and stopped taking their diabetes medication for two days. A fasting blood sample was taken (t =0) and then the 50g OGC was repeated. Blood glucose and plasma insulin were determined throughout protocol (Figure 5.1) and blood flow measures were again taken at basal and in response to the OGC. Testing conditions were as described in section 2.1.1.

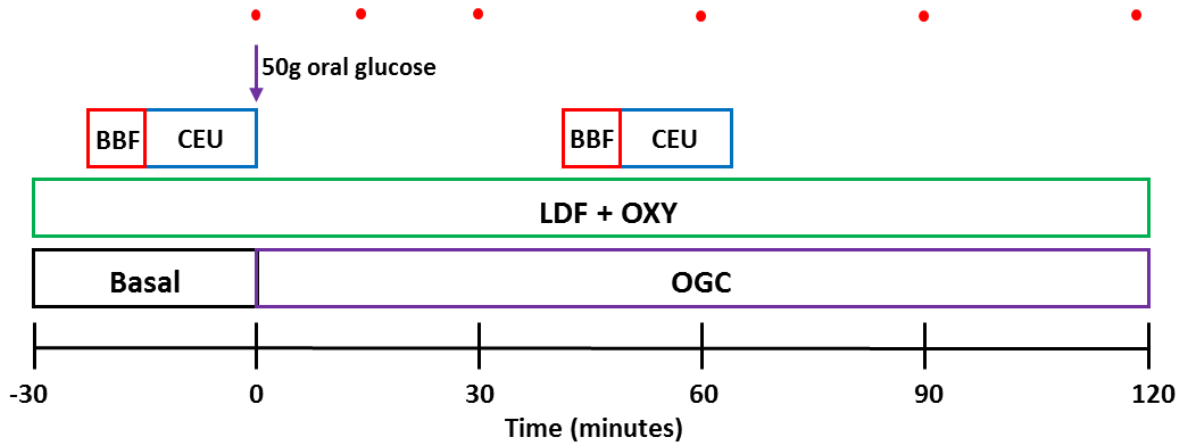

Figure 5.1: *Study protocol.* Participants lay in a semi-recumbent position throughout testing. An initial **basal** period was observed and then 50g of liquid glucose was orally consumed. Forearm skin+SC **LDF + OXY** measures were taken throughout **basal** and oral glucose challenge (**OGC**). Total forearm blood flow was determined by measuring brachial blood flow (**BBF**) during **basal** and at t = 45min into **OGC**. Skeletal muscle microvascular perfusion was determined using contrast enhanced ultrasound (**CEU**) at rest and at = 60min of **OGC**. Venous blood samples were taken before and then throughout **OGC** (●).

5.2.2.1 Skin and subcutaneous tissue microvascular blood flow

The LDF + OXY probe (described in section 2.1.2) was attached to the midsection of the ventral side of the right forearm. Skin+SC LDF flux and tissue oxygenation measures were continuously recorded throughout basal and during the OGC (Figure 5.1). Skin+SC microvascular flowmotion was assessed with LDF flux and tissue oxygenation measures over two 20min time periods during basal (t = -30 to -10min) and then during the OGC (t = 35 to 45min).

5.2.2.2 Total forearm blood flow

Total flow into the forearm was determined by measuring the brachial artery blood flow with 2D-ultrasound (describe in section 2.1.4). Brachial artery diameter and blood velocity were measured, and brachial blood flow (BBF) calculated as described previously in 2.1.4. BBF measures were taken at basal (t = -20min) and then at t = 45min into OGC (Figure 5.1).

5.2.2.3 Forearm skeletal muscle microvascular perfusion

Microvascular blood volume, filling rate and perfusion of forearm deep flexor muscle were determined as described in section 2.1.3. CEU measure were taken in triplicate during basal period (t = -10min) and then at t = 60min of OGC.

5.2.2.4 Blood analysis

Fasting blood samples were taken from antecubital vein of the non-dominant arm and analysed for HbA1c and lipid profile as described in section 2.1.6. Blood samples taken at fasting and then throughout the OGC (Figure 5.1) were analysed for blood glucose and plasma insulin as described in section 2.1.6.

5.2.3 Data analysis

5.2.3.1 Microvascular blood flow averages

Mean LDF flux and tissue oxygenation measures over a 10min time period during basal (t = -30 to -20min) and at t = 50 to 60min during the OGC were determined as described in section 2.1.8.1.

5.2.3.2 Flowmotion measures

Flowmotion analysis using wavelet transformation was performed on 20min of basal (t = -30 to -10min) and OGC (t = 35 to 55min) LDF flux and tissue oxygenation measures. Wavelet transformation data were then quantified by determining AUC of peaks within each flowmotion frequency component and peak frequency, as described in section 2.1.8.3.

5.2.4 Statistical analysis

Two-way repeated measures ANOVA were performed to determine difference at basal and during the OGC between Pre-RT and Post-RT groups, as described in section 2.4. Paired Student's t-test was used to determine the difference in change during OGC from basal between Pre-RT and Post-RT groups. The correlation between change from basal during OGC (Δ) in LDF flux and microvascular perfusion measures in the Post-RT group was performed with a Spearman Correlation analysis, as described in section 2.4.

5.3 Results

5.3.1 Participant characteristics

Table 5.1 shows the difference in anthropometrics and blood chemistries Pre-RT (reported in chapter 3) and Post-RT. RT resulted in a small but significant (p = 0.003) decrease in percentage body fat and a decrease in fasting blood glucose in these type 2 diabetic participants (p = 0.013).

Table 5.1: *Changes in participant anthropometrics and blood chemistries after 6 weeks of resistance training in type 2 diabetics.*

	Pre-RT	Post-RT	P value
Age (yr)	52 ± 2	52 ± 2	-
Sex (M/F)	9/5	9/5	-
Weight (kg)	96. ± 7.5	94.6 ± 3.6	0.547
Body Fat (%)	32.7 ± 1.8	31.4 ± 2.0	**0.003**
BMI (kg/m^2)	33.8 ± 2.2	31.8 ± 0.8	0.380
Blood Pressure (mmHg)			
Systolic	130.4 ± 3.8	131.4 ± 3.5	0.819
Diastolic	78.9 ± 2.3	80.4 ± 2.5	0.354
Fasting Blood glucose (mM)	10.2 ± 1.0	9.2 ± 0.9	**0.013**
HbA1c (%)	8.1 ± 0.5	7.8 ± 0.4	0.102
Plasma Insulin (pM)	106.2 ± 19.5	102.3 ± 18.1	0.562
Fasting Blood Lipids (mmol/L)			
HDL	1.5 ± 0.3	1.3 ± 0.1	0.910
LDL	2.7 ± 0.3	2.5 ± 0.3	0.505
Total Cholesterol	3.9 ± 0.4	3.7 ± 0.3	0.127

Anthropometric and blood chemistry differences between Pre-RT and Post-RT. Data expressed as mean ± SE.

5.3.1 Strength improvement with resistance training

The strength of participants was improved over the 6-week training program. The calculated 1RM for bench press and leg press exercises, as well as total weight lifted was significantly ($p < 0.01$) increased with RT (Table 5.2). Relative strength (corrected for body weight) was also significantly improved from Pre-RT to Post-RT ($p < 0.001$).

Table 5.2: *Improvement in strength (1RM) after 6-week resistance training program in type 2 diabetic participants.*

	Pre-RT	Post-RT	Improvement	P value
1RM (kg)				
Bench press	61.1 ± 7.9	85.6 ± 13.6	24.5 ± 7.8	**0.004**
Leg press	135.1 ± 11.1	221.4 ± 21.2	86.3 ± 15.0	**< 0.001**
Dead lift	46.0 ± 10.4	59.9 ± 7.8	14.0 ± 11.9	0.084
Total	247.8 ± 22.3	364.5 ± 32.1	122.4 ± 15.8	**< 0.001**
Relative strength (kg/kg body weight)	2.6 ± 0.20	3.8 ± 0.28	1.2 ± 0.14	**< 0.001**

Average strength at baseline (Pre-RT) and after (Post-RT) resistance training (n = 14). 1RM calculated with Epley formula (274). Data expressed as mean ± SE.

5.3.2 OGC blood glucose and plasma insulin

The results of a 50g OCG used to measure insulin sensitivity are shown in Figure 5.2. Fasting blood glucose was significantly decreased Post-RT ($p = 0.019$). Interestingly, there was no difference in the blood glucose levels before and after training at any time point during the OGC (Figure 5.2A), however, the blood glucose AUC was significantly decreased ($p = 0.002$) after RT (Figure 5.2B). Despite the significantly lower fasting blood glucose measures, there was no difference in the change from basal of blood glucose during between Pre and Post-RT. There was no difference in plasma insulin levels at fasting or throughout the OGC between Pre-RT and Post-RT (Figure 5.2D-F).

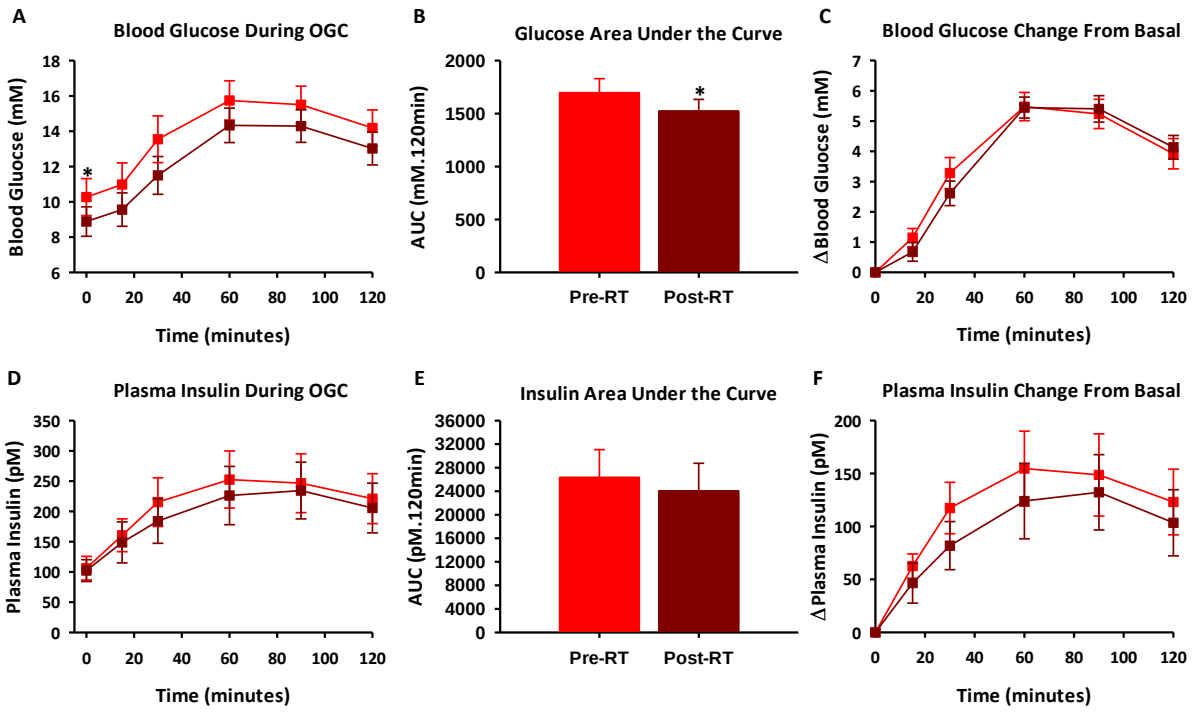

Figure 5.2: *Blood glucose and plasma insulin pre and post 6-week resistance training program in type 2 diabetic participants.* A) Blood glucose response to OGC, the B) resulting AUC of time course and the C) blood glucose during OGC represented as change from basal. D) Plasma insulin response to OGC, the E) resulting AUC of time course and F) plasma insulin during OGC represented as change from basal. **Pre-RT** and **Post-RT** (n=12) groups. Data expressed as mean ± SE. * indicates significant difference between **Pre-RT** and **Post-RT** ($p < 0.05$).

5.3.2 Forearm total flow

Total flow to the forearm determined by 2D-ultrasound at basal (t = -20min) and during OGC (t = 45min) is shown in Figure 5.3. There is a significant increase in BBF in response to OGC, both Pre-RT and Post-RT (p = 0.007 and 0.037 respectively), however these responses were not significantly different Pre- versus Post-RT.

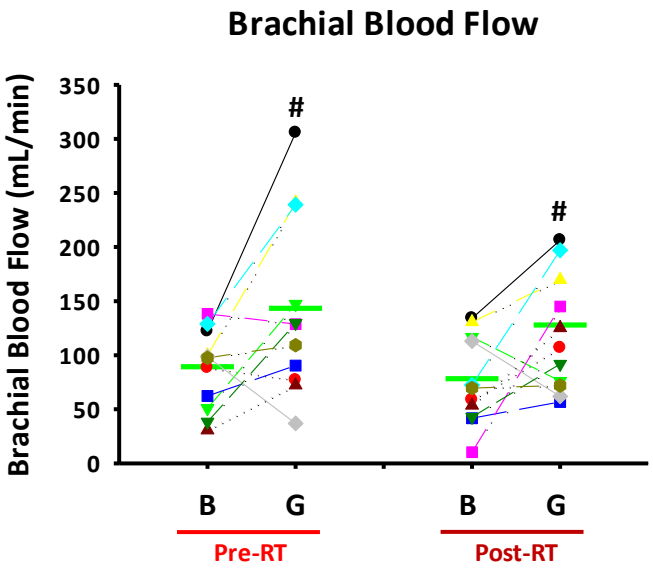

Figure 5.3: *Brachial artery blood flow change with 6-week resistance training program in type 2 diabetic participants.* Brachial artery blood flow (mL/min) measured during basal (B) and 45min after OGC (G). **Pre-RT** and **Post-RT** (n=11) groups. Time points of each individual participant is represented by a different signal, — indicates mean. **#** indicates significant difference between healthy basal and OGC ($p < 0.05$).

5.3.3 Skin and subcutaneous tissue microvascular blood flow and tissue oxygenation

The average skin+SC microvascular blood flow measures (LDF flux, O_2 Sat and tHb) were assessed over a 10min period at basal (t = -30 to -20) and OGC (t = 50 to 60min) to determine blood flow changes resulting from 50g oral glucose load. There were no changes in LDF flux, O_2 Sat or tHb in response to the OGC, and RT has no effect on these measures (Figure 5.4A-C). The change during the OGC from basal in LDF flux, O_2 Sat and tHb measures was no different from Pre-RT to Post-RT (Figure 5.4D-F).

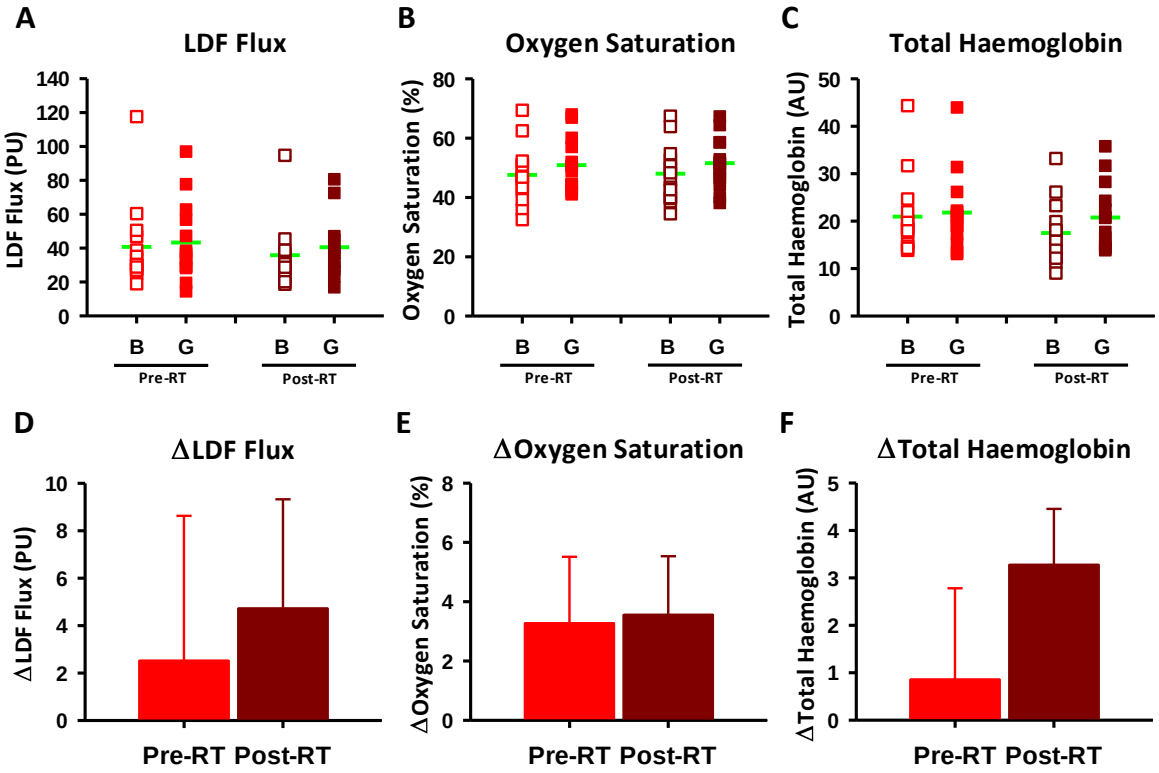

Figure 5.4: *Skin and subcutaneous tissue LDF flux and tissue oxygenation change with 6-week resistance training program in type 2 diabetic participants.* Average skin+SC A) LDF flux, B) O_2 Sat, and C) tHb measures assessed over 10mins during basal (B, open symbol) and OGC (G, filled symbol). — indicates mean. Change from basal to OGC was calculated for LDF flux (D), O_2 Sat (E) and tHb (F). **Pre-RT** and **Post-RT** (n=14) groups. Data expressed as mean ± SE.

5.3.4 Forearm skeletal muscle microvascular perfusion

Blood flow in the skeletal muscle of forearm was measured using CEU Pre-RT and Post-RT to determine if exercise training improved basal muscle microvascular perfusion and in response to OGC. No significant difference at basal or in response to the OGC, Pre or Post-RT was seen in the skeletal muscle microvascular perfusion measures (Figure 5.5A-B). However, training did result in a near significant ($p = 0.052$) reduction in microvascular filling rate at basal. Figure 5.5D-F shows the change in forearm skeletal muscle microvascular perfusion in response to OGC. Skeletal muscle microvascular perfusion measures tended to decrease in response to OGC Pre-RT, whereas Post-RT microvascular perfusion tended to increase during OGC. The change from basal was therefore significantly different between Pre and Post-RT for microvascular filling rate ($p = 0.021$) and perfusion ($p = 0.002$).

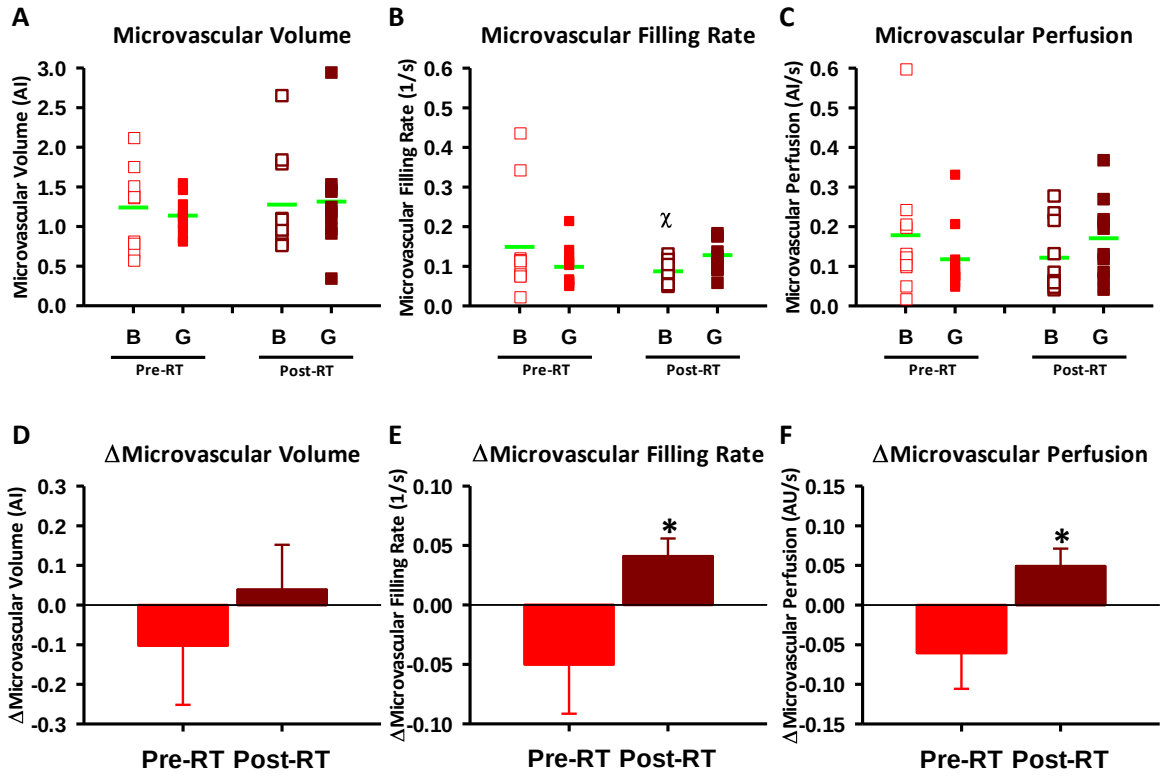

Figure 5.5: *Skeletal muscle microvascular blood perfusion change with 6-week resistance training program in type 2 diabetic participants.* CEU was used to determine A) microvascular blood volume, B) microvascular filling rate and C) microvascular perfusion during basal (B, open symbol) and OGC (G, filled symbol). — indicates mean. Change from basal during OGC in forearm skeletal was calculated for D) Δmicrovascular blood volume, E) Δmicrovascular filling rate and F) Δmicrovascular perfusion. **Pre-RT** and **Post-RT** (n=10) groups. Data expressed as mean ± SE. χ indicates a near significant difference between **Pre-RT** and **Post-RT** groups ($p = 0.052$) at basal. * indicates significant difference between **Pre-RT** and **Post-RT** groups ($p < 0.05$).

5.3.5 Correlation between skin and subcutaneous tissue flux and skeletal muscle perfusion

To determine if skeletal muscle and skin+SC had a similar vascular response to the OGC Post-RT, a correlation analysis was performed. The change in skin+SC LDF flux was compared to the change in skeletal muscle microvascular blood volume (Figure 5.6A) and perfusion (Figure 5.6B) in response to the OGC. There was no correlation between change in LDF flux in skin+SC and change in microvascular blood volume in skeletal muscle (Figure 5.6A), where R = 0.290 and p = 0.182. Similarly, there was no correlation between change in LDF flux in skin+SC and change in microvascular perfusion of skeletal muscle (Figure 5.6B), R = 0.109 and p = 0.885.

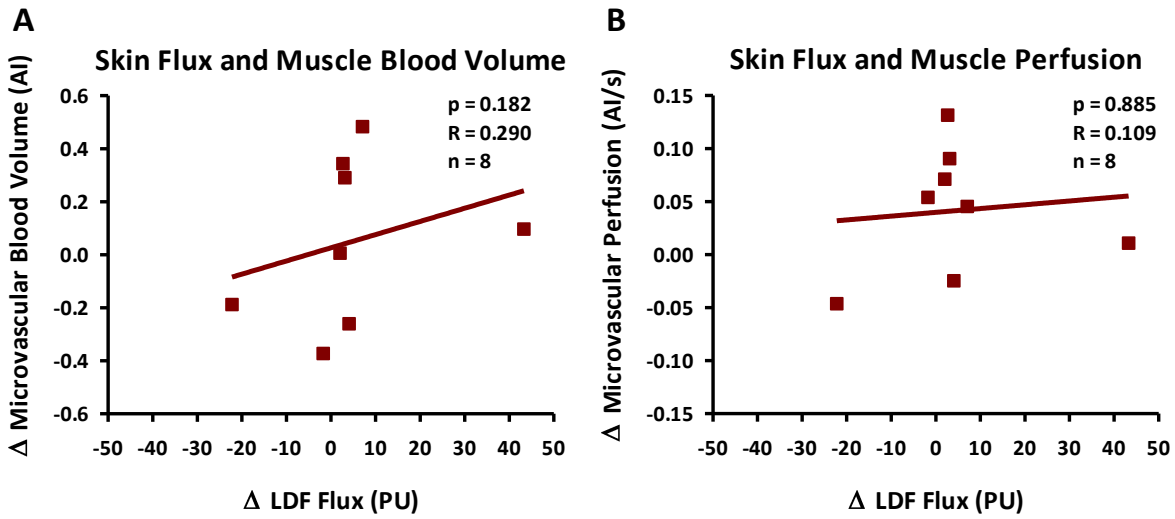

Figure 5.6: *Correlation of skin and subcutaneous tissue with skeletal muscle blood flow after 6-week resistance training program in type 2 diabetic participants.* The correlation between the change during OGC from basal of skin+SC LDF flux and skeletal muscle A) microvascular blood volume and B) microvascular perfusion was determined in Post-RT (■) group (n = 8).

5.3.6 Skin and subcutaneous tissue flowmotion measures

To determine of the effect of RT on flowmotion, representative traces from an individual Pre-RT and Post-RT participant during basal and the OGC are shown in Figure 5.7.

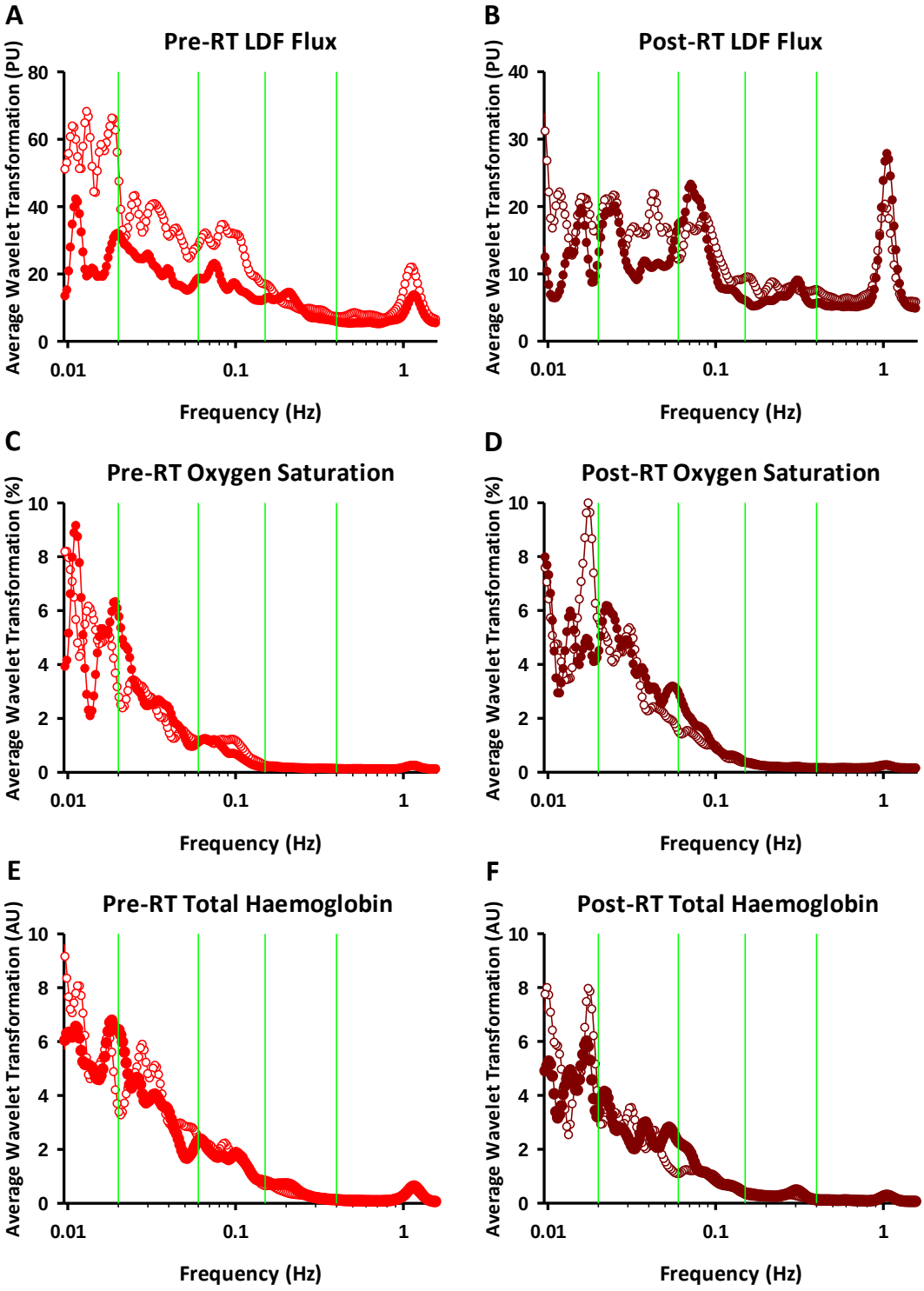

Figure 5.7: *Wavelet transformation of skin and subcutaneous tissue blood flow measures before and after RT.* This figure shows wavelet transformation during basal (open symbol) and OGC (filled symbol) of skin+SC A) LDF flux B) O_2 Sat and C) tHb measures of one subject **Pre-RT** and **Post-RT**.

Wavelet transformations resulting from LDF flux skin+SC microvascular blood flow measures were not affected by 6-week resistance training as there was no difference in peak AUC from basal to OGC Pre or Post-RT (Figure 5.8).

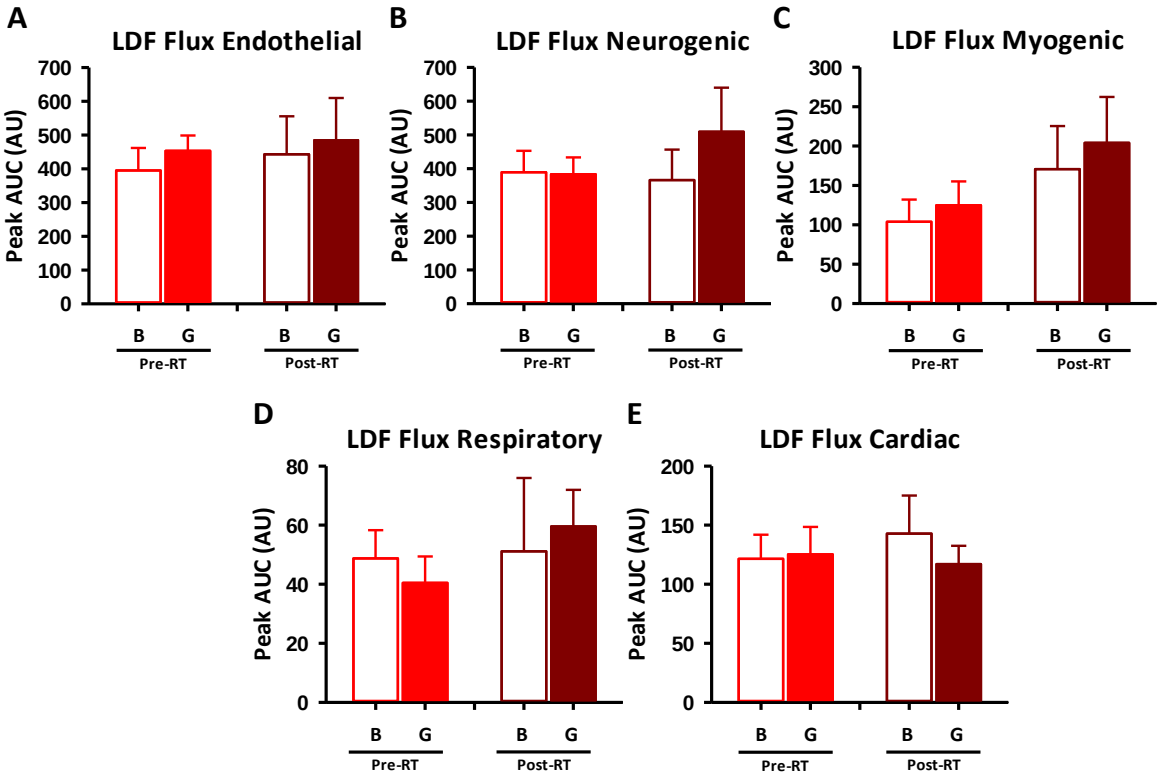

Figure 5.8: *LDF flux wavelet transformation: peak area under the curve for flowmotion component changes with 6-week resistance training program in type 2 diabetic participants.* Average peak AUC of wavelet transformed LDF flux measures during basal (B, open bars) and OGC (G, filled bars) for frequency regions A) endothelial B) neurogenic C) myogenic D) respiratory and E) cardiac. **Pre-RT** and **Post-RT** (n=14) groups. Data expressed as mean ± SE.

In both the Pre-RT and Post-RT measures, the OGC resulted in a significant elevation in the peak frequency of the cardiac input ($p= 0.002$ and $p < 0.001$ respectively, Table 5.3). No change in peak frequency in the lower frequency components of flowmotion were seen in the Pre-RT measurements. In the Post-RT group, the neurogenic and myogenic peak frequency were both significantly decreased during the OGC compared to basal ($p = 0.027$ and $p = 0.016$ respectively), which did not occur in the Pre-RT group, indicating a training effect.

Table 5.3: *LDF flux wavelet transformation: peak frequency changes with 6-week resistance training program in type 2 diabetic participants.*

LDF Flux							
		Pre-RT			Post-RT		
		Basal	OGC	P value	Basal	OGC	P value
Endothelial	*Hz*	0.014 ±0.001	0.013 ± 0.001	NS	0.013 ± 0.001	0.014 ± 0.001	NS
	Secs	75.1 ± 4.2	78.9 ± 5.5		81.0 ± 3.9	74.7 ± 4.5	
Neurogenic	*Hz*	0.033 ± 0.002	0.028 ± 0.001	NS	0.036 ± 0.003	0.029 ± 0.002	**0.027**
	Secs	31.8 ± 2.1	36.8 ± 1.8		30.0 ± 2.2	36.4 ± 2.2	
Myogenic	*Hz*	0.075 ± 0.003	0.072 ± 0.003	NS	0.08 ± 0.004	0.074 ± 0.004	**0.016**
	Secs	13.7 ± 0.54	14.0 ± 0.54		12.3 ± 0.56	13.8 ± 0.60	
Respiratory	*Hz*	0.270 ± 0.015	0.278 ± 0.016	NS	0.25 ± 0.017	0.287 ± 0.018	NS
	Secs	3.84 ± 0.21	3.78 ± 0.29		4.24 ± 0.30	3.68 ± 0.32	
Cardiac	*Hz*	1.12 ± 0.04	1.20 ± 0.040	**0.006**	1.09 ± 0.032	1.20 ± 0.044	**<0.001**
	Secs	0.901 ± 0.03	0.841 ± 0.03		0.928 ± 0.03	0.846 ± 0.03	

Average peak frequency in each frequency region during basal and OGC, expressed as frequency (Hz) and cycle period (seconds). Pre-RT and Post-RT (n=14) groups. Data expressed as Mean ± SE.

The cycles per second change from basal in the cardiac component was significantly different (p = 0.003) from Pre-RT to Post-RT (Table 5.4). There were no other significant differences in cycle per second change from basal between the two groups, though the neurogenic component showed a trend (p = 0.055) of increased cycle period during OGC from basal in Post-RT compared to Pre-RT.

Table 5.4: *LDF flux wavelet transformation: change from basal in peak frequency.*

Change from basal to OGC LDF Flux				
		Pre-PT	**Post-RT**	**P value**
Endothelial	*Cycle period (secs)*	4.1 ± 7.8	-4.9 ± 5.9	0.967
Neurogenic	*Cycle period (secs)*	5.4 ± 2.7	6.3 ± 2.5	0.055
Myogenic	*Cycle period (secs)*	0.44 ± 0.72	1.4 ± 0.68	0.143
Respiratory	*Cycle period (secs)*	-0.13 ± 0.43	-0.35 ± 0.28	0.137
Cardiac	*Cycle period (secs)*	-0.06 ± 0.02	-0.08 ± 0.02	**0.003**

Average change from basal the in peak frequency at each frequency region, expressed as cycle period (seconds). Pre-RT and Post-RT (n=14) groups. Data expressed as Mean ± SE.

Quantification of the O_2 Sat wavelet transformation data showed only one significant difference during the OGC compared to basal in the Pre-RT and Post-RT measures. Pre-RT there was a significant reduction in the endothelial peak AUC during the OGC as compared to basal (p = 0.006). This significant change was no longer present after RT intervention. While not significant, a similar trend in the neurogenic and myogenic components of decreased input during OGC Pre-RT, and an improvement Post-RT was also observed.

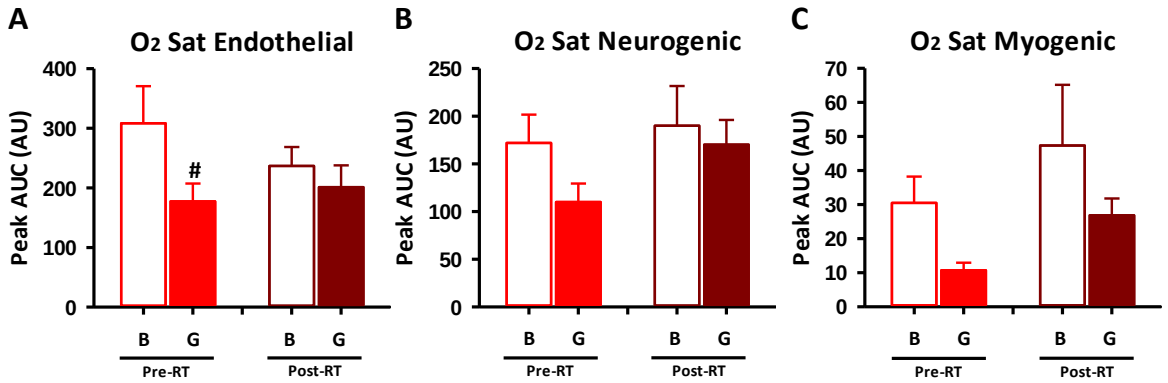

Figure 5.9: *O_2 Sat wavelet transformation: peak area under the curve for flowmotion component changes with 6-week resistance training program in type 2 diabetic participants.* Average peak AUC of wavelet transformed O_2 Sat measures during basal ((B, open bars) and OGC (G, filled bars) for frequency regions A) endothelial B) neurogenic and C) myogenic. **Pre-RT** and **Post-RT** (n=14) groups. Data expressed as mean ± SE. **#** indicates significant difference from basal to OGC in **Pre-RT** group (p = 0.012).

Pre-RT the myogenic component peak frequency significantly decreased (p = 0.026) in response to the OGC compared to basal (Table 5.5). This significant change was no longer present after RT intervention.

Table 5.5: *O_2 Sat wavelet transformation peak: peak frequency changes with 6-week resistance training program in type 2 diabetic participants.*

Oxygen Saturation							
		Pre-RT			Post-RT		
		Basal	OGC	P value	Basal	OGC	P value
Endothelial	*Hz*	0.013 ± 0.001	0.013 ± 0.001	NS	0.014 ± 0.00	0.013 ± 0.00	NS
	Secs	78.6 ± 4.8	77.8 ± 3.3		77.1 ± 4.2	77.7 ± 4.1	
Neurogenic	*Hz*	0.030 ± 0.002	0.028 ± 0.002	NS	0.031 ± 0.004	0.030 ± 0.002	NS
	Secs	35.1 ± 1.8	37.4 ± 2.1		33.3 ± 1.9	35.3 ± 2.0	
Myogenic	*Hz*	0.078 ± 0.003	0.067 ± 0.003	**0.026**	0.075 ± 0.004	0.078 ± 0.005	NS
	Secs	13.0 ± 0.5	15.3 ± 0.6		13.9 ± 0.9	13.3 ± 0.6	

Average peak frequency in each frequency region during basal and OGC, expressed as frequency (Hz) and cycle period (seconds). Pre-RT and Post-RT (n=14) groups. Data expressed as Mean ± SE.

There was no difference in the peak frequency change from basal to OGC between the Pre-RT and Post-RT groups (Table 5.6).

Table 5.6: *O_2 Sat wavelet transformation: change from basal in peak frequency.*

Change from basal to OGC Oxygen Saturation				
		Pre-PT	Post-RT	P value
Endothelial	*Cycle period (secs)*	-0.79 ± 6.7	-0.77 ± 6.1	0.903
Neurogenic	*Cycle period (secs)*	2.3 ± 2.3	0.74 ± 3.1	0.810
Myogenic	*Cycle period (secs)*	2.1 ± 0.69	-0.73 ± 1.1	0.521

Average change from basal the in peak frequency at each frequency region, expressed as cycle period (seconds). Pre-RT and Post-RT (n=14) groups. Data expressed as Mean ± SE.

Flowmotion measures determined from the tHb wavelet transformation showed no significant difference in peak AUC during the OGC compared to basal in Pre-RT or Post-RT. However, as with O_2 Sat measures, there was a trend for a decrease in the lower frequency components (endothelial, neurogenic and myogenic) input in the Pre-RT group, which appears to have been improved with RT.

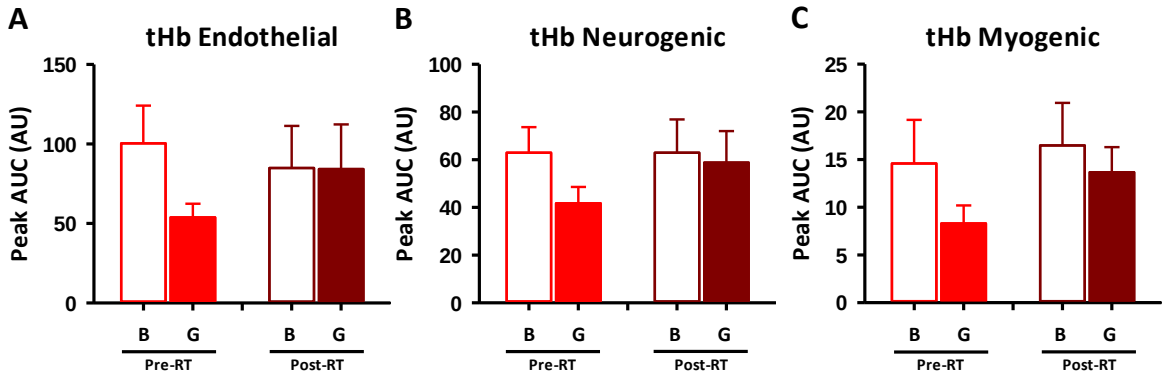

Figure 5.10: *tHb wavelet transformation: peak area under the curve for flowmotion component changes with 6-week resistance training program in type 2 diabetic participants.* Average peak AUC of wavelet transformed tHb measures during basal (B, open bars) and OGC (G, filled bars) for frequency regions A) endothelial B) neurogenic and C) myogenic. **Pre-RT** and **Post-RT** (n=14) groups. Data expressed as mean ± SE.

There was no difference in the peak frequency in Pre-RT or Post-RT during the OGC when compared to basal (Table 5.7).

Table 5.7: *tHb wavelet transformation peak: peak frequency changes with 6-week resistance training program in type 2 diabetic participants.*

Total Haemoglobin							
		Pre-RT			Post-RT		
		Basal	OGC	P value	Basal	OGC	P value
Endothelial	*Hz*	0.012 ± 0.001	0.014 ± 0.001	NS	0.013 ± 0.001	0.014 ± 0.001	NS
	Secs	86.8 ± 4.7	76.8 ± 4.9		80.6 ± 5.1	75.8 ± 5.2	
Neurogenic	*Hz*	0.031 ± 0.002	0.033 ± 0.003	NS	0.029 ± 0.001	0.030 ± 0.003	NS
	Secs	33.5 ± 2.0	32.8 ± 2.3		35.1 ± 1.6	35.6 ± 2.8	
Myogenic	*Hz*	0.074 ± 0.002	0.073 ± 0.003	NS	0.080 ± 0.004	0.078 ± 0.007	NS
	Secs	13.7 ± 0.4	13.9 ± 0.6		12.8 ± 0.6	13.7 ± 0.9	

Average peak frequency in each frequency region during basal and OGC, expressed as frequency (Hz) and cycle period (seconds). Pre-RT and Post-RT (n=14) groups. Data expressed as Mean ± SE.

The peak frequency changes from basal during OGC (Table 5.8) were not different between the Pre-RT and Post-RT groups.

Table 5.8: *tHb wavelet transformation: change from basal in peak frequency.*

Change from basal to OGC Total Haemoglobin				
		Pre-PT	**Post-RT**	**P value**
Endothelial	*Cycle period (secs)*	-10.0 ± 6.8	-6.7 ± 6.1	0.590
Neurogenic	*Cycle period (secs)*	-0.64 ± 3.8	0.13 ± 2.7	0.876
Myogenic	*Cycle period (secs)*	0.31 ± 0.97	0.87 ± 0.91	0.979

Average change from basal the in peak frequency at each frequency region, expressed as cycle period (seconds). Pre-RT and Post-RT (n=14) groups. Data expressed as Mean ± SE.

5.4 Discussion

A 6-week RT intervention in T2D participants resulted in improvement in strength (Table 5.2), glucoregulatory function (Figure 5.2) and a small change in body composition (Table 5.1). While the total forearm blood flow (Figure 5.3) and average skin+SC microvascular flux (Figure 5.4) response to the OGC was unaltered with training, skeletal muscle perfusion (Figure 5.5) and skin+SC flowmotion (Table 5.3 and Figure 5.9) responses to the OGC were significantly alter from basaline Post-RT.

The increase in relative strength (as measured by 1RM, Table 5.2) over the 6-week RT intervention showed participants successfully engaged in the exercise program, facilitating their progression. As a result of this training program, there was a small, but significant decrease in percentage body fat of participants, with no total body weight change (Table 5.1), suggesting a small improvement in body composition. The enhancement in physical strength and body composition was accompanied by an improvement in blood glucose levels, both fasting (Table 5.1) and in response to the OGC (Figure 5.2), while plasma insulin levels were unaltered. The exercise intervention therefore appears to have improved insulin-sensitivity of participants, as has been previously reported in T2D participants (224, 275), resulting in increased glucose disposal in response to OGC and lower fasting blood glucose levels. While these measures improved with training, fasting blood glucose and blood glucose response to OGC were still elevated in comparison to the healthy controls (described in Table 3.1 and Figure 4.2), demonstrating that while there has been improvement in glucoregulation, participants still display an overt diabetic disease state. Additionally, while the improvements in fasting blood glucose and body composition are statistically significant, this may not translate into significant clinical improvements in the short term. Post-RT no change was made to the medication of any participants, indicating that the changes over the short RT intervention have not yet become clinically significant. However, with continued exercise in the T2D participant's further improvements on health parameters are likely to occur and therefore have a greater long-term clinical significance and improvement.

Previously, RT interventions in T2D and insulin resistance have shown improvement in cardiovascular function in cardiac output, large vessel function (212, 272) and in NO-dependent flow mediated dilation of conduit and resistance vessels, indicating an improvement in endothelial function (213, 265, 269). In the current study a short term 6-week exercise intervention did not improve blood pressure (Table 5.1), total forearm blood flow (Figure 5.3) or skin+SC microvascular flux (Figure 5.4), either at basal or in response to the OGC. Post-RT, bulk blood flow to the forearm was still significantly elevated in response to the OGC, as was skin+SC microvascular blood flow at basal and during the OGC, in comparison to healthy controls (as described in sections 4.3.2 and 4.3.3). The lack of improvement in blood pressure and macrovascular blood flow is perhaps due to the short duration of the exercise intervention as studies showing blood pressure changes with RT tend to occur over longer periods of time (12 weeks or more (270, 272)).

While skin+SC flux and total blood flow, at basal or during OGC was not altered with RT, the response to OGC in the underlying skeletal muscle microvascular perfusion was improved (Figure 5.5). Prior to RT skeletal muscle microvascular perfusion decreased in response to the OGC (Figure 5.5). In contrast, Post-RT microvascular perfusion tended to increase in response to the OGC, indicating improved insulin-mediated vasodilation in the skeletal muscle. These improvements were primarily driven by an improvement in basal perfusion levels Post-RT (Figure 5.5). The RT intervention may have improved baseline skeletal muscle microvascular perfusion levels and insulin sensitivity of the endothelium, and thus augmented insulin-mediated vasodilation in the skeletal muscle. Improved insulin-mediated vasodilation enhances nutritive capillary recruitment, potentially then enabling a greater glucose disposal in skeletal muscle (41). While this change in response to the OGC Post-RT does differ from the decrease in skeletal muscle perfusion seen in the healthy control group (described in section 4.3.5), it is important to note that the decrease seen in the healthy controls was surprising. An increased skeletal muscle microvascular perfusion in response to a mixed meal challenge (65) and euglycemic hyperinsulinemic clamp (37) has previously been seen in healthy populations. As discussed

in chapter 4, this surprising result in the healthy controls is possibly due to an increased activation of the SNS. (258). It appears that in the already insulin resistant T2D group, where blood glucose levels are chronically elevated, the OGC-mediated activation of SNS is blunted, as has previously been observed in an insulin resistant population (253). This blunted response may be due to an already elevated neurogenic activity, which is commonly associated with T2D (autonomic dysfunction) (199). Therefore, the increased perfusion in response to OGC Post-RT shows an improvement in vascular insulin sensitivity and increase in muscle perfusion.

RT resulted in a significant decrease in the rate of the neurogenic and myogenic components of flowmotion in response to the OGC (measured by LDF, Figure 5.8). Pre-RT the contribution of the endothelial component was decreased during the OGC, while Post-RT there was no change observed in the endothelial component in response to the OGC (measured by O_2 Sat, Figure 5.9), indicating a partial restoration of endothelial function. Based on the data from this study, the RT intervention has modified skin+SC flowmotion in the T2D group. Again, these findings differ from the skin+SC flowmotion changes seen in response to the OGC in the healthy control group (as described in section 4.3.5), where lower frequency component contribution decreased and rate of components increased during the OGC. An increased activation of the SNS is likely to account for this observation in healthy controls (253). Previously, Jonk *et.al.* (247) observed an increase in all components of skin+SC flowmotion after endogenous release of insulin induced by a mixed meal in healthy controls. Flowmotion Post-RT, where the endothelial component was no longer decreased, does therefore appear to be improved, but not normalised in these T2D participants.

An additional consideration for the current study may be that in the Post-RT group the measurement of flowmotion in the skin+SC, where RT did not alter average microvascular blood flow measured by LDF flux and tissue oxygenation (Figure 5.4), may not reflect the flowmotion occurring in the underlying skeletal muscle, which showed improved response to the OGC (Figure 5.5). It is possible

the minimal changes during the OGC in the lower frequency component contributions that occurred in the skin+SC (improvements seen in endothelial component only), does not reflect the skeletal muscle flowmotion changes, where insulin-mediated vasodilation seems to have improved with RT, and a greater change in flowmotion may occur.

A further factor that needs consideration is the potential decrease in subcutaneous fat of T2D participants after RT intervention. RT caused a decrease in the percentage body fat of T2D participants (Table 5.1), therefore if there was a change in forearm subcutaneous fat content, it is likely that the skin+SC flowmotion measures are sampling different volumes of skin+SC after RT compared to baseline. The different blood volumes of the tissue potentially measured by the LDF + OXY probe may also explain the difference in skin+SC flowmotion measures before and after RT. Unfortunately, despite CEU imaging being performed on forearm muscle, any difference in subcutaneous fat from Pre-RT to Post-RT was not able to be determined as ultrasound images were focused on muscle tissue and adequate imaging of subcutaneous mass was not obtained for each subject.

The results of this study, and those described in chapters 3 and 4 of this thesis, highlight an issue with the assessment of flowmotion in healthy and diseased populations, where, for primarily practical (non-invasive) reasons, flowmotion is assessed in skin+SC using LDF flux. The response to the OGC in healthy controls and in the T2D participants Pre and Post-RT, show a difference in skin+SC and muscle blood flow, indicating that skin+SC flowmotion measures may not reflect the flowmotion occurring in the underlying skeletal muscle tissue. Furthermore, there was no correlation in skin+SC and muscle blood flow in healthy controls and type 2 diabetics, Pre or Post RT (Figure 4.7 and 5.6 respectively). Understanding flowmotion in skeletal muscle and how it changes with metabolism, is of great importance in discerning the dysfunction that occurs in T2D given the critical role skeletal muscle blood flow plays in glucose disposal. Adaptation of the CEU technique, used to measures skeletal muscle microvascular perfusion in the clinical studies of this thesis, could potentially assess

flowmotion in skeletal muscle tissue in a non-invasive manner and allow assessment of flowmotion in large regions of tissue simultaneously.

Chapter 6 - *Adaption of contrast enhanced ultrasound to measure skeletal muscle flowmotion*

6.1 Introduction

The ability to vary blood flow patterns and distribution in tissues is important for normal physiological function, optimising the delivery of nutrients and removal of wastes under different metabolic demands (80, 276, 277). Altering both total blood flow and flow distribution is believed to be of particular importance in tissues such as skeletal muscle. Nutrient requirement in skeletal muscle undergoes dramatic changes during different states of metabolic demand. During rest demand is low and therefore only about 1/3 of capillaries are perfused at any one time, allowing for greater blood flow distribution to other tissues in the body (reviewed in (6)). In contrast, during exercise demand for fuel significantly increases and (dependent upon level of intensity) many or all capillaries become perfused to meet heightened nutrient requirements of the myocytes (278). The mechanism by which changes in blood flow distribution occur is not well understood, however it is thought to be influenced by a number of factors, both centrally mediated and locally acting.

Changes in blood flow distribution within skeletal muscle can be brought about by altering the vascular tone of 3^{rd}-5^{th} order arterioles which feed into the capillaries (16). Additionally, pre-capillary sphincters may contract or relax to allow or impede the passage of blood flow (35). Of particular interest in this thesis is the process of flowmotion as it is believed to be important for normal physiological function in skeletal muscle. However, the precise mechanisms which control this process and the influence of different metabolic states is still poorly understood.

Elucidating the mechanisms which control skeletal muscle flowmotion is impeded by the technologies available to assess the phenomena. Intravital microscopy has been used to assess flowmotion in small specialised, surgically exposed animal muscle (279) or in the nailfold microvasculature of humans (92, 100). However, this technique is limited in the study of flowmotion due to its inability to study larger sections of deeper more metabolically relevant tissues, without significant disruption to the blood flow. The primary technique used to assess flowmotion has been LDF. Due to its ability to non-invasively assess skin+SC blood flow, LDF has been a useful tool in the discovery of flowmotion and

the categorisation of the different frequency components which influence blood flow distribution (56, 90, 91, 96, 279). LDF does however have a number of limitations which prevent a complete understanding of flowmotion function. A major limitation with the LDF technique in the context of flowmotion is that it can only measure a small section of tissue at any one time. The LDF laser illuminates up to a volume of ~0.55-0.79mm^2 section of tissue (61), thus assessing flowmotion in that area alone, giving no indications of possible differing flowmotion patterns occurring outside of this sample area. LDF is also limited in the types of tissues in which it can be used to assess flowmotion, especially in humans, as in deeper tissues such as skeletal muscle a LDF probe must be inserted into the tissues itself (or the skin above the muscle surgically removed). The need to implant the LDF probe presents a number of issues, such as the discomfort caused in participants, as well as the potential damage to the tissue and alteration of blood flow patterns. As such, the majority of flowmotion assessment using LDF has been in skin+SC, which is a non-invasive LDF measure where the probe is placed directly onto the skin surface. The previous chapters of this thesis have demonstrated a difference in microvascular perfusion between skin+SC and the underlying skeletal muscle as measured by LDF and CEU respectively. As such, it is unlikely skin+SC flowmotion measurements are representative of flowmotion in more metabolically active tissues such as skeletal muscle. LDF also measures both red blood cell number and velocity, meaning the influence of each of these components upon the overall measure of flowmotion cannot be separated. Thus, with LDF measures it is unclear if changes in flowmotion detected are a result of increased blood volume to a tissue (indicating greater capillary recruitment) or increased velocity (indicating an increase in total blood flow to the tissue), or a combination of the two.

Originally developed to detect blood flow blockages in the heart (280, 281), the novel technique of CEU is a minimally invasive technique which has been adapted to measure skeletal muscle microvascular volume changes in humans and animals (282). The CEU technique allows continuous monitoring of blood volume in a section of skeletal muscle, and therefore any changes in

microvascular recruitment under different treatment conditions can be determined. The adaptation of the CEU technique for the measurement of skeletal muscle flowmotion would provide a means of overcoming a number of the limitations of LDF flowmotion measures. Unlike LDF, CEU is able to measure flowmotion across larger sections of skeletal muscle tissue, i.e. a 2D image of a whole rat calf muscle. CEU measurements are non-invasive in regards to the tissue being assessed (only requiring intravenous infusion of contrast agent), making the technique appropriate for human use, and limiting any experimental induced changes in skeletal muscle blood flow patterns. CEU is also a measure of blood volume alone and as such any changes observed can be directly related to blood volume changes within the tissue and not changes in RBC velocity like LDF. The adaptation of CEU to assess flowmotion therefore provides the opportunity to establish if flowmotion changes result purely from altered velocity of blood flow, or if blood volume also contributes.

A novel idea is to not only measure skeletal muscle flowmotion with wavelet transformation of LDF flux and tissue oxygenation data, but to also apply the same processing principles to CEU data acquired during various treatment protocols. The use of CEU in the assessment of flowmotion gives a new approach to its study and can potentially improve the ability to evaluate different components of skeletal muscle flowmotion. Thus the aim of this study was to use CEU to assess skeletal muscle flowmotion with the wavelet transformation technique. The CEU measures were validated with a comparison to the well-established LDF technique. In order to validate the CEU technique, skeletal muscle flowmotion was altered with the infusion of phentolamine (PT). PT is an alpha-adrenoceptor antagonist known to cause vasodilation of arteries and arterioles via the inhibition of neurogenic-mediated vasoconstriction (283). The systemic infusion of PT therefore results in an inhibition of the neurogenic component of flowmotion. LDF and CEU data were analysed by wavelet transformation to determine changes in skeletal muscle flowmotion.

6.2 Methods

6.2.1 Animal care

Male Sprague Dawley rats (288g ± 8) were used in these experiments. Animals were raised as described in 2.1.1.

6.2.2 *In vivo* surgery

The anaesthetised rat model was used for these experiments. Surgery was performed as described in section 2.1.2.

6.2.3 Experimental procedure

The systemic infusion of contrast agent during CEU measures causes an interference with the ultrasonic flow probe used to measure FBF, therefore, systemic and microvascular blood flow were measured in separate experiments (protocol A and protocol B, Figure 6.1). Protocol A allows the assessment of LDF flowmotion and FBF, while protocol B assesses flowmotion with LDF and CEU. These were performed on separate animals.

6.2.3.1 Protocol A

After post-surgery stabilisation, a 30min basal period was followed by a 60min systemic PT infusion (5mg/kg/min). Skeletal muscle microvascular blood flow in the tibialis anterior muscle was assessed with the LDF + OXY probe (LDF flux, O_2 Sat and tHb measures). LDF flux, tissue oxygenation and FBF measures (as per section 2.1.2.1) were taken constantly throughout protocol (Figure 6.1). LDF + OXY flowmotion was assessed by wavelet transformation on data from the 30min basal period and last 30min of PT infusion. Animals were euthanized at completion of experiment with an overdose of sodium pentobarbital.

6.2.3.2 Protocol B

Protocol B also consisted of a 30min basal period followed by 60min of systemic PT infusion (5mg/kg/min). Tibialis anterior LDF + OXY flux was again measured throughout protocol. Calf or upper thigh CEU acoustic intensity (AI) measures were constantly recorded during 30min basal period, and for the last 30min of PT infusion (t=60-90min, Figure 6.1). Flowmotion measures from calf and upper thigh CEU and LDF + OXY data from 30min basal capture and last 30min of PT infusion was determined with wavelet transformation. Calf microvascular perfusion was determined at t=30min (basal) and t=90min (PT), as describe in section 2.1.2.3. Animals were euthanized at completion of experiment with an overdose of sodium pentobarbital.

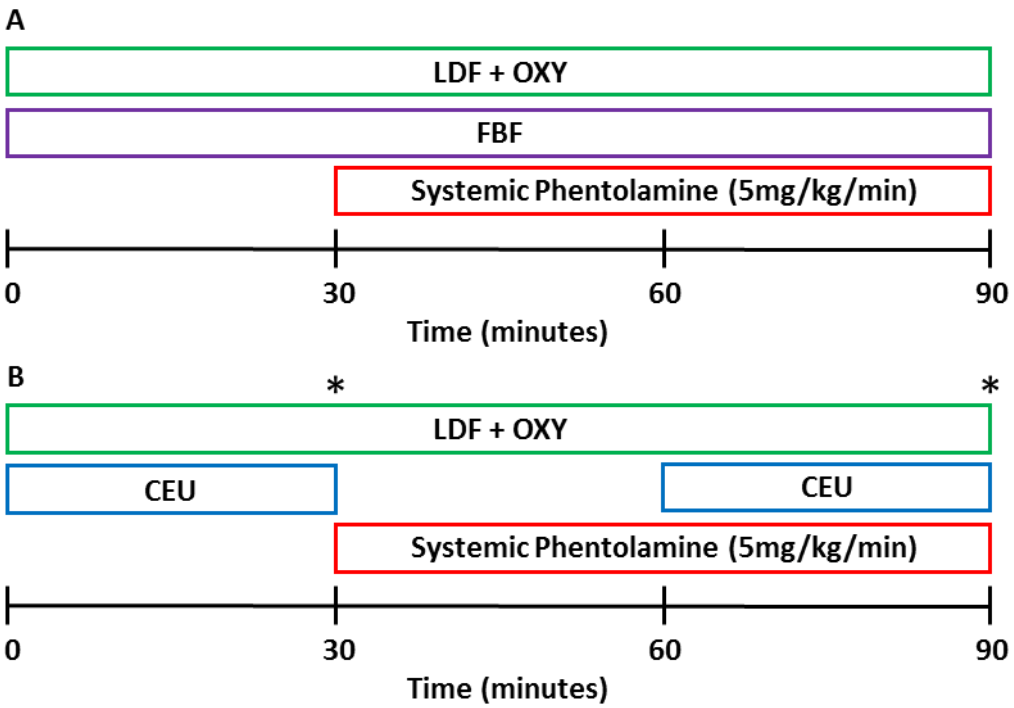

Figure 6.1: *Microvascular experimental protocols*. A) Protocol A: LDF flux, O_2 Sat, tHb (**LDF + OXY**) and femoral blood flow (**FBF**) was recorded continuously throughout experiment. Following 30min basal recording phentolamine (**PT**) was systemically infused (5mg/kg/min) for remainder of experiment (60min). Wavelet transformation analysis was performed on 30min basal and last 30min of **PT** infusion **LDF + OXY** data. B) Protocol B: **LDF + OXY** was again recorded continuously throughout experiment. Contrast enhanced ultrasound (**CEU**) measures were taken on either calf or upper thigh skeletal muscle. A 30min basal **CEU** capture was taken. **PT** was then systemically infused (5mg/kg/min) for remainder of experiment. Continuous **CEU** capture was taken on the last 30min of **PT** infusion. CEU microvascular perfusion measures were taken at the end of basal and PT captures (*), t=30 and 90min. **CEU** and **LDF + OXY** data from the 30min basal and **PT** time points was used in the wavelet transformation analysis.

6.2.4 Data analysis

6.2.4.1 Haemodynamic and LDF flux analysis

Data were determined as described in section 2.2.3. MAP, HR and FBF were calculated every 5min over the course of experiment. LDF + OXY 5min LDF flux, O_2 Sat and tHb averages were calculated throughout entire experiment.

6.2.4.2 LDF + OXY flowmotion analysis

Data from each 30min time period measured by LDF + OXY was exported from Moor instruments software and analysed as per section 2.2.4. To determine changes from basal to PT in lower frequency components of flowmotion in LDF + OXY measures, AUC of peaks in endothelial (0.095-0.02Hz), neurogenic (0.02-0.06Hz) and myogenic (0.06-0.15Hz) frequency ranges were determined using PeakFit as describe in section 2.1.8.3. As these experiments were performed on an animal model, but the frequency regions defined in the literature are based on human participants, less stringent parameters on frequencies rangers were applied when prudent. Where there were clear peaks for each component shown that were not necessarily within the defined frequency bands leniency was applied to allow for the potential difference between the animal model and human participants.

6.2.4.3 CEU flowmotion analysis

After extensive investigation, a region of 1mm^2 was determined to be most appropriate for analysis. Qlab software allows for a maximum of 10 ROI to be used during any one analysis. A range of different ROI box sizes were analysed to determine the best means of assessing CEU data to then be compared to LDF + OXY. Figure 6.2 demonstrates the differences in wavelet transformation output at various box sizes. The decision was made to use ten x 1mm^2 boxes as the data output was of a sufficient quality and comparable to the LDF + OXY measures as LDF has been shown to sample ~0.55-0.79mm^2 volume of tissue (61).

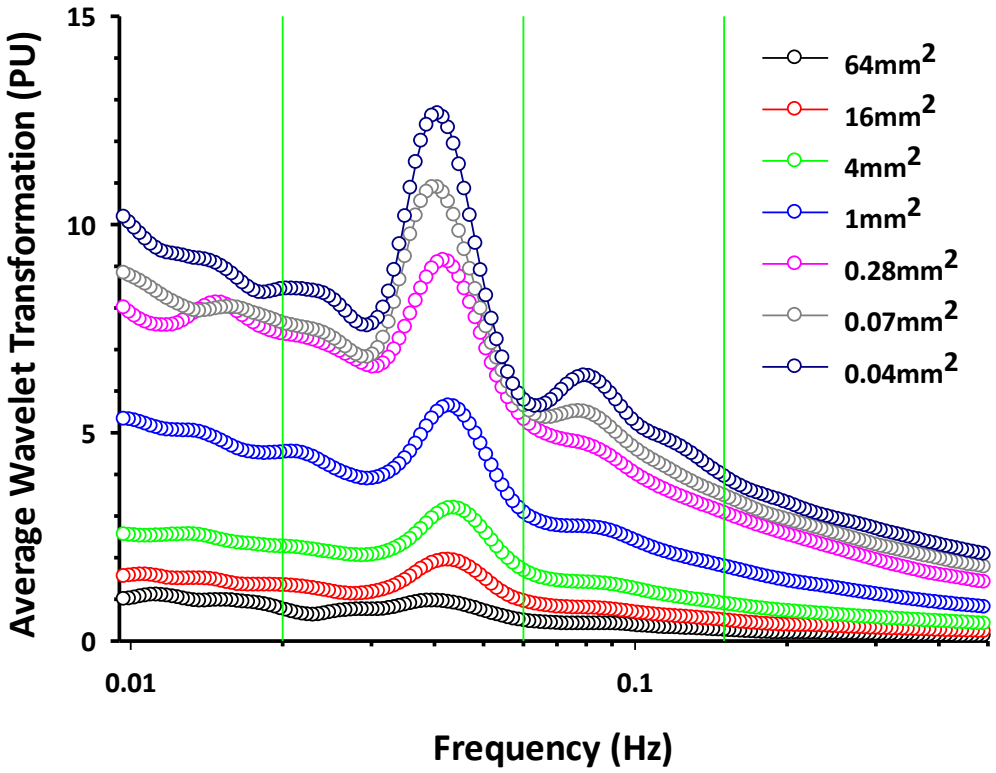

Figure 6.2: *Average wavelet transformation for different ROI sizes.* As size of ROI measured decreases, the clarity of peaks in each frequency component becomes higher and more pronounced, without a significant change in frequency. Under 1mm^2 decreasing ROI box size has less effect upon wavelet transformation. The 1mm^2-sized ROI gives well defined peaks in the wavelet transformation output and is comparable to LDF measures, therefore was used in analysis.

For calf and upper thigh CEU measures, both a predominantly white region and a mixed fibre region (Figure 6.3) in each muscle mass was assessed with ten 1mm^2 regions of interest (ROI's). Data for each ROI was exported and wavelet transformation per section 2.2.4 was performed. Analysis was performed this way to investigate if flowmotion varies in different sections with differing fibre types. It is not appropriate to use large ROI to assess flowmotion in skeletal muscle tissue as it is thought different sections of the muscle will have different flowmotion patterns. The output of large ROI analysis will thereby be an average of all the flowmotion patterns and not representative of the differing blood flow occurring across the tissue. Due to the observed highly variable nature of flowmotion across skeletal muscle, the basal wavelet transformation graph of each ROI for each experiment and each fibre type region was de-identified, randomised and given to informed, but impartial selectors. In duplicate, these selectors determined the three 1mm^2 ROI's of each experiment

and fibre type that displayed the strongest neurogenic peak in the basal recording. The experimental average was determined from these three ROI's for both basal and PT treatment. As per LDF + OXY, to determine changes from basal to PT in lower frequency components of flowmotion in CEU measures PeakFit software was used to determine AUC of peaks in each frequency region as described in section 2.1.8.3.

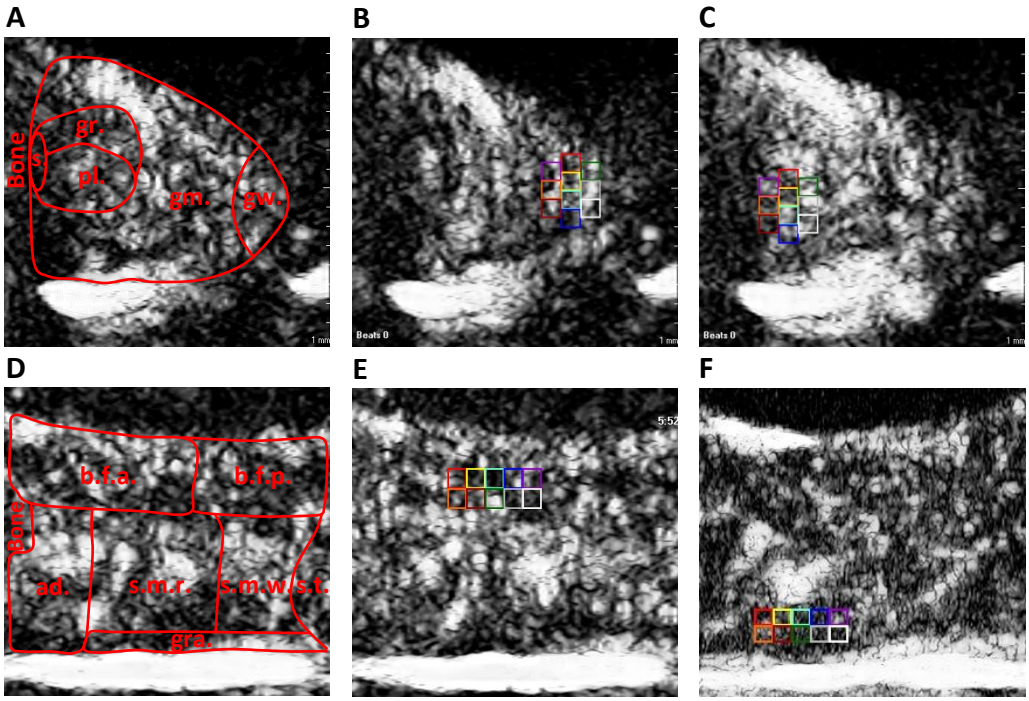

Figure 6.3: *Rat calf and upper thigh contrast enhanced ultrasound regions of interest.* A) CEU image of rat calf with overlay of individual muscle positioning based upon R. Armstrong and O. Phelps 1982 (229). Abbreviations: s., soleus; pl., plantaris; gr., gastrocnemius red; gm., gastrocnemius mixed; gastrocnemius white. B) Example of 10 regions of interest (ROI) placement in calf predominantly white fibre region. C) Example of 10 ROI placement in calf mixed fibre region. D) CEU image of rat upper thigh with overlay of individual muscle positioning based upon R. Armstrong and O. Phelps 1982 (229). Abbreviations: b.f.a., biceps femoris anterior; b.f.p., biceps femoris posterior; ad., adductor magnus and brevis; s.m.r., semimembranosus red; s.m.w., semimembranosus white; s.t. semitendinosus; gra., gracilis. E) Example of 10 ROI placement in thigh predominantly white fibre region. F) Example of 10 ROI placement in thigh mixed fibre region.

6.2.5 Statistical analysis

All tests were performed using SigmaStat software (Systat Software Inc. CA, USA) as described in section 2.4. Significant change in LDF flux, O_2 Sat, tHb, MAP and FBF over time were determined using one-way repeated-measures ANOVA. Statistical difference between basal and PT was determined using a paired Student's t-test.

6.3 Results

6.3.1 Systemic haemodynamic changes

PT inhibits the neurogenic input to the vascular system and thus causes haemodynamic changes systemically (Figure 6.4). HR was not significantly altered throughout experiment (Figure 6.4B). MAP remained steady at 113.6 ± 0.5mmHg throughout basal period and then significantly decreased ($p < 0.001$) within 5min of PT infusion (Figure 6.4A). This drop in MAP plateaued at 45mins and remained at 79.2 ± 1.0mmHg for the rest of the experiment. FBF followed a similar pattern with an average of 1.00 ± 0.01mL/min at basal becoming significantly increased upon PT infusion ($p < 0.05$) (Figure 6.4C). FBF however, continued to increase throughout experiment reaching 2.48 ± 0.19mL/min (2.5-fold increase from basal) at experiment end (t = 90min).

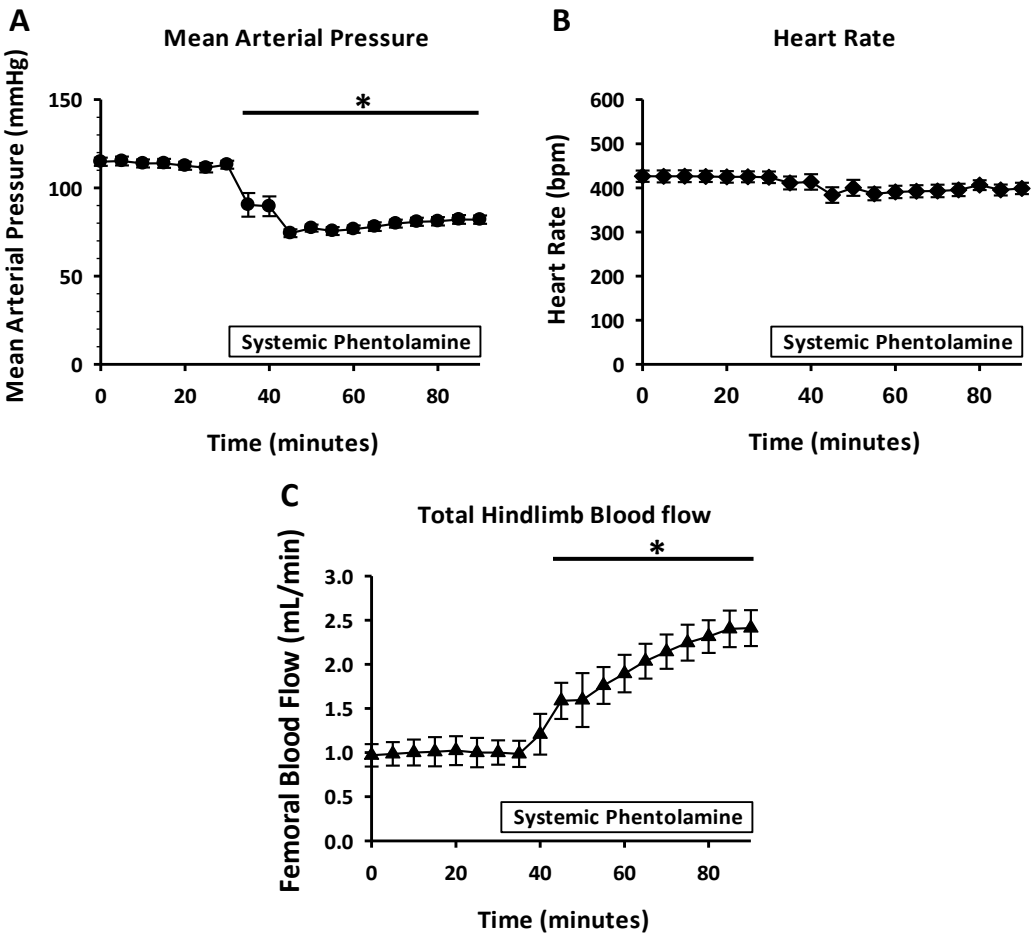

Figure 6.4: *Systemic hemodynamic changes with PT.* Systemic PT induced changes in A) mean arterial pressure (n=14) and B) heart rate (n=14) C) total hindlimb blood flow (n=5). Data expressed as mean ± SE. * significantly different from basal, $p<0.05$.

6.3.2 Microvascular haemodynamic changes

Inhibition of neurogenic input to the vasculature resulted in altered microvascular blood flow in skeletal muscle. Change from basal in LDF + OXY measures (LDF flux, O_2 Sat and tHb) for the tibialis anterior muscle are shown in Figure 6.5. LDF measures tended to increase from basal (173.4 ± 27.6PU) over course of experiment, becoming significant ($p < 0.05$) from t = 0 at t = 80 and 90min. O_2 Sat remained steady throughout basal period (58.4 ± 0.1%) and then significantly increased at t = 40min, remaining elevated (70.6 ± 0.5%) for the rest of experiment. tHb was constant throughout basal (156.9 ± 16.1AU) and then continually increased upon PT infusion, reaching significantly different from basal ($p < 0.05$) at t = 60min. Peak increase of 24.4 ± 9.3AU was at achieved at t = 90min.

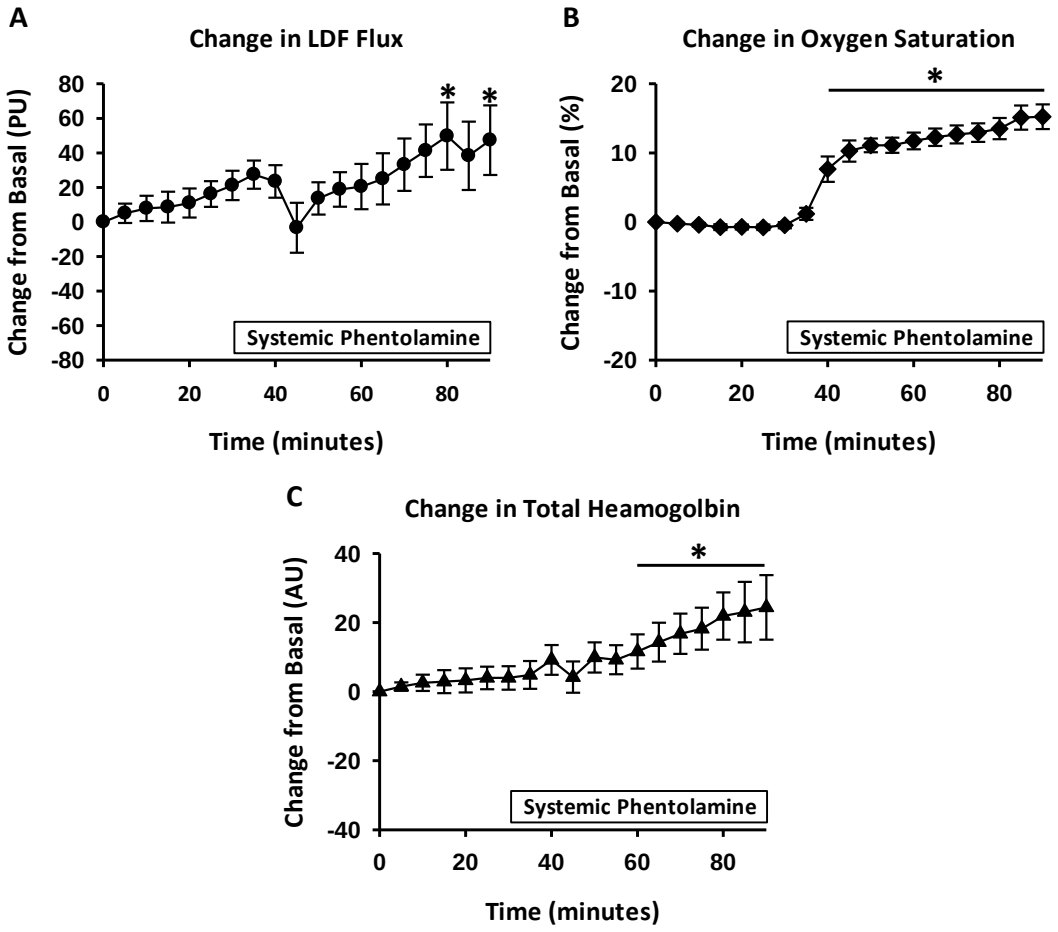

Figure 6.5: *Microvascular blood flow changes from basal in tibialis anterior muscle.* Systemic PT induced A) LDF flux change from basal B) O_2 Sat change from basal C) tHb change from basal. Data expressed as mean ± SE, n=14. * Significantly different from t=0, $p<0.05$.

Infusion of PT resulted in increased capillary perfusion from basal (t=30min) to PT treatment (t=90min) in calf muscle as shown in Figure 6.6. Microvascular blood volume and microvascular filling rate of the calf muscle both significantly increased upon PT treatment (p = 0.002 and 0.004 respectively). When combined these two parameters give a measure of microvascular perfusion, which also increased significantly (p = 0.015) with PT infusion, indicating significant microvascular recruitment in the calf upon PT infusion.

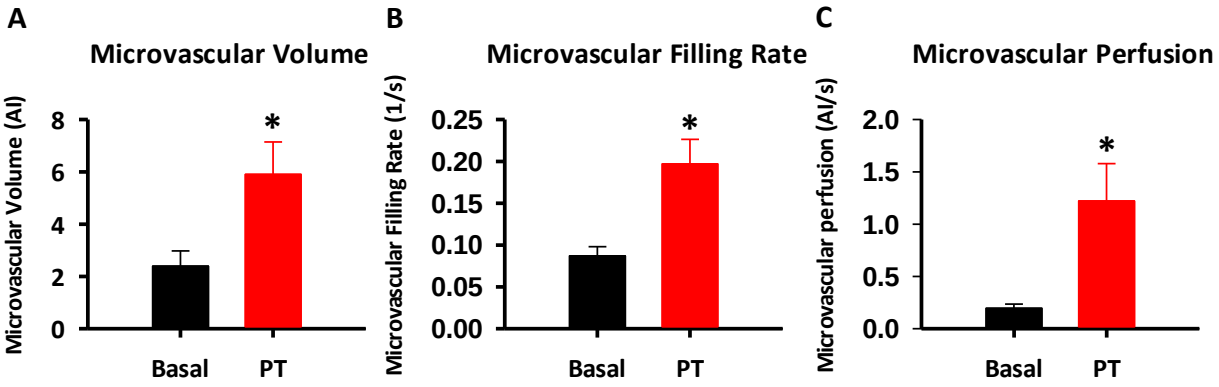

Figure 6.6: *Microvascular perfusion in calf muscle as measure by contrast enhanced ultrasound.* Calf microvascular perfusion pre (t = 30) and 60min (t = 90) into PT infusion. A) Microvascular volume (A) B) microvascular filling rate (β) C) Microvascular perfusion (Axβ) n=5. * Significantly increased from basal, p<0.05.

6.3.3 Skeletal muscle flowmotion changes

Data from wavelet transformation indicates the contribution of each frequency component to flowmotion and can be graphed on a log scale. Figure 6.7 shows typical wavelet transformations from each different microvascular blood flow measure. During basal capture a clear peak in the neurogenic frequency range (0.02-0.06Hz) is observed, upon PT infusion there is a prominent loss of the signal within the neurogenic frequency component.

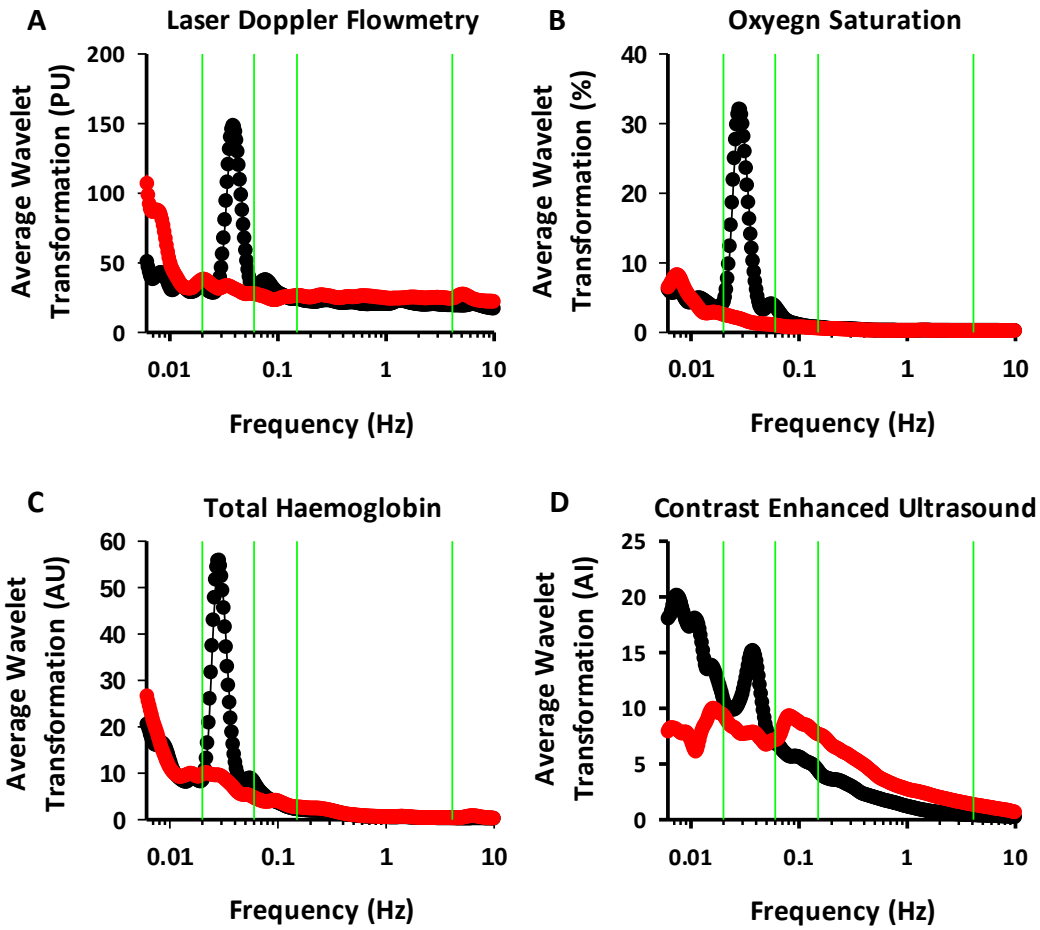

Figure 6.7: *Typical wavelet transformation of skeletal muscle blood flow measures Laser Doppler Flowmetry, oxygen saturation, total haemoglobin and contrast enhanced ultrasound.* Typical wavelet transformations of **basal** and **PT** treatment over low frequency components endothelial (0.095-0.02Hz), neurogenic (0.02-0.06Hz) and myogenic (0.06-0.15Hz) in tibialis anterior muscle measured by A) LDF flux B) O_2 Sat C) tHb measures and calf muscle measured by D) CEU.

The change in each of the flowmotion frequency components upon PT infusion can be quantified by determining the AUC of the peaks in each frequency range. Figure 6.8 shows the basal to PT changes in the lower frequency components of flowmotion (endothelial, neurogenic and myogenic) in the tibialis anterior muscle measured by the LDF + OXY probe. Flowmotion measures by LDF show a significant reduction ($p < 0.001$) in peak AUC from basal in both neurogenic and myogenic frequency ranges. Similarly, O_2 Sat and tHb flowmotion measures show a significant reduction in both neurogenic ($p < 0.001$, $p = 0.00125$ respectively) and myogenic ($p = 0.00088$, $p < 0.001$ respectively) frequency ranges.

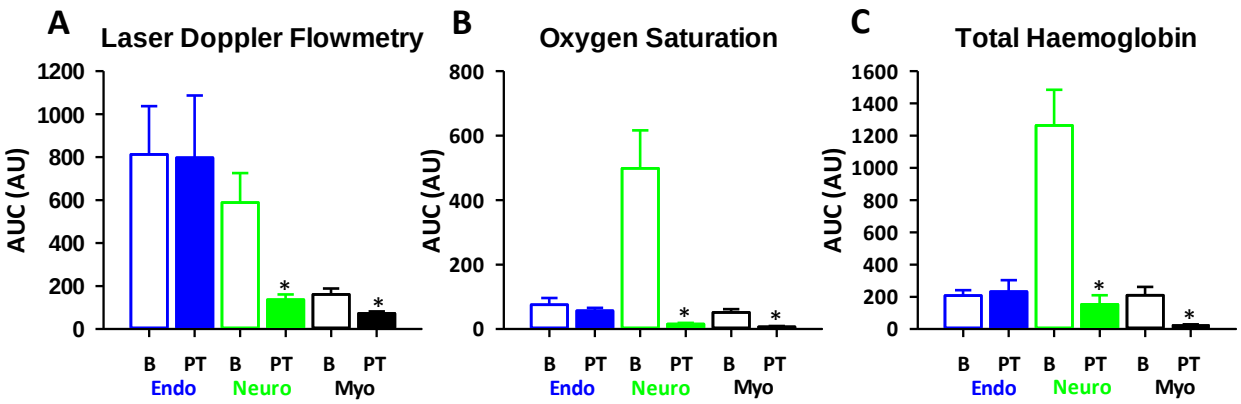

Figure 6.8: *Phentolamine induced flowmotion changes in tibialis anterior muscle measured by Laser Doppler Flowmetry, oxygen saturation and total haemoglobin.* Changes in flowmotion from basal (▫) with systemic PT (▪) infusion determined by area under the curve of the peaks in component frequencies endothelial (**Endo**, 0.095-0.02Hz), neurogenic (**Neuro**, 0.02-0.06Hz) and myogenic (**Myo**, 0.06-0.15Hz). Data measured by A) LDF B) oxygen saturation C) total haemoglobin (n=14). Data expressed as mean ± SE. * significant decrease from basal $p<0.05$.

Quantified data from the LDF + OXY probe was used for comparison (as this it is the standard technique for flowmotion measures) to determine if CEU can adequately measure skeletal microvascular flowmotion. Figure 6.9 shows the CEU flowmotion measures from different muscle types (calf and upper thigh), as well as different fibre type regions (predominantly white fibre and mixed fibre regions). There was a significant reduction ($p = 0.050$) in calf predominantly white fibre neurogenic component from basal to PT treatment. No significant change in contribution in any frequency component in the calf mixed fibre was observed. In the upper thigh predominantly white fibre region there was a significant decrease in both neurogenic ($p = 0.00134$) and endothelial ($p = 0.016$) frequency regions. Similarly, in the upper thigh mixed fibre region only the endothelial region was significantly decreased ($p = 0.030$) with PT infusion.

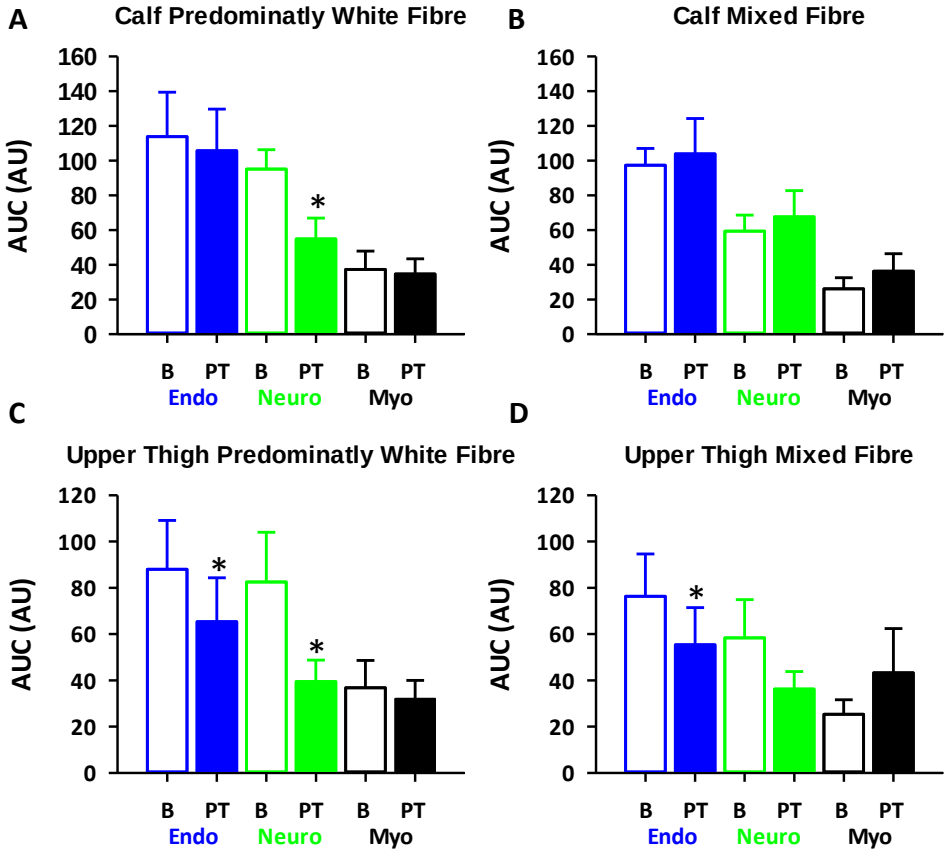

Figure 6.9: *Phentolamine induced flowmotion changes in calf and upper thigh skeletal muscle measured by contrast enhanced ultrasound.* Changes in flowmotion from basal (▫) with systemic PT (▪) infusion determined by area under the curve of peaks in component frequencies endothelial (Endo, 0.095-0.02Hz), neurogenic (Neuro, 0.02-0.06Hz) and myogenic (Myo, 0.06-0.15Hz) as measured by CEU. A) calf predominantly white fibre region (n=5) B) calf mixed fibre region (n=5) C) upper thigh predominantly white fibre (n=9) D) upper thigh mixed fibre (n=9). Data expressed as mean ± SE. * significantly decreased from basal, $p<0.05$.

6.4 Discussion

This study demonstrates for the first time that CEU can be adapted for the determination of skeletal muscle flowmotion. Assessment of skeletal muscle flowmotion using the CEU technique enables the study of blood flow patterns over large sections of muscle tissue, with the ability to identify different regional patterns of flowmotion. The infusion of PT allowed similar changes in flowmotion patterns to be identified by both the LDF + OXY (traditionally used for determination of flowmotion, Figure 6.8) and CEU data (Figure 6.9). The changes in flowmotion pattern identified with CEU show that microvascular flowmotion is in part brought about by changes in blood volume. Additionally, differences in fibre type flowmotion patterns within one muscle region were identified in this initial study, a further advantage of the CEU technique (Figure 6.9).

A systemic dose of PT produced the expected changes in haemodynamic parameters, including a reduction in mean arterial pressure and increase in total hindlimb flow (Figure 6.4). These changes resulted from the inhibition of sympathetic-mediated vascular tone, thereby producing a dilation of blood vessels (283). These changes in systemic haemodynamics indicate an appropriate dose of PT was used to elicit change in microvascular flow and inhibit sympathetic nervous system-mediated neurogenic flowmotion contributions.

PT infusion produced a significant change in all measures of blood flow in rat hindlimb. Total flow to hindlimb was shown to be increase with the FBF measures (Figure 6.4). Microvascular blood flow was shown to be greater with LDF flux (indicating an increase in RBC number and velocity in tibialis anterior muscle, Figure 6.5) and CEU (increased microvascular filling rate in the calf muscle, Figure 6.6). Changes in FBF, LDF flux and microvascular filling rate indicate an overall increase in the velocity of skeletal muscle total and microvascular blood flow during PT infusion. Tissue oxygenation was shown to be enhanced after PT infusion with the increase in O_2 Sat measures in the tibialis anterior muscle (Figure 6.5). The increase in calf acoustic intensity (AI, measured by CEU) and tibialis anterior muscle

tHb measures show an increase in microvascular perfusion in response to PT (Figure 6.6), and thus indicates that PT has also increased microvascular blood volume. PT infusion is therefore producing both the expected systemic changes and a significant change in blood flow patterns and distribution in the microvasculature.

Flowmotion measured by the LDF + OXY probe show a reduction in contribution to the neurogenic and myogenic components (Figure 6.8). Flowmotion measures by CEU show a similar reduction in the contribution of the neurogenic component, while also showing a reduction in the endothelial component (Figure 6.9). In addition to the expected reduction of the neurogenic flowmotion component induced by PT (an adrenoceptor antagonists) the LDF, O_2 Sat and tHb measures show a concurrent decrease in the myogenic component of flowmotion. It appears that with the removal of neurogenic influence upon the vessel smooth muscle, there has been a subsequent change in the activity of vasomotion (the intrinsic contractility of the smooth muscle), thereby producing a change in the myogenic component of flowmotion as well as the neurogenic. What the specific changes that occur in the smooth muscle to produce an alteration in the myogenic component of flowmotion is not known. A possible explanation is the removal of neurogenic input altered the synchronised oscillation of Ca^{2+} in the smooth muscle cells, which is believed to be responsible for the generation of vasomotion (11). Similarly, the CEU measures in the upper thigh show an alteration in the endothelial component of flowmotion (Figure 6.9). The significant reduction in endothelial component was only seen in the CEU measures. This suggests that the removal of neurogenic input upon PT infusion is altering the endothelial component in some way to result in blood volume changes within the skeletal muscle tissue.

Interestingly fibre type differences in flowmotion were revealed through the analysis of different regions of the calf and upper thigh muscles (as imaged by CEU, Figure 6.9). In the calf muscle significant changes in flowmotion from basal to PT were only observed in the predominantly white fibre region,

not the mixed fibre region. Changes to flowmotion measures in the upper thigh predominantly white fibre region occurred in both the neurogenic (as expected) and endothelial regions. Whereas only the endothelial region was significantly altered in the upper thigh mixed fibre region. Unfortunately due to the spatial resolution of the CEU technique, a predominantly red fibre region could not be analysed as these muscles tend to be small in size and deeper inside the tissue in rats (229). The flowmotion LDF + OXY measures on the tibialis anterior were taken via placing the probe on the surface of the outer muscle tissue. The tibialis anterior muscle is separated into two components, tibialis anterior white which is superficially located and tibialis anterior red which is located deeper in the hindlimb (229), therefore due to tissue penetration of the CP3 probe the LDF + OXY flowmotion measures are of a predominantly white fibre muscle region. The LDF + OXY measures of the tibialis anterior complement the predominantly white fibre calf and upper thigh CEU measures as a change in neurogenic component is seen in wavelet transformation of all measures. This data demonstrates the limitations of LDF. However, with the CEU technique allowing analysis of flowmotion across larger tissue regions, more intricate and subtle changes in flowmotion can be detected and analysed. It is thought that blood flow patterns are altered based on the specific needs of each different tissue region. As such, at any given time flowmotion patterns in different sections of a muscle may be not be acting in the same way. The CEU technique allows analysis of flowmotion across the whole tissue, which permits investigation of differing flowmotion patterns over a larger tissue region. Further development of the analysis of the CEU data may allow a pixel-by-pixel determination of flowmotion to highlight regional difference in flowmotion patterns across larger skeletal muscle sections.

The difference in flowmotion fibre type changes observed in this study indicate an interesting observation about blood flow control over large regions of skeletal muscle tissue. It may be that flowmotion control differs over a tissue, and here in the rat hindlimb it appears that central nervous system control is more pronounced in predominantly white fibre regions, hence the greater change produced with PT infusion. Mixed and predominantly red fibre regions may have greater control exerted over flowmotion by a different mechanism, for example locally generated factors (myogenic

or endothelial). Further investigation of the differing influences over different skeletal muscle fibre types is required.

The aim of this study was to determine if CEU could be used to assess flowmotion in skeletal muscle. By using LDF measures for comparison, it appears that the data generated by this CEU technique can indeed be analysed in a similar manner, with the resulting data providing a new comprehensive view of flowmotion changes in a large tissue region. Assessment of flowmotion by CEU in this anaesthetised rat model has also indicated that the frequency regions defined by Stefanovska *et. al.* (55) in humans may not be the same in this model. Leniency was shown in interpretation of results where clear peaks for each contribution were evident, but not necessarily exactly within predefined regions, indicating there may be variation in frequency regions in different species and under anaesthetic. Given this initial study, further research can now begin to assess how flowmotion is influenced by the metabolic state of the tissue and how the five components of flowmotion change in response to changes in substrate metabolism and oxygen uptake in the muscle. A previous study by Newman *et al.* (57) performed in a similar anaesthetised rat model, showed an increase in the contribution of the myogenic frequency component during insulin infusion (10mU/min/kg). Hindlimb glucose uptake was also increased during the insulin infusion, thereby linking changes in muscle metabolism with changes in flowmotion patterns. Flowmotion changes were measured in the tibialis anterior muscle using an implanted LDF probe. Further study with CEU technique is needed to further elucidate the interaction of flowmotion and metabolic state.

In conclusion, the data in this thesis chapter indicates that the adaptation of the CEU technique, used in conjunction with the well-established LDF technique, provides a new way of assessing skeletal muscle flowmotion. Further investigation of the factors controlling flowmotion and differing flowmotion patterns with changes in muscle metabolic state can now be performed. A difference in

skeletal muscle fibre type flowmotion control was additionally demonstrated in this study and prompts further research into this area to establish if this interesting observation can be replicated.

Chapter 7 – *Discussion*

7.1 Summary of findings

The aim of this thesis was to investigate the importance of flowmotion, with a particular focus on the dysfunction that occurs in T2D. A number of vascular processes become dysregulated in the disease (284), and thus it was thought that changes to flowmotion would be apparent. It is hypothesised that altered flowmotion contributes to pathological changes to metabolism, particularly decreased glucose uptake in the skeletal muscle, adding to the characteristic chronic elevation of blood glucose in T2D.

The first aim of this thesis was to investigate flowmotion in healthy control and T2D participants at basal and in response to an OGC (which induces endogenous insulin release). Secondly, this thesis aimed to assess if a RT intervention, which has previously been shown to improve glucoregulatory control and cardiovascular function (266), could restore any flowmotion dysfunction in the T2D participants. Skin+SC flowmotion in the forearm was measured via LDF flux and tissue oxygenation. Wavelet transformation of these data measured the rate and contribution of each of the components that influence flowmotion (cardiac, respiratory, myogenic, neurogenic and endothelial). Differences between healthy control and T2D participants were seen at both basal and in response to the OGC, indicating dysfunction in flowmotion in T2D participants. The short-term RT intervention in these participants resulted in modest improvements in skin+SC flowmotion.

While measures of skin+SC flowmotion are useful in investigating microvascular dysfunction in T2D, knowledge of changes to skeletal muscle flowmotion is of greater interest as this tissue plays a key role in whole body glucose disposal (162). Changes to blood flow and consequently glucose uptake in skeletal muscle in T2D is thought be an important process in the development of the disease (230, 285). As such, a further aim of this thesis was to determine if the changes to blood flow in response to the OGC were similar in skin+SC and skeletal muscle. The forearm total blood flow, skin+SC microvascular flux and skeletal muscle perfusion in response to the OGC was therefore compared. There were clear differences in the response to the OGC in skin+SC and muscle blood flow measures,

indicating that the skin+SC flowmotion measures taken in this study are unlikely to represent the flowmotion occurring in the underlying skeletal muscle.

The data in this thesis therefore highlight an issue in the current investigation of flowmotion, where predominantly skin+SC LDF flux measures are used. A non-invasive means of investigating skeletal muscle flowmotion is required to further knowledge of flowmotion changes in this tissue, which are of great importance in understanding the pathology of T2D. Thus, the final aim of this thesis was to adapt the CEU technique (currently used for the determination of skeletal muscle perfusion) to measure skeletal muscle flowmotion. An anaesthetised rat model was used to allow for invasive LDF blood flow measures in skeletal muscle and the pharmacological inhibition of the neurogenic component of flowmotion. To validate the CEU technique, results obtained from skeletal muscle flowmotion measured by LDF flux and tissue oxygenation (skin removed and LDF probe directly onto skeletal muscle) were compared to results obtained via CEU measures of flowmotion. The successful adaption of CEU to measure skeletal muscle flowmotion described in chapter 6 provides exciting opportunities to investigate flowmotion in this tissue during normal physiological function and in disease.

7.2 Flowmotion in healthy controls

The detection of skin+SC flowmotion during basal conditions in the healthy controls illustrates the occurrence of flowmotion at rest in this tissue. In this thesis, changes in flowmotion observed in the skin+SC were detected by both LDF flux and tissue oxygenation measures. The LDF technique determines both RBC number and velocity in the region of tissue illuminated by the laser (which cannot be separated, flux is a relative measure of the change in volume), whereas the tissue oxygenation measures (O_2 Sat and tHb) are thought to determine only RBC number (with O_2 Sat also being a measure of tissue oxygen use). The detection of flowmotion with these two different

measurement types indicates that flowmotion involves changes in both the velocity and volume of blood flow through tissue. In this thesis blood flow measured in the skin+SC was hypothesized to represent general flowmotion patterns in the body, but results presented in chapters 3, 4 and 5 indicate that this may not be true for skeletal muscle and thereby potentially other tissues as well.

It is thought that in skeletal muscle, blood flow distribution across the tissue is constantly changing, with only a portion of capillaries perfused at one time and constant variation in which capillaries are perfused (6). It is hypothesised that this constant variation in blood flow is, at least in part, controlled by flowmotion to produce optimal blood flow across the skeletal muscle tissue. Thereby, flowmotion at rest (in skeletal muscle) is thought to allow for adequate nutrient delivery to tissue to maintain basal metabolic activity, while supporting low total volumes of blood to a tissue. In response to changes in cellular metabolism, flowmotion is thought to alter to allow greater blood flow in support of enhanced metabolism (3).

Previously, changes in skeletal muscle flowmotion have been observed during a hyperinsulinemic clamp (133), which is hypothesised to allow enhanced blood flow directly to cells, augmenting glucose uptake. Studies in skeletal muscle observed an increased microvascular capillary perfusion in response to endogenous insulin release, induced by consumption of a mixed meal (65) and during a euglycemic hyperinsulinemic clamp (37). This increased capillary perfusion was stimulated by insulin action on the vascular endothelium, resulting in vasodilation. Hyperinsulinemia has also been shown to activate the SNS (244) and increase cardiac output and respiratory rate (200). These changes induced by insulin in the components that may influence flowmotion are believed to enhance tissue metabolism (286). It was an aim of this thesis to investigate flowmotion changes in healthy controls in response to increased plasma insulin levels. However, the use of an OGC to induce endogenous insulin release produced unexpected decreases in skeletal muscle blood flow in the healthy controls. This surprising response during the OGC, where plasma insulin levels were shown to increase, may be due to a

concurrent excessive activation of the SNS resulting from acute high levels of glucose in the insulin sensitive population (253). Consumption of a large glucose load alone has been shown to increase noradrenaline (NA) plasma concentrations (258) and increase SNS activity in skeletal muscle (244) in insulin sensitive participants. Data in chapter 4 of this thesis, where the OGC induced an increased in the rate of neurogenic activity in healthy controls and a decrease in the T2D participants (Table 4.3), possibly indicates an increase of SNS activity in insulin sensitive participants, as has been previously described (253). This increased SNS response to ingested glucose appears to be absent in insulin resistant participants. It is thought in this population where autonomic dysfunction is common (199), neurogenic input is already increased at basal compared to healthy controls. As such, an increase in circulating NA does not induce a further activation of the SNS. The results of this thesis highlight an important implication for future studies looking at blood flow and flowmotion response to insulin. A study by Jonk *et. al.* (247), where skin+SC flowmotion in healthy controls was examined in response to a 75g oral glucose load and a 495-kcal liquid mixed meal (60% carbohydrate, 25% protein and 15% fat), highlights the difference between methods used to induced insulin release. In response to the two different meal types, all components of flowmotion were enhanced by consumption of the mixed meal, whereas only the endothelial component was increased with 75g glucose load. Based on the observations by Jonk *et. al.* (247) and the data in this thesis, it is recommended that in the study of insulin mediated changes in blood flow, elevated insulin should be induced via consumption of a mixed meal or with a euglycemic hyperinsulinemic clamp, which appear not to result in excessive SNS activation.

7.3 Flowmotion in type 2 diabetes

Data in this thesis highlight the general microvascular dysfunction that occurs in T2D, with changes in both the rate of input and contribution of the five components that influence flowmotion. A change in microvascular flowmotion, whether it be caused by insulin resistance or itself contributing to insulin

resistance, is believed to impact on the function of a tissue (80). Pathological changes to vascular function in metabolic tissues such as skeletal muscle attenuates glucose uptake, but changes in other tissues (e.g. skin+SC) are also important. Changes to skin+SC flowmotion caused by insulin resistance and as a result of direct glucose damage to vessels, may be used to identify early dysfunction in peripheral blood flow, which may indicate the potential occurrence of damage to other cell types such as nerves in T2D, which leads to the development of neuropathy. Further investigation into the dysfunction of flowmotion in insulin resistance and T2D is therefore potentially of great importance. It may lead to the identification of the mechanisms that become dysfunctional in the disease, providing drug targets for future treatment. However, the investigation of flowmotion in normal physiological function and T2D has so far shown inconsistent results.

The primary means of investigating flowmotion has been through LDF measures of the skin+SC, due to its minimally invasive nature. These measures do provide valuable information about blood flow dysfunction occurring in insulin resistance and T2D, but the changes to flowmotion seen in different studies is highly variable. Changes in the five components that influence flowmotion at rest and in response to insulin are inconsistent between studies. A number of different factors may account for the variation of results, which need to be addressed before skin+SC LDF flowmotion measures could have diagnostic applications.

Table 7.1 summarises a number of recent studies investigating skin+SC flowmotion in healthy, obese and T2D populations and highlights a number of variables (population studied, probe position, analysis technique, and treatment type) that may account for the inconsistency of the results between studies.

Table 7.1: *Variations in skin and subcutaneous tissue flowmotion studies in healthy, obese and type 2 diabetic populations*

Year	Author	Population	Probe position	Analysis technique	Treatment	Observations
2014	de Boer *et. al.*	Healthy controls	Hand	Wavelet analysis	Euglycemic hyperinsulinemic clamp	All five components of flowmotion increased with insulin stimulation
2014	de Boer *et. al.*	Healthy controls	Hand	Wavelet analysis	Rest	BMI inversely associated with the contribution of neurogenic component
2011	Clough *et. al.*	Central obesity but otherwise healthy	Calf	Welch's method	Euglycemic hyperinsulinemic clamp	Increased endothelial component in response to insulin
2015	Vinet *et. al.*	Healthy control and metabolic syndrome	Forearm	Fourier analysis	Transdermal iontophoresis of insulin	Metabolic syndrome subjects showed a reduction in all components of flowmotion except respiratory in response to insulin, compared to healthy controls
2014	Montero *et. al.*	Severely obese and normal weight adolescents	Foot	Wavelet analysis	Transdermal iontophoresis of insulin	Severely obese adolescents showed impaired myogenic response in obesity during insulin stimulation, compared to normal weight
2008	de Jongh *et. al.*	Healthy control compared to obese women	Hand	Fourier analysis	Transdermal iontophoresis of insulin	Obese subjects showed blunted response to insulin in endothelial and neurogenic components in obesity, compared to healthy controls
2011	Rossi *et. al.*	Healthy controls compared to obese	Forearm	Fourier analysis	Rest	Reduced endothelial, neurogenic an myogenic contribution in obesity compared to healthy
2013	Sun *et. al.*	Healthy control compared to T2D with and without sympathetic skin response	Foot	Wavelet analysis	Rest	Decreased endothelial component in T2D at risk of neuropathy. Reduced neurogenic component in T2D with no sympathetic skin response.
2014	Sun *et. al.*	Healthy control compared to T2D with no, moderate or sever neuropathy	Foot	Wavelet analysis	Rest	Increased myogenic and decreased neurogenic activity associated with the development of neuropathy

One variable contributing to the inconsistent findings is the different populations of participants which have been assessed. It is likely that the level and type of dysfunction in flowmotion varies over the development and progression of T2D. Pathological changes to the five factors of flowmotion may possibly alter at different stages of the disease. Thereby, skin+SC flowmotion measures in clinically diagnosed T2D may vary significantly from those seen in early stages of disease development such as obesity. The age of the population may also influence skin+SC flowmotion. Changes to flowmotion have been reported with advancing age (287) and T2D populations tend to be older. The differences in subject populations are highlighted in studies by Montero *et. al.* (216) and de Jongh *et. al.* (219). Both studies investigated skin+SC flowmotion changes in obese populations during insulin

iontophoresis. However, participants in the Montero *et. al.* (216) study were adolescents of both sexes (aged between 12-17 years old), whereas the de Jongh *et. al.* (219) study population were obese women with a mean age of 40.1 ± 6.6 years. Montero *et. al.* (216) reported an impaired myogenic response to insulin, while de Jongh *et. al.* (219) reported blunted endothelial and neurogenic response to insulin. The studies by Montero *et. al.* (216) and de Jongh *et. al.* (219) also highlights the potential impact of gender in flowmotion studies, as flowmotion measures may differ between the sexes. Of particular note is the difference in subcutaneous adipose volume being assessed, as women tend to have a greater amount of subcutaneous adipose as compared to men (288). This has implications for LDF flux measures in the skin, where different combinations and volumes of tissue types may be measured, which may affect the flowmotion observed.

Another important variable is the positioning of the probe on the body. Blood flow patterns in the forearm may vary significantly from those on the hand, foot or calf, yet each of these has been used in the investigation of skin+SC flowmotion. There are differences in skin+SC at these different sites, as well as differences in the underlying tissue. The forearm and calf have larger subcutaneous tissue content compared to the foot or hand, and the underlying tissue is predominantly muscle in the forearm and calf, as opposed to bone in the foot and hand (288). These differences have the potential to greatly impact LDF flux measures as the composition of tissue sampled at each site can vary considerably.

The spectral analysis technique employed to analyses LDF data may also contribute to the inconsistency of the literature. Primarily, either Fourier analysis or wavelet transformation is used to determine flowmotion in skin+SC LDF flux measures. While both analysis techniques are able to detect the five frequency components of flowmotion, there are differences in the spectral analyses that may influence the results. For example, the wavelet transformation technique is thought to better elucidate the activity of the lower frequency components of flowmotion, compared to Fourier analysis

which is particularly adept at detecting higher frequency signals (55, 103). As such, the different flowmotion analysis techniques used in the literature may contribute to the observed variations in flowmotion response to insulin and changes in disease.

An additional consideration in the investigation of skin+SC flowmotion changes in response to insulin, both in healthy and T2D participants, is the method used to elicit an insulin response. The gold standard technique in the investigation of insulin sensitivity and insulin-mediated responses is an euglycemic hyperinsulinemic clamp, where insulin is infused at a constant concentration and glucose at a variable rate to maintain a steady state blood glucose concentration during hyperinsulinemia. This technique produces a systemic response to insulin (138), therefore in the context of flowmotion it may activate both local and centrally acting components. The changes in skin+SC flowmotion in response to this systemic exogenous infusion of insulin may vary considerably to changes induced by another common technique, insulin iontophoresis where insulin is introduced locally in the skin+SC (250). Local insulin introduced through the skin will not activate the centrally mediated flowmotion components, while the forced introduction of insulin through the skin may cause changes in blood flow in itself. Additionally, issues associated with iontophoresis such as the indirect effects of the current used and the fact that the concentration of insulin is unknown with this technique (289), complicate flowmotion measures. Therefore, the method of insulin stimulation used could greatly effect which of the frequency components are alter by insulin.

If these issues could be addressed and greater consistency in skin+SC flowmotion studies achieved, there is potential for this technique to be incorporated into clinical practice. Skin+SC flowmotion measures could perhaps be used to identify vascular dysfunction early on in disease pathology, and also be used to monitor disease progression and to identify early the development of secondary conditions such as neuropathy. The early detection of changes in flowmotion is potentially of great

importance as treatment programs such as exercise intervention or weight loss could be implemented to stop progression to clinically diagnosed T2D.

Previous studies, particularly in early stages of disease progression (obesity) have identified changes in skin+SC flowmotion and then implemented a treatment to correct these changes. Rossi *et. al.* (243) identified changes to the endothelial, neurogenic and myogenic components in skin+SC flowmotion at rest, in morbidly obese participants (BMI 47.0 ± 8kg/m^2), both with and without T2D. These participants then had gastric bypass surgery and subsequently, had significant weight loss (~40kg on average) 1-year post surgery when flowmotion was reassessed. As a consequence of the weight loss in these participants, the changes in skin+SC flowmotion seen at baseline were normalised. As such, it appears the weight loss is able to reverse flowmotion defects in obese participants.

Exercise training interventions have enormous potential to improve health outcomes and quality of life in T2D patients as it promotes weight loss, increases insulin sensitivity and improves cardiovascular function. Importantly, in early stages of disease development (obesity and insulin resistance) an exercise intervention can normalise pathological changes in flowmotion. Vinet et. al. (273) showed a 6-month exercise and dietary intervention in participants with metabolic syndrome (a precursor state for a number of different diseases including T2D) normalised the response to insulin of endothelial, neurogenic and cardiac components of flowmotion measured in the skin+SC. Identification of skin+SC flowmotion dysfunction at early stages of disease development could thus be used to prompt early pharmaceutical and exercise intervention in an attempt to stop progression towards T2D. Exercise intervention may also improve long-term health outcomes in participants already diagnosed with T2D. In this thesis a 6-week RT exercise intervention in clinically diagnosed type 2 diabetics improved a number of health parameters over the short intervention. Body composition and glucoregulatory control was improved, as has been previously shown with RT (271), as well as partial restoration of skin+SC flowmotion. Long-term exercise interventions in T2D has the potential to greatly improve

vascular function, and thereby flowmotion. With improvement in flowmotion in T2D, processes such as glucose disposal can potentially be improved and thus long-term outcomes and quality of life greatly enhanced.

The studies describe this thesis highlights further considerations for the assessment of flowmotion in healthy control and T2D participants. Basal and OGC induced changes in skin+SC flowmotion give further evidence that flowmotion is altered in clinically diagnosed T2D participants. The next step is to understand how these changes develop in T2D, thereby potentially identifying drug targets for future pharmaceutical intervention. The data in chapter 5 indicates that long term RT intervention in type 2 diabetics may be a means of improving flowmotion, potentially in a number of tissues including skeletal muscle, which may lead to improved glucose disposal.

To aid in the detection and treatment of microvascular dysfunction, this thesis hoped to develop complexity analysis of skin+SC LDF flux and tissue oxygenation measures as a means to easily identify microvascular dysfunction in a clinical setting. Previously, decreasing skin+SC LDF flux complexity was observed with increasing severity of insulin resistance and T2D in monkeys (226). Data in chapters 3 and 4 of this thesis show differences in flowmotion between healthy control and T2D groups identified with spectral analysis of skin+SC blood flow data, but no differences between the two groups was identified with complexity analysis. Therefore, it appears that complexity analysis of skin+SC blood flow measures is not able to adequately detect skin+SC microvascular dysfunction in humans.

Another outcome from the data in this thesis is the recommendation that investigation of insulin-mediated changes in flowmotion in healthy and disease states should not use an oral glucose load, due to the unexpected decreased in blood flow it induced in the healthy controls. Instead consumption of a mixed meal or an euglycemic hyperinsulinemic clamp should be used, which have previously been

shown to increase blood flow in healthy controls (37, 65, 248, 256), as would be expected with an increase in insulin levels.

The difference in skin+SC and skeletal muscle microvascular blood flow response to OGC observed in chapters 3, 4 and 5 have important implications for the future study of skeletal muscle flowmotion. This thesis highlights that skin+SC flowmotion measures may not be representative of skeletal muscle flowmotion, and thus to ascertain the changes in flowmotion that occur in response to stimuli such as insulin or during disease states like T2D, different techniques are required. While skin+SC flowmotion measures are still useful in the identification of microvascular dysfunction in T2D, these data suggest skin+SC flowmotion may not represent skeletal muscle flowmotion patterns. In T2D there are two important tissues in glucose metabolism that become dysfunctional, liver and skeletal muscle (290). Blood flow in the liver differs greatly from that in the skeletal muscle due to the both the structural and functional differences of the tissues (252). Changes in flowmotion in T2D are not likely to be important in the liver, but may have great importance in skeletal muscle tissue where 65-90% of glucose is stored after a meal (162-164). It is therefore of great interest to understand the normal physiological role of flowmotion at rest in skeletal muscle and the dysfunction which may occur in insulin resistance and T2D.

Only a limited number of studies have directly investigated skeletal muscle flowmotion. Newman *et. al.* (57), using the anaesthetised rat model, measured flowmotion using a LDF probe invasively implanted directly into skeletal muscle tissue. This study showed an increase in the myogenic component of flowmotion during an euglycemic hyperinsulinemic clamp, which was then bunted during an acute insulin-resistant state induced by the vasoconstrictor α-methylserotonin. In healthy humans de Jongh *et. al.* (249) also used an invasively implanted LDF probe in the calf and showed an increase in the endothelial and neurogenic components of flowmotion during a euglycemic hyperinsulinemic clamp. While implanted LDF probes have allowed this investigation of skeletal

muscle flowmotion, there are a number of limitations that need to be considered with this technique. By inserting the LDF probe directly into the skeletal muscle tissue there is the potential for this invasion to alter blood flow patterns being investigated. Thereby the blood flow measures may not be a true representation of skeletal muscle flowmotion. Additionally, a considerable limitation of LDF is the relatively small amount of tissue (~0.55-0.79mm^2 volume (61)) that can be sampled at any one time. Large tissue regions and differences in blood flow in different sections of muscle tissue therefore cannot be examined with this technique. There is potentially great variation in skeletal muscle blood flow across the tissue, particularly between different fibre types and between nutritive and non-nutritive capillary networks (24). To overcome these limitations and greatly expand the potential for investigation of skeletal muscle flowmotion, the data in chapter 6 of this thesis shows the successful adaptation of the CEU technique in the assessment of skeletal muscle flowmotion.

CEU is non-invasive to skeletal muscle, requiring only an intravenous infusion of the contrast agent (282). As such, it does not artificially alter the blood flow in skeletal muscle, thus flowmotion measurements are a true representation of blood flow patterns in the tissue. An exciting additional benefit of CEU flowmotion measures is the larger sections of tissue in which blood flow can be assessed by this technique, as the ultrasound technique is able to visualised large sections of skeletal muscle tissue. The data in chapter 6 demonstrates how the CEU technique allows analysis of differing flowmotion in different sections of the same tissue. In Figure 6.9 the differing flowmotion patterns in both a predominantly white fibre region and a mixed fibre region in the calf and upper thigh muscles upon inhibition of the neurogenic component are shown. These observations highlight the exciting potential for CEU to determine differences in flowmotion patterns across the same muscle section occurring at the same time. Also demonstrated by the successful measurement of flowmotion using CEU (which is a measure of blood volume alone), is that flowmotion changes are, in part, brought about but changes in blood volume, not just velocity.

The adaptation of CEU has great potential to investigate skeletal muscle flowmotion and significantly enhance knowledge of its physiological role and how flowmotion becomes altered in disease. The most exciting outcome of this thesis is the potential human application of CEU flowmotion measures, allowing for the first-time non-invasive measures of human skeletal muscle flowmotion. CEU could be used to assess skeletal muscle flowmotion in human participants to build our understanding of healthy patterns of flowmotion, as well as investigate how dysfunction develops in disease states.

7.4 Limitations of study

The data in this thesis allows a unique insight into microvascular blood flow patterns and distribution, however there are several limitations to consider in the interpretation of results. As shown in Table 7.2, the size of the cohort in the clinical studies was under-powered for some measures and hence a limitation of this study. Underpowering of a study can lead to the occurrence of a type 2 statistical error. Potentially there are differences in blood flow and flowmotion measures between the T2D and healthy control groups that has not been identified in these studies due to insufficient numbers. Power calculations to determine the number of participants required to achieve a 60% change in the T2D group compared to the healthy controls were performed as this is the magnitude change previously seen in blood flow measures under different metabolic conditions (65, 282). The percentage change able to be detected with the actual number of participants in the study was also calculated. Power calculations were performed on skin+SC perfusion measures, total forearm blood flow and LDF flux flowmotion contribution of lower frequency components. Of the measures on which the power calculation was performed brachial blood flow, LDF flux, O_2 Sat, and tHb were sufficiently powered, indicating no type 2 statistical error. However, the measures of skeletal muscle perfusion (microvascular volume, filling rate and perfusion) and LDF flux flowmotion appear to be underpowered in this study which leads to the possible occurrence of a type 2 statistical error.

Table 7.2: *Size of cohorts and power calculations.*

	Number of people required	Power	Actual number		Outcome	
Measure	**60% Change**	**% change**	**Control**	**T2D**	**% change**	**P value**
Brachial Blood Flow	13	63	22	12	64	0.003
LDF Flux	17	58	23	18	54	0.006
O_2 Sat	3	15	23	18	10	0.093
tHb	7	34	23	18	14	0.242
Microvascular Volume	18	48	20	11	-15	0.225
Microvascular Filling Rate	26	97	20	11	16	0.788
Microvascular Perfusion	24	90	20	11	-0.3	0.757
LDF Myogenic Peak AUC	27	45	23	18	-24	0.072
LDF Neurogenic Peak AUC	23	67	23	18	-10	0.579
LDF Myogenic Peak AUC	27	74	23	18	-9	0.990

The tissue oxygenation component of the LDF + OXY Moor Industries probe measures oxygenated and deoxygenated RBC in the section of tissue sampled. In this thesis O_2 Sat and tHb, which are calculated from oxygenated and deoxygenated RBC measures, were chosen as determinates of microvascular blood flow. Each of these measures give further insight into metabolism occurring within the tissue site (O_2 Sat) and a measure of microvascular blood volume (tHb), which can be compared to CEU measures. A limitation of this study is therefore the potential for error in the calculation of these measures from the raw oxygenated and deoxygenated RBC determined by the LDF + OXY Moor instruments probe. Kuliga *et. al.* (63) has previously shown that the relationship between blood flow

and O_2 Sat measure in the LDF + OXY probe is best described by a one-phase association curve fit with a plateau in O2 Sat of 84%. As the O_2 Sat measures in this thesis not exceed 80% at any point the impact of using the O_2 Sat measure is considered negligible.

A new technique, peak frequency analysis, was used in this study to better quantify the components of flowmotion. The use of this novel analysis technique allowed the determination of both the contribution through determination of peak AUC and peak frequency of each flowmotion component, giving novel insight into the control of microvascular blood flow patterns. However, validation studies to determine reproducibility and reliability are yet to be performed. Instead in this thesis, acceptable variation in the data was determined through observations made during analysis process. Official validation of this technique is still required.

These limitations may have bearing on the mechanistic interpretation of the complex and unique data in this thesis. It is believed that the best analysis process (based on extensive investigation of various analysis techniques) was utilised. However, it may have influenced the interpretation of the results potentially selecting for the desired outcome. Bias may have been introduced through the manual selection of peak AUC and frequency in PeakFit. To overcome this limitation, analysis was completed by one person to ensure consistency, analysis was done in a random order and the parameters for the selection of peak area were set by the PeakFit program. The under powering of the clinical studies may have masked potential differences between healthy control and T2D groups, but due to experimental and practical issues such as difficulty with participant recruitment and loss of data, this could not be avoided. The studies where significantly powered to determine expected difference between the two groups (skin perfusion, clinical chemistries and total limb flow) to then allow investigation into the unknown flowmotion changes.

7.5 Conclusion

It is believed that flowmotion plays an important role in the optimisation of blood flow throughout different tissues, allowing for small volumes of blood to support basal metabolic rate, while maintain the ability to greatly enhanced blood flow directly to working cells when metabolic activity is increased. Due to the importance of flowmotion in normal physiological processes, it is believed that its dysregulation is involved in the development and progression of T2D. It is still unclear if changes to flowmotion occur in response to insulin resistance and vessel damage caused by high glucose concentrations, or if dysfunction develops in the disease through other mechanisms and itself contributes to insulin resistance. Nevertheless, the changes in flowmotion function are believed to be involved in the subsequence attenuation of glucose uptake that is characteristic of the disease. The data in this thesis demonstrate changes in skin+SC flowmotion that occur in T2D, both at rest and in response to OGC. It also addresses the potential for RT intervention to improve flowmotion in T2D. If flowmotion can be improved in T2D participants, potentially glucose uptake can be enhanced, leading to better glucoregulatory control and thereby better health outcomes and quality of life for patients. This thesis also addresses the current issues with measuring flowmotion in skin+SC. Skeletal muscle flowmotion is more relevant in the metabolic T2D disease. Therefore, this thesis also provides a new technique to non-invasively assess skeletal muscle flowmotion. There is great potential for this technique to overcome current limitations in the literature and investigate changes in flowmotion during different disease states, as well as regional variation of flowmotion across a large muscle mass. Using the new CEU technique to investigate skeletal muscle flowmotion can potentially expand knowledge of flowmotion function, to better help understand the changes that occur in disease progression and perhaps provide new drug targets for therapeutic intervention, particularly in early stages of disease development.

Chapter 8 – *References*

1. Johnson PC. Autoregulation of blood flow. Circulation Research. 1986;59(5):483-95.
2. Janssen I, Heymsfield SB, Wang Z, Ross R. Skeletal muscle mass and distribution in 468 men and women aged 18–88 yr. Journal of Applied Physiology. 2000;89(1):81-8.
3. Clark MG, Rattigan S, Dora KA, Newman JM, Vincent MA, Hargreaves M, et al. Interactions between blood flow, metabolism and exercise. Biochemistry of Exercise X. Champaign, IL: Human Kinetics; 1998. p. 35-46.
4. Coyle E. Substrate utilization during exercise in active people. The American Journal of Clinical Nutrition. 1995;61(4):968S-79S.
5. Clark MG, Colquhoun EQ, Rattigan S, Dora KA, Eldershaw TP, Hall JL, et al. Vascular and endocrine control of muscle metabolism. American Journal of Physiology - Endocrinology And Metabolism. 1995;268(5):E797-E812.
6. Clark MG, Wallis MG, Barrett EJ, Vincent MA, Richards SM, Clerk LH, et al. Blood flow and muscle metabolism: a focus on insulin action. American Journal of Physiology - Endocrinology And Metabolism. 2003;284(2):E241-E58.
7. Slaaf DW, Tangelder GJ, Teirlinck HC, Reneman RS. Arteriolar vasomotion and arterial pressure reduction in rabbit tenuissimus muscle. Microvasc Res. 1987;33(1):71-80.
8. Meyer JU, Borgstrom P, Lindbom L, Intaglietta M. Vasomotion patterns in skeletal muscle arterioles during changes in arterial pressure. Microvasc Res. 1988;35(2):193-203.
9. Schmidt JA. Periodic Hemodynamics in Health and Disease: Chapman & Hall; 1996.
10. Aalkjær C, Boedtkjer D, Matchkov V. Vasomotion – what is currently thought? Acta Physiologica. 2011;202(3):253-69.
11. Aalkjaer C, Nilsson H. Vasomotion: cellular background for the oscillator and for the synchronization of smooth muscle cells. British Journal of Pharmacology. 2005;144(5):605-16.
12. de Boer MP, Meijer RI, Newman J, Stehouwer CD, Eringa EC, Smulders YM, et al. Insulin-induced changes in microvascular vasomotion and capillary recruitment are associated in humans. Microcirculation. 2014.
13. Boron WF, Boulpaep EL. Medical Physiology, A Cellular and Molecular Approach. 1st Edition ed: Saunders, Elsevier Science; 2003. 449 p.
14. Sweeney TE, Sarelius IH. Arteriolar control of capillary cell flow in striated-muscle. Circulation Research. 1989;64(1):112-20.
15. Williams DA, Segal SS. Microvascular architecture in rat soleus and extensor digitorum longus muscles. Microvasc Res. 1992;43(2):192-204.
16. Murrant CL, Sarelius IH. Coupling of muscle metabolism and muscle blood flow in capillary units during contraction. Acta Physiologica Scandinavica. 2000;168(4):531-41.
17. Utriainen T, Nuutila P, Takala T, Vicini P, Ruotsalainen U, Ronnemaa T, et al. Intact insulin stimulation of skeletal muscle blood flow, its heterogeneity and redistribution, but not of glucose uptake in non-insulin-dependent diabetes mellitus. Journal of Clinical Investigation. 1997;100(4):777-85.
18. Lindbom L, Arfors K-E. Non-homogeneous blood flow distribution in the rabbit tenuissimus muscle Differential control of total blood flow and capillary perfusion. Acta Physiologica Scandinavica. 1984;122(3):225-33.
19. Piiper J, Marconi C, Heisler N, Meyer M, Weitz H, Pendergast DR, et al. Spatial and temporal variability of blood flow in stimulated dog gastrocnemius muscle. Adv Exp Med Biol. 1989;248:719-28.
20. Intaglietta M. Vasomotor activity, time-dependent fluid exchange and tissue pressure. Microvasc Res. 1981;21(2):153-64.
21. Segal SS. Integration of blood flow control to skeletal muscle: key role of feed arteries. Acta Physiologica Scandinavica. 2000;168(4):511-8.
22. Honig CR, Odoroff CL, Frierson JL. Active and passive capillary control in red muscle at rest and in exercise. Am J Physiol. 1982;243(2):H196-H206.

23. Clark MG, Rattigan S, Newman JMB, Eldershaw TPD. Vascular control of nutrient delivery by flow redistribution within muscle: Implications for exercise and post-exercise muscle metabolism. International Journal of Sports Medicine. 1998;19(6):391-400.
24. Clark MG, Rattigan S, Clerk LH, Vincent MA, Clark ADH, Youd JM, et al. Nutritive and non-nutritive blood flow: rest and exercise. Acta Physiologica Scandinavica. 2000;168(4):519-30.
25. Pappenheimer JR. Vasoconstrictor nerves and oxygen consumption in the isolated perfused hindlimb muscles of the dog. J Physiol. 1941;99(2):182-200.
26. Lindbom L, Arfors K. Non-homogeneous blood flow distribution in the rabbit tenuissimus muscle. Differential control of total blood flow and capillary perfusion. Acta Physiol Scand. 1984;122(3):225-33.
27. Grant RT, Wright HP. Anatomical basis for non-nutritive circulation in skeletal muscle exemplified by blood vessels of rat biceps femoris tendon. Journal of Anatomy. 1970;106:125-&.
28. Vincent MA, Rattigan S, Clark MG, Bernard SL, Glenny RW. Spatial distribution of nutritive and nonnutritive vascular routes in perfused rat hindlimb muscle using microspheres. Microvasc Res. 2001;61(1):111-21.
29. Newman JM, Steen JT, Clark MG. Vessels supplying septa and tendons as functional shunts in perfused rat hindlimb. Microvasc Res. 1997;54(1):49-57.
30. Clerk LH, Smith ME, Rattigan S, Clark MG. Increased chylomicron triglyceride hydrolysis by connective tissue flow in perfused rat hindlimb. Implications for lipid storage. J Lipid Res. 2000;41(3):329-35.
31. Poole DC, Copp SW, Ferguson SK, Musch TI. Skeletal muscle capillary function: contemporary observations and novel hypotheses. Experimental Physiology. 2013;98(12):1645-58.
32. Clark MG, Rattigan S, Barrett EJ, Vincent MA. Point:Counterpoint: There is/is not capillary recruitment in active skeletal muscle during exercise. Journal of Applied Physiology. 2008;104(3):889-91.
33. Poole D, Brown M, Hudlicka O. Last Word on Point:Counterpoint: There is/is not capillary recruitment in active skeletal muscle during exercise. Journal of Applied Physiology. 2008;104(3):901.
34. Boushel R, Langberg H, Olesen J, Nowak M, Simonsen L, Bülow J, et al. Regional blood flow during exercise in humans measured by near-infrared spectroscopy and indocyanine green. Journal of Applied Physiology. 2000;89(5):1868-78.
35. González-Alonso J, Olsen DB, Saltin B. Erythrocyte and the Regulation of Human Skeletal Muscle Blood Flow and Oxygen Delivery. Circulation Research. 2002;91(11):1046-55.
36. Vincent MA, Dawson D, Clark ADH, Lindner JR, Rattigan S, Clark MG, et al. Skeletal Muscle Microvascular Recruitment by Physiological Hyperinsulinemia Precedes Increases in Total Blood Flow. Diabetes. 2002;51(1):42-8.
37. Coggins M, Lindner J, Rattigan S, Jahn L, Fasy E, Kaul S, et al. Physiologic Hyperinsulinemia Enhances Human Skeletal Muscle Perfusion by Capillary Recruitment. Diabetes. 2001;50(12):2682-90.
38. Eggleston EM, Jahn LA, Barrett EJ. Hyperinsulinemia Rapidly Increases Human Muscle Microvascular Perfusion but Fails to Increase Muscle Insulin Clearance: Evidence That a Saturable Process Mediates Muscle Insulin Uptake. Diabetes. 2007;56(12):2958-63.
39. Baron AD, Tarshoby M, Hook G, Lazaridis EN, Cronin J, Johnson A, et al. Interaction between insulin sensitivity and muscle perfusion on glucose uptake in human skeletal muscle: evidence for capillary recruitment. Diabetes. 2000;49(5):768-74.
40. Vincent MA, Barrett EJ, Lindner JR, Clark MG, Rattigan S. Inhibiting NOS blocks microvascular recruitment and blunts muscle glucose uptake in response to insulin. American Journal of Physiology - Endocrinology And Metabolism. 2003;285(1):E123-E9.
41. Vincent MA, Clerk LH, Lindner JR, Klibanov AL, Clark MG, Rattigan S, et al. Microvascular Recruitment Is an Early Insulin Effect That Regulates Skeletal Muscle Glucose Uptake In Vivo. Diabetes. 2004;53(6):1418-23.

42. Dela F, Larsen JJ, Mikines KJ, Ploug T, Petersen LN, Galbo H. Insulin-Stimulated Muscle Glucose Clearance in Patients With NIDDM: Effects of One-Legged Physical Training. Diabetes. 1995;44(9):1010-20.
43. Laakso M, Edelman SV, Brechtel G, Baron AD. Decreased effect of insulin to stimulate skeletal muscle blood flow in obese man. A novel mechanism for insulin resistance. J Clin Invest. 1990;85(6):1844-52.
44. Gelfand RA, Barrett EJ. Effect of physiologic hyperinsulinemia on skeletal muscle protein synthesis and breakdown in man. J Clin Invest. 1987;80(1):1-6.
45. Ueda S, Petrie JR, Cleland SJ, Elliott HL, Connell JM. The vasodilating effect of insulin is dependent on local glucose uptake: a double blind, placebo-controlled study. J Clin Endocrinol Metab. 1998;83(6):2126-31.
46. Utriainen T, Malmstrom R, Makimattila S, Yki-Jarvinen H. Methodological aspects, dose-response characteristics and causes of interindividual variation in insulin stimulation of limb blood flow in normal subjects. Diabetologia. 1995;38(5):555-64.
47. Raitakari M, Nuutila P, Ruotsalainen U, Laine H, Teras M, Iida H, et al. Evidence for dissociation of insulin stimulation of blood flow and glucose uptake in human skeletal muscle - Studies using O-15 H2O, F-18 fluoro-2-deoxy-D-glucose, and positron emission tomography. Diabetes. 1996;45(11):1471-7.
48. Rattigan S, Clark MG, Barrett EJ. Hemodynamic actions of insulin in rat skeletal muscle - Evidence for capillary recruitment. Diabetes. 1997;46(9):1381-8.
49. Clark MG, Clark ADH, Rattigan S. Failure of laser Doppler signal to correlate with total flow in muscle: Is this a question of vessel architecture? Microvasc Res. 2000;60(3):294-301.
50. Oberg PA. Laser-Doppler flowmetry. Crit Rev Biomed Eng. 1990;18(2):125-63.
51. Oberg PA, Tenland T, Nilsson GE. Laser-Doppler flowmetry--a non-invasive and continuous method for blood flow evaluation in microvascular studies. Acta Med Scand Suppl. 1984;687:17-24.
52. Obeid AN, Barnett NJ, Dougherty G, Ward G. A critical review of laser Doppler flowmetry. Journal of Medical Engineering & Technology. 1990;14(5):178-81.
53. Clark ADH, Youd JM, Rattigan S, Barrett EJ, Clark MG. Heterogeneity of laser Doppler flowmetry in perfused muscle indicative of nutritive and nonnutritive flow. American Journal of Physiology - Heart and Circulatory Physiology. 2001;280(3):H1324-H33.
54. Clark ADH, Barrett EJ, Rattigan S, Wallis MG, Clark MG. Insulin stimulates laser Doppler signal by rat muscle in vivo, consistent with nutritive flow recruitment. Clin Sci. 2001;100(3):283-90.
55. Stefanovska A, Bracic M, Kvernmo HD. Wavelet analysis of oscillations in the peripheral blood circulation measured by laser Doppler technique. Biomedical Engineering, IEEE Transactions on. 1999;46(10):1230-9.
56. Bracic M, Stefanovska A. Wavelet-based analysis of human blood-flow dynamics. Bulletin of Mathematical Biology. 1998;60(5):919-35.
57. Newman JMB, Dwyer RM, St-Pierre P, Richards SM, Clark MG, Rattigan S. Decreased microvascular vasomotion and myogenic response in rat skeletal muscle in association with acute insulin resistance. The Journal of Physiology. 2009;587(11):2579-88.
58. Liao F, Struck BD, Macrobert M, Jan YK. Multifractal analysis of nonlinear complexity of sacral skin blood flow oscillations in older adults. Med Biol Eng Comput. 2011;49(8):925-34.
59. Liao FY, O'Brien WD, Jan YK. Assessing complexity of skin blood flow oscillations in response to locally applied heating and pressure in rats: Implications for pressure ulcer risk. Physica a-Statistical Mechanics and Its Applications. 2013;392(20):4905-15.
60. Avery MR, Voegeli D, Byrne CD, Simpson DM, Clough GF. Age and cigarette smoking are independently associated with the cutaneous vascular response to local warming. Microcirculation. 2009;16(8):725-34.
61. Fredriksson I, Larsson M, Strömberg T. Measurement depth and volume in laser Doppler flowmetry. Microvasc Res. 2009;78(1):4-13.

62. Liu H, Kohl-Bareis M, Huang XEDRN, Popp J, editors. Design of a tissue oxygenation monitor and verification on human skin. Clinical and Biomedical Spectroscopy and Imaging II; 2011 2011/05/22; Munich: Optical Society of America.
63. Kuliga KZ, McDonald EF, Gush R, Michel C, Chipperfield AJ, Clough GF. Dynamics of Microvascular Blood Flow and Oxygenation Measured Simultaneously in Human Skin. Microcirculation. 2014;21(6):562-73.
64. Hellsten-Westing Y. Immunohistochemical localization of xanthine oxidase in human cardiac and skeletal muscle. Histochemistry. 1993;100(3):215-22.
65. Vincent MA, Clerk LH, Lindner JR, Price WJ, Jahn LA, Leong-Poi H, et al. Mixed meal and light exercise each recruit muscle capillaries in healthy humans. American Journal of Physiology - Endocrinology And Metabolism. 2006;290(6):E1191-E7.
66. Correas JM, Bridal L, Lesavre A, Mejean A, Claudon M, Helenon O. Ultrasound contrast agents: properties, principles of action, tolerance, and artifacts. European Radiology. 2001;11(8):1316-28.
67. Podell S, Burrascano C, Gaal M, Golec B, Maniquis J, Mehlhaff P. Physical and biochemical stability of Optison®, an injectable ultrasound contrast agent. Biotechnology and Applied Biochemistry. 1999;30(3):213-23.
68. Zhang L, Vincent MA, Richards SM, Clerk LH, Rattigan S, Clark MG, et al. Insulin Sensitivity of Muscle Capillary Recruitment In Vivo. Diabetes. 2004;53(2):447-53.
69. Hudetz AG. Blood Flow in the Cerebral Capillary Network: A Review Emphasizing Observations with Intravital Microscopy. Microcirculation. 1997;4(2):233-52.
70. Jain RK. Determinants of Tumor Blood Flow: A Review. Cancer Research. 1988;48(10):2641-58.
71. Kindig CA, Poole DC. A Comparison of the Microcirculation in the Rat Spinotrapezius and Diaphragm Muscles. Microvasc Res. 1998;55(3):249-59.
72. Bek T, Jeppesen P, Kanters JK. Spontaneous high frequency diameter oscillations of larger retinal arterioles are reduced in type 2 diabetes mellitus. Investigative ophthalmology & visual science. 2013;54(1):636-40.
73. Masedunskas A, Sramkova M, Parente L, Weigert R. Intravital Microscopy to Image Membrane Trafficking in Live Rats. In: Taatjes DJ, Roth J, editors. Cell Imaging Techniques: Methods and Protocols. Totowa, NJ: Humana Press; 2013. p. 153-67.
74. Krogh A, Lindhard J. A comparison between voluntary and electrically induced muscular work in man. The Journal of Physiology. 1917;51(3):182-201.
75. Barrett EJ, Eggleston EM, Inyard AC, Wang H, Li G, Chai W, et al. The vascular actions of insulin control its delivery to muscle and regulate the rate-limiting step in skeletal muscle insulin action. Diabetologia. 2009;52(5):752-64.
76. Poole DC, Brown MD, Hudlicka O. Counterpoint: There is not capillary recruitment in active skeletal muscle during exercise. Journal of Applied Physiology. 2008;104(3):891-3.
77. Clark M, Rattigan S, Barrett E, Vincent M. Last Word on Point:Counterpoint: There is/is not capillary recruitment in active skeletal muscle during exercise. Journal of Applied Physiology. 2008;104(3):900.
78. Verbeuren TJ, Vallez MO, Lavielle G, Bouskela E. Activation of thromboxane receptors and the induction of vasomotion in the hamster cheek pouch microcirculation. Br J Pharmacol. 1997;122(5):859-66.
79. Jones TW. Discovery That the Veins of the Bat's Wing (Which are Furnished with Valves) are Endowed with Rythmical Contractility, and That the Onward Flow of Blood is Accelerated by Each Contraction. Philosophical Transactions of the Royal Society of London. 1852;142:131-6.
80. Nilsson H, Aalkjaer C. Vasomotion: mechanisms and physiological importance. Molecular Interventions. 2003;3(2):79-89.
81. Collin O, Zupp JL, Setchell BP. Testicular vasomotion in different mammals. Asian J Androl. 2000;2(4):297-300.

82. Kano T, Shimoda O, Hashiguchi A, Satoh T. Periodic abnormal fluctuations of blood pressure, heart rate and skin blood flow appearing in a resuscitated comatose patient. J Auton Nerv Syst. 1991;36(2):115-22.
83. Schechner JS, Braverman IM. Synchronous vasomotion in the human cutaneous microvasculature provides evidence for central modulation. Microvasc Res. 1992;44(1):27-32.
84. Porret CA, Stergiopulos N, Hayoz D, Brunner HR, Meister JJ. Simultaneous ipsilateral and contralateral measurements of vasomotion in conduit arteries of human upper limbs. Am J Physiol. 1995;269(6 Pt 2):H1852-8.
85. Colantuoni A, Bertuglia S, Intaglietta M. The effects of a- or b-adrenergic receptor agonists and antagonists and calcium entry blockers on the spontaneous vasomotion. Microvasc Res. 1984;28(2):143-58.
86. Colantuoni A, Bertuglia S, Intaglietta M. Microvessel diameter changes during hemorrhagic shock in unanesthetized hamsters. Microvasc Res. 1985;30(2):133-42.
87. Colantuoni A, Bertuglia S, Intaglietta M. Variations of rhythmic diameter changes at the arterial microvascular bifurcationsV. Pflugers Archiv-European Journal of Physiology. 1985;403(3):289-95.
88. Colantuoni A, Bertuglia S, Coppini G, Donato L. Superposition of arteriolar vasomotion waves and regulation of blood flow in skeletal muscle microcirculation. Piiper J, Goldstick TK, Meyer M, editors1990. 549-58 p.
89. Wilkin JK. Periodic cutaneous blood flow during postocclusive reactive hyperemia. American Journal of Physiology - Heart and Circulatory Physiology. 1986;250(5):H765-H8.
90. Bollinger A, Hoffmann U, Franzeck UK. Evaluation of flux motion in man by the laser Doppler technique. Blood Vessels. 1991;28 Suppl 1:21-6.
91. Welsh M, Sharpe RM, Moffat L, Atanassova N, Saunders PT, Kilter S, et al. Androgen action via testicular arteriole smooth muscle cells is important for Leydig cell function, vasomotion and testicular fluid dynamics. PLoS One. 2010;5(10):e13632.
92. Mahler F, Muheim MH, Intaglietta M, Bollinger A, Anliker M. Blood pressure fluctuations in human nailfold capillaries. Am J Physiol. 1979;236(6):H888-93.
93. Ances BM, Greenberg JH, Detre JA. Interaction between nitric oxide synthase inhibitor induced oscillations and the activation flow coupling response. Brain Res. 2010;1309:19-28.
94. Stefanovska A. Coupled oscillators: complex but not complicated cardiovascular and brain interactions. Conf Proc IEEE Eng Med Biol Soc. 2006;1:437-40.
95. Rossi M, Nannipieri M, Anselmino M, Pesce M, Muscelli E, Santoro G, et al. Skin Vasodilator Function and Vasomotion in Patients with Morbid Obesity: Effects of Gastric Bypass Surgery. Obesity Surgery. 2011;21(1):87-94.
96. Kvernmo HD, Stefanovska A, Bracic M, Kirkeboen KA, Kvernebo K. Spectral analysis of the laser Doppler perfusion signal in human skin before and after exercise. Microvasc Res. 1998;56(3):173-82.
97. Kvandal P, Stefanovska A, Veber M, Kvernmo HD, Kirkeboen KA. Regulation of human cutaneous circulation evaluated by laser Doppler flowmetry, iontophoresis, and spectral analysis: importance of nitric oxide and prostaglandines. Microvasc Res. 2003;65(3):160-71.
98. Bocchi L, Evangelisti A, Barrella M, Scatizzi L, Bevilacqua M. Recovery of 0.1Hz microvascular skin blood flow in dysautonomic diabetic (type 2) neuropathy by using Frequency Rhythmic Electrical Modulation System (FREMS). Med Eng Phys. 2010;32(4):407-13.
99. Thorn CE, Matcher SJ, Meglinski IV, Shore AC. Is mean blood saturation a useful marker of tissue oxygenation? Am J Physiol Heart Circ Physiol. 2009;296(5):H1289-95.
100. Fagrell B, Fronek A, Intaglietta M. A microscope-television system for studying flow velocity in human skin capillaries. Am J Physiol. 1977;233(2):H318-21.
101. Lio P. Wavelets in bioinformatics and computational biology: state of art and perspectives. Bioinformatics. 2003;19(1):2-9.

102. Addison PS. Wavelet transforms and the ECG: a review. Physiological Measurement. 2005;26(5):R155-R99.
103. Torrence C, Compo GP. A practical guide to wavelet analysis. Bulletin of the American Meteorological Society. 1998;79(1):61-78.
104. Haddock RE, Hill CE. Rhythmicity in arterial smooth muscle. The Journal of Physiology. 2005;566(3):645-56.
105. Haddock RE, Hirst GD, Hill CE. Voltage independence of vasomotion in isolated irideal arterioles of the rat. J Physiol. 2002;540(Pt 1):219-29.
106. Peng H, Matchkov V, Ivarsen A, Aalkjaer C, Nilsson H. Hypothesis for the initiation of vasomotion. Circ Res. 2001;88(8):810-5.
107. Sell M, Boldt W, Markwardt F. Desynchronising effect of the endothelium on intracellular Ca2+ concentration dynamics in vascular smooth muscle cells of rat mesenteric arteries. Cell Calcium. 2002;32(3):105-20.
108. Lamboley M, Schuster A, Beny JL, Meister JJ. Recruitment of smooth muscle cells and arterial vasomotion. Am J Physiol Heart Circ Physiol. 2003;285(2):H562-9.
109. Matchkov VV. Mechanisms of cellular synchronization in the vascular wall. Mechanisms of vasomotion. Dan Med Bull. 2010;57(10):B4191.
110. Jacobsen JC, Aalkjaer C, Nilsson H, Matchkov VV, Freiberg J, Holstein-Rathlou NH. A model of smooth muscle cell synchronization in the arterial wall. Am J Physiol Heart Circ Physiol. 2007;293(1):H229-37.
111. Matchkov VV, Aalkjaer C, Nilsson H. A cyclic GMP-dependent calcium-activated chloride current in smooth-muscle cells from rat mesenteric resistance arteries. J Gen Physiol. 2004;123(2):121-34.
112. Salter KJ, Kozlowski RZ. Differential electrophysiological actions of endothelin-1 on Cl- and K+ currents in myocytes isolated from aorta, basilar and pulmonary artery. J Pharmacol Exp Ther. 1998;284(3):1122-31.
113. Salter KJ, Turner JL, Albarwani S, Clapp LH, Kozlowski RZ. Ca(2+)-activated Cl- and K+ channels and their modulation by endothelin-1 in rat pulmonary arterial smooth muscle cells. Exp Physiol. 1995;80(5):815-24.
114. ZhuGe R, Sims SM, Tuft RA, Fogarty KE, Walsh JV, Jr. Ca2+ sparks activate K+ and Cl- channels, resulting in spontaneous transient currents in guinea-pig tracheal myocytes. J Physiol. 1998;513 (Pt 3):711-8.
115. Bakhramov A, Hartley SA, Salter KJ, Kozlowski RZ. Contractile agonists preferentially activate CL- over K+ currents in arterial myocytes. Biochem Biophys Res Commun. 1996;227(1):168-75.
116. Bartlett IS, Crane GJ, Neild TO, Segal SS. Electrophysiological basis of arteriolar vasomotion in vivo. J Vasc Res. 2000;37(6):568-75.
117. Matchkov VV, Rahman A, Bakker LM, Griffith TM, Nilsson H, Aalkjaer C. Analysis of effects of connexin-mimetic peptides in rat mesenteric small arteries. Am J Physiol Heart Circ Physiol. 2006;291(1):H357-67.
118. Chaytor AT, Evans WH, Griffith TM. Peptides homologous to extracellular loop motifs of connexin 43 reversibly abolish rhythmic contractile activity in rabbit arteries. J Physiol. 1997;503 (Pt 1):99-110.
119. Matchkov VV, Rahman A, Peng H, Nilsson H, Aalkjaer C. Junctional and nonjunctional effects of heptanol and glycyrrhetinic acid derivates in rat mesenteric small arteries. Br J Pharmacol. 2004;142(6):961-72.
120. Tsai ML, Watts SW, Loch-Caruso R, Webb RC. The role of gap junctional communication in contractile oscillations in arteries from normotensive and hypertensive rats. J Hypertens. 1995;13(10):1123-33.
121. Guyenet PG. The sympathetic control of blood pressure. Nat Rev Neurosci. 2006;7(5):335-46.

122. Kastrup J, Bulow J, Lassen NA. Vasomotion in human skin before and after local heating recorded with laser Doppler flowmetry. A method for induction of vasomotion. Int J Microcirc Clin Exp. 1989;8(2):205-15.
123. Talke P, Lobo E, Brown R. Systemically administered alpha2-agonist-induced peripheral vasoconstriction in humans. Anesthesiology. 2003;99(1):65-70.
124. Cauvin C, Malik S. Induction of Ca++ influx and intracellular Ca++ release in isolated rat aorta and mesenteric resistance vessels by norepinephrine activation of alpha-1 receptors. Journal of Pharmacology and Experimental Therapeutics. 1984;230(2):413-8.
125. Khan ZP, Ferguson CN, Jones RM. Alpha-2 and imidazoline receptor agonistsTheir pharmacology and therapeutic role. Anaesthesia. 1999;54(2):146-65.
126. Starke K. Regulation of noradrenaline release by presynaptic receptor systems. Reviews of Physiology, Biochemistry and Pharmacology. Berlin, Heidelberg: Springer Berlin Heidelberg; 1977. p. 1-124.
127. Jackson WF. Oscillations in active tension in hamster aortas: role of the endothelium. Blood Vessels. 1988;25(3):144-56.
128. Kvernmo HD, Stefanovska A, Kirkeboen KA, Kvernebo K. Oscillations in the human cutaneous blood perfusion signal modified by endothelium-dependent and endothelium-independent vasodilators. Microvasc Res. 1999;57(3):298-309.
129. Jackson WF, Mulsch A, Busse R. Rhythmic smooth muscle activity in hamster aortas is mediated by continuous release of NO from the endothelium. Am J Physiol. 1991;260(1 Pt 2):H248-53.
130. Gustafsson H, Mulvany MJ, Nilsson H. Rhythmic contractions of isolated small arteries from rat: influence of the endothelium. Acta Physiol Scand. 1993;148(2):153-63.
131. Rahman A, Matchkov V, Nilsson H, Aalkjaer C. Effects of cGMP on coordination of vascular smooth muscle cells of rat mesenteric small arteries. J Vasc Res. 2005;42(4):301-11.
132. Mauban JR, Wier WG. Essential role of EDHF in the initiation and maintenance of adrenergic vasomotion in rat mesenteric arteries. Am J Physiol Heart Circ Physiol. 2004;287(2):H608-16.
133. Jonk AM, Houben AJHM, de Jongh RT, Serné EH, Schaper NC, Stehouwer CDA. Microvascular Dysfunction in Obesity: A Potential Mechanism in the Pathogenesis of Obesity-Associated Insulin Resistance and Hypertension. Physiology. 2007;22(4):252-60.
134. Abramson DI, Schkloven N, Margolis MN, Mirsky IA. Influence of massive doses of insulin on peripheral blood flow in man. American Journal of Physiology -- Legacy Content. 1939;128(1):124-32.
135. Tack CJJ, Lutterman JA, Vervoort G, Thien T, Smits P. Activation of the sodium-potassium pump contributes to insulin-induced vasodilation in humans. Hypertension. 1996;28(3):426-32.
136. Yki-Jarvinen H, Young AA, Lamkin C, Foley JE. Kinetics of glucose disposal in whole body and across the forearm in man. J Clin Invest. 1987;79(6):1713-9.
137. Kelley DE, Reilly JP, Veneman T, Mandarino LJ. Effects of insulin on skeletal-muscle glucose storage, oxidation, and glycolysis in humans. Am J Physiol. 1990;258(6):E923-E9.
138. Jackson RA, Hamling JB, Blix PM, Sim BM, Hawa MI, Jaspan JB, et al. The influence of graded hyperglycemia with and without physiological hyperinsulinemia on forearm glucose uptake and other metabolic responses in man. J Clin Endocrinol Metab. 1986;63(3):594-604.
139. Ferrannini E, Taddei S, Santoro D, Natali A, Boni C, Del Chiaro D, et al. Independent stimulation of glucose metabolism and Na+-K+ exchange by insulin in the human forearm. Am J Physiol. 1988;255(6 Pt 1):E953-8.
140. Eringa EC, Stehouwer CDA, Merlijn T, Westerhof N, Sipkema P. Physiological concentrations of insulin induce endothelin-mediated vasoconstriction during inhibition of NOS or P13-kinase in skeletal muscle arterioles. Cardiovascular Research. 2002;56(3):464-71.
141. Fryer LG, Hajduch E, Rencurel F, Salt IP, Hundal HS, Hardie DG, et al. Activation of glucose transport by AMP-activated protein kinase via stimulation of nitric oxide synthase. Diabetes. 2000;49(12):1978-85.

142. Dimmeler S, Fleming I, Fisslthaler B, Hermann C, Busse R, Zeiher AM. Activation of nitric oxide synthase in endothelial cells by Akt-dependent phosphorylation. Nature. 1999;399(6736):601-5.
143. Moncada S, Palmer RMJ, Higgs EA. Biosynthesis of nitric oxide from L-arginine - a pathway for the regulation of cell-function and communication. Biochemical Pharmacology. 1989;38(11):1709-15.
144. Ignarro LJ. Nitric oxide as a unique signaling molecule in the vascular system: A historical overview. Journal of Physiology and Pharmacology. 2002;53(4):503-14.
145. Friebe A, Koesling D. Regulation of Nitric Oxide-Sensitive Guanylyl Cyclase. Circulation Research. 2003;93(2):96-105.
146. Sauzeau V, Le Jeune H, Cario-Toumaniantz C, Smolenski A, Lohmann SM, Bertoglio J, et al. Cyclic GMP-dependent Protein Kinase Signaling Pathway Inhibits RhoA-induced Ca2+ Sensitization of Contraction in Vascular Smooth Muscle. Journal of Biological Chemistry. 2000;275(28):21722-9.
147. Barman SA, Zhu S, Han G, White RE. cAMP activates BKCa channels in pulmonary arterial smooth muscle via cGMP-dependent protein kinase. American Journal of Physiology - Lung Cellular and Molecular Physiology. 2003;284(6):L1004-L11.
148. Archer SL, Huang JM, Hampl V, Nelson DP, Shultz PJ, Weir EK. Nitric oxide and cGMP cause vasorelaxation by activation of a charybdotoxin-sensitive K channel by cGMP-dependent protein kinase. Proceedings of the National Academy of Sciences. 1994;91(16):7583-7.
149. Surks HK, Mochizuki N, Kasai Y, Georgescu SP, Tang KM, Ito M, et al. Regulation of myosin phosphatase by a specific interaction with cGMP-dependent protein kinase I alpha. Science. 1999;286(5444):1583-7.
150. Cardillo C, Nambi SS, Kilcoyne CM, Choucair WK, Katz A, Quon MJ, et al. Insulin Stimulates Both Endothelin and Nitric Oxide Activity in the Human Forearm. Circulation. 1999;100(8):820-5.
151. Muniyappa R, Montagnani M, Koh KK, Quon MJ. Cardiovascular actions of insulin. Endocr Rev. 2007;28(5):463-91.
152. Kim J-a, Montagnani M, Koh KK, Quon MJ. Reciprocal Relationships Between Insulin Resistance and Endothelial Dysfunction: Molecular and Pathophysiological Mechanisms. Circulation. 2006;113(15):1888-904.
153. Mather KJ, Lteif A, Steinberg HO, Baron AD. Interactions Between Endothelin and Nitric Oxide in the Regulation of Vascular Tone in Obesity and Diabetes. Diabetes. 2004;53(8):2060-6.
154. Scherrer U, Sartori C. Insulin as a vascular and sympathoexcitatory hormone: implications for blood pressure regulation, insulin sensitivity, and cardiovascular morbidity. Circulation. 1997;96(11):4104-13.
155. Rowe JW, Young JB, Minaker KL, Stevens AL, Pallotta J, Landsberg L. Effect of insulin and glucose infusions on sympathetic nervous system activity in normal man. Diabetes. 1981;30(3):219-25.
156. Clerk LH, Vincent MA, Jahn LA, Liu Z, Lindner JR, Barrett EJ. Obesity blunts insulin-mediated microvascular recruitment in human forearm muscle. Diabetes. 2006;55(5):1436-42.
157. Lembo G, Napoli R, Capaldo B, Rendina V, Iaccarino G, Volpe M, et al. Abnormal sympathetic overactivity evoked by insulin in the skeletal muscle of patients with essential hypertension. J Clin Invest. 1992;90(1):24-9.
158. Sartori C, Trueb L, Nicod P, Scherrer U. Effects of sympathectomy and nitric oxide synthase inhibition on vascular actions of insulin in humans. Hypertension. 1999;34(4 Pt 1):586-9.
159. Oltman CL, Kane NL, Gutterman DD, Bar RS, Dellsperger KC. Mechanism of coronary vasodilation to insulin and insulin-like growth factor I is dependent on vessel size. Am J Physiol Endocrinol Metab. 2000;279(1):E176-81.
160. Marshall JM. The influence of the sympathetic nervous system on individual vessels of the microcirculation of skeletal muscle of the rat. J Physiol. 1982;332:169-86.

161. Dela F, Stallknecht B, Biering-Sorensen F. An intact central nervous system is not necessary for insulin-mediated increases in leg blood flow in humans. Pflugers Archiv-European Journal of Physiology. 2000;441(2-3):241-50.
162. Katz LD, Glickman MG, Rapoport S, Ferrannini E, Defronzo RA. Splanchnic and peripheral disposal of oral glucose in man. Diabetes. 1983;32(7):675-9.
163. Defronzo RA, Ferrannini E, Sato Y, Felig P. Synergistic interaction between exercise and insulin on peripheral glucose-uptake. Journal of Clinical Investigation. 1981;68(6):1468-74.
164. Defronzo RA, Jacot E, Jequier E, Maeder E, Wahren J, Felber JP. The effect of insulin on the disposal of intravenous glucose - results from indirect calorimetry and hepatic and femoral venous catheterixation. Diabetes. 1981;30(12):1000-7.
165. Kolka CM, Bergman RN. The endothelium in diabetes: Its role in insulin access and diabetic complications. Rev Endocr Metab Disord. 2013;14(1):13-9.
166. Kubota T, Kubota N, Kumagai H, Yamaguchi S, Kozono H, Takahashi T, et al. Impaired Insulin Signaling in Endothelial Cells Reduces Insulin-Induced Glucose Uptake by Skeletal Muscle. Cell Metab. 2011;13(3):294-307.
167. de Luca JP, Garnache AK, Rulfs J, Miller TB. Wortmannin inhibits insulin-stimulated activation of protein phosphatase 1 in rat cardiomyocytes. American Journal of Physiology - Heart and Circulatory Physiology. 1999;276(5):H1520-H6.
168. Clerk LH, Vincent MA, Lindner JR, Clark MG, Rattigan S, Barrett EJ. The vasodilatory actions of insulin on resistance and terminal arterioles and their impact on muscle glucose uptake. Diabetes/Metabolism Research and Reviews. 2004;20(1):3-12.
169. Meijer RI, De Boer MP, Groen MR, Eringa EC, Rattigan S, Barrett EJ, et al. Insulin-Induced Microvascular Recruitment in Skin and Muscle are Related and Both are Associated with Whole-Body Glucose Uptake. Microcirculation. 2012;19(6):494-500.
170. Bradley EA, Willson KJ, Choi-Lundberg D, Clark MG, Rattigan S. Effects of central administration of insulin or l-NMMA on rat skeletal muscle microvascular perfusion. Diabetes, Obesity and Metabolism. 2010;12(10):900-8.
171. Baron AD. The Coupling of Glucose Metabolism and Perfusion in Human Skeletal Muscle: The Potential Role of Endothelium-Derived Nitric Oxide. Diabetes. 1996;45(Supplement 1):S105-S9.
172. Kahn SE, Hull RL, Utzschneider KM. Mechanisms linking obesity to insulin resistance and type 2 diabetes. Nature. 2006;444(7121):840-6.
173. Kelley DE. Skeletal Muscle Triglycerides. Annals of the New York Academy of Sciences. 2002;967(1):135-45.
174. Shulman GI. Cellular mechanisms of insulin resistance. Journal of Clinical Investigation. 2000;106(2):171-6.
175. Hotamisligil GS, Arner P, Caro JF, Atkinson RL, Spiegelman BM. Increased adipose tissue expression of tumor necrosis factor-alpha in human obesity and insulin resistance. The Journal of Clinical Investigation. 1995;95(5):2409-15.
176. Straczkowski M, Dzienis-Straczkowska S, Stepien A, Kowalska I, Szelachowska M, Kinalska I. Plasma interleukin-8 concentrations are increased in obese subjects and related to fat mass and tumor necrosis factor-alpha system. Journal of Clinical Endocrinology & Metabolism. 2002;87(10):4602-6.
177. Zeyda M, Stulnig TM. Obesity, Inflammation, and Insulin Resistance – A Mini-Review. Gerontology. 2009;55(4):379-86.
178. Ravussin E, Smith SR. Increased Fat Intake, Impaired Fat Oxidation, and Failure of Fat Cell Proliferation Result in Ectopic Fat Storage, Insulin Resistance, and Type 2 Diabetes Mellitus. Annals of the New York Academy of Sciences. 2002;967(1):363-78.
179. Stumvoll M, Goldstein BJ, van Haeften TW. Type 2 diabetes: principles of pathogenesis and therapy. Lancet. 2005;365(9467):1333-46.

180. Zierath J, He L, Gumà A, Wahlström E, Klip A, Wallberg-Henriksson H. Insulin action on glucose transport and plasma membrane GLUT4 content in skeletal muscle from patients with NIDDM. Diabetologia. 1996;39(10):1180-9.
181. King PA, Horton ED, Hirshman MF, Horton ES. Insulin resistance in obese Zucker rat (fa/fa) skeletal-muslce is associated with a failure of gulconse transporter translocation. Journal of Clinical Investigation. 1992;90(4):1568-75.
182. Rattigan S, Bussey CT, Ross RM, Richards SM. Obesity, Insulin Resistance, and Capillary Recruitment. Microcirculation. 2007;14(4-5):299-309.
183. Rattigan S, Clark MG, Barrett EJ. Acute vasoconstriction-induced insulin resistance in rat muscle in vivo. Diabetes. 1999;48(3):564-9.
184. Youd JM, Rattigan S, Clark MG. Acute impairment of insulin-mediated capillary recruitment and glucose uptake in rat skeletal muscle in vivo by TNF-alpha. Diabetes. 2000;49(11):1904-9.
185. Cusi K, Maezono K, Osman A, Pendergrass M, Patti ME, Pratipanawatr T, et al. Insulin resistance differentially affects the PI 3-kinase– and MAP kinase–mediated signaling in human muscle. The Journal of Clinical Investigation. 2000;105(3):311-20.
186. Pasceri V, Chang J, Willerson JT, Yeh ETH. Modulation of C-Reactive Protein–Mediated Monocyte Chemoattractant Protein-1 Induction in Human Endothelial Cells by Anti-Atherosclerosis Drugs. Circulation. 2001;103(21):2531-4.
187. Pasceri V, Willerson JT, Yeh ETH. Direct Proinflammatory Effect of C-Reactive Protein on Human Endothelial Cells. Circulation. 2000;102(18):2165-8.
188. Muniyappa R, Iantorno M, Quon MJ. An Integrated View of Insulin Resistance and Endothelial Dysfunction. Endocrinology and Metabolism Clinics of North America. 2008;37(3):685-711.
189. Clerk LH, Rattigan S, Clark MG. Lipid infusion impairs physiologic insulin-mediated capillary recruitment and muscle glucose uptake in vivo. Diabetes. 2002;51(4):1138-45.
190. Caballero AE. Metabolic and Vascular Abnormalities in Subjects at Risk for Type 2 Diabetes: The Early Start of a Dangerous Situation. Archives of Medical Research. 2005;36(3):241-9.
191. Caballero AE. Endothelial dysfunction in obesity and insulin resistance: A road to diabetes and heart disease. Obesity Research. 2003;11(11):1278-89.
192. Wheatley CM, Rattigan S, Richards SM, Barrett EJ, Clark MG. Skeletal muscle contraction stimulates capillary recruitment and glucose uptake in insulin-resistant obese Zucker rats. American Journal of Physiology - Endocrinology And Metabolism. 2004;287(4):E804-E9.
193. Wallis MG, Wheatley CM, Rattigan S, Barrett EJ, Clark ADH, Clark MG. Insulin-Mediated Hemodynamic Changes Are Impaired in Muscle of Zucker Obese Rats. Diabetes. 2002;51(12):3492-8.
194. Premilovac D, Bradley EA, Ng HLH, Richards SM, Rattigan S, Keske MA. Muscle insulin resistance resulting from impaired microvascular insulin sensitivity in Sprague Dawley rats. Cardiovascular Research. 2013.
195. Muris DM, Houben AJ, Schram MT, Stehouwer CD. Microvascular dysfunction: an emerging pathway in the pathogenesis of obesity-related insulin resistance. Rev Endocr Metab Disord. 2013;14(1):29-38.
196. Benedict KF, Coffin GS, Barrett EJ, Skalak TC. Hemodynamic Systems Analysis of Capillary Network Remodeling During the Progression of Type 2 Diabetes. Microcirculation. 2011;18(1):63-73.
197. Barchetta I, Riccieri V, Vasile M, Stefanantoni K, Comberiati P, Taverniti L, et al. High prevalence of capillary abnormalities in patients with diabetes and association with retinopathy. Diabetic Medicine. 2011;28(9):1039-44.
198. Carnethon MR, Jacobs DR, Sidney S, Liu K. Influence of Autonomic Nervous System Dysfunction on the Development of Type 2 Diabetes. The CARDIA study. 2003;26(11):3035-41.
199. Segel SA, Paramore DS, Cryer PE. Hypoglycemia-Associated Autonomic Failure in Advanced Type 2 Diabetes. Diabetes. 2002;51(3):724-33.
200. Stehouwer CDA, Henry RMA, Ferreira I. Arterial stiffness in diabetes and the metabolic syndrome: a pathway to cardiovascular disease. Diabetologia. 2008;51(4):527-39.

201. Alberti K, Zimmet PZ, Consultation WHO. Definition, diagnosis and classification of diabetes mellitus and its complications part 1: Diagnosis and classification of diabetes mellitus - Provisional report of a WHO consultation. Diabetic Medicine. 1998;15(7):539-53.
202. Inzucchi SE. Oral antihyperglycemic therapy for type 2 diabetes: Scientific review. JAMA. 2002;287(3):360-72.
203. Zanuso S, Jimenez A, Pugliese G, Corigliano G, Balducci S. Exercise for the management of type 2 diabetes: a review of the evidence. Acta diabetologica. 2010;47(1):15-22.
204. Yokoyama H, Emoto M, Fujiwara S, Motoyama K, Morioka T, Koyama H, et al. Short-term aerobic exercise improves arterial stiffness in type 2 diabetes. Diabetes Res Clin Pract. 2004;65(2):85-93.
205. Segal KR, Edano A, Abalos A, Albu J, Blando L, Tomas MB, et al. Effect of exercise training on insulin sensitivity and glucose metabolism in lean, obese, and diabetic men. Journal of Applied Physiology. 1991;71(6):2402-11.
206. Mourier A, Gautier J-F, Kerviler ED, Bigard AX, Villette J-M, Garnier J-P, et al. Mobilization of Visceral Adipose Tissue Related to the Improvement in Insulin Sensitivity in Response to Physical Training in NIDDM: Effects of branched-chain amino acid supplements. Diabetes Care. 1997;20(3):385-91.
207. Church TS, Blair SN, Cocreham S, et al. Effects of aerobic and resistance training on hemoglobin a1c levels in patients with type 2 diabetes : A randomized controlled trial. JAMA. 2010;304(20):2253-62.
208. Thijssen DH, Maiorana AJ, O'Driscoll G, Cable NT, Hopman MT, Green DJ. Impact of inactivity and exercise on the vasculature in humans. European journal of applied physiology. 2010;108(5):845-75.
209. Laughlin MH. Endothelium-mediated control of coronary vascular tone after chronic exercise training. Med Sci Sports Exerc. 1995;27(8):1135-44.
210. Moyna NM, Thompson PD. The effect of physical activity on endothelial function in man. Acta Physiol Scand. 2004;180(2):113-23.
211. Maiorana A, O'Driscoll G, Taylor R, Green D. Exercise and the nitric oxide vasodilator system. Sports medicine (Auckland, NZ). 2003;33(14):1013-35.
212. Stewart KJ. Exercise training and the cardiovascular consequences of type 2 diabetes and hypertension: Plausible mechanisms for improving cardiovascular health. JAMA. 2002;288(13):1622-31.
213. Cohen ND, Dunstan DW, Robinson C, Vulikh E, Zimmet PZ, Shaw JE. Improved endothelial function following a 14-month resistance exercise training program in adults with type 2 diabetes. Diabetes Res Clin Pract. 2008;79(3):405-11.
214. Green DJ, Maiorana A, O'Driscoll G, Taylor R. Effect of exercise training on endothelium-derived nitric oxide function in humans. J Physiol. 2004;561(Pt 1):1-25.
215. Clough GF, L'Esperance V, Turzyniecka M, Walter L, Chipperfield AJ, Gamble J, et al. Functional dilator capacity is independently associated with insulin sensitivity and age in central obesity and is not improved by high dose statin treatment. Microcirculation. 2011;18(1):74-84.
216. Montero D, Walther G, Perez-Martin A, Santamaria C, Roche E, Mercier C, et al. Decreased microvascular myogenic response to insulin in severely obese adolescents. Clin Hemorheol Microcirc. 2014;57(1):23-32.
217. Sun PC, Chen CS, Kuo CD, Lin HD, Chan RC, Kao MJ, et al. Impaired microvascular flow motion in subclinical diabetic feet with sudomotor dysfunction. Microvasc Res. 2012;83(2):243-8.
218. Sun P-C, Kuo C-D, Chi L-Y, Lin H-D, Wei S-H, Chen C-S. Microcirculatory vasomotor changes are associated with severity of peripheral neuropathy in patients with type 2 diabetes. Diabetes and Vascular Disease Research. 2012.
219. de Jongh RT, Serne EH, RG IJ, Jorstad HT, Stehouwer CD. Impaired local microvascular vasodilatory effects of insulin and reduced skin microvascular vasomotion in obese women. Microvasc Res. 2008;75(2):256-62.

220. Ding H, Triggle CR. Endothelial dysfunction in diabetes: multiple targets for treatment. Pflügers Archiv - European Journal of Physiology. 2010;459(6):977-94.
221. de Boer MP, Wijnstok NJ, Serné EH, Eringa EC, Stehouwer CDA, Flyvbjerg A, et al. Body mass index is related to microvascular vasomotion, this is partly explained by adiponectin. European Journal of Clinical Investigation. 2014;44(7):660-7.
222. Russell RD, Nelson AG, Kraemer RR. Short bouts of high-intensity resistance-style training produce similar reductions in fasting blood glucose of diabetic offspring and controls. Journal of strength and conditioning research / National Strength & Conditioning Association. 2014;28(10):2760-7.
223. Roberts CK, Hevener AL, Barnard RJ. Metabolic syndrome and insulin resistance: underlying causes and modification by exercise training. Comprehensive Physiology. 2013;3(1):1-58.
224. Holten MK, Zacho M, Gaster M, Juel C, Wojtaszewski JF, Dela F. Strength training increases insulin-mediated glucose uptake, GLUT4 content, and insulin signaling in skeletal muscle in patients with type 2 diabetes. Diabetes. 2004;53(2):294-305.
225. Tallroth K, Kettunen JA, Kujala UM. Reproducibility of regional DEXA examinations of abdominal fat and lean tissue. Obesity facts. 2013;6(2):203-10.
226. Tigno XT, Hansen BC, Nawang S, Shamekh R, Albano AM. Vasomotion Becomes Less Random as Diabetes Progresses in Monkeys. Microcirculation. 2011;18(6):429-39.
227. Lempel A, Ziv J. On the Complexity of Finite Sequences. IEEE Transactions on Information Theory. 1976;22(1):75-81.
228. Mahajan H, Richards SM, Rattigan S, Clark MG. Local methacholine but not bradykinin potentiates insulin-mediated capillary recruitment and glucose uptake in muscle in vivo. Diabetes. 2004;53:A369-A.
229. Armstrong RB, Phelps RO. Muscle fiber type composition of the rat hindlimb. American Journal of Anatomy. 1984;171(3):259-72.
230. Clark MG. Impaired microvascular perfusion: a consequence of vascular dysfunction and a potential cause of insulin resistance in muscle. American Journal of Physiology - Endocrinology And Metabolism. 2008;295(4):E732-E50.
231. Goh S-Y, Cooper ME. The Role of Advanced Glycation End Products in Progression and Complications of Diabetes. The Journal of Clinical Endocrinology & Metabolism. 2008;93(4):1143-52.
232. Singh R, Barden A, Mori T, Beilin L. Advanced glycation end-products: a review. Diabetologia. 2001;44(2):129-46.
233. Forbes JM, Cooper ME. Mechanisms of Diabetic Complications. Physiological Reviews. 2013;93(1):137-88.
234. WHO. Global Database on Body Mass Index 2016 [cited 2016 25/7/16]. Available from: http://apps.who.int/bmi/index.jsp?introPage=intro_3.html.
235. Allen J, Frame JR, Murray A. Microvascular blood flow and skin temperature changes in the fingers following a deep nspiratory gasp. Physiol Meas. 2002;23(2):365-73.
236. Laakso M, Edelman SV, Brechtel G, Baron AD. Impaired Insulin-Mediated Skeletal Muscle Blood Flow in Patients With NIDDM. Diabetes. 1992;41(9):1076-83.
237. Levy BI, Schiffrin EL, Mourad JJ, Agostini D, Vicaut E, Safar ME, et al. Impaired tissue perfusion: a pathology common to hypertension, obesity, and diabetes mellitus. Circulation. 2008;118(9):968-76.
238. Fowler MJ. Microvascular and Macrovascular Complications of Diabetes. Clinical Diabetes. 2008;26(2):77-82.
239. Sachidanandam K, Harris A, Hutchinson J, Ergul A. Microvascular Versus Macrovascular Dysfunction in Type 2 Diabetes: Differences in Contractile Responses to Endothelin-1. Experimental Biology and Medicine. 2006;231(6):1016-21.
240. Keen H, Clark C, Laakso M. Reducing the burden of diabetes: Managing cardiovascular disease. Diabetes-Metabolism Research and Reviews. 1999;15(3):186-96.

241. Creager MA, Lüscher TF, Cosentino F, Beckman JA. Diabetes and Vascular Disease. Pathophysiology, Clinical Consequences, and Medical Therapy: Part I. 2003;108(12):1527-32.
242. Stansberry KB, Shapiro SA, Hill MA, McNitt PM, Meyer MD, Vinik AI. Impaired peripheral vasomotion in diabetes. Diabetes Care. 1996;19(7):715-21.
243. Rossi M, Nannipieri M, Anselmino M, Guarino D, Franzoni F, Pesce M. Subcutaneous adipose tissue blood flow and vasomotion in morbidly obese patients: long term effect of gastric bypass surgery. Clin Hemorheol Microcirc. 2012;51(3):159-67.
244. Vollenweider P, Tappy L, Randin D, Schneiter P, Jequier E, Nicod P, et al. Differential effects of hyperinsulinemia and carbohydrate metabolism on sympathetic nerve activity and muscle blood flow in humans. J Clin Invest. 1993;92(1):147-54.
245. Baron AD. Hemodynamic actions of insulin. American Journal of Physiology - Endocrinology And Metabolism. 1994;267(2):E187-E202.
246. Pereda SA, Eckstein JW, Abboud FM. Cardiovascular responses to insulin in the absence of hypoglycemia. American Journal of Physiology -- Legacy Content. 1962;202(2):249-52.
247. Jonk AM, Houben AJ, Schaper NC, de Leeuw PW, Serné EH, Smulders YM, et al. Meal-Related Increases in Microvascular Vasomotion Are Impaired in Obese Individuals: A potential mechanism in the pathogenesis of obesity-related insulin resistance. Diabetes Care. 2011;34(Suppl 2):S342-S8.
248. Steinberg HO, Brechtel G, Johnson A, Fineberg N, Baron AD. Insulin-mediated skeletal muscle vasodilation is nitric-oxide dependent - a novel action of insulin to increase nitric oxide release. Journal of Clinical Investigation. 1994;94(3):1172-9.
249. de Jongh RT, Clark ADH, Ijzerman RG, Serne EH, de Vries G, Stehouwer CDA. Physiological hyperinsulinaemia increases intramuscular microvascular reactive hyperaemia and vasomotion in healthy volunteers. Diabetologia. 2004;47(6):978-86.
250. Rossi M, Maurizio S, Carpi A. Skin blood flowmotion response to insulin iontophoresis in normal subjects. Microvasc Res. 2005;70(1-2):17-22.
251. Schmiedel O, Schroeter ML, Harvey JN. Microalbuminuria in Type 2 diabetes indicates impaired microvascular vasomotion and perfusion. American Journal of Physiology - Heart and Circulatory Physiology. 2007;293(6):H3424-H31.
252. Shaw P. Ross and Wilson Anatomy and Physiology in Health and Illness – Twelfth edition. Nursing Standard. 2014;28(49):32-.
253. Straznicky NE, Lambert GW, Masuo K, Dawood T, Eikelis N, Nestel PJ, et al. Blunted sympathetic neural response to oral glucose in obese subjects with the insulin-resistant metabolic syndrome. Am J Clin Nutr. 2009;89(1):27-36.
254. Russell RD, Kraemer RR, Nelson AG. Metabolic dysfunction in diabetic offspring: deviations in metabolic flexibility. Med Sci Sports Exerc. 2013;45(1):8-15.
255. Kahn SE. The relative contributions of insulin resistance and beta-cell dysfunction to the pathophysiology of Type 2 diabetes. Diabetologia. 2003;46(1):3-19.
256. Keske MA, Clerk LH, Price WJ, Jahn LA, Barrett EJ. Obesity Blunts Microvascular Recruitment in Human Forearm Muscle After a Mixed Meal. Diabetes Care. 2009;32(9):1672-7.
257. Dawson D, Vincent MA, Barrett EJ, Kaul S, Clark A, Leong-Poi H, et al. Vascular recruitment in skeletal muscle during exercise and hyperinsulinemia assessed by contrast ultrasound. American Journal of Physiology-Endocrinology and Metabolism. 2002;282(3):E714-E20.
258. Welle S, Lilavivathana U, Campbell RG. Increased plasma norepinephrine concentrations and metabolic rates following glucose ingestion in man. Metabolism. 1980;29(9):806-9.
259. Ross RM, Downey K, Newman JMB, Richards SM, Clark MG, Rattigan S. Contrast-enhanced ultrasound measurement of microvascular perfusion relevant to nutrient and hormone delivery in skeletal muscle: A model study in vitro. Microvasc Res. 2008;75(3):323-9.
260. Baron AD, Steinberg H, Brechtel G, Johnson A. Skeletal muscle blood flow independently modulates insulin-mediated glucose uptake. American Journal of Physiology - Endocrinology And Metabolism. 1994;266(2):E248-E53.

261. Laakso M, Edelman SV, Brechtel G, Baron AD. Decreased effect of insulin to stimulate skeletal muscle blood flow in obese man. A novel mechanism for insulin resistance. Journal of Clinical Investigation. 1990;85(6):1844-52.
262. Williams SB, Goldfine AB, Timimi FK, Ting HH, Roddy M-A, Simonson DC, et al. Acute Hyperglycemia Attenuates Endothelium-Dependent Vasodilation in Humans In Vivo. Circulation. 1998;97(17):1695-701.
263. Russell RD, Nelson AG, Kraemer RR. Short Bouts of High-Intensity Resistance-Style Training Produce Similar Reductions in Fasting Blood Glucose of Diabetic Offspring and Controls. The Journal of Strength & Conditioning Research. 2014;28(10):2760-7.
264. Castaneda C, Layne JE, Munoz-Orians L, Gordon PL, Walsmith J, Foldvari M, et al. A Randomized Controlled Trial of Resistance Exercise Training to Improve Glycemic Control in Older Adults With Type 2 Diabetes. Diabetes Care. 2002;25(12):2335-41.
265. Maiorana A, O'Driscoll G, Cheetham C, Dembo L, Stanton K, Goodman C, et al. The effect of combined aerobic and resistance exercise training on vascular function in type 2 diabetes. Journal of the American College of Cardiology. 2001;38(3):860-6.
266. Davis J-K, Green JM. Resistance Training and Type-2 Diabetes. Strength & Conditioning Journal. 2007;29(1):42-8.
267. Boulé NG, Haddad E, Kenny GP, Wells GA, Sigal RJ. Effects of exercise on glycemic control and body mass in type 2 diabetes mellitus: A meta-analysis of controlled clinical trials. JAMA. 2001;286(10):1218-27.
268. Snowling NJ, Hopkins WG. Effects of Different Modes of Exercise Training on Glucose Control and Risk Factors for Complications in Type 2 Diabetic Patients. A meta-analysis. 2006;29(11):2518-27.
269. Watts K, Beye P, Siafarikas A, Davis EA, Jones TW, O'Driscoll G, et al. Exercise training normalizes vascular dysfunction and improves central adiposity in obese adolescents. Journal of the American College of Cardiology. 2004;43(10):1823-7.
270. Dunstan DW, Daly RM, Owen N, Jolley D, de Courten M, Shaw J, et al. High-Intensity Resistance Training Improves Glycemic Control in Older Patients With Type 2 Diabetes. Diabetes Care. 2002;25(10):1729-36.
271. Gordon BA, Benson AC, Bird SR, Fraser SF. Resistance training improves metabolic health in type 2 diabetes: A systematic review. Diabetes Res Clin Pract. 2009;83(2):157-75.
272. Croymans DM, Krell SL, Oh CS, Katiraie M, Lam CY, Harris RA, et al. Effects of resistance training on central blood pressure in obese young men. Journal of human hypertension. 2014;28(3):157-64.
273. Vinet A, Obert P, Dutheil F, Diagne L, Chapier R, Lesourd B, et al. Impact of a lifestyle program on vascular insulin resistance in metabolic syndrome subjects: the RESOLVE study. J Clin Endocrinol Metab. 2015;100(2):442-50.
274. Epley B. Boyd Epley Workout. Poundage Chart. 1985.
275. Ibañez J, Izquierdo M, Argüelles I, Forga L, Larrión JL, García-Unciti M, et al. Twice-Weekly Progressive Resistance Training Decreases Abdominal Fat and Improves Insulin Sensitivity in Older Men With Type 2 Diabetes. Diabetes Care. 2005;28(3):662-7.
276. Kislukhin VV. Stochasticity of flow through microcirculation as a regulator of oxygen delivery. Theoretical Biology and Medical Modelling. 2010;7.
277. Thorn CE, Kyte H, Slaff DW, Shore AC. An association between vasomotion and oxygen extraction. American Journal of Physiology - Heart and Circulatory Physiology. 2011;301(2):H442-H9.
278. Rattigan S, Wheatley C, Richards SM, Barrett EJ, Clark MG. Exercise and insullin-mediated capillary recruitment in muscle. Exercise and Sport Sciences Reviews. 2005;33(1):43-8.
279. Kvandal P, Landsverk SA, Bernjak A, Stefanovska A, Kvernmo HD, Kirkebøen KA. Low-frequency oscillations of the laser Doppler perfusion signal in human skin. Microvasc Res. 2006;72(3):120-7.

280. Achenbach S, Giesler T, Ropers D, Ulzheimer S, Derlien H, Schulte C, et al. Detection of Coronary Artery Stenoses by Contrast-Enhanced, Retrospectively Electrocardiographically-Gated, Multislice Spiral Computed Tomography. Circulation. 2001;103(21):2535-8.
281. Caiati C, Montaldo C, Zedda N, Bina A, Iliceto S. New Noninvasive Method for Coronary Flow Reserve Assessment: Contrast-Enhanced Transthoracic Second Harmonic Echo Doppler. Circulation. 1999;99(6):771-8.
282. Sjoberg KA, Rattigan S, Hiscock N, Richter EA, Kiens B. A new method to study changes in microvascular blood volume in muscle and adipose tissue: real-time imaging in humans and rat. American Journal of Physiology-Heart and Circulatory Physiology. 2011;301(2):H450-H8.
283. Das PK, Parratt JR. Myocardial and haemodynamic effects of phentolamine. British Journal of Pharmacology. 1971;41(3):437-44.
284. Jansson PA. Endothelial dysfunction in insulin resistance and type 2 diabetes. J Intern Med. 2007;262(2):173-83.
285. Dhananjayan R, Koundinya KS, Malati T, Kutala VK. Endothelial Dysfunction in Type 2 Diabetes Mellitus. Indian journal of clinical biochemistry : IJCB. 2016;31(4):372-9.
286. Barrett EJ, Rattigan S. Muscle Perfusion. Its Measurement and Role in Metabolic Regulation. 2012;61(11):2661-8.
287. Bari F, Tóth-Szűki V, Domoki F, Kálmán J. Flow motion pattern differences in the forehead and forearm skin: Age-dependent alterations are not specific for Alzheimer's disease. Microvasc Res. 2005;70(3):121-8.
288. D'Antoni AV. Gray's Anatomy, the Anatomical Basis of Clinical Practice, 41st edition. Clinical Anatomy. 2016;29(2):264-5.
289. Ledger PW. Skin biological issues in electrically enhanced transdermal delivery. Advanced Drug Delivery Reviews. 1992;9(2):289-307.
290. Stumvoll M, Goldstein BJ, van Haeften TW. Type 2 diabetes: principles of pathogenesis and therapy. The Lancet. 2005;365(9467):1333-46.